

2003-2006

**China National Report on Meteorology  
and Atmospheric Sciences**

*For*

The 24rd General Assembly of IUGG

Perugia, Italy, 2-13 July, 2007

By Chinese National Committee for

The International Union of Geodesy and Geophysics

Beijing, China

**June, 2007**

## **PREFACE**

As a rule, the International Association of Meteorology and Atmospheric Sciences (IAMAS) requests each of her member countries to submit, every four years, a progress report on the relevant operational and research fields, and exchange the report with other members during the International Union of Geodesy and Geophysics (IUGG) Assembly that is held every four years as well. During the last thirty years, the China National Committee for IAMAS has regularly composed its report. This National Report of the China National Committee for IAMAS is prepared for the XXIV General Assembly of IUGG, Perugia, Italy, July 2007 and introduces some advances and achievements in meteorology and atmospheric sciences in China mainly during 2003-2006.

The National Report consists of 15 papers that cover the following fields: Observation, numerical weather prediction, climate and climate change, climate model, nonlinear dynamics and predictability, monsoon, meso-scale meteorology, cloud physics, and etc. Those papers were also sent out for peer-review. If they are accepted, they will be published in a Special Issue of “Advances in Atmospheric Sciences” which is the journal of the China National Committee for IAMAS.

Through this report you could briefly understand what Chinese Scientists have done and what they are going to do in China. We hope that this report will strengthen domestic exchanges and enhance international cooperation so that meteorology and atmospheric sciences in China will develop further, and we will be able to contribute more to the outside world.

Chinese National Committee for IAMAS  
WU Guoxiong, Chairman  
ZHENG Guoguang, Vice-Chairman  
LI Jianping, Secretary-General  
June, 2007

# RECENT PROGRESSES IN THE ATMOSPHERIC OBSERVATION RESEARCHES IN CHINA

*Qiu Jinhuan, Chen Hongbin, Wang Pucai, Liu Yi, and Xia Xiang'ao*

Institute of Atmospheric Physics, Beijing 100029

## ABSTRACT

Recent progresses in atmospheric observation techniques, observation systems and applications in China are reviewed. According to different observation platforms, the reviewing is presented in three sections, i.e. Satellite Remote Sensing (SRS), ground-based observation technologies and applications, and airborne/balloon measurements. The section “satellite remote sensing” presents research advances on SRS techniques, SRS of cloud and aerosol, SRS of trace gases and temperature/moisture profiles. The section “ground-based observation technologies and applications” focuses on researches such as lidar systems and applications, sun/sky radiometer and radiation observations, weather radar and wind profiler, GPS measurements, and some new concept systems.

## 1. Introduction

Modern atmospheric observation, mainly composed of satellite remote sensing and advanced ground-based observation systems, plays a very important role in many research fields such as modern atmospheric science, environment science, global change and so on. In recent years, atmospheric observations have received much attention and great advantage in China. In a paper from Qiu and Chen (2004a), progresses in the atmospheric remote sensing research in China during 1999-2003 were reviewed. The paper paid more attention to atmospheric remote sensing applications. In the present paper, we will review research progresses in the atmospheric observation techniques, observation systems and applications in China mainly since 2003. Our emphasis is not only atmospheric observation applications, but also atmospheric observation technologies and systems. According to different observation platforms, satellite remote sensing, ground-based observation technologies and applications, and airborne/balloon measurements will be reviewed, respectively.

## **2. Satellite remote sensing**

### **2.1 Satellite remote sensing techniques**

There is a great progress in satellite remote sensing technique developments for atmospheric observation applications in China in recent years. The second generation of polar orbit satellite, FY-3 is scheduled to be launched in the next year. The main payloads of FY-3 are Medium Resolution Spectral Imager (MERSI), Infrared Atmospheric Sounder (IRAS), Microwave Temperature Sounder (MWTS), Microwave Humidity Sounder (MWHS), Total Ozone Unit (TOU), Solar Backscattering Ultraviolet Sounder (SBUS), and Earth Radiation Measurement (ERM).

The MERSI instrument has 20 channels with two spatial resolutions, 250 m and 1000 m, respectively for visible and infrared bands. MERSI has similar features to MODIS, of which the channels are good for retrieving Aerosol Optical Thickness (AOT) over ocean as well as over land, atmospheric water vapor, dust monitoring, surface albedo, ocean color, and so on. The IRAS scans from 49.5° negative to the positive value across the track, the spatial resolution is 17 km at nadir. 26 channels in CO<sub>2</sub> absorption 15 μm band, water vapor band, ozone band, and atmospheric window are designed for retrieving atmospheric temperature and humidity profiles. The MWTS scans from 48.3° negative to the same degree but positive, a pixel at nadir stands for about 50 km. While the MWHS scans within 53.35°, with a swath of 2700 km and a resolution of 15 km at nadir. The TOU instrument has 6 channels, ranging from 308 nm to 360 nm, of which 5 channels are sensitive to ozone absorption, and 1 insensitive. The spatial resolution is about 50 km at nadir. The SBUS has 12 channels, ranging from 252 nm to 340 nm, and its spatial resolution is about 200 km. The retrieval algorithms for these four kinds of applications are developing.

### **2.2 Satellite remote sensing of aerosol and cloud**

Satellites remote sensing of aerosol and cloud can provide their optical properties over global coverage; it is thought to be the unique approach to obtain temporal and spatial distribution of aerosols and clouds with high resolution on a global scale. Aerosol and cloud particles can change the intensity of incoming radiation by scattering and absorbing, so we can get their optical properties by measuring the changing of incoming radiation. Aerosol can be served as CCN, and its interaction with sunlight and their effect on cloud microphysics form a major uncertainty in

predicting climate change.

During last 5 years, after the successfully launching of MODIS/Terra and MODIS/Aqua, some Chinese authors have contributed great efforts to remote sensing research of aerosol and cloud from space. The researches are summarized in four aspects: 1) development of aerosol retrieval algorithms, 2) validation of satellite remote sensing of AOT, 3) applications of satellite aerosol products to atmospheric and environmental researches, 4) development of cloud retrieval algorithms and applications.

### **2.2.1 Development of aerosol retrieval algorithms**

After successful launching of MODIS/Terra, several works had been done based on MODIS data. Based on the 6S radiative transfer code, the dense dark vegetation method and contrast reduction method are used to retrieve AOT over land surface from MODIS/Terra data over Beijing and its surrounding area. It is found that the dense dark vegetation method fails to retrieve AOT over urban area because of bright surface and strongly absorbing urban aerosol. By selecting suitable combinations of the two methods, the reasonable retrieval of AOT can be achieved (Li et al., 2003a). Synergy of MODIS/Terra and MODIS/Aqua data are applied to retrieve AOT and surface reflectance simultaneously, this method can be used over many kinds of ground types (Tang et al., 2005). Based on MODIS aerosol operational algorithm, an AOT retrieval method with 1 km resolution is developed, and it is used for obtaining the AOT over Hong Kong. Comparing these products with long-term sunphotometer observations, it is found that the relative error of the products is about 20%, which indicates that this method applied in Hong Kong has precision enough to capture the urban aerosol distribution (Li et al., 2005a)

LANDSAT/TM5 high spatial resolution images are used to discriminate cloud and the shadow since they are projected on the surface from cloud free pixels in the visible band. Over a nontransparent cloud shadow, the radiance obtained from satellite measurement is the contribution of atmospheric path radiance and surface diffuse reflection; while, over a bright area surrounding the cloud shadow, besides the contribution of atmospheric radiance and surface diffuse reflection, the surface direct reflection also contributes to the radiance measured from satellite. Based on this theory, the difference between the two radiances and its relationship with the surface reflectance and AOT are analyzed, and a new method to retrieve surface reflectance and AOT simultaneously over land is developed (Duan et al., 2002).

#### **2.4.2 Validation of satellite remote sensing of AOT**

MODIS AOT-products are compared with ground-based sunphotometer observations. The comparison in Beijing area, presented by Mao et al. (2002), shows the two data fit very well with high correlations. Over East Asian, MODIS aerosol retrievals are evaluated by comparison with AERONET aerosol observations, the preliminary validation results showed a moderate agreement between MODIS and AERONET AOT. Seasonal variation and uncertainties of surface reflection in northern inland of East Asia produce large random errors in MODIS aerosol retrievals. It is particularly important to improve MODIS aerosol retrieval algorithm in these regions (Xia et al. 2004). But new studies show that on a global scale over land, MODIS/AOT retrievals are overestimated except at a few AERONET sites in Africa and eastern Asia. This is likely due to uncertainty of surface reflectance, but issues with the AERONET cloud screening methodology remain open. More research concerning cloud contamination should be done (Xia, 2006a).

#### **2.4.3 Applications of satellite observation to atmospheric and environmental researches.**

Some Chinese authors use the satellite data to analyze aerosol process and properties. Li et al. (2003b) applies MODIS L1B data to retrieve 1km-resolution AOT products and apply the products on studying the aerosol distribution patterns and the air pollution problems over China. Li et al. (2004a) also use MODIS AOT-data and aerosol extinction coefficient profiles from MPL LIDAR to study an aerosol pollution episode in the Pear River Delta on June 18 and 19, 2003. In addition, using TOMS historical aerosol index data, Gao et al. (2004) study the aerosol spatial distribution, its variation trend, and the influence of dust aerosol on solar radiation.

#### **2.2.4 Development of cloud retrieval algorithms and applications**

It is well known that clouds strongly modulate the energy balance of the Earth and its atmosphere through their interaction with solar and terrestrial radiation. Knowledge of cloud properties and their variation in space and time is crucial to study of a global climate change.

In the visible spectral region, cloud reflection function depends mainly on the Cloud Optical Thickness (COT). In the near infrared and middle infrared spectral region, the cloud reflection function depends mainly on cloud particle effective radius. Based on this consideration, an iterative algorithm is developed to retrieve cloud properties from NOAA-AVHRR imagery (Zhao et al., 2002). The algorithm is applied to analyze the radiative properties of stratocumulus over East China Sea. The results indicate that their iterative algorithm has a reasonable accuracy.

Chinese meteorological satellite FY-1C was successfully launched on May 10, 1999. It has ten spectral channels. Some of them, such as channel 1 (0.58~0.68 $\mu\text{m}$ ), channel 4(10.3~11.3 $\mu\text{m}$ ) and channel 6 (1.58~1.64 $\mu\text{m}$ ), can be used for cloud particles phased detection. As shown in the study by Liu et al. (2003a), the 1.6 $\mu\text{m}$  can be used to analyze the thermodynamic phase of cloud particles. The FY-1C data are also used to retrieve COT and effective radius of water clouds. The results show that the reflection function of clouds at a non-absorbing band (such as channel 1) in the visible wavelength region is primarily a function of the cloud optical thickness, while the reflection function at water (or ice) absorbing band (such as channel 6) in the near infrared is primarily a function of cloud particles size. COT and effective particle radius of water clouds can be determined solely from reflection function measurements at channel 1 and channel 6 or from function measurements at channel 1 and brightness temperature at channel 3 of FY-1C/CHPRT data when COT is larger (Liu et al., 2003b).

### **2.3 Satellite remote sensing of gases**

Much attention has been paid to the measurement of trace gases in atmospheric remote sensing because of their significances in climate as well as in environment. SO<sub>2</sub>, NO<sub>x</sub>, O<sub>3</sub> are main air pollutants, and CO<sub>2</sub>, CH<sub>4</sub> are green-house gases for climate.

Satellite-borne DOAS (Differential Optical Absorption Spectroscopy) techniques have been applied in the Institute of Atmospheric Physics. Benefiting the MOST-ESA coordinated Dragon Program, the Chinese scientists work together with the European scientists. The SCIMACHY data on ENVISAT were used to retrieve NO<sub>2</sub> in monitoring the air pollution over the whole China. Some very important features of NO<sub>2</sub> distribution over China were found. The high value of NO<sub>2</sub> over north China, Yangtze delta region was observed.

### **2.4 Satellite remote sensing of temperature/moisture profiles**

Recent interests of some Chinese authors were paid to develop retrieval algorithm for satellite remote sensing of atmospheric temperature/moisture profiles. Wu et al. (2005) presented the physical retrieval algorithm of atmospheric temperature and moisture distribution from the Atmospheric InfraRed Sounder (AIRS). The algorithm applied to AIRS clear-sky radiance measurements. The algorithm employs a statistical retrieval followed by a subsequent nonlinear

physical retrieval. The regression coefficients for the statistical retrieval are derived from a dataset of global radiosonde observations (RAOBs) comprising atmospheric temperature, moisture, and ozone profiles. Evaluation of the retrieved profiles is performed by a comparison with RAOBs from the Atmospheric Radiation Measurement (ARM) Program Cloud And Radiation Testbed (CART) in Oklahoma, USA. Comparisons show that the physically-based AIRS retrievals agree with RAOBs from the ARM CART site with a Root Mean Square error of 1 k on average for temperature profiles above 850 hPa, and approximately 10 % on average for relative humidity profiles.

### **3. Ground-based observation technologies and applications**

#### **3.1 Lidar systems and applications**

Lidar is a powerful means for remote sensing of the atmosphere. Recently, there has been a considerable development in lidar systems and applications in China.

A Differential Absorption Lidar (DIAL) and a transportable Raman-Mie lidar system were recently developed in Anhui Institute of Optics and Fine Mechanics (AIOFM), Chinese Academy of Sciences (CAS). In the DIAL system, the fourth harmonic of Nd:YAG laser was used to pump CH<sub>4</sub> and D<sub>2</sub> gas cell. The system was applied to measure trace gases such as SO<sub>2</sub>, O<sub>3</sub>, NO<sub>2</sub> and so on (Hu et al., 2004a). The DIAL measurements of the trace gases were validated by the chemical analyzers. The Raman-Mie lidar system is used to measure vertical profiles of water vapor mixing ratio by Raman scattering as well as aerosol extinction coefficient by Mie scattering (Xie et al., 2005, 2006). By using the lidar, water vapor mixing ratio is measured over the city of Hefei. In the study, the characteristics and the errors of typical water vapor mixing ratio profiles detected by the lidar are analyzed.

Two Doppler lidar systems for wind field profile measurements are developing in China in recent years. AIOFM has constructed a 1064nm Doppler lidar system for measuring three-dimensional wind profiles in the low troposphere (Sun et al., 2005; Zhong et al., 2006). The system uses a double-edging technique with Fabry-Perot standard. Comparison observations of the lidar wind profile were performed with CINRAD/SA Doppler weather radar, Airda16000

microwave radar and Vaisala balloon. Quite good agreement was obtained between them, and the capability of continuous monitoring the 3-D wind field was proven. It was shown that this Doppler lidar is able to detect the atmosphere up to 9 km at night. Another Doppler Lidar is developing in Institute of Atmospheric Physics, CAS.

A dual-wavelength lidar for detecting upper atmosphere was developed in Wuhan Institute of Physics and Mathematics, CAS (Hu et al., 2004b). The Lidar was applied for detecting the solar activities and disastrous space weather. It is capable of detecting the atmosphere of 30-110 km, including middle and upper atmospheres and the lower ionosphere. It became effective observation equipment for studying middle and upper atmospheres and the sun-earth relationship.

The Mie-Rayleigh-Na lidar system has been developed at the University of Science and Technology of China in Hefei. The lidar system is applied for measuring the vertical profiles of aerosol extinction coefficient by Mie scattering, temperature by Rayleigh scattering and density of Na atom by fluorescence. The reliability of the measured data by the lidar was checked by comparison with nearby lidar of NIES (National Institute for Environmental Study, Japan), good agreement has obtained.

Mie scattering lidars are very useful in detecting the atmospheric aerosol, planet boundary layer structure, and cloud height and thickness. This kind of lidar was widely used in China to monitor the transport behavior of dust during the dust storm event, aerosol extinction coefficient profiles, regional air pollutant transport and so on (Yuan et al., 2005; Zhou et al., 2002; Zhou et al., 2006; Hu et al., 2004a). In addition, AIOFM has actively jointed national and international projects on lidar monitoring of the atmosphere. These projects include AD-Net (Asian Dust lidar observation NETWORK), ADEC (Aeolian Dust Experiment on Climate impact), SKYNET, ABC (Atmospheric Brown Cloud), and GALION (GAW Aerosol Lidar Observation Network).

### **3.2 Sun/sky radiometer and radiation measurements**

Much attention has been paid to the connection between the greenhouse effect brought on by human activities and global climate change. Human activities also result in the emission of large

amounts of aerosols, which can significantly influence global climate. The global annually averaged direct radiative forcing at the top of the atmosphere by aerosols is estimated to be in the range of  $-0.5$  to  $0.2 \text{ Wm}^{-2}$ . Because of the relatively short lifetime of aerosol particles and their large regional variability, instances of strong localized direct forcing can occur. On a regional scale, it is suggested that aerosols are already affecting surface forcing, atmospheric heating, and precipitation. The importance role of aerosol played in the climate and environment system is widely recognized. However, large uncertainties in the chemical, physical, and optical properties of atmospheric aerosols render the quantitative assessment of aerosol effects on climate and environment problematic. It should be noted that long-term continuous observations of aerosol properties are still very limited, so we should maintain the existing observations and make an effort to augment aerosol observations across China. A combination of ground-based and satellite remote sensing and the integration and assimilation of all aerosol data available into models is a feasible way to reduce the uncertainties in the effects of aerosols on environment and climate.

Sunphotometer is a classical yet reliable means to measure aerosol optical properties, including its AOT. In recent years, three main Sunphotometer or sun/sky radiometer networks have been established in China and played an important role in measuring aerosol optical properties. One is CSHNET (Chinese Sun Hazemeter Network), using hand-held sunphotometers to measure AOT (Xin et al., 2006). Using these measurements, the spatial and temporal distributions of AOT were derived and the MODIS AOTs were assessed (Wang L.L. et al., 2006). CSHNET is a part of Chinese Ecological Research Network (CERN). Along with sunphotometers, a set of broadband solar radiometers is installed in CERN stations. The spatial-temporal variations of solar radiation were discussed by Hu et al. (2006). Another is four Chinese sites of AERONET (Aerosol Robotic Network), i.e. Beijing, Xianghe, Taihu and Xinglong. AERONET (Holben et al., 1998) is a worldwide aerosol monitoring network, initiated in 1990s and expanded rapidly to more than 200 sites across the world. In the Chinese sites, the CIMEL sun/sky radiometers measure direct spectral solar radiation with a  $1.2^\circ$  fully-viewing field at 440, 675, 870, 940, and 1020 nm (nominal wavelength) every 15 minutes. These solar extinction measurements are used to derive AOT except for the forth, which is used to retrieve column water vapor amount. The AOT-accuracy was estimated to be 0.01~0.02. The radiometer also performs sky radiance scans at 440, 675, 870, and 1020 nm (nominal wavelengths) at optical

air masses of 4, 3, and 2 in the morning and afternoon, and once per hour in between. Aerosol microphysical properties including size distribution and refractive index are retrieved at solar zenith angles greater than 45 degrees. Aerosol optical quantities such as phase function, asymmetry factor and single scattering albedo are computed from the retrieved microphysical properties. The third is CE-318 Sunphotometer Network, set up by China Meteorological Administration since 2002. Using the CE-318 sunphotometer data, dust aerosol optical properties in south Tarim Basin were studied (Li et al., 2005b), and the AOT over urban area in Urumqi and Beijing were retrieved (Li et al., 2005c, Zhang et al., 2002). In addition, in order to monitor dust events, a national network and several intense regional networks have been established in recent years. Main equipments in these dust monitoring networks include Cimel sun/sky radiometers. The dust storm monitoring and forecasting centers use also satellite remote sensing data and provide numerical model prediction services (Liu et al., 2004; Wang et al., 2005a).

On the basis of aerosol optical property data from the above three aerosol networks as well as other satellite and ground-based measurements, aerosol optical properties in China were actively instigated recently. Rapid economic growth and population expansion over the last twenty years has led to a significant increase in AOT over much of China. The average AOT at 750 nm observed at 46 stations in China increased from 0.38 in 1960 to 0.47 in 1990 (Luo et al., 2001). High aerosol loading over much of China was evident from satellite and ground-based measurements (Li et al., 2003c; Xia et al., 2005; Zhang et al., 2002). An extremely wide range of aerosol loading, size and absorption were derived from multiyear ground-based network observations in Beijing (Xia et al., 2006b; Fan et al., 2006). The increase in aerosol loading partly accounted for a notable decrease of sunshine duration and downward surface solar irradiance (Che et al., 2005a; Liang et al., 2005; Xia et al., 2006c).

Heavy aerosol loading and notable temporal and spatial variation over Beijing and Xianghe sites in spring were revealed by AERONET data in spring 2001. Aerosol loading and size between Beijing and Xianghe, an urban and suburban site in North China, were highly correlated, illustrating a clear picture of regional air pollution (Xia et al., 2005). The climatologic aspects of aerosol optical properties in Beijing were studied using AERONET data from 2001 to 2004 (Xia et al., 2006b). The AOT increased from January gradually to June, and then decreased gradually to December. However, the surface  $PM_{10}$  concentration showed quite different seasonal variation,

with higher  $PM_{10}$  in spring and winter and relatively lower values in summer and autumn. The seasonal variations of pollution boundary layer height and relative humidity might be responsible for this inconsistency. Aerosol Single Scattering Albedo (SSA) in Beijing was about 0.90 at 440 nm and decreased slightly in the near infrared wavelength. SSA increased notably and the spectral dependence reversed if Beijing was impacted by dust weather. Aerosol absorption in Beijing was close to AERONET data in urban regions such as in Mexico City and Kanpur. By using AERONET data, Che et al. (2004, 2005b) studied the aerosol optical characteristics in Mu Us desert and also compared the aerosol optical and physical characteristics under two different weather conditions of dust storm and haze.

In September 2004, scientists from China and United States cooperated to establish a comprehensive radiation site in Xianghe. A set of state-of-the-art broadband pyranometers was installed side-by-side with a CIMEL sun-photometer (see Fig.1). The first objective is to establish a test-bed for validation of satellite estimates of aerosol, cloud and energy budget in North China. Secondly, the effects of aerosols on energy budget at the surface and at the top of the atmosphere will be explored based on long-term ground-based and satellite observations. Xianghe site became one new Baseline Surface Radiation Network (BSRN) station officially by having its data accepted by the BSRN archive in 2005. BSRN is a project of the World Climate Research Programme (WCRP) and the Global Energy and Water Experiment (GEWEX) and as such is aimed detecting important changes in the earth's radiation field at the earth's surface and supporting the validation and confirmation of satellite and computer model estimates of these quantities. It is important to point out that Xianghe is the only one BSRN station in vast Asia Continent.



Fig.1. The picture of Xianghe radiation site, located at the top of a four-floor building.

Using fifteen months of ground-based broadband and spectral radiation data in Xianghe, aerosol loading and effects on surface solar radiation were analyzed. The mean 500nm AOT is 0.66, and standard AOT-deviation is up to 0.67, implying a large day-to-day variation. Approximate 23% of AOT data exceeded 1.0 in spring and winter, and 34% was larger than 1.0 in summer and autumn. About 37% of AOT data were less than 0.15 in winter, but the frequency was only 10% in spring and summer. The aerosol extinction was primarily contributed by fine particles with radii less than 0.6 except a few cases of dust events. Aerosols seriously impacted the downward solar radiation. The collocated aerosol and surface solar radiation data were utilized to estimate quantitatively aerosol effects on total shortwave radiation (TSW) and Photosynthetically Active Radiation (PAR), which was supported by radiative transfer model simulations. The monthly aerosol direct radiative forcing (ADRF) for TSW at the surface varied from  $-13 \text{ W m}^{-2}$  in January to  $-45 \text{ W m}^{-2}$  in June and then to  $-15 \text{ W m}^{-2}$  in December, which was about 1.73 times ADRF for PAR (see Figure 2). The normalized ADRF, i.e., the ratio of ADRF to AOT at 500 nm, ranged from  $-40 \text{ W m}^{-2}$  in winter to  $-72 \text{ W m}^{-2}$  in June. The estimates from observations were in good agreement with radiative transfer model simulations.

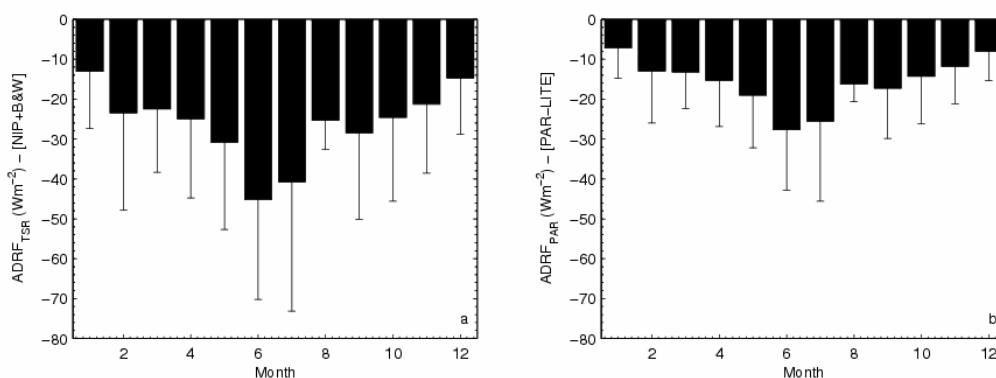


Fig.2. Monthly diurnal mean aerosol direct radiative forcing at the surface (ADRF) for TSW (a) and PAR (b), respectively. The results were derived from a parameterization equation.

In the spring of 2005, a sunphotometer and a set of broadband pyranometers were installed in Liaozhong, a suburban region in northeastern China (Xia et al., 2006d). Aerosol properties derived from sunphotometer measurements and aerosol-induced changes in downwelling shortwave surface irradiances were explored based on four-month data. The result showed that the mean aerosol optical depth (AOT) at 500 nm was 0.63. The day-to-day variation of aerosol optical depth

was dramatic, with a maximum daily AOT close to 2.0 and a minimum value close to the background level. Dust activities generally produced heavy aerosol loading characterized by larger particle sizes and less absorption than those observed under normal conditions. The reduction of instantaneous direct shortwave surface irradiance per unit of AOT was  $404.5 \text{ Wm}^{-2}$ . About 63.8% of this reduction was offset by an increase in diffuse irradiance, consequently, one unit increase in AOT led to a decrease in global surface irradiance of  $146.3 \text{ Wm}^{-2}$ . The diurnal aerosol direct radiative forcing efficiency was about  $-47.4 \text{ Wm}^{-2}$ . Overall, aerosols reduced about  $30 \text{ Wm}^{-2}$  of surface net shortwave irradiance in this suburban region.

An unprecedented change has taken place due to rapid economic development and population growth in China in recent twenty years. One of byproducts was that aerosol properties had changed significantly along with this change. This provided a unique natural laboratory for studying aerosols. It should be noted that long-term continuous observations of aerosol properties are still very limited, so we should maintain the existing observations and make an effort to augment aerosol observations across China. A combination of ground-based and satellite remote sensing and the integration and assimilation of all aerosol data available into models is a feasible way to reduce the uncertainties in the effects of aerosols on climate and environment.

Trends in Chinese global radiation, direct horizontal radiation, diffuse radiation, clearness index, diffuse fraction and percentage of possible sunshine duration for the period 1961–2000 were evaluated based on data for daily surface solar radiation and monthly sunshine duration. Annual means for all six variables were calculated for each station and for China as a whole. Linear regression analysis was used to characterize long-term annual trends in these variables. Over the latter half of the 20th century, there have been significant decreases in global radiation ( $-4.5 \text{ W/m}^2$  per decade), direct radiation ( $-6.6 \text{ W/m}^2$  per decade), clearness index ( $-1.1\%$  per decade), and the percentage of possible sunshine duration ( $-1.28\%$  per decade), but diffuse fraction has increased ( $1.73\%$  per decade). Although there is some evidence that conditions have improved in the last decade, the consistent spatial and temporal variations of these variables support the theory that increased aerosol loadings were at least partially responsible for the observed decreases in global radiation and direct radiation, the clearness index, and the monthly percentage of possible sunshine duration over much of China.

### 3.3 Pyrheliometer/paranometer measurements of aerosol and cloud optical properties

There is a denser worldwide network using relatively inexpensive but reliable pyrheliometer and pyranometer instruments for broadband solar radiation measurements from the surface. In China, pyrheliometer and pyranometer measurements started in the 1950s, and now there are more 90 (40) meteorological observatories performing routine pyranometer (pyrheliometer) measurements. Available yet quantitative methods to derive aerosol and cloud optical properties from these broadband radiation data should be very significant and useful. Impelled by this application, some Chinese authors have contributed their considerable effort to develop the methods.

Based on Broadband Diffuse Solar Radiation method (BDRM) for Aerosol Imaginary Part (AIP) retrieval, presented by Wei and Qiu (1998), an improved BRDM for the AIP and  $1\mu\text{m}$ -wavelength SSA retrievals is proposed by Qiu et al. (2004b). The first improvement is to determine diffuse radiation from combined pyrheliometer and pyranometer data. Secondly, available approaches to input parameters demanded for AIP retrievals are presented, including the approach to determine aerosol extinction coefficient profile from visibility and aerosol optical depth data. This method is used in retrieving AIP and SSA from routine pyrheliometer and pyranometer observation data measured in 1993-2001 over 6 meteorological observatories in northern China. As shown in the retrieval results, 9-year-mean yearly-mean AIP during 1993-2001 changes 0.0207 to 0.0301 for the 6 cities, and the corresponding SSA from 0.851 to 0.803 with a mean value of 0.832. This BDRM is available to retrieve  $1\mu\text{m}$ -wavelength SSA. Generally, SSA is closely wavelength-dependent. In order to take account into the dependence, Qiu (2006a) developed a new BDRM to retrieve radiation-weighted-mean SSA. As shown in retrieval simulations, if the error of Ångström index is within  $\pm 0.2$ , the errors of the SSA retrievals are within  $\pm 0.0227$  and  $\pm 0.0345$  for continent and urban-industrial aerosols, respectively. The larger aerosol optical thickness is, the larger the error of the SSA solution caused by the error of radiation data. Under the condition of  $0.55\mu\text{m}$ -wavelength aerosol optical thickness being larger than 0.312, the errors of SSA solutions are within  $\pm 0.0149$  and  $\pm 0.0317$  if radiation data errors are within  $\pm 2\%$  and  $\pm 4\%$ , respectively.

Using Broadband Extinction Method (BEM) for AOT retrieval (Qiu, 2001), Zong et al. (2005a) compared AOT from BEM with AOT from AERONET in Beijing site. Comparative results show that both AOT-data are in good agreement in clear (no cloud) days. Furthermore, they developed a

method to weaken cloud effect on the monthly-average AOT-estimation. The method feasibility is tested through a comparison of the BEM AOT with AERONET AOT. Based on AOT data from BEM, Zong et al. (2005b) also analyzed variation characteristics of monthly/seasonally/ yearly mean AOT in sixteen sites during 1993~2002. It is concluded that AOT has an increasing trend over Shenyang and Zhengzhou but a decreasing trend over Harbin, Lanzhou, Guangzhou, and Beijing.

Qiu et al. (2005) developed a method to determine a so-called scaling height of the tropospheric aerosol and the exponent-type aerosol extinction coefficient profile from the pyrheliometer or sunphotometer measurements and surface visibility data. Using this method, characteristics of seasonally/yearly mean scaling heights and aerosol extinction profiles over 11 sites in China during 1994-2001 are analyzed. The yearly-mean scaling heights over the 11 sites change between 1.30km and 2.67km, and they are very variable for different seasons, being usually larger in spring. As far as the yearly-mean scaling heights of all 11 sites are concerned, they change between 1.88km and 2.11km during 1994-2001, having an increasing trend.

In addition, Qiu (2006b) developed a method to retrieve COT from global solar radiation detected by ground-based pyranometer. Based on numerical simulations and comparative tests, main error factors of COT retrievals are analyzed. COTs ( $\tau_{\text{pyr}}$ ) from pyranometer data at two meteorological observatories are compared with COTs ( $\tau_{\text{ISCCP}}$ ) from ISCCP and COTs ( $\tau_{\text{MODIS}}$ ) from MODIS. The relative standard deviations between monthly-mean  $\tau_{\text{pyr}}$  and  $\tau_{\text{MODIS}}$ , or  $\tau_{\text{pyr}}$  and  $\tau_{\text{ISCCP}}$ , are all less than 45.4% for both sites. The agreement among the yearly-mean  $\tau_{\text{pyr}}$ ,  $\tau_{\text{MODIS}}$  and  $\tau_{\text{ISCCP}}$  is satisfactory. The absolute (relative) deviations between the yearly-mean  $\tau_{\text{pyr}}$  and  $\tau_{\text{MODIS}}$  are within  $\pm 1.55$  (8%) for both sites, and the deviations between the  $\tau_{\text{pyr}}$  and  $\tau_{\text{ISCCP}}$  are within  $\pm 1.94$  (25%).

### 3.4 Weather radar and wind profiler

The China Meteorology Administration (CMA) has planned to deploy 158 sets of new generation Doppler weather radar (CINRAD) over the main continent. Over last 4 years, more than half of them have been set up mainly in Southern China where heavy rainfall and typhoon events frequently occur. The national and regional mosaics of radar product images are now available on the web sites of national and regional meteorological centers.

To improve the capability of precipitation estimation and hailstorm detection, several X-band and C-band dual-polarization radars have been developed in the Institute of Atmospheric Physics (IAP) and Institute of Cold and Arid Regions Environmental and Engineering Research in collaboration with radar manufacture units. A theoretical study of estimations of rain and hail rates in mixed-phase areas with dual-polarization radar was carried out by Liu (2002). The results show that the reflectivity of hail measured by a C-band dual-polarization radar decreases with hail rate when hail rate is very large.  $K_{DP}$  in hailstorm is related with the shape, orientation, size of hails. In the mixture of rain and hail, major contribution of  $Z_H$  is from hail; raindrops are main factor to affect  $K_{DP}$ ; both rain and hail have contributions to  $Z_{DR}$ ; and  $Z_H$  and  $K_{DP}$  in rain have good correlation. Then, a simple method is proposed to estimate hail and rain rates in mixed phase area with  $Z_H$ ,  $Z_{DR}$ , and  $K_{DP}$  with error analysis.

For the purpose of obtaining the information of 3-D wind field, the X-band bistatic Doppler weather radar system is being developed by Nanjing Research Institute of Electronics Technology in collaboration with the IAP (Li, 2005d). Based on the specifications and functions of X-band radar, slotted wave-guide antenna and GPS timer are used to solve the synchronization problems of space, phase, and time. The system is characterized by the simple structure, cheapness, reliability, and high sensitivity.

In addition, the design of the phase array Doppler weather radar is also under way to improve the time resolution of radar observation.

The wind profiler is a powerful tool to profile the vertical wind structure in the troposphere. In recent years, a number of wind profilers both home- and overseas-made have been deployed in many big cities and used in some field experiments. For example, Wang X. et al. (2005b) conducted a comparison study between the radiosonde and the wind profiler measurements during the 973 heavy rain field campaign in the summer 2002 in Anhui Province. The wind profiler WPR 1300 was used. Results show that the vertical structure of wind can be well detected by the wind profiler during the meso-scale precipitation.

### **3.5 GPS measurements of ozone profile and water vapor**

The ozonesonde system, an effective technique for direct measurement of vertical ozone structure in the atmosphere, has been developed (Wang et al., 2003). This system is one

combination of single cell ozone sensor with GPS sonde. Before its application for routine operation, the performance of the system was tested in laboratory and compared with that commonly used in the world ozone monitoring network. The main technical specifications, components, and the performance test results can be found in Wang et al. 's (2003, 2004a), and Xuan et al.'s(2004).

At present, ground-based GPS meteorology focuses on such three main targets as: 1) the measurement of precipitable water vapor at the zenith direction; 2) the remote sensing of slant-path water vapor; 3) the retrieval of water vapor three-dimensional structures in the local region (water vapor tomography). In this research aspect, Bi et al. (2006) developed a GPS approach to measure 4-D Water Vapor Tomography in the Troposphere, and Li et al. (2004b) presented the concepts of hydrostatic delay and wet delay in remote sensing water vapor with ground based GPS receivers. In the Bi et al.'s approach, a tomographic method was utilized to retrieve the local horizontal and vertical structure of water vapor over a local GPS receiver network using SWV amounts as observables in the tomography. The method of obtaining SWV using ground-based GPS is described first, and then the theory of tomography using GPS is presented. A water vapor tomography experiment was made using a small GPS network in the Beijing region. The tomographic results were analyzed in two ways: (1) a pure GPS method, i.e., only using GPS observables as input to the tomography; (2) combining GPS observables with vertical constraints or a priori information, which come from average radiosonde measurements over three days. It is shown that the vertical structure of water vapor is well resolved with a priori information. Comparisons of profiles between radiosondes and GPS show that the RMS error of the tomography is about 1-2 mm. It is demonstrated that the tomography can monitor the evolution of tropospheric water vapor in space and time. The vertical resolution of the tomography is tested with layer thicknesses of 600 m, 800 m and 1000 m. Comparisons with radiosondes show that the result from a resolution of 800 m is slightly better than results from the other two resolutions in the experiment. Water vapor amounts recreated from the tomography field agree well with precipitable water vapor (PWV) calculated using GPS delays. Hourly tomographic results are also shown using the resolution of 800 m. Water vapor characteristics under the background of heavy rainfall development are analyzed using these tomographic results. The water vapor spatio-temporal structures derived from the GPS network show a great potential in the

investigation of weather disasters.

As shown in the study by Li and Mao (2004), the concepts of hydrostatic delay and wet delay in remote sensing water vapor using ground based GPS receivers are reviewed. The common formula of calculating precipitable water from GPS troposphere delay is inferred based on the refractive index and air state equation expressions.

### **3.5 UAV sounding system**

Ma et al.(2004) present a miniature robotic plane meteorological sounding system (RPMSS), which consists of three major subsystems: a miniature robotic plane, an air-borne meteorological sounding and flight control system, and a ground-based system. Taking-off and landing of miniature aircraft are guided by radio control and the flight of robotic plane along a pre-designed trajectory is automatically piloted by an onboard navigation system. The observed meteorological data as well as all flight information are sent back in real time to the ground, then displayed and recorded on the ground-based computer. Ground-based subsystem can also emit some instruction signals to the air-borne control subsystem. Good system performance has been demonstrated by more than 300 hours flight for atmospheric sounding.

The miniature robot aircraft (MRA) has innovatively been used for weather modification, i.e., precipitation enhancement (Ma et al., 2006). The system is composed of three parts: the miniature aircraft, the mission loading (the airborne seeding device and meteorological measurement device), and the ground monitor control sub-system. Before each launch, flight path is designed and transferred to the airborne control system. After reaching the altitude operation and receiving the instruction from the remote control terminal, the cloud seeding is conducted. During the flight course, the meteorological parameters are measured and transferred in real-time to the ground. Through a number of flight tests, the performance of MRA for weather modification and its capability for meteorological observation have been proved. The MRA can fly up to 6000m of altitude carrying the seeding materials of 1kg (silver iodide), and its operation radius can reach 25 km. The operation can be done under the severe weathers.

The Vaisala RS92 radiosonde was introduced by Ma et al.(2005). RS92 adopts the digital technology with greatly improved sounding precision and anti-jamming capability in information transmission. The bandwidth of its transmitter is only one tenth of RS80's. By using GPS frequency-extending technology, RS92 wind data acquirement is greatly enhanced. The sensors of

temperature, pressure, and humidity as well as their calibration techniques are also significantly improved. The CMA is planning to use the RS92 radiosondes in some climate monitoring observatories.

In parallel, the GPS-based radiosonde system has been successfully developed in China (Wang et al., 2004b). The request and design of the software system for new generation radiosonde are described by Yao et al.(2004).

A new pattern of digital atmospheric turbulence detector designed with the adoption of the dipole sensor device is presented by Luo et al.(2004). The analog and digital filters are also optimized. The MA (Moving Average) and the incremental processing algorithms are provided to give a solution to the problem of the high frequency and gusty interference. Both the simulation and experimental results show that the performance of the new pattern is much better than the traditional systems, in sensitivity, data reliability, and noise level.

### **3.7 Other systems of atmospheric observations and applications**

Several innovative instruments have been developed in the Laboratory for middle Atmosphere and Global Environment Observations (LAGEO) of the IAP, including the trail-tracked advice for multi-target albedo observation, the scanning infrared thermometer for simultaneously measuring sky and surface IR brightness temperatures, and a high resolution whole sky imager based on a up-looking fish-eye camera (Huo et al., 2005).

In order to fill in the data gaps between upper air sounding and the surface meteorological and environmental observation stations, Chen and Zheng (2005) suggested that it is necessary and feasible, along with the advance of transport platform and communication technology, to build up a 3-D dimension mobile system for monitoring the global atmosphere and its environment by using commercial transport platforms such as aircraft, ship, train, and autobus. Some perspectives for atmospheric sounding can be founding in Zhang et al's(2003).

To automatically analyze on-line the concentrations of water-soluble ions in ambient particles, a system of rapid collection of fine particles and ion chromatography (RCFP-IC) was developed by combining the system of rapid collection of ambient particles and ion chromatography (Wen et al., 2006). The detection limit of RCFP-IC for  $\text{SO}_2$ ,  $\text{NO}_2$ ,  $\text{NO}$ ,  $\text{Cl}^-$  and  $\text{F}^-$  is below  $0.3 \mu\text{g m}^{-3}$ . The collection efficiency of RCFP-IC increases rapidly with increasing sized particles. For particles larger than 300 nm, the collection efficiency approaches 100%. The precision of

RCFP-IC is more than 90% over 28 repetitions. The response of RCFP-IC is very sensitive and no obvious cross-pollution is found during measurement. A comparison of RCFP-IC with an integrated filter measurement indicates that the measurement of RCFP-IC is comparable in both laboratory experiments and field observations. The results of the field experiment prove that RCFP-IC is an effective on-line monitoring system and is helpful in source apportionment and pollution episode monitoring.

A study by Si et al. (2006) has shown that the continuous operation of the DOAS system has the capability of profiling atmospheric aerosols. The correlation study using diurnal datasets shows that, on the average, the MEE values vary over a range of 2.6–13.7  $\text{m}^2 \text{g}^{-1}$ . On the basis of the simulation study, it is likely that high MEE values indicate the dominance of fine particles, while low MEE values suggest the dominance of coarse particles. It is also obvious that MEE changes with the RH. These findings are supported by both the Angstrom coefficient and the one month variation of the RH.

The aircraft observations of the size distributions of particles (0.47-3 $\mu\text{m}$ , 57 channels, including number concentration distribution, surface area concentration distribution and mass concentration distribution) were carried out by Wang et al. (2005c) at an altitude of 2000 m over eastern coastal areas of China from Zhuhai, Guangdong to Dalian, Liaoning. The TSI APS-3310A Aerodynamic Particle Sizer were used on aircraft to sample particle size distributions. It consists of the Model 3310A Aerodynamic Particle Sizer Spectrometer (APS) and data analysis system. It uses 57 channels to analyze particles with diameters in the range 0.43-3  $\mu\text{m}$  and gives number size distribution automatically. Air was introduced into the instrument through a Teflon tube and stainless steel tube at a rate of 5  $\text{Lmin}^{-1}$ . The inside of the tube was treated with glycerin in order to reduce the static charge and to further reduce the loss of particles. The measurements show that the average daily concentrations of  $\text{PM}_{10}$  are very high in the cities along the flight leg. These cities are among the most heavily polluted cities in China. The main pollution sources are anthropogenic activities such as wood, coal and oil burning. The observed size distributions show a broad spectrum and unique multi-peak characteristics, indicating no significant impacts of individual sources from urban areas.

Ozone vertical profiles are retrieved from the Dobson Umkehr observations of Beijing from 1990 to 2002 (Yang et al., 2006). Using the derived profiles combined with the total ozone data

measured by the Dobson spectrophotometer, the characteristics and variations of the ozone vertical distributions of Beijing during 1990-2002 are studied. The results show that in the fall of 1992 and the spring of 1993, the seasonal average ozone concentrations in layers 2-4, corresponding to heights of 10.3-23.5km, were unusually lower than normal, and at the same time, the total ozone underwent a marked decline; During the period 1990-2002, the monthly mean total ozone decreased slightly, but the trends of change of ozone concentrations at different altitudes were different.

## **4 Airborne/balloon measurements**

### **4.1 Airborne microwave radiometer**

An airborne up-looking microwave radiometer for measuring column supercooled cloud liquid water path was developed by Lei et al. (2003). The tests of the instrument both in laboratory and on the airplane suggest that under certain conditions the instrument sensibility can be better than or equal to 0.2 K. The calibration methods are also introduced and the measurement uncertainties are discussed in their paper. And the retrieval method is described in Jiang et al.'s (2004).

### **4.2 Tethered balloon**

The tethered balloon sounding system has great applications for meteorological and environmental observations in the boundary layer. A home-made one named XLS-II is introduced by Wang et al. (2004). The technical specifications of the main components are given as follows: the winch weight of 36 kg, the motor power of 600 W, the maximum pulling force of 175 kg, and a cord of 1500 m. The payload can be the meteorological sensors, ozone sensor, aerosol sampler, optical particle counter and so on.

**Acknowledgments.** This research work was supported by National Natural Science Foundation of China (Grant No. 40333029).

## **References**

- Bi Yangmeng, Mao Jietai, and Li Chengcai, 2006: Preliminary Results of 4-D Water Vapor Tomography in the Troposphere Using GPS. *Advan. Atmos. Sci.*, **23**, 551-560.
- Chen Hongbin, and G.G. Zheng, 2005: Mobile systems for monitoring the atmosphere and its environments based

- on commercial transport platforms. *Adv. in Earth Sci.*, **20**(5), 520-524.
- Che, H. Z., G. Y. Shi, X. Y. Zhang, R. Arimoto, J. Q. Zhao, L. Xu, B. Wang, and Z. H. Chen, 2005a: Analysis of 40 years of solar radiation data from China, 1961–2000. *Geophysical Research Letters*, **32**, L06803, doi: 10.1029/2004GL022322.
- Che Huizheng, Zhang Xiaoye, Shi Guangyu, Li Yang, Zhao Jianqi, Qu Wenjun, and Wang Dan, 2005b: Aerosol optical characteristics in Mu Us desert under weather conditions of dust storm and haze. *China Powder Science and Technology*, **11**(3), 4-7 (in Chinese).
- Che Huizheng, Zhang Xiaoye, Shi Guangyu, Li Yang, and B. Chatenet, 2004: Elementary researches on aerosol optical characteristics in the Mu Us desert. *The Chinese Journal of Process Engineering*, **4**(3), 772-776. (in Chinese)
- Duan Minzheng, Lu Daren, Cui Kejian, and Hao Wenqiang, 2002: Retrieval of Surface Reflectance and Aerosol Optical Thickness Simultaneously from Space Measurement over land: Basic Theory and Simulation. *Journal of Remote Sensing*, **6**(5), 321~327.
- Fan X. H., H. B. Chen, P. Goloub, X.A. Xia, W.X. Zhang, and B. Chatenet, 2006: Analysis of Column-Integrated Aerosol Optical Thickness in Beijing from AERONET Observations. *Particology*, in press.
- Gao Qingxian, Ren Zhenghai, Li Zhanqing, and Pubu Ciren, 2004: Spatial and Temporal Distribution of Dust Aerosol and Its Impacts on Radiation Based on Analysis of EP/TOMS Satellite Data. *Resources Sci.*, **26** (5): 2~10.
- Holben, B.N., T.F. Eck, I. Slutsker, D. Tanre, J.P. Buis, , A. Setzer, E. Vermote, J.A. Reagan, Y. Kaufman, T. Nakajima, F. Lavenue, I. Jankowiak, and Smirnov, A , 1998: AERONET - A federated instrument network and data archive for aerosol characterization. *Rem. Sens. Environ.*, **66**, 1-16.
- Hu Bo, Wang Yuesi, and Liu Guangren, 2006: The spatio-temporal characteristics of Photosynthetically Active Radiation in China. *J. Geophys. Res.*, revised.
- Hu Huanling, Wu Yonghua, Xie Chenbo, Yan Fengqi, Weng Ningquan, Fan Aiyuan, Xu Chidong, Ji Yufeng, Yu Tong, Ren Zhenhai, 2004a: Aerosol pollutant boundary layer measured by lidar at Beijing, *Research of Environmental Sciences*, **17**, 59-66(Chinese).
- Hu Shunxing, Hu Huanling, Zhang Yinzhao, et al., 2004b: Differential absorption lidar for environmental SO<sub>2</sub> measurements. *Chinese Laser*, **31**, 1121-1126.
- Huo, J., and D. R. Lu, 2005: Analysis of cloud's distribution in Beijing with all-sky images. *Scientia Meteorologica Sinica*, **25**(3), 239-243.
- Jiang, F., C. Wei, H.C. Lei, D.Z. Ji, J.H. Zhang, and, S.F. Gu, 2004: Measurement of column cloud liquid water

- content by airborne upward-looking microwave radiometer I: retrieval method. *Plateau Meteorology*, **23**(1), 34-39.
- Lei, H.C., C. Wei, Z.L. Sheng, X.Q. Zhang, D.Z. Jin, S.F. Gu, M.L. Li, and J.H. Zhang, 2003: Measurement of column cloud liquid water content by airborne upward-looking microwave radiometer I: instrument and its calibration. *Plateau Meteorology*, **22**(6), 551-557.
- Li Xiaojing, Liu Yujie, Qiu Hong, and Zhang Yuxiang, 2003a: Retrieval Method for Optical Thickness of Aerosols over Beijing and Its Vicinity by Using the MODIS Data. *ACTA Meteorological Sinica*, **61**(5), 580~591.
- Li Chengcai, Mao Jietai, Liu Qihan, 2003b: Remote Sensing Aerosol with MODIS and the Application of MODIS Aerosol Products. *Acta Scientiarum Naturalium Universitatis Pekinensis*, **39**(supplement), 108~117.
- Li Chengcai, Mao Jietai, Liu Qihan, Chen Jiezhong, Yuan Zibin, Liu Xiaoyang, Zhu Aihua, and Liu Guiqing, 2003c: Characteristics of distribution and seasonal variation of aerosol optical depth in eastern China with MODIS products. *Chinese Sci. Bull.*, **48**, 2488-2495.
- Li Chengcai, Mao Jietai, and Alexis Kai-Hon Lau, 2005a: Remote Sensing of High Spatial Resolution Aerosol Optical Depth with MODIS Data over Hong Kong. *Chinese Journal of Atmospheric Sciences*, **29**(3), 335-342.
- Li Chengcai, Liu Qihan Mao Jietai, Chen Aizhong, 2004a: An Aerosol Pollution Episode in Hong Kong with Remote Sensing Products of MODIS and Lidar. *Journal of Applied Meteorological Science*. 2004, **15** (6): 641~651
- Li Chengcai, and Mao Jietai, 2004b: The concepts of hydrostatic delay and wet delay in remote sensing water vapor with ground based GPS receivers. *Chinese J. Atmos. Sci.* **28**, 795-800.
- Li Xia, Hu Xiuqing, Cui Caixia, and Li Juan, 2005b: Research on dust aerosol optical properties in south Tarim Basin and classification of different dusty weather in China. *Journal of Desert Research*, **25**(4), 488-495. (in Chinese)
- Li Xia, Chen Yonghang, Hu Xiuqing, Ren Yiyong, and Wei Wenshou, 2005c: Analysis of atmospheric aerosol optical properties over Urumqi. *China Environmental Science*, **25**(Suppl.), 22~25. (in Chinese)
- Li, C., 2005d: Design of X-band bistatic Doppler weather radar system. *Modern Radar*, **27**(2), 11-14.
- Liang F., and X. Xia, 2005: Long-term trends in solar radiation and the associated climatic factors over China for 1961-2000, *Annales Geophys.*, 23,2425-2432
- Liu Jian, Dong Chaohua Zhu Yuanjing, Zhu Xiaoxiang, and Zhang Wenjian, 2003a: Thermodynamic Phase Analysis of Cloud Particles with FY-1C Data, *Chinese Journal of Atmospheric Sciences*, **27**(5), 901~908.
- Liu Jian, Dong Chaohua, and Zhang Wenjian, 2003b: Determination of the Optical Thickness and Effective Radius

- of Water Clouds by FY-1C Data. *J. Infrared Millim. Waves*, **22**(6), 436~440.
- Liu, L.P., 2002: A theoretical study of estimations of rain and hail rates in mixed-phase areas with dual-polarization radar. *Chinese J. Atmos. Sci.*, **26**(6), 761-772.
- Liu, W.D., C.L. Cheng, M.Y. Zhang, X.L. Zhang, and Y.C. Wang, 2004: Sand-dust weather monitoring, forecasting, and pre-warning system in Beijing. *Meteorol. Sci. and Tech.*, **32**(z1), 50-53.
- Luo, H., Y. Li, S.D. Du, and D.T. Gao, 2004: A new pattern of digital atmospheric turbulence detector and its data reliability. *Transportation and Computer*, **22**(4), 44-47.
- Luo, Y. F., D.R., Lu, X.J. Zhou, W.L. Li, and Q. He, 2001: Characteristics of the spatial distribution and yearly variation of aerosol optical depth over China in last 30 years. *J. Geophys. Res.*, **106**, D13, 14501-14513.
- Mao Jietai, Li Chengcai, Zhang Junhua, Liu Xiaoyang, and Liu Qihan, 2002: The Comparison of Remote Sensing Aerosol Optical Depth from MODIS Data and Ground Sun-photometer Observations. *Journal of Applied Meteorological Science*, **13**, 127~135.
- Ma Shuqing, Chen Hongbin, Wang Gai, Pan Yi, and Li Qiang, 2004: A miniature robotic plane meteorological sounding system. *Adv. Atmos. Sci.*, **21**(6), 890~896.
- Ma, S. Q., Z.Q. Zhao, and Y. Xing, 2005: Vaisala Radiosonde technology and advance in radiosonde technology in China. *Meteorol. Sci. & Tech.*, **33**(5), 390-393.
- Ma, S.Q., G.G. Zheng, G. Wang, L. Wu, X.P. Zhang, Y. Pan, Q. Li, Q. Cai, 2006: The study of miniature robot aircraft for weather modification. *Adv. in Earth Sci.*, **21**(5), 544-550.
- Qiu Jinhuan, 2001: Broadband extinction method to determine atmospheric aerosol optical properties. *Tellus*, **53B**(1), 72-82.
- Qiu Jinhuan, and Chen Hongbin, 2004a: Recent progresses in atmospheric remote sensing research in China. *Adv. Atmos. Sci.*, **21**, 475-484.
- Qiu Jinhuan, Yang Liquan, and Zhang Xiaoye, 2004b: Characteristics of imaginary part and single scattering albedo of urban aerosol in northern China. *TELLUS*, 2004, 53B, 72-82.
- Qiu Jinhuan, Zong Xuemei, and Zhang Xiaoye. 2005: A study of the scaling height of the tropospheric aerosol and its extinction coefficient profile, *Journal of Aerosol Science*, 361-371.
- Qiu Jinhuan, 2006a: Broad band diffuse radiation method to retrieve radiation-weighted mean aerosol single scattering albedo. *Chinese J. Atmos. Sci.*, **30**(5), 767-777.
- Qiu Jinhuan, 2006b: Cloud optical thickness retrievals from ground-based pyranometer measurements, *J. Geophys.*

- Res.*, in press.
- Si, F.Q., J.G. Liu, P.H. Xue, Y.J. Zhang, W.Q. Liu, H. Kuze, N. Lagrosas, and N. Takeuchi, 2006: Correlation Study Between Suspended Particulate Matter and DOAS Data. *Adv. Atmos. Sci.*, **23**(3), 461-467.
- Sun Dongsong, Zhong Zhiqing, Zhou Jun, Hu Huanling, and T. Kobayashi, 2005: Accuracy analysis of the Fabry-Perot etalon based Doppler wind lidar, *Optical Review*, **12**, 409-414.
- Tang Jiakui, Xue Yong, Yu Tong, Guan Yanning, Cai Guoyin, and Hu Yincui, 2005: Remote sensing of aerosol over land surface from synergy data of MODIS/Terra and MODIS/Aqua. *Science in China (Series D)*, **35** (5), 474-481.
- Wang, S.C., P.X. Wang, and Z.Y. Wang, 2005a: The synthetic system of operation and service on dust and sand storm monitoring and forecasting in Northern China. *Arid Meteorology*, **23**(4), 83-87.
- Wang, X., L. G. Bian, H. Peng, and J.D. Li, 2005b: The atmospheric wind profiler and radio acoustic sounding system with its applications. *J. Appl. Meteorol. Sci.*, **16**(5), 693-697.
- Wang, W., H.J. Liu, X. Yue, H. Li, J.H. Chen, and D.G. Tang, 2005c: Study on Size Distributions of airborne particles by aircraft observation in Spring over eastern coastal areas of China. *Adv. Atmos. Sci.*, **22**(3), 328-336.
- Wang, G. C., L.Q., Li, Y. Wang, Y.J. Xuan, X.W. Wan, Q.X. Kong, and H. B. Chen, 2004a: XLS-II tethered balloon sounding system. *Meteorol. Sci. & Tech.*, **32**(4),
- Wang, G. C., Q. X. Kong, Y.J. Xuan, X.W. Wan, H.B. Chen, S.Q. Ma, Q. Zhao, 2004b: Preliminary analysis on parallel sounding comparison of GPSO3 and Vaisala ozonesones, *J. Appl. Meteorol. Sci.*, **15**(6), 672-679.
- Wang, G. C., Q. X. Kong, Y.J. Xuan, X.W. Wan, H.B. Chen, and S.Q. Ma, 2003: Development and application of ozonesonde system in China, *Adv. in Earth Sci.*, **18**(3), 471-475.
- Wang Lili, Xin Jinyuan, Wang Yuesi, Li Zhanqing, Wang Pucui, Liu Guanren, and Wen Tianxue, 2006: The assessment of MODIS aerosol data using CSHNET observations. *Chinese Science Bulletin*, accepted.
- Wen, T. X., Y. S. Wang, S.Y. Chang, and G.R. Liu, 2006: On-line Measurement of Water-Soluble Ions in Ambient Particles. *Adv. Atmos. Sci.*, **23**(4), 586-592.
- Xin Jinyuan, Wang Yuesi, Li Zhang, Wang Pucui, Hao Weimin, Nordgren B.L., Wang Shigong, Liu Guanren, Wang Lili, Wen Tianxue, Sun Yang, and Hu Bo, 2006: AOT and Angstrom exponent of aerosols observed by the Chinese sun hazemeter network from August 2004 to September 2005. *J. Geophys. Res.*, in press.
- Xia Xiangao, Chen Hongbin, and Wang Pucui, 2004: Validation of MODIS aerosol retrievals and evaluation of potential cloud contamination in East Asia. *J. Environmental Sciences*, **16** (5), 832-837.
- Xia Xiangao, Chen Hongbin, Wang Pucui, Zong Xuemei, Qiu Jinhuan, and Phillipe Gouloub, 2005: Aerosol

- properties and their spatial and temporal variations over North China in spring 2001. *Tellus*, **57B**, 28-39.
- Xia Xiangao, 2006a: Significant overestimation of global aerosol optical thickness by MODIS over land. *Chinese Science Bulletin*, **51** (1), 1-7.
- Xia X., Chen H., Wang P., Zhang W., Goloub P., Chatenet B., Eck, T.F., and Holben B.N., 2006b: Variation of column-integrated aerosol properties in a Chinese urban region. *J. Geophys. Res.*, D06204, doi:10.1029/2005JD006203.
- Xia Xiangao, Wang Pucai, Chen Hongbin, and Liang Feng, 2006c: Analysis of downwelling surface solar radiation in China from National Centers for Environmental Prediction reanalysis, satellite estimates, and surface observations. *J. Geophys. Res.*, doi:10.1029/2005JD006405.
- Xia Xiangao, Chen Hongbin, Li Zhanqing, Wang Pucai, and Wang Jiankai, 2006d: Significant reduction of surface solar irradiance induced by aerosols in a suburban region in northeastern China. *J. Geophys. Res.*, in press.
- Xie Chenbo, Zhou Junyue, Gu Ming, Qi Fudi, and Fan Aiyuan, 2006: New Mobile Raman Lidar for Measurement of Tropospheric Water Vapor. *Acta Optica Sinica*, **26**, 1281-1286 (in Chinese).
- Xie Chenbo, Han Yong, Li Chao et al., 2005: Mobile lidar for visibility measurement. *High power laser and particle beams*, **17**, 971-975(in Chinese).
- Xu, Q., 2001: Abrupt change of the midsummer climate in central east China by the influence of atmospheric pollution, *Atmos. Environ.*, **35**, 5029- 5040.
- Xuan, Y. J. , S.Q. Ma , H.B. Chen G.C. Wang, Q.X. Kong, Q. Zhao, and X.W. Wan, 2004: Intercomparison of PGSO3 and Vaisala ECC ozone sondes. *Plateau Meteorol.*, **23**(3), 395-399.
- Yang Jingmei, Qiu Jinhuan, and Zhao Yanliang, 2005: Umkehr Observations of Vertical Ozone Distributions of Beijing in Recent 13 Years. *Proceedings of SPIE*, 5832, 300-307.
- Yao, W., G.G. Zheng, Y.T. Guo, B.X. Huang, and B.Y. Du, 2004: Standardization of the software design for upper-air observation. *J. Appl. Meteorol. Sci.*, **15**(1), 88-94.
- Yuan S., X.Yu, and Zhou Jun, 2005: Lidar observations of the lower atmospheric layer in Hefei. *Chinese Journal of Atmosphere Sciences*, **29**, 387-395 (in Chinese).
- Zhang Yuxiang, Hu Xiuqing, Liu Yujie, and Rong Zhiguo, 2002a: Measurement of atmospheric aerosol optical characteristics in Beijing urban area. *Journal of Applied Meteorological Science*, **13**(Suppl.), 136-143 (in Chinese).
- Zhang Junhua, Mao Jietai, and Wang Meihua, 2002b: Analysis of aerosol extinction characteristics in different area of China. *Advan. Atmos. Sci.*, **19**, 136-152.
- Zhang, Q.Y., Y. Zhang, L. Li, and J. Tian, 2003: Tendency of atmospheric sounding. *Meteorol. Sci. & Tech.*, **31**(2),

119-123.

Zhao Fengsheng, Ding Qiang, Sun Tongming, Kong Qingxing, Hu Wen, Xun Shangpei, and Shao Hengfei, 2002:

An iterative algorithm for the retrieval of cloud properties from NOAA-AVHRR imagery, *Acta Meteorologica Sinica*, **60**(5), 594~601.

Zhong Z., Sun Dong song, B. X. Wang et al., 2006: Low tropospheric wind measurement with 1.06 $\mu$ m Doppler lidar. *23th ILRC, Nara, Japan*.

Zhou, J., G. Yu, C. Jin, F. Qi, D. Liu, H. Hu, Z. Gong, G. Shi, T. Nakajima and T. Takamura, 2002: Lidar Observations of Asian Dust over Hefei, China in the Spring of 2000, *JGR*, 107, D15, AAC51-58.

Zhou Jun, D. Liu, G. Yue, et al., 2006: Vertical distribution and temporal variation of Asian dust observed by lidar over Hefei, China. *Journal of Korean Physical Society*, **49**, 320-326.

Zong Xuemei, Qiu Jinhuan and Wang Pucai, 2005a: Characteristics of atmospheric aerosol optical depth over 16 radiative stations in the last 10 years. (Chinese) *Climatic and Environment Research*, **10**(2), 201-208.

Zong Xuemei, Qiu Jinhuan and Wang Pucai, 2005b: A comparison study of aerosol optical depths retrieved from broadband extinction method and aerosol robotic network observation. *Chinese J. Atmos. Sci.*, **29**(4), 645-653.

Wei, Dongjiao, and Qiu, Jinhuan, 1998: Wideband method to retrieve the imaginary part of complex refractive index of atmospheric aerosols, part I: Theory. *Chinese J. Atmos. Sci.*, **22**, 677-685.

Wu Xuebao, Li Jun, Zhang Wenjian, and Wang Fang, 2005: Atmospheric profile retrieval with AIRS data and validation of the ARM CART site. *Advan. Atmos. Sci.*, **22**, 647-654.

# PROGRESSES ON OBSERVATIONS OF CRYOSPHERIC COMPONENTS AND CLIMATE-RELATED STUDIES IN CHINA

*Xiao Cunde<sup>1,2</sup>, Qin Dahe<sup>1</sup>, Yao Tandong<sup>1,3</sup>, Ding Yongjian<sup>1</sup>  
Liu Shiyin<sup>1</sup>, Zhao Lin<sup>1</sup>, Liu Yujie<sup>4</sup>*

(1. Joint Key Laboratory of Cryosphere and Environment, Cold and Arid Regions Environmental and Engineering Research Institute, Chinese Academy of Sciences, Lanzhou 730000, China; 2. Chinese Academy of Meteorological Sciences, Beijing 100081, China; 3. Institute of Tibetan Plateau Research, Chinese Academy of Sciences, Beijing 100085, China; 4. National Satellite Meteorological Centre of China, CMA, Beijing 100081, China

## ABSTRACT

Systematic studies on cryosphere in China started in late 1950s. Significant achievements have been made by continuous efforts on glacier inventory (investigations), frozen ground observations, paleo-climate recovery from ice cores, processes studies and the modeling of the cryospheric/atmospheric interactions. The general facts and understanding of these changes include: (1) Solid precipitation, such as the frost days and hailstone fallings, shows a decreasing tendency in the past half centuries. (2) Glaciers in various areas in west China have experienced different changes in the past decades. Although, in most areas, glaciers are retreating or have even completely vanished (>80%), some glacier are still advancing (5-20% according to different time periods). The annual glacial melt water in China amounts to  $600 \times 10^8 \text{ m}^3$ , and it has been increased since 1980s. The supply of melt water to river runoff in northwest China is about 10-13%. (3) Snow cover in western China did not experience a continual decrease during the great warming periods of the 1980s and 1990s, without clear correlation between temperature and precipitation in the snow cover season. The long-term variability of snow cover in western China is characterized by a large inter-annual variation superimposed on a small increasing trend. Snow cover variability in the Qinghai-Xizang Plateau (QXP) is influenced by Indian monsoon, and reversely impacts monsoon onset and strength, eventually the drought and flood events in middle-low reaches of Yangtze River. (4) Frozen ground, including permafrost, is decaying both in QXP and in Northeast China. The most significant changes occurred in the regions with thickest seasonal frozen ground

(SFG), i.e., inland QXP, then northeastern and northwestern QXP. The duration of shortened SFG varied in different regions. Significant changes also occurred in the inland and northeastern regions of QXP. The cold season air temperature is the main factor controlling SFG change. The warming of ground surface temperatures are more significant than air temperature. (5) The sea ice coverage over the Bohai- and Yellow seas has decreased since 1980s. (6) River ice duration and ice thickness is also decreasing in the northern China.

In 2002, Chinese National Committee of WCRP/CliC (CNC-CliC) was organized in order to strengthen researches on climate and cryosphere in China. Future monitoring of cryosphere in China will be enhanced both in spatial coverage and the usages of techniques. Interaction between atmosphere/cryosphere/hydrosphere/ land-surface will be performed to a better understanding of the mechanism on cryospheric changes.

**KEY WORDS:** CNC-WCRP/CliC, Cryosphere, observations, climate change, global warming

## 1. CRYOSPHERE IN CHINA AND RELATED OBSERVATIONS

The cryosphere, portions of the Earth's surface where water is in solid form, has shown a widespread shrinkage in the 20th century, the warmest century for the past 2000 years (IPCC, 2001). Cryosphere is considered as one of the sensitive indicators of climate change. Chinese cryosphere, one of the largest cryospheric areas on Earth, has also been undergoing rapid changes in the past decades.

In China, the cryosphere is mainly located in the Qinghai-Xizang (Tibetan) Plateau (hereafter QXP), East Tianshan Mountain, Altai Mountain, east Pamir and northeast China (Figure 1). The total number of glaciers in China is 46,298 with an area of 59,406 km<sup>2</sup> and an ice volume 5,590 km<sup>3</sup>. The permafrost and the seasonal frozen ground (SFG) cover an area of  $1.49 \times 10^6$  km<sup>2</sup> and  $5.28 \times 10^6$  km<sup>2</sup>, accounting for 11.5% and 55% of China's land territory, respectively. Snow covered area is around  $9.0 \times 10^6$  km<sup>2</sup>, and among this, an area over  $4.8 \times 10^6$  km<sup>2</sup> consists of unstable snow cover (duration <20 d). Stable snow cover (duration >60 d) is mainly located in the QXP, North Xinjiang (including Tianshan Mountains), and the Inner Mongolia-Northeast China

(hereafter IM-NEC) regions. The mean snow cover areas of the above three regions are  $2.3 \times 10^6$  km<sup>2</sup>,  $0.5 \times 10^6$  km<sup>2</sup> and  $1.4 \times 10^6$  km<sup>2</sup>, respectively. Seasonal sea ice forms in Bohai Sea and in the northern Yellow Sea of China. Sea ice forms in mid-to-late November and reaches its maximum area in late January to early February and melts away in late March. River ice forms in most of rivers in north China, including Yellow River, Songhuajiang River, Nengjiang River, Liaohe River and others.

**Figure 1.** Distributions of major cryospheric components (a: Glacier, b. frozen ground, c: snow cover) in China.

In order to coordinate the relevant researches of cryosphere in China, Chinese National Committee on WCRP/CliC (CNC-CliC) was established in 2002. CNC-CliC consists of 9 research panels such as: (1) Climate and glacier and frozen ground; (2) Climate and cold regions hydrology; (3) Climate and polar marine/terrestrial ecology; (4) Interactions of atmosphere/ocean/sea-ice; (5) Cryospheric change and climate prediction; (6) Remote sensing and data base; (7) Cold regions sustainable development; (8) Cold regions engineer and technology; (9) Integrated assessment.

Systematic studies on cryosphere in China commenced late 1950s. Comprehensive investigations on glacier for water storages were performed in the west China. Later, frozen ground and snow cover surveys were also included. Sea ice and river ice were monitored by Chinese Hydrology Ministry and Chinese Ocean Administration, respectively. Progresses on observations of cryospheric components have been achieved during past decades.

## 1.1 Solid precipitation

Solid precipitation includes snowfall, frost, hailstones and other solid forms of precipitation. In China, there are few studies on snowfall changes in national scale (such as annual changes of snowfall days and duration, etc.), only some studies on disaster-related snowfall. Snowfall disasters, the extreme events of the heavy snowfall which kills animals and sometimes human beings, usually occurs over the QXP, north Xinjiang, Inner Mongolia and the northwest China. For

instance, Totally 11 snowfall disasters were occurred in Qinghai province, east QXP, during 1956-1996, which kills  $854 \times 10^4$  animals. Heavy snowfall events in Xinjiang in both 1970s and 1980s were doubled than in the 1960s. But in Inner Mongolia, heavy snowfall events in the 1970s were less than in the 1960s and the 1980s. In the Tibet Plateau, the frequency of heavy snowfall increases from the 1960s to 1980s, the most severe disasters occurred in the late 1980s.

Frost days are defined as the minimum daily temperatures below  $0^{\circ}\text{C}$ . The frost days in north China show a decreasing trend for the last decades. This is specifically shown in east China and north part of Xinjiang. In these regions, the mean non-frost days increased around 40 days. Frost days in China deceased by 2.4 days/10a (Figure 2), amounting to a total decreasing of 12 days in the last 50 years (Zhai and Pan, 2003). The decreasing was probably attribute to the global warming, especially winter warming in the last decades.

**Figure 2.** Changes of frost days in China during 1951-1999 (Zhai and Pan, 2003)

Recent studies show an obvious decreasing in frost days in the north China during the last 50 years. Frost days also show different annual variability in different regions. Large annual variabilities occur over the north part of the east China, east part of Northeast China and the southwest part of Northeast China, the maximum of the variability is as large as 30 days/50a. In general, the variability in the east China is larger than in the west China. The end dates of frost in spring is becoming earlier in most regions, most obviously in east part of northwest China, southwest part of the northeast China, north part of east China, as well as the most part of Inner Mongolia. The start dates of frost is becoming later in most regions, most obviously in the east part of northwest China, north part of northeast China, as well as the low reach of the Yangtze River.

China is one of the most suffered countries by hailstone disasters in the world. The mean area of annual hailstone falling is  $173 \times 10^4 \text{ hm}^2$ , and in some extreme cases it can be as large as  $400 \times 10^4 \text{ hm}^2$ . The hailstone days in the last 40 years in the northwest China showing a general decreasing trend (Figure 3a). Three periods of the heavy hailstone fallings were 1960-1965, 1967-1974 and 1979-1988, respectively. After 1990, hailstone days display a rapid decrease trend. The decrease of the cold air masses under the background of the global warming could be the

major reason for the decreasing of hailstone days, while the enhanced weather modification activities also contribute to, but believed to be minor, the decrease after 1990s (Li et al., 2005). There are three major geographical centers of hailstone fallings in the northwest China. The largest one (area I in Figure 3b) locates in the south of Qinghai Province and the Southwest of Gansu Province, where high mountains such as Tanggula, Kekexili, Bayankala and Animaqin are located. The mean annual hailstone days are more than 20 days in the last 40 years. Area II locates in the central and west section of Tianshan Mountain. The hailstone days in the central area II are more than 9 days, with the high hailstone days (averaged to be 19 days) occurred in Zhaosu. Area III locates on the south slope of Qilian Mountain, or Beihai of Qinghai Province, where the average hail days are less than 9 days.

**Figure 3.** Distribution and changes of hailstone fallings in the northwest China (a. changes of annual hailstone falling events in NW China during 1960-2000; b. spatial distribution of hailstone falling in NW China)

There are no studies on the historical changes of hailstone fallings in whole China for the last decades. But since hailstone fallings generally occur in the high mountains and plateaus, the study on the northwest China, where high mountains and plateau locate, can represent the general trend of hailstone fallings in China.

Little studies have been operated on amount measurements of solid precipitation in China. Early study was operated on Glacier No.1 at the headwater of Urumuqi River, Central Tianshan. Recently, experiment on solid precipitation measurement is carried out over the several sites in the northeast and northwest China by Chinese Meteorological Administration (CMA). These studies are primary and no results have been published yet.

## **1.2 Glacier inventory and recent observations on glacier changes**

Glacier inventory in China commenced 1979 and lasted for 24 years until completed in 2002. Totally 342,000 aerial photos, more than 200 satellite images and 2000 topography maps were used for the project. There have been 13 expeditions organized for this study over the high altitudes of the west China. It is estimated that 43677 glaciers, with the total area 59425 km<sup>2</sup> and

ice volume  $5600 \text{ km}^3$ , are distributed in the high mountains in the west China. Totally 12 volumes containing 23 series of glacier inventory books have been published. For each glacier, 34 parameters were described, including the geophysical position, size, orientation, physical characteristics, etc. Glacier inventory in China provides the fundamental and plentiful information for glacier studies in China, and has important contribution to the socio-economic aspects, especially to water resources management.

Glacier changes for the last decades have been studied based on measurements of mass balance and the variations of glacier terminals. Mass balance has been measured on several relatively easily accessible glaciers such as Glacier No.1, Xiao Dongkemadi (XDKMD), Meikuang (MK), Qiyi and Hailuogou (Xiao et al., 2007). Glacier No.1 at the headwater of Urumqi River (Tianshan) is the only glacier in China that included into the network of World Glacier Monitoring Service (WGMS (ISCS-IAHS)). The cumulative mass loss of the Glacier No.1 during 1959-2002 equals to a lowering of glacier surface up to 10.6 m. The mass loss is accelerated since 1995. For instance, the cumulative mass loss between 1995/96 and 2000/01 accounts for 42% of the total loss since 1959. Mass balance at XDKMD turned into negative since 1993, and displaying accelerated mass loss since then. Mass balance at MK is displaying a parallel trend to that of XDKMD. Mass balance at Qiyi from 1979/80 to 1977/78 was averaged to be 256 mm, from 1984/85 to 1987/88 it was 4 mm, while in 2001/02 and 2002/03 was -861 mm and -360 mm, respectively. It is calculated that the rate of mass loss was  $25.2 \text{ mm a}^{-1}$  between 1976-86 and  $-35.4 \text{ mm a}^{-1}$  between 1986-2002. Hailuogou Glacier, locating at the east margin of the Tibetan Plateau, displayed a continuously negative mass balance since 1960.

In the 20th century, the glaciers in the High Asia in China have retreated intensively with climatic warming. The glacial changes can be divided into several stages as follows: The first stage was the first half of the 20th century during which glaciers had advanced or shifted from advance to retreat. The second stage was between the 1950s and 1960s during which many glacial observations had been started. Glaciers in China had begun to retreat intensively during this stage (Table1). According to previous studies (Zhang et al., 1981; Ren et al., 1988; Shi et al., 2002), there were about two thirds of glaciers retreating and ten percents advancing, with some glaciers were stable. The third stage was between the late 1960s and 1970s when the proportion of advancing glaciers increased and that of retreating glaciers decreased. The fourth stage was the

1980s during which glaciers retreated intensively again. The fifth stage was the 1990s during which glacial retreat was more intensive than that of any other periods in the 20th century (Yao et al., 1991).

**Table 1.** Proportions of advancing and retreating glaciers in the High Asia in China in different stages (Yao et al., 2004)

On the plateau scale, the magnitude of glacial retreat in recent decades is smaller at the interior and larger at the margin. The magnitude of glacial retreat was much large in the Southeast Tibetan Plateau and Karakorum Mountains. The annual glacial retreat rate in Karakorum Mountains reached 30 m, and 40 m in the Southeast Tibetan Plateau. However, the annual glacial retreat rates in the Kunlun Mountains and Tanggula Mountains (central Tibetan Plateau) were small and less than 10 m. This kind of regional difference of glacial retreat forms an elliptical shape of the glacial retreat in recent years on the Tibetan Plateau, and the distribution feature was similar to that of the glacial shrinkages since the Maximum of the Little Ice Age to present (Figure 4). The central part of the elliptical regional distribution is located in the Tanggula Mountains, Kunlun Mountains, Qiangtang Plateau of the inland of the Tibetan Plateau with minimum magnitude of glacial retreat. The glacial retreat increased from inland to margin of the Tibetan Plateau, and reaches to the maximum in the Southeast Tibetan Plateau and Karakorum Mountains.

**Figure 4.** Regional features of the glacial fluctuations since the Little Ice Age (LIA) in the west China (Yao et al., 2004).

### 1.3 Snow cover changes

Qin et al (2005) studied the geographical distribution and spatial and temporal variability of the western China snow cover in the past 47 years between 1951 and 1997. The data used consist of Scanning Multichannel Microwave Radiometer (SMMR) 6-day snow-depth charts, NOAA weekly snow extent charts, and the daily snow depth and number of snow cover days from 106

selected meteorological stations across western China. Empirical orthogonal function was performed on the SMMR dataset to better understand the spatial pattern and variability of the QXP snow cover. A multiple linear regression analysis was conducted to show the association of interannual variations between snow cover and snow season temperature as well as precipitation. Further, the autoregressive moving average model was fitted to the snow and climate time series to test for their long-term trends. Results show that western China did not experience a continual decrease in snow cover during the great warming period of the 1980s and 1990s. It is of interest to note that no correlation was identified between temperature and precipitation in the snow cover season. However, year-to-year fluctuation of snow cover responds to both snowfall and snow season temperature. About one-half to two-thirds of the total variance in snow cover is explained by the linear variations of snowfall and snow season temperature. The long-term variability of western China snow cover is characterized by a large interannual variation superimposed on a small increase trend. The positive trend of the western China snow cover is consistent with increasing snowfall, but is in contradiction to regional warming. In addition, many constraints of the Qinghai–Xizang (Tibet) snow cover force the author’s challenge of Blanford’s hypothesis.

Figure 5a shows a time series of the annual and spring ablation season (March and April), number of days with snow cover, and annual cumulative daily snow-cover depth over northwest China from 1951 through 1997. It demonstrates that long-term variability of snow cover is normally characterized by random oscillation. Snow cover fluctuated around the mean, alternating between heavy- and light snow-cover. Neither abrupt changes nor continuation of snow minima from the late 1980s and early disappearance of spring snow cover were found. But from the end of the 1980s, a prolonged decrease in snow cover was evidenced but not as great as the three previous snow-deficit periods. In the 1960s and the early 1970s, snow cover was measured lower than at any other time in the second half of the 20th century.

Over the QXP long-term variability of snow cover is characterized by large inter-annual variabilities superimposed on a continuous increasing trend. Furthermore, the annual amplitude of snow-cover variability has increased significantly since the 1980s (Figure 5b). Both extremely heavy- and light snow-cover years occurred more frequently. The anomalies did not appear to be outside the range of natural variability.

In the IM-NEC region, there are several scattered areas with deep snow cover where large

inter-annual variabilities in snow depth were observed. These areas include Da Hingan, Xiao Hingan and Xilinguole. There are also big seasonal variations in snow depth. The deepest snow cover appears in mid-winter, the same season as when the largest inter-annual snow depth variations occur. The overall trend in the IM-NEC regions shows a very slight decrease (0.1% per year) in snow depth. (Figure 5c)

The annual snow cover variations depend both on the amount of winter snowfall and of the winter temperatures. Li (2000) established relationships between snow cover and winter air temperatures and precipitation, respectively for the Xinijing, QXP and IM-NEC regions. These are:

$$\text{Xinjiang: } Sd = 20.86P - 150.39T - 738.8$$

$$Sn = 0.48P - 4.51T + 35.2$$

$$\text{QXP: } Sd = 1.99P - 14.21T - 121.1$$

$$\text{IM-NEC: } Sd = 11.95P - 43.2T - 279$$

Whereas  $Sd$  and  $Sn$  are the annual daily cumulative snow depth data (cm) and annual snow-cover days (d), respectively.  $P$  is the amount of winter snowfall (mm), and  $T$  is the mean air temperature during snow-cover season.

The inter-annual snow-cover variations based on the above functions coincide well with the observed results, with an error range within 10%. But these functions can not properly reproduce long-term changes in snow cover, probably due to the large errors in measuring solid precipitations.

**Figure 5.** Interannual variability of snow cover over China during the past 50 years. a) Xinjiang, b) Qinghai-Xizang Plateau (QXP) and c) Inner Mongolian-Northeast China (IM-NEC) region

Zhao and Moore (2004) suggested that there exists an east-west dipole-like correlation pattern between snow cover over the Tibetan plateau and Indian summer monsoon rainfall that underwent a change in sign around 1985. They argue that variability in the Tibetan plateau monsoon is responsible for the spatial and temporal variability in the relationship between Tibetan snow cover and the Indian summer monsoon.

## 1.4 Frozen ground changes

### *Permafrost*

Since 1964, a 35 m deep hole for measuring soil temperature was measured at Fenghuoshan, central QXP. Ground temperatures in different depths were read in 1964, 1984, 1992 and 1996. Stable ground temperatures were observed between 1964 and 1984, but after the mid-1980s turned into a warming trend for the surface soil within 20 m (Zhang et al., 2000). According to Zhao and other's study (2003), permafrost temperatures over the hinterland of the Tibetan Plateau increased about  $+0.2^{\circ}\text{C}$  to  $+0.5^{\circ}\text{C}$  from the 1970s to the 1990s. Permafrost temperatures were measured at four sites along the northern section of Qinghai-Xizang Highway, these sites are Chumaer River, Kekexili, Kunlun Pass and Fenghuoshan. At these sites, ground temperature increases at 5-m depth were averaged to have increased up to  $0.5^{\circ}\text{C}$  over the period 1995-2002 (Wu and Liu, 2003; Zhao et al., 2004). Permafrost temperatures increased from about  $0.2^{\circ}\text{C}$  to  $0.4^{\circ}\text{C}$  from 1973 to 2002 at 16-to-20 m depths in the Tianshan Mountain region (Qiu et al., 2000; Zhao et al., 2004). Permafrost surface temperatures increased from about  $0.7^{\circ}\text{C}$  to  $1.5^{\circ}\text{C}$  over a period from 1978 through 1991 from the valley bottom to the north-facing slopes in the Da Hinggan Mountains in northeastern China (Zhou et al., 1996). Permafrost temperature at the depth of the zero annual temperature variation increased about  $2.1^{\circ}\text{C}$  on the valley bottom,  $0.7^{\circ}\text{C}$  on the north-facing slopes, and  $0.8^{\circ}\text{C}$  on south facing slopes. The active layer has increased by about 40 cm at Jiagedaqi over permafrost, from an average of 240 cm in the 1960s to an average of 280 cm in the 1990s (Liu J., et al., 2003). In the south-facing slope areas where no permafrost exists, soil temperatures at the lower limits of the seasonally frozen ground increased by about  $2.4^{\circ}\text{C}$  (Zhou et al., 1996).

### *Seasonal frozen ground (SFG)*

We discuss SFG changes over three major regions in China, they are QXP, northwest China (including Xinjiang, Hexi Corridor of Gansu Province) and northeast China (Xiao et al., 2007).

Over the QXP, the thickness of seasonally frozen ground has decreased from 0.05 m to 0.22 m from 1967 through 1997 (Zhao et al., 2004). The driving force for the decrease is the significant warming in cold seasons, while changes in snow cover depth plays a minor role. Over the Tibetan

Plateau, the duration of seasonally frozen ground shortened by more than 20 days from 1967 through 1997, this was mainly due to the earlier onset of thaw in spring rather than the late onset of freeze in autumn.

The average and maximum SFG depths and the duration of the frost period at 10 cm deep in Xinjiang during the period of 1961-2002 are analyzed (Wang et al., 2005). The results show that the average and maximum depths of the freezing front are decreasing and that the duration of the frost period is becoming shorter due to warmer climate in Xinjiang in the past decades. Such changes have become more significant since 1986, after an obvious local change towards a warmer-wetter climate. A significant decrease of the maximum depths reached by the freezing front occurred in the mid-1980s, both in South and North Xinjiang.

Data of the upper and lower limits of SFG, as well as on the duration of the frost period, collected from 17 meteorological stations in the Hexi Corridor in the Gansu Province from 1958-2003, show a rapid decrease in the depth reached by the freezing front in the mid-1980s. This coincides with an increase in winter temperature over the same period. The minimum air temperature in winter controls the maximum depth reached by the freezing front and the duration of the frost period (Guo et al., 2005).

There are few SFG studies in northeast China. But since an obvious trend in increased air temperatures has been observed for the past 50 years, it is clear there has been a reduction of the SFG in the past decades. Observations show a rapid increase of winter air temperature in NE China in the past five decades (Sun et al., 2005), which is harmful to the preservation of SFG.

### **1.5 Sea ice and river ice**

The Bohai Sea and the northern part of the Yellow Sea located on the south edge of the Northern Hemisphere sea ice, it lies between the latitudes 37°05'N-40°55'N, and longitudes 117°30'E-125°30'E. Since the early 1950s, sea ice coverage and thickness over the oceans were monitored for harbor disasters' assessment and prediction. Sea-ice disasters are classified into five grades according to the sea ice cover and thickness (Zhang, 1993). Heavy sea-ice disasters occurred in the year of 1956/1957 and the winter of 1968/1969, and less heavy disasters occurred in the winters of 1967/1968 and 1976/1977.

During the past five decades, the Bohai Sea sea ice cover has shown a declining trend, while

there is no obvious trend over the north Yellow Sea area. But, for the whole area, a general decline in sea-ice coverage has been shown since late 1960s.

Zhang (1993) detected the relationships between sea-ice cover and climate, showing that solar cycle activities and El Nino events correlate to the anomalous sea-ice conditions. The maxima and minima of solar activities, and the intensity and timing of the El Nino events, play a very important role in the occurrence of severe ice conditions.

We discuss the changes in river ice over two key areas—Inner Mongolia and Northeast China—where river ice data are available. River ice of the Inner-Mongolia section of the Yellow River has been observed at the Sanhuhekou-, Shizuishan-, Baotou-, Zhaojunfeng- and Toudaogui-Hydrological Stations. River ice of Songhuajiang River has been observed at the Harbin Hydrological Station, and the Nengjiang River was observed at Fulaerji Station.

Changes in river ice can be described as changes in freeze-up and breakup dates, length of frost period, as well as ice thickness.

Over the Inner-Mongolia section of the Yellow River, freeze-up dates are five days later in the 1990s than that of the 1950s-1990s average, and the breakup date in the 1990s is three days earlier than the average. The frost period duration and the maximum ice thickness in the 1990s are nine days shorter and 0.16 m thinner, respectively, than the average (Xiao et al., 2007).

At Harbin of Songhuajiang River, freeze-up date is one day later and breakup date is one day earlier in 1990s later than that of the 1950s-1990s average. The duration of the frost period and the maximum ice thickness in the 1990s are respectively four days shorter and 0.21 m thinner than the average.

At Fulaerji of Nengjiang River, the freeze-up date is six days later and breakup date was 2.5 days earlier in the 1990s later than that of the 1950s-1990s average. The frost period duration and the maximum ice thickness in the 1990s are respectively ten days shorter and 0.06 m thinner than the average.

At three study areas, the frost period and the maximum ice thickness decreased since late 1970s, when the global and regional climate warming is most prominent. During the period 1959-2002, annual mean air temperature increased by  $0.48^{\circ}\text{C}/\text{a}$ , and winter air temperatures increased by  $0.72^{\circ}\text{C}/\text{a}$  over northeast China (Sun and Yuan, 2005), where the Songhuajiang River and Nengjiang River are located.

## 1.6 Ice core records for climate changes

More than 20 ice cores have been drilled in the Chinese High-Asia regions in the last approximately 20 years (Figure 6). These ice cores cover the time scales from several decades to tens of thousands, providing plentiful information on climatic and environmental changes of the west China (Yao, 2002).

Major progresses on ice-core studies can be summarized as follows:

(1) Quantitative relationships between stable water isotopes ( $\delta^{18}\text{O}$ ,  $\delta\text{D}$ ) and air temperature ( $\delta\text{-T}$ ) have been established over a vast area over the QXP and the surrounding regions based on precipitation sampling at the meteorological stations (Tian et al., 2003). This study has been performed since 1989 and has laid a solid foundation for interpreting the temperature changes in the ice core records. For instance,  $\delta\text{-T}$  relations at Delingha (Qinghai Province) is  $1.5^{\circ}\text{C}/\text{‰}$ , while at the headwater of Urumqi River, Middle Tianshan, it is  $1.2^{\circ}\text{C}/\text{‰}$ .

(2) Long-term climate records in Guliya Ice Core. Hundreds of thousands years' climate was believed contained in the Guliya ice core, with the average time

**Figure 6.** Distribution of ice cores that have been drilled in west China

resolution around 50 years. It shows that Guliya ice core recorded the MIS1, 2, 3, 4 and 5, corresponding to the records in the Vostok ice core in Antarctica and GRIP ice core in Greenland. MIS5 contains 5 sub-stages as 5a, 5b, 5c, 5d and 5e (Yao et al., 1997; Thompson et al., 1997). Although most Guliya climate events coincides with that of GRIP records, there are still differences between them. Firstly, the frequency and amplitudes of climate change in Guliya are bigger than in GRIP; Secondly, the rapid change from warm to cold stages, and the slow changes from cold to warm stages are more dominant in Guliya ice core than GRIP. Finally, the warm period in the 30,000 a BP is prominent in Guliya while in Vostok and GRIP it was medium warm. Abrupt climate events with time scales approximately 200 years were shown in Guliya ice core during 18ka to 35 ka BP, with their frequency and amplitudes higher than the polar regions.

(3) Quaternary climate change were shown clearly as three stages—early Quaternary, mid-late

Quaternary and the late Quaternary, divided by two major warm periods 8.4ka-8.5ka BP and 2.9ka-3ka BP, respectively. The early stage of quaternary in QXP was unstable, with the remarkable cooling events occurred about 8.8 ka BP.

(4) High resolution climate records in different ice cores for the last 2000 years have been recovered over the QXP. Based on Guliya and Dunde ice cores, it shows three cooling periods and three warm periods since the Little Ice Age (LIA) over the north QXP. This is in coincidence with the three moraine ranges at the most glacier terminals in the west China. Furthermore, climate records in Guliya and Dunde were shown similar variations with the records from the east China, where the Medium Warm Period (MWP) is more prominent. Methane changes of the last 2000 years have been recovered in Dasuopu ice core in the middle Himalayas, showing high concentration and high amplitude of changes than polar regions (Yao et al., 2002).

(5) Annual and decadal records of climate in other ice cores show climate and precipitation changes both in the north and south plateau (Duan et al., 2004; Qin et al, 2002; Yao et al, 2001; Wang et al, 2003; Hou et al, 2000; Kang et al, 2000). These records display increasing trends of precipitation in the north and decline trends in the south for the last decades. Also, dust records show decline trends in the north plateau (Wang et al, 2005). The decline precipitation in Himalayas was suggested to be attributable to the strength change of Indian monsoon.

### 1.7 Estimation of glacial water resources and changes in west China

During the 1980s-1990s, glacier water resources were assessed based on the method of glacier melt water runoff modulus, runoff-temperature relations, and in situ experiments. It was estimated the total melt-water discharge is  $563.3 \times 10^8 \text{m}^3$  (Yang, 1991), and this data recently has been modified as  $604.65 \times 10^8 \text{m}^3$  (Kang et al., 2000; Xie et al., 2006. Table 2).

**Table 2.** The Estimated glacier runoff in China (Based on Kang et al., 2000; Xie et al., 2006)

According to the study of Yang (1991), the annual glacial melt water runoff in China was about  $56.4 \text{ km}^3$  or  $564 \times 10^8 \text{m}^3$ , which is close to the total annual runoff of the Yellow River, it is 2% of the total runoff in China, 10% of the total runoff in Northwest China and 13% of the total

runoff ( $4431 \times 10^8 \text{m}^3$ ) of West China's Gansu, Qinghai, Xinjiang and Tibet. In fact, glacial water resource is much important to the arid inland mainly including Northwest China's Xinjiang, Qinghai and Gansu. According to the results of Yang (1995), the total glacial melt water runoff in Northwest China was about  $220.07 \times 10^8 \text{m}^3$ . Given the fact that intensive glacial melting began in 1972/1973, the supply of glacial melt water runoff reached 5.5% in the past 27 a. According to Yao (1996, 1997), obvious climate warming appeared in the 1980s, and became more intensive in the 1990s, we therefore estimate that the supply of glacial melt-water runoff was more than 5.5% in the 1990s.

To discuss this in more details, we use estimation of the glacial volume changes based on the experimental formula by Liu (2002). In doing so, average glacial areas and its decreases in the past 40a were studied. According to the studies in recent years, the glacial area in China decreased by about 7% in the past 40 a. Therefore, the result calculated with the experimental formula is that glacial volume decreased  $500 \times 10^9 \text{m}^3$  in the past 40 a. The results estimated with the two different methods are comparable.

Decreasing of glacial volume is estimated to be between  $452.770 \text{ km}^3$  and  $586.94 \text{ km}^3$  in China in the past 40a. Although the result is still not precise, this raises the importance of glacial retreat to the water resource in Northwest China. If we take  $502 \text{ km}^3$ , an average of  $452.77$  and  $586.94 \text{ km}^3$ , as an average of glacial volume decrease, the value is equal to the sum of six years of the total runoff in Xinjiang. Glacial volume decrease, in turn, results in the increasing of melt water runoff. A recent study of Shi and others (2001; 2002) showed that river runoff in Xinjiang had increased significantly. The increase of the total runoff of 6 tributaries of the Tarim River increased even more obviously. The increase of the annual runoff of the Aksu River is particularly intensive. Because the Tarim River Basin is the most glacial concentrated area in the High Asia in China, it is much important to study the impacts of glacial fluctuation on the water resource in the Tarim River Basin.

There are 14285 glaciers in the Tarim River Basin, the total glacial area is  $23628.98 \text{ km}^2$ , the glacial volume is  $2669.435 \text{ km}^3$  and the average glacial depth is 113 m. Liu (1999) had shown a similar data set including about 12182 glaciers,  $20271.02 \text{ km}^2$  in glacial area and  $2347.317 \text{ km}^3$  in glacial volume in the Tarim River Basin. The magnitude of glacial change in the Tarim River Basin was much larger than that in the Tianshan Mountains, and the glacial length change reached

13.8%, the glacial volume decrease is  $280 \times 10^8 \text{m}^3$ . And the glacial volume decrease calculated with the experimental formula is  $222 \times 10^8 \text{m}^3$ . The results estimated with the two methods are comparable. According to a previous study (Shi et al., 2002), the total annual runoff of six tributaries of the Tarim River is  $310 \times 10^8 \text{m}^3$ . Therefore, the runoff of the Tarim River supplied with the glacier volume decrease reached about 50% in the past 40 a, which is equal to net supply of 13% per decade. According to the study of Shen (2003), a stronger glacial melting period started in 1972/1973. If so, the net supply of the glacial volume decrease would be much larger after 1972/1973. According to the study of Shi (2002), the runoff in the Tarim River Basin increased from  $310 \times 10^8 \text{m}^3$  to  $350 \times 10^8 \text{m}^3$  in the 1990s, which is equal to a runoff increase of 13%. According to his study, the climatic warming and wetting are the major causes of runoff increase in the Tarim River Basin. The results show that the climatic warming and glacial melt water increasing are much important in this area. According to the study of mass balance change of the Tailan Glacier in the upper reaches of the Tarim River Basin in 1997 by Shen and others (2003), the glacial depth thinned 1.6 m with an average thinning of 0.29 m per year between 1957 and 2000, and the supply of the melt water of the Tailan Glacier reached to 13% between 1957 and 1986 and 23% between 1987 and 2000. That is to say, the glacial melt water runoff increased by 10% in the 1990s, which is similar to the above estimation. According to the study of Yang (1991, 1992), the glacial melt water runoff in the Tarim River Basin was  $202.26 \times 10^8 \text{m}^3$ . If the glacial melt water runoff began to increase in 1972/1973, the glacial ice volume decrease of  $280.291 \times 10^8 \text{m}^3$  would make the glacial melt water runoff increasing by 5% per year since 1972/1973. In fact, the climate was not warm obviously in the 1970s. Evident climatic warming started in the 1980s, and the glacial melt water runoff supply should therefore increased obviously since the 1980s. The study of Ye and others (1999) showed that the runoff in Xinjiang had increased by about 32% since the 1980s, which is equal to an increase of 16% per decade.

According to the previous studies (Yang et al., 1996; Wang et al., 1991), there are 24752 glaciers in Gansu, Qinghai and Xinjiang, the total glacial area is  $31351.09 \text{ km}^2$ , and glacial volume  $3107.8 \text{ km}^3$  with an average glacial thickness of 99.1 m. The estimated glacial volume decrease caused by the glacial retreat is  $258 \times 10^9 \text{ m}^3$  in Northwest China, based on the experimental formula. It is within the range of the value estimated using the relationship between glacial length, area and volume.

## 2. STATE AND ONGOING PROGRAMS OF CHINESE CLIC

The routine monitoring of cryospheric components in China is operated at several overwinter stations (National Stations and Institute-based Stations), as well as some sites that are annually investigated in summer (Figure 7). Year-around monitoring of glacier is operated at Glacier No.1, headwater of Urumuqi River, Tianshan. Summer measurements of glaciers are carried out at institute-based stations and monitoring sites. Year-around monitoring of frozen ground over the Qinghai-Tibetan Plateau is carried out by Germud National Cryosphere Observatory Station, while at some stations, such as Qomulangma, Namuco, Lijiang, Ranwu, integrated observations of atmosphere, cryosphere, hydrosphere and land surface processes were performed. These observations were engaged to a better understanding of the interactions between land surface and atmosphere.

Snow cover (depth) and frozen ground (soil temperature) monitoring has being done at most meteorological stations across Chinese land territory. River ice measurements are performed at hydrological stations over the Yellow River, Songhuajiang River, Lengjiang, Lihe River and rivers in Northwest China. Sea ice observation in Bohai and the north Yellow Seas is carried out using the methods including (1) ground stations (2) remote sensing - including air photos and satellite images (3) ice breaker observations.

**Figure 7** Stations and observation sites that are operated for cryospheric monitoring in the west China

### 2.1 Glacier change monitoring and the second phase glacier inventory in China

For the statistical estimations of glacial changes over specific regions, studies are based on the 1950-1970 topography map and on Landsat TM/ETM+ and Terra ASTERN photos taken during 2000-2002, glacier changes for more than 5000 glaciers in the western China have been studies. The geometrically correct errors of the photos in different areas is usually smaller than two units (30-60 m for TM/ETM+, and 30 m for ASTER). The glaciers are not included in the

statistics where the amplitude of the changes is less than the errors.

Totally 15 areas were selected for this study at present (Figure 8). For the last approximately 50 years and for the forthcoming years. Overall 82.2% percent of measured glaciers have been retreated (Liu et al., 2006). The annual mean percentages of area changes (APAC) of glaciers were vary in different areas. Areas of 3, 5, 6, 8, 11 and 14 in Figure 8 were the least rate of arial retreating ( $APAC < 0.1\%/a$ ), bigger retreating rate were occurred in areas of 2, 4, 10 and 13 ( $0.1\%/a < APAC < 0.2\%/a$ ), while biggest retreating rate occurred in areas of 1, 7, 9, 12 and 15 ( $APAC > 0.2\%/a$ ).

As the first stage (since 2007) of the second phase of Chinese glacier inventory, the above 15 areas have been approved by the Ministry of Science and Technology of China (MoST) for long-term monitoring glacier regions using methods of remote sensing and in situ investigations.

To better understand the overall changes of glaciers in China, higher resolution and tree dimension satellite images such as ASTER, SAR/InSAR and altimetry technique are essential to this purpose. Information of glacier size and ice volume should both be obtained for assessing its contribution to global sea level changes, as well as its impact to the water resources of the arid and semi-arid regions in central Asia.

**Figure 8.** Distribution of monitoring sites of glacier changes using remote sensing methods (Liu et al., 2006). The numbers denotes the sites, they are 1. Gaiz River basin, 2. Yerkant River basin, 3. Hetian River basin, 4. Keriya River basi, 5. Xinqingfeng Ice Cap, 6. Geladangdong Mountian, 7. Pengqu River basin, 8. Gangri Gabu Mountian, 9. A'nyêmaqên mountains, 10. west Qilian Mountains, 11. Aksu River basin, 12. Kaidu River basin, 13. Kashi River basin, 14. Sikesu River basin, 15. Urumuqi River Basin

## 2.2 Routine monitoring of snow cover in China

There are two methods for routine snow survey in China. One is routine observation in weather stations and another is snow mapping from satellite data.

For the conventional observation, there are 612 weather stations for snow observation

routinely. The survey elements include snow fall, snow depth, snow surface temperature, frozen soil.

There is the operational snow cover mapping system in National Satellite Meteorological Center of China in CMA. The research of snow cover remote sensing with satellite data have been started since 1990. An operational system for snow cover mapping over China was set up in December 1996. Based on the analysis of the spectral characteristics between snow, cloud and other types of earth surface with AVHRR data from NOAA-14, a multi-channel thresholds testing method is used to separate snow from cloud. With a spatial resolution of  $0.05^{\circ} \times 0.05^{\circ}$ , pixels covered with snow and the other types of land surface have been discriminated in China and surrounding areas. Extent of the seasonal snow cover can be produced every 10-day from satellite data with the spatial coverage of  $65^{\circ}$ - $145^{\circ}$  E,  $17^{\circ}$ - $57^{\circ}$  N.

With the successful launches of FY-1C,-1D, 2D and NOAA-16, -17 and NOAA-18, The modification study has been done for the multi-spectral thresholds methods. The improved system was set up in 2002. It can produce snow map automatically every 10 day. The spatial resolution of snow data is  $0.02^{\circ} \times 0.02^{\circ}$ .

The satellite snow data from the system have been compared with the NOAA operational snow products and validated against land surface observations. The new system produces more accurate snow cover products over China.

Based on the research on snow survey with satellite data, there are research works carried out on estimating of regional snow depth (SD) and snow water equivalent (SWE) in China with passive microwave SSM/I and ASMR data. The regional algorithms for SD and SWE determination have been developed. Figure 9 shows an example of the results from SSM/I data using the above method.

**Figure 9.** Distribution of snow depth (a,b) and snow water equivalent (c,d) in China from SSM/I data

### **2.3 Frozen ground and related observations along the Qinghai-Tibetan Railway and Highway**

Borehole observations for soil temperature were operated 32 sites, water/heat exchanges at 21 sites over the permafrost zones along the Qinghai-Xizang Railway and Highway (they are almost parallel) (Figure 10). The related measurements also include boundary layer meteorology

(10 sites), automatic weather stations (6 sites), balloon-born (1 site) and energy/mass fluxes (5 sites). Also, in order to monitor the stability of the ground base of railway and highway, there are several sites/ temporal stations were established over the frozen ground areas of the plateau.

**Figure 10.** Permafrost monitoring sites along the Qinghai-Tibet Highway (QTH). The solid dots represent sites for active layer monitoring by GAME-Tibet, open circle and red triangle for borehole monitoring (red triangle by Garmud Observatory Station) (by Zhao Lin, personal communication).

### 2.3 Projects that relates to CliC

There are several ongoing programs and projects focused on or closely related to cryospheric research in China. These projects were funded by the Ministry of Science and Technology of China (MoST), National Natural Science Foundation of China (NSFC), Chinese Academy of Sciences (CAS), China Meteorological Administration (CMA), as well as bilateral cooperation sources. For example: (1) Environmental changes in Tibetan Plateau and its response to global change, as well as adaptation strategy studies (funded by MoST); (2) Observational studies for the glacio-hydrology in the typical areas in Himalayas responding to climate change (CAS); (3) Present processes study on the cryospheric changes in the Qinghai-Tibetan Plateau (CAS); (4) Hydrological effects of the typical glacial and frozen ground changes under global warming (CAS); (5) The study on the response of glaciers in the south Tibetan Plateau to the climate change (CAS); (6) The effect of Indian monsoon and glacial changes to the resources and sustainable development of Li Jiang and Yulong Mountain areas (NSFC); (7) The frozen/thaw processes of the soil in the Tibetan Plateau and its effect on the seasonal transition (CAS). (8) The active layer changes of permafrost on the Tibetan Plateau as well as the seasonal frozen ground changes in the surrounding areas of the plateau during the past decade (CAS); (9) Glacial changes surrounding the Tarim Basin and their impact to water resources (NSFC); (10) Ice-core records, glacial changes and water resources assessment of the Mutztag Glacier, Pamir Plateau (MoST).

There are more than 20 projects specifically for ice-core studies which are not included into

the above summary.

The total amount of funds for the above programs and projects are over 80 million Chinese Yuan, equaling to 12 million US dollars.

### **3. SUMMARY**

Vast cryospheric regions were distributed in China, The major cryospheric components, mountains glaciers, high altitudes frozen ground and snow cover, are distributed over the QXP and surrounding mountains. These components have shown widespread shrinkage over the past decades. More than 80% glaciers are retreating, all parts of frozen ground (including permafrost) are decaying, river ice and sea ice duration are becoming shorter and their extents are becoming smaller. Only snow cover extent in QXP shows an increasing trend, which is different from the overall trend of Eurasian continent.

More than 20 ice cores were retrieved from high altitudes of the west China. These ice cores have illustrated past climate changes from decades to tens of thousands years. In the long term (orbital scale) trend, climate change in QXP shows similar variations, although different in frequencies and amplitudes of the rapid climate events. Climate change in west China for the last two thousands years shows clearly the LIA and MWP, also coincide with the records in East China. In the past decades, climate records in Himalayas show good indicator for the variations of the Indian monsoon.

Snow cover over the plateau exerts big impact on the monsoon onset and its north extent, which determines the drought events or floods in the middle-low reaches of Yangtze River. But monsoon development in turn influences the amount of snow cover over the plateau. This is an important issue in studying the interactions of atmosphere/cryosphere in China.

Monitoring stations or sporadic survey sites for cryosphere in west China are becoming larger in spatially extent. Integrated observations for atmosphere /cryosphere/hydrosphere/land-surface have been operated over several sites and by expeditions in order to gain a better understanding of their interactions and mechanisms.

Increasing financial supports are provided by national sources in recent years. With the facts of global warming, Chinese government pays more and more attention to the cryosphere changes

in China. The relevant studies are valuable to policymakers for socio-economic assessments and managements.

**ACKNOWLEDGEMENTS:** This study is supported by the Ministry of Science and Technology of China (MoST, 2005DFA20930). The authors are grateful to other members of the Chinese National Committee of WCRP/CliC (CNC-CliC) for providing the relevant materials.

**References:**

- Duan, K. Q., T. D. Yao, and L. G. Thompson, 2004: Low-frequency of Southern Asian monsoon variability using a 295-year record from the Dasuopu ice core in the central Himalayas. *Geophys. Res. Lett.*, **31**:doi:10.1029/2004GL020015
- Guo Hui, Li Dongliang, Zhang Qiang, Lu Dengrong, Fen Jianying, Qing Jizu, Tang Maochang, and Shen Zhibao, 2005: Interdecadal variability of seasonal frozen ground depth and its climatic reasons in Hexi Corridor of Gansu. *J. Glaciol. Geocryol.*, **27**(4), 503-508. (in Chinese with English abstract)
- Hou Shugui, Qin Dahe, C. P. Wake, P. A. Mayewski, Ren Jiawen, and Yang Qinzhaohao, 2000: Climatological significance of ice core net-accumulation record at Mt. Qomolangma (Everest). *Chin. Sci. Bull.*, **45**(3), 259-264.
- Kang Ersi, Yang Zhenniang, Lai Zuming, Liu Fengjing, and Ye Baisheng. 2000: Runoff of snow and ice melt water and mountainous rivers. In Shi Yafeng, ed., *Glaciers and Related Environments in China—The Past, Present and the Future*. Beijing: Science Press, 190-233. (in Chinese)
- Kang Shichang, C. P. Wake, Qin Dahe, P. A. Mayewski and Yao Tandong, 2000: Monsoon and dust signals recorded in the Dasuopu firn core, central Himalayas. *J. Glaciol.*, **46** (153), 222-226.
- Li Peiji, 2000: Distribution, annual variations of snow cover in China and its response to the climate change. In Shi Yafeng, ed., *Glaciers and Related Environments in China—The Past, Present and the Future*. Beijing: Science Press, 101-131. (in Chinese)
- Li Zhaorong, Ding Ruijing, Dong Anxiang, Li Rongqin, and Pang Chaoyun, 2005: Distribution of hail falling in the northwest China. In: Zhang Qiang and Kang Fengqin, ed., *Study on Hail Falling in the Northwest China*. Beijing: Chinese Meteorological Press, 359-363. (in Chinese)
- Liu Chaohai, Kang Ersi, and Liu Shiyin, 1999: Study on glacier variation and its runoff responses in the arid region of Northwest China. *Sci. in China (D)*, **42** (supp.): 64-71.

- Liu Jingshi, Norio Hayakawa, Lu Mingjiao, Dong Shuhua, and Yuan Jinying. 2003: Winter streamflow, ground temperature and active-layer thickness in Northeast China. *Permaf. and Perigl. Proc.*, **14**: 11–18.
- Liu Shiyin, Ding Yongjian, Li Jingshi, Shangguan Donghui, and Zhang Yong, 2006: Glaciers in response to recent climate warming in western China. *Quat. Sci.*, **26** (5): 762-771. (in Chinese with English abstract)
- Liu Shiyin, Shen Yongping, Sun Wenxin, and Li Gang, 2002: Glaciers variation since the Maximum of the Little Ice Age in the western Qilian Mountain, Northwest China. *J. Glaciol. Geocryol.*, **24**(3), 227-233. (in Chinese with English abstract)
- Qin Dahe, Hou Shugui, Zhang Dongqi, Ren Jiawen, Kang Shichang, P.A. Mayewski and C.P. Wake, 2002: Preliminary results from the chemical records of an 80.4 m ice core recovered from East Rongbuk Glacier, Qomolangma (Mount Everest), Himalaya. *Ann Glaciol.*, **35**: 278-284.
- Qin Dahe, Liu Shiyin, and Li Peiji, 2006. Snow cover distribution, variability, and response to climate change in western China. *J. Climate*, **19**: 1820-1833.
- Qiu Guoqing, Zhou Youwu and Guo Dongxin, 2000: Chapter 10: Frozen Ground in Northwest China. In: Zhou Youwu, Guo Dongxin, Qiu Guoqing, and Cheng Guodong eds., *Geocryology in China*. Beijing: Science Press, 220-298. (in Chinese).
- Ren Binghui, 1988: Recent fluctuation of glaciers in China. In: Shi Yafeng, Huang Maoheng, Ren Binghui eds., *An Introduction to the Glaciers in China*. Beijing: Science Press, 171-186. (in Chinese)
- Shen Yongping, and Liu Shiyin, 2003: Glaciers mass balance change in Tailanhe River water sheds on the south slope of the Tianshan Mountains and its impact on water resource. *J. Glaciol. Geocryol.*, **25** (2), 124-129. (in Chinese with English abstract)
- Shen Yongping, 2003: Mechanism and Future Regime of Glacial Lake Outburst Flood from Lake Marzbacher in North Inylchek Glacier, Central Asia Tianshan, *J. Glaciol. Geocryol.*, **25** (6), 611-615. (in Chinese with English abstract)
- Shi Yafeng, 2001: Estimation of the water resources affected by climatic warming and glacier shrinkage before 2050 in West China, *J. Glaciol. Geocryol.*, **23** (4), 333-341. (in Chinese with English abstract)
- Shi Yafeng, Shen Yongping, and Hu Ruji, 2002: Preliminary study on signal, impact and outlook of climatic shift from warm-dry to warm-humid in Northwest China, *J. Glaciol. Geocryol.*, **24**(3), 219-225. (in Chinese with English abstract)
- Sun Fenghua, and Yuan Jian, 2005: Characteristics of spatial-temporal variability of maximum and minimum temperatures in northeast China during 1959-2002. *Adv. Clim. Change Res.*, **1**(4), 168-171. (in Chinese)

- Sun Fenghua, Ren Guoyu, Zhao Chunyu, and Yand Suyin. 2005: An analysis of temperature abnormal change in northeast China and type underlying surface. *Sci. Geograph. Sinica*, **25**(2), 167-171.
- Thompson, L.G., T. Yao, M.E. Davis, K.A. Henderson, E. Mosley-Thompson, P.-N. Lin, J. Beer, H.-A. Synal, J. ColeDai, and J. F. Bolzan, 1997: Tropical climate instability : the last glacial cycle from Qinghai-Tibetan Plateau. *Science*, **276**, 1821-1825.
- Tian, L., T. Yao , P. F. Schuster, J. W. C. White, E. Ichiyangi, E. Pendall, J. Pu, and W. Yu, 2003: Oxygen-18 concentrations in recent precipitation and ice cores on the Tibetan Plateau, *J. Geophys. Res.*, **108**, D9, ACH 16-10.
- Wang Ninglian, 2005: Decrease trend of dust event frequency over the past 200 years recorded in the Malan ice core from the northern Tibetan Plateau. *Chin. Sci. Bull.*, **50**(24), 2866-2871.
- Wang Ninglian, Yao Tandong, Pu Jianchen, Zhang Yongliang, Sun Weizhen, and Wang Youqing. 2003: Variations in air temperature during the last 100 years revealed by  $\delta^{18}\text{O}$  in the Malan ice core from the Tibetan Plateau. *Chin. Sci. Bull.*, **48** (19), 2134-2138.
- Wang Qiuxiang, Li Hongjun, Wei Rongqing, and Wang Xiaomei. 2005: Annual change and abrupt change of the seasonal frozen soil in Xinjiang, China during 1961-2002. *J. Glaciol. Geocryol.*, **27** (6), 820-826. (in Chinese with English abstract)
- Wang Zongtai, and Yang Huian, 1991: Characteristics of the distribution of glaciers in China. *Ann. Glaciol.*, **6**: 17-20.
- Wu Qingbai, and Liu, Yongzhi, 2003: Ground temperature monitoring and its recent change in Qinghai-Tibet Plateau. *Cold Regions Sci. Technol.*, **18**: 85-92.
- Xiao Cunde, Liu Shiyin, Zhao Lin, Wu Qingbai, Li Peiji, Liu Chunzhen, Zhang Qiwen, Ding Yongjian, Yao Tandong, Li Zhongqin, and Pu Jiancheng, 2007: Observed changes of cryosphere in China over the second half of the 20th century: an overview. *Ann. Glaciol.*, **46** (in press)
- Xie Zichu, Wang Xin, Feng Qinghua, Kang Ersi, Li Qiaoyuan, and Cheng Lei, 2006: Glacier runoff in China: an evaluation and prediction for the future 50 years. *J. Glaciol. Geocryol.*, **28** (4), 457-466. (in Chinese with English abstract)
- Yang Hui'an, Mi Desheng and Kang Xingcheng, 1996: The distribution and features of glacier resource in Northwest China. In: *Proceeding of the Fifth Chinese Conference on Glaciology and Geocryology (Vol.1)* (edited by the Glaciology and Geocryology Society of China), Lanzhou: Gansu Culture Press, 175-181. (in Chinese)

- Yang Zhengniang, 1991: Glacier water resources in China. Lanzhou: Gansu Science and Technology Press, 1-158.  
(in Chinese)
- Yang Zhenniangu, 1995: Glacier meltwater runoff in China and its nourishment to river, *Chin. Geograph. Sci.*, **5**, 66-76.
- Yang Zhenniangu, and Hu Xiaogang, 1992: Study of glacier melt water resources in China, *Ann. Glaciol.*, **16**, 141-145.
- Yao Tandong, 2002: An introduction of the ice core research over the Qinghai-Tibetan Plateau. *Bullet. NSFC*, **16** (2), 96-98. (in Chinese)
- Yao Tandong, L.G. Thompson, Shi Yafeng, Qin Dahe, Jiao Keqing, Yang Zhihong, Tian Lide, and E. M. Thompson, 1997: Climate changes since the Last Interglacial recorded in the Guliya ice core. *Sci in China (D)*, **40**, 662-668.
- Yao Tandong, Y. Ageta, and T. Ohata, 1991: Preliminary results from China-Japan Glaciological Expedition in Tibetan Plateau in 1989. *J. Glaciol. Geocryol.*, 13(1), 1-8. (in Chinese with English abstract)
- Yao Tandong, Duan Keqin, Tian Lide, et al., 2001: Changes of the accumulation rate in Dasuopu ice core and summer monsoon. *Geophys. Res. Lett.*, **28** (23): 4499-4502.
- Yao Tandong, Jiao Keqin, Tian Lide et al., 1996: Climatic variations since the Little Ice Age recorded in the Guliya ice core, *Sci. in China (D)*, **39**, 588-596.
- Yao Tandong, L. G. Thompson, Duan Keqin, Xu Baiqing, Wang Ninglian, Pu Jianchen, Tian Lide, Sun Weizhen, Kang Shichang, and Qin Xiang, 2002: Temperature and methane records over the last 2 ka in Dasuopu ice core. *Sci. in China (D)*, **45** (12), 1068-1074.
- Yao Tandong, Lonnie Thompson, Qin Dahe et al., 1997: Variations in temperature and precipitation in the past 2000 years on the Xizang (Tibet) Plateau— Guliya ice core record. *Sci. in China (D)*, **39**, 425-433.
- Yao Tandong, Wang Youqing, Liu Shiyong, Pu Jianchen, Shen Yongping, and Lu Anxin, 2004: Recent glacial retreat in High Asia in China and its impact on water resource in Northwest China. *Sc. in China (D)*: **47** (12), 1065-1075.
- Ye Baisheng, Ding Yongjian, Kang Ersi et al. 1999: Response of the snowmelt and glacier runoff to the climate warming-up in the last 40 years in Xinjiang Uygur Autonomous Region, China. *Sci. in China (D)*, **42**, 44-51.
- Zhai P., and X. H. Pan, 2003: Trends in temperature extremes during 1951-1999 in China. *Geophys. Res. Lett.*, **30** (17), 1913.

- Zhang Luxin, 2000: Regularity of ground temperature variation in Qinghai-Tibet Plateau permafrost region and its effect on subgrade stability. *China Railway Science*, **21**(1): 37-47. (in Chinese with English abstract)
- Zhang Qiwen, 1993: On forecasting disastrous sea ice conditions in the Bohai Sea. In: Yu Zhouwen, C. L. Tang, R. H. Preller, and Wu Huiding eds., *Proceedings of 93's International Symposium on Sea Ice*. Beijing, China Ocean Press, 189-197.
- Zhang Xiangsong, Zheng Benxing, and Xie Zichu, 1981: Recent variations of existing glaciers on the Qinghai-Xizang (Tibet) Plateau. In: *Geological and Ecological Studies of Qinghai-Xizang Plateau Science* (edited by China Society on the Tibetan Plateau), Beijing: Science Press, 1625-1629.
- Zhao H, and G. Moore, 2004: On the relationship between Tibetan snow cover, the Tibetan plateau monsoon and the Indian summer monsoon. *Geophys. Res. Lett.*, **31**, L14204, doi:10.1029/2004GL020040.
- Zhao Lin, C. Ping, D. Yang, et al., 2004: Changes of Climate and Seasonally Frozen Ground over the Past 30 Years in Qinghai-Xizang (Tibetan) Plateau, China. *Global and Planetary Change*, **43**, 19-31.
- Zhao Lin, Cheng Guodong, and Li Shuxun, 2003: Changes of plateau frozen-ground and environmental engineering effects. In: Zheng Du eds., *The formation environment and development of Qinghai-Tibet Plateau*. Shijiazhuang: Hebei Science and Technology Press, 143-150. (In Chinese)
- Zhou Youwu, Gao Xingwang, and Wang Yinxue, 1996: The ground temperature changes of seasonally freeze-thaw layers and climate warming in Northeast China in the past 40 years. In: *Proceeding of the 5th Chinese conference on glaciology and geocryology (Vol. 1)*. Lanzhou: Gansu Culture Press. 3-9. (In Chinese)

## Caption of Tables

**Table 1.** Proportions of advancing and retreating glaciers in the High Asia in China in different stages (Yao et al., 2004)

<i>Time</i>	<i>Glaciers</i>	<i>Retreating Glaciers (5)</i>	<i>Advancing glaciers (%)</i>	<i>Stable glaciers (%)</i>	<i>Reference</i>
1950-1870	116	53.44	30.17	16.37	
1970-1980	224	44.2	26.3	29.5	
1980-1990	612	90	10	0	
1990-present	612	95	5	0	

**Table 2.** The Estimated glacier runoff in China (Based on Kang et al., 2000; Xie et al., 2006)

Discharge basin	Glacier area (km <sup>2</sup> )	River runoff (×10 <sup>8</sup> m <sup>3</sup> )	Glacier melt water supply (×10 <sup>8</sup> m <sup>3</sup> )		Percentage of the supply (%)	
			Xie	Kang	Xie	Kang
Hexi Corridor	1334.75	72.40	11.94	9.99	16.5	13.8
Zhunger Basin	2254.10	125.0	33.65	16.89	26.9	13.5
Tulufan-Hami Basin	252.73	--	3.6	1.9	--	--
Yili River	2022.66	193.0	37.14	26.41	19.2	13.7
Tarim Basin	19878	347.0	126.5	133.42	36.2	38.5
Chadamu Basin	1865.05	66.9	13.51	6.31	28.4	9.4
Hala Lake	25.50	3.2	0.11	0.12	3.4	3.8
Qiangtang Plateau	7836	246.0	29.18	39.10	11.9	15.9
<b>Subtotal of inflow</b>	35389.71	1053.5	255.6	234.14	24.3	22.2
Yangtze River	1895.00	177.0	15.52	32.71	8.8	18.5
Yellow River	171.41	209.0	1.74	2.86	0.8	1.3
E'rqisi River	289.29	100.0	7.73	3.62	7.7	3.6
Nancangjiang River	316.32	109.0	4.43	7.16	4.0	6.6
Nujiang River	1730.20	409.0	24.26	35.98	5.9	8.8
Ganges River	18161.44	3103.1	299.5	280.48	9.7	9.1
Indus River	1451.26	17.2	6.95	7.70	40.4	44.8
<b>Subtotal of outflow</b>	24016.44	4122.3	360.0	370.51	8.7	9.0
<b>Total</b>	59425	5157.8	615.7	604.65	11.9	11.7

## Caption of Figures

**Figure 1.** Distribution of major cryospheric components in China. Glacier distribution (a), frozen ground distribution (b) and snow cover distribution (c).

**Figure 2.** Changes of days with frost in China during 1951-1999 (Zhai and Pan, 2003)

**Figure 3.** Distribution and changes of hailstone fallings in the northwest China (a. changes of annual hailstone falling events in NW China during 1960-2000; b. spatial distribution of hail falling in NW China) (Li et al., 2005)

**Figure 4.** Regional features of the glacial fluctuations since the Little Ice Age (LIA) in the west China.

**Figure 5.** Interannual variability of snow cover over China during the past 50 years. a) Xinjiang, b) Qinghai-Xizang Plateau (QXP) and c) Inner Mongolian-Northeast China (IM-NEC) region

**Figure 6.** Distribution of ice cores that have been drilled in west China

**Figure 7.** Stations and observation sites that are operated for cryospheric monitoring in the west China

**Figure 8.** Distribution of monitoring sites of glacier changes using remote sensing methods (Liu et al., 2006). The numbers denotes the sites, they are 1. Gaiz River basin, 2. Yerkant River basin, 3. Hetian River basin, 4. Keriya River basi, 5. Xinqingfeng Ice Cap, 6. Geladandong Mountian, 7. Pengqu River basin, 8. Gangri Gabu Mountian, 9. A'nyêmaqên mountains, 10. west Qilian Mountains, 11. Aksu River basin, 12. Kaidu River basin, 13. Kashi River basin, 14. Sikeshu River basin, 15 Urumuqi River Basin

**Figure 9.** Distribution of snow depth (a,b) and snow water equivalent (c,d) in China from SSM/I data

**Figure 10.** Permafrost monitoring sites along the Qinghai-Tibet Highway (QTH). The solid dots represent sites for active layer monitoring by GAME-Tibet, open circle and red triangle for borehole monitoring (red triangle by Garmud Observatory Station) (by Zhao Lin, personal communication).

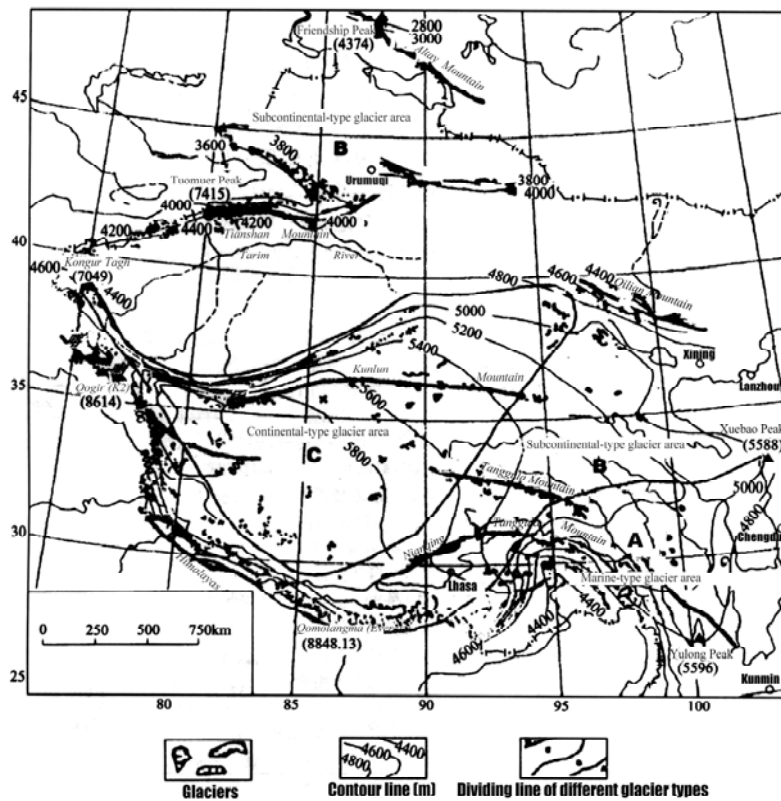


**Figure 1a.** Distribution of major cryospheric components in China. Glacier distribution (a)

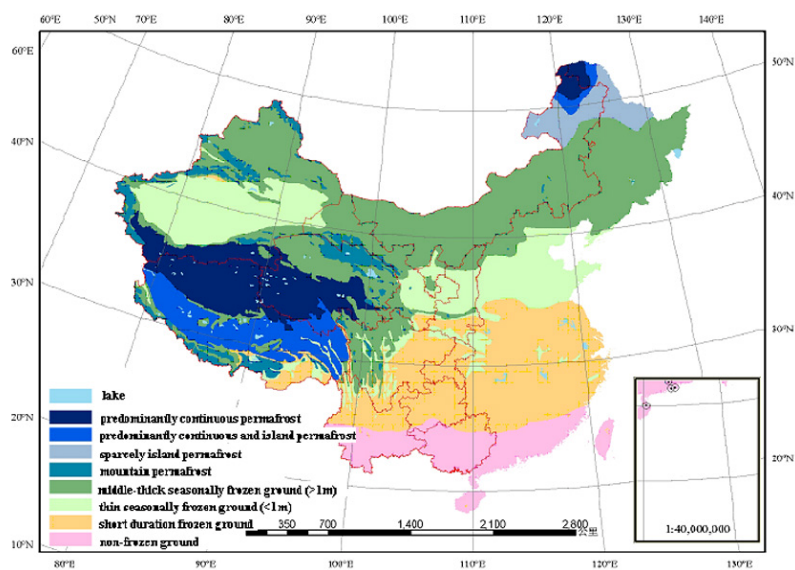


**Figure 1b.** Distribution of major cryospheric components in China. Frozen ground distribution (b)

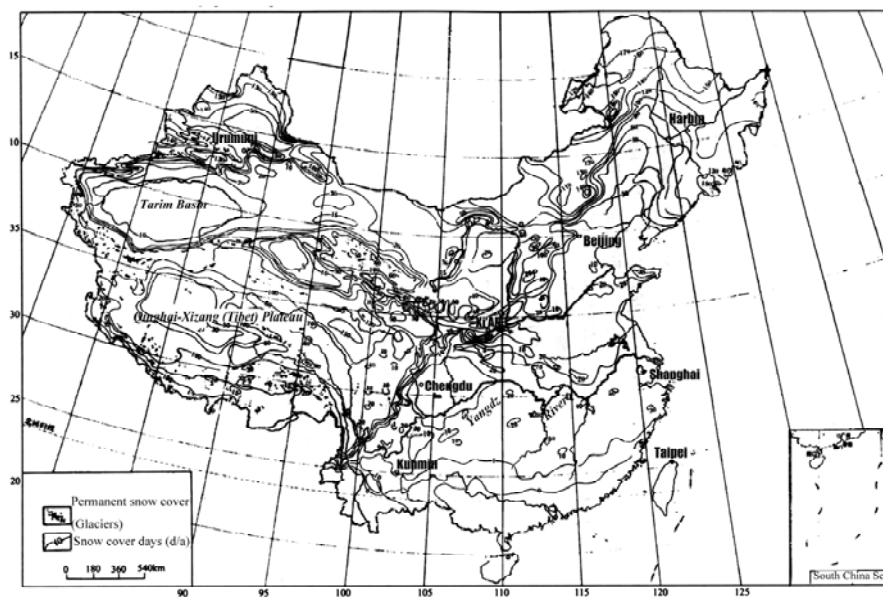


**Figure 1c.** Distribution of major cryospheric components in China. Snow cover distribution (c).

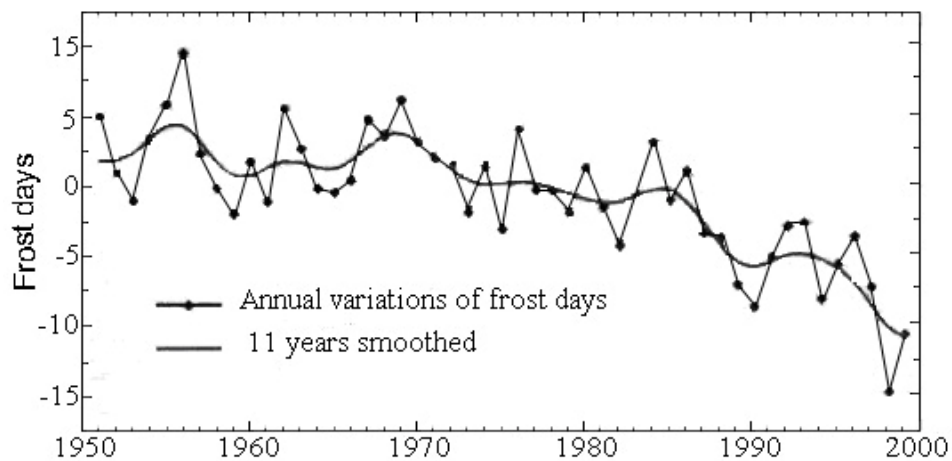


**Figure 2.** Changes of days with frost in China during 1951-1999 (Zhai and Pan, 2003)

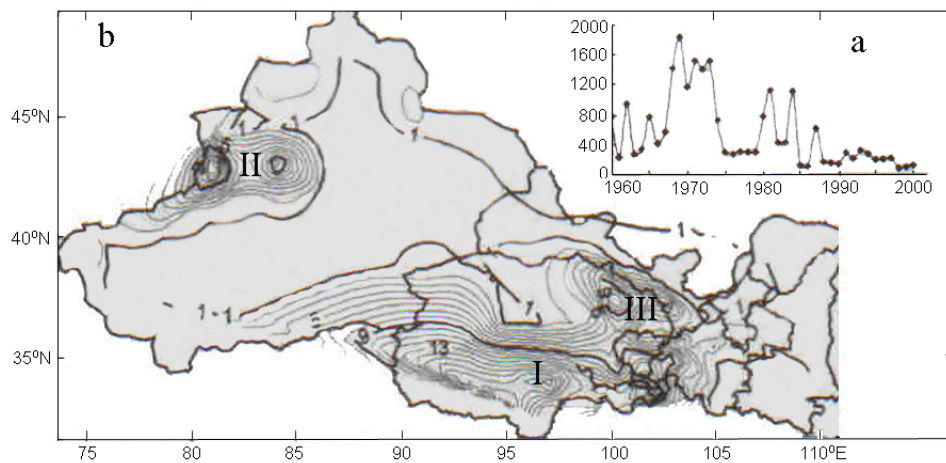


**Figure 3.** Distribution and changes of hailstone fallings in the northwest China (a. changes of annual hailstone falling events in NW China during 1960-2000; b. spatial distribution of hail falling in NW China) (Li et al., 2005)

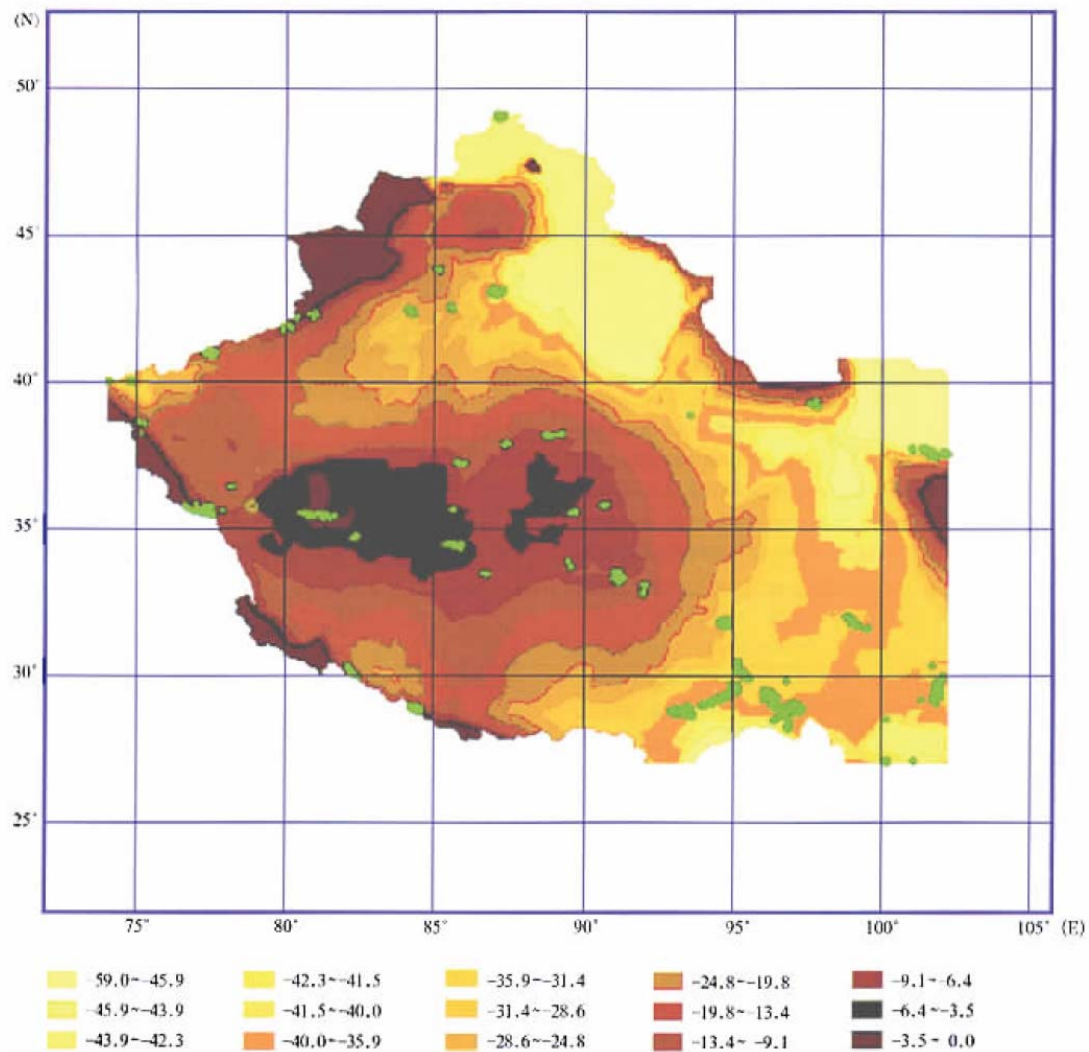


**Figure 4.** Regional features of the glacial fluctuations since the Little Ice Age (LIA) in the west China.

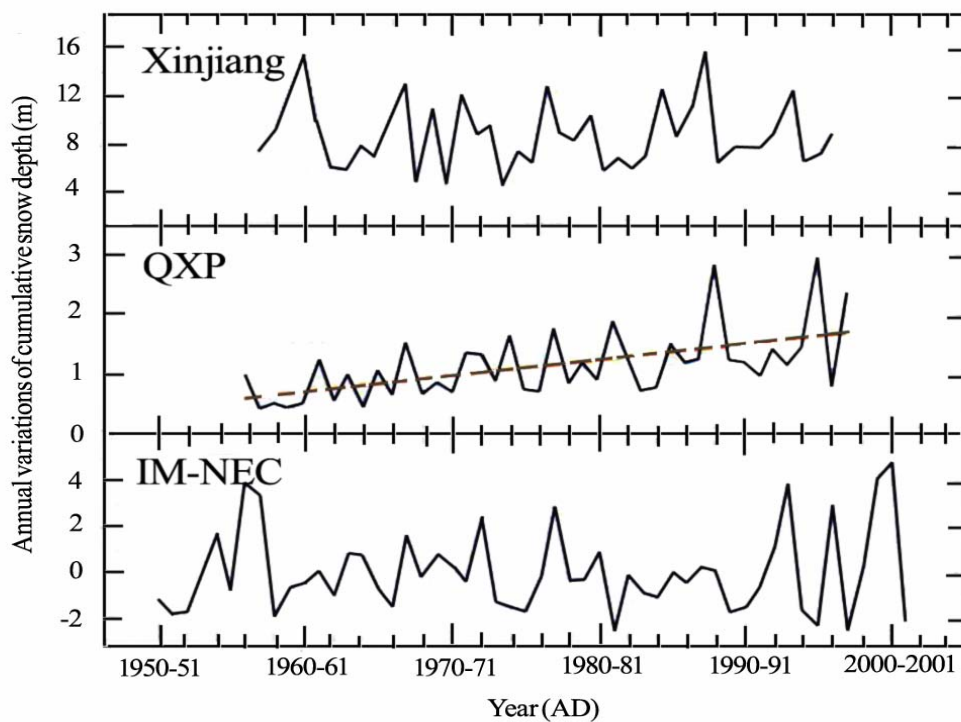


**Figure 5.** Interannual variability of snow cover over China during the past 50 years. a) Xinjiang, b) Qinghai-Xizang Plateau (QXP) and c) Inner Mongolian-Northeast China (IM-NEC) region.



**Figure 6.** Distribution of ice cores that have been drilled in west China

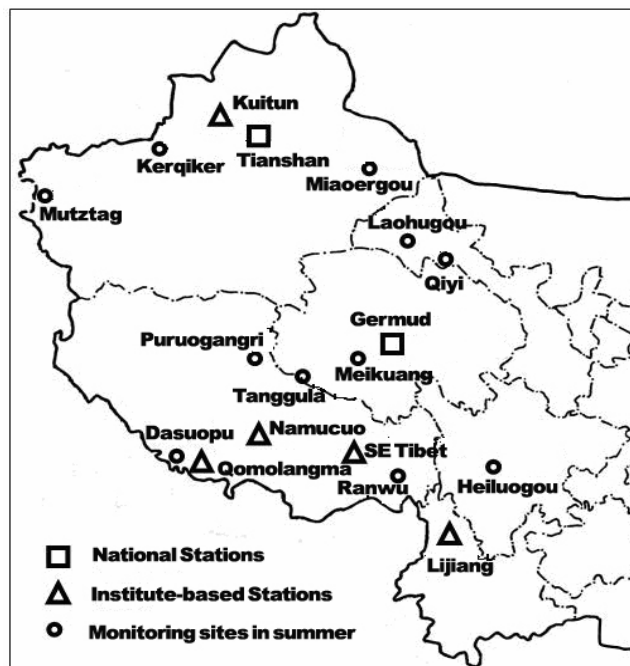


**Figure 7.** Stations and observation sites that are operated for cryospheric monitoring in the west China.

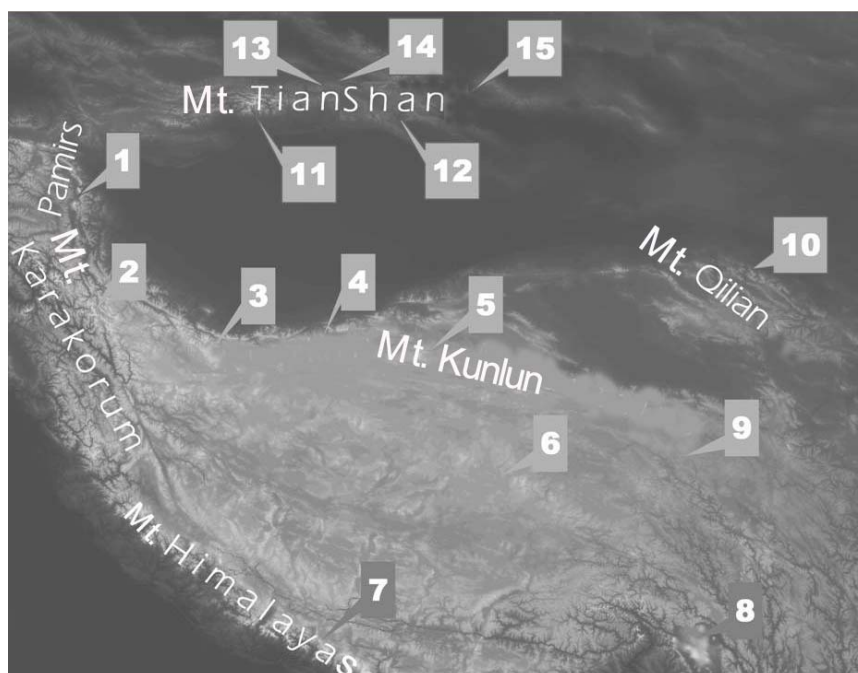


**Figure 8.** Distribution of monitoring sites of glacier changes using remote sensing methods (Liu et al., 2006). The numbers denotes the sites, they are 1. Gaiz River basin, 2. Yerkant River basin, 3. Hetian River basin, 4. Keriya River basin, 5. Xinqingfeng Ice Cap, 6. Geladangdong Mountain, 7. Pengqu River basin, 8. Gangri Gabu Mountain, 9. A'nyêmaqên mountains, 10. west Qilian Mountains, 11. Aksu River basin, 12. Kaidu River basin, 13. Kashi River basin, 14. Sikeshu River basin, 15. Urumuqi River Basin

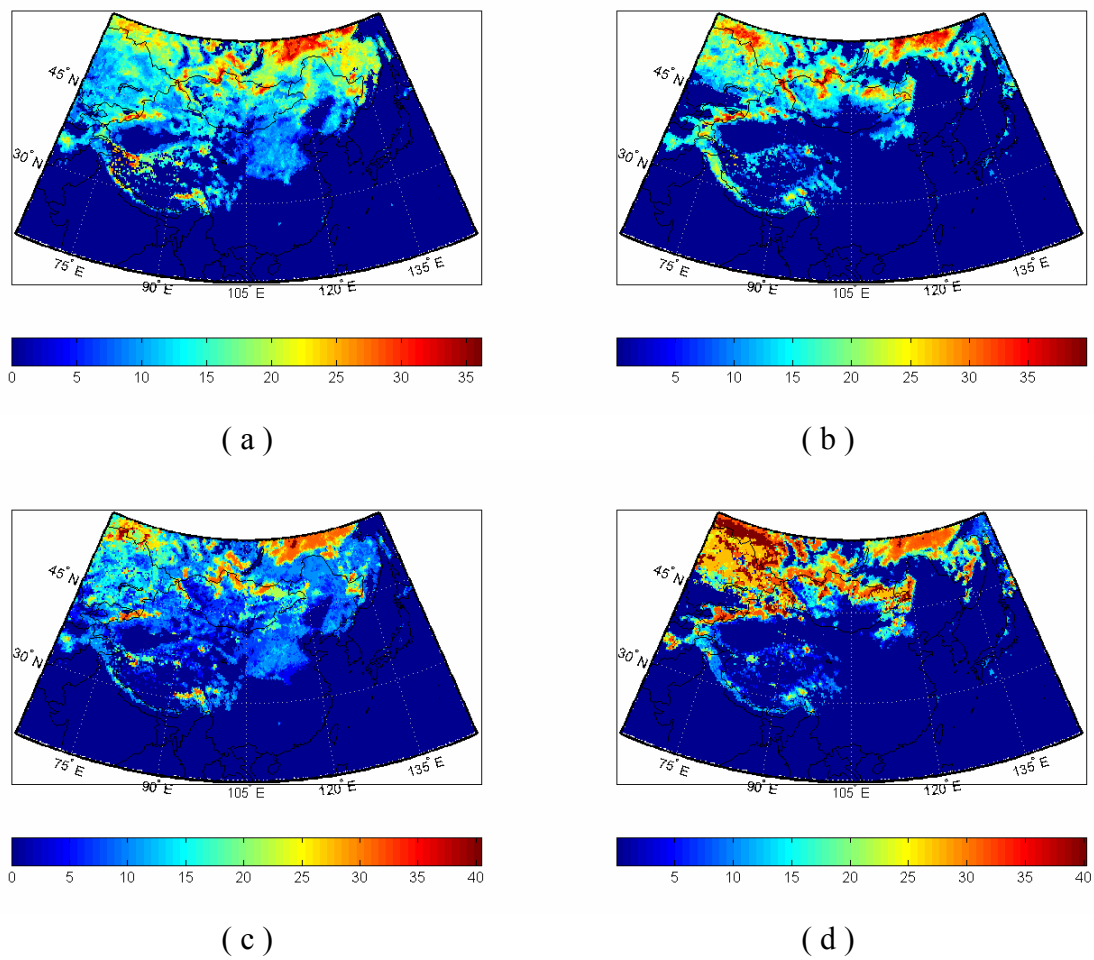


**Figure 9.** Distribution of snow depth (a,b) and snow water equivalent (c,d) in China from SSM/I data

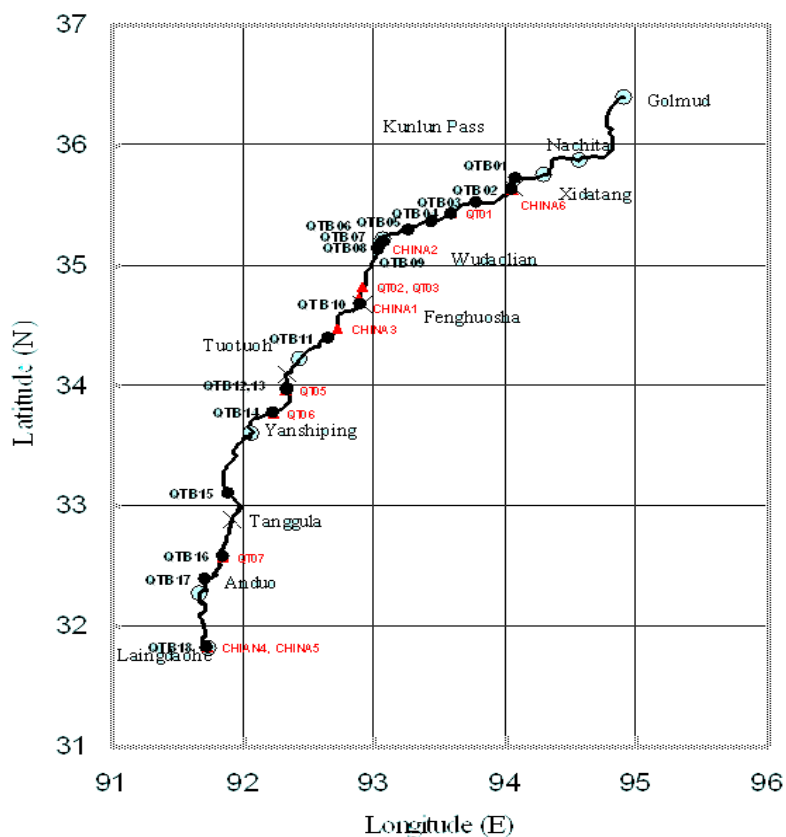


**Figure 10.** Permafrost monitoring sites along the Qinghai-Tibet Highway (QTH). The solid dots represent sites for active layer monitoring by GAME-Tibet, open circle and red triangle for borehole monitoring (red triangle by Garmud Observatory Station) (by Zhao Lin, personal communication).

# NUMERICAL WEATHER PREDICTION IN CHINA IN THE NEW CENTURY- PROGRESS, PROBLEMS AND PROSPECT

*XUE Jishan (薛纪善) LIU Yan (刘艳)*

State Key Laboratory of Severe Weather, Chinese Academy of Meteorological Sciences, Beijing 100081

Email of corresponding author: jsxue@cma.gov.cn

## Abstract

The progresses in the research and development of numerical weather prediction (NWP) in China during 2003 and 2006 are review in this paper, focusing on the new methodologies of data assimilation, high resolution NWP model, global medium range assimilation and prediction system, model physics, ensemble prediction and application of NWP models in environmental problems. GRAPES ( Global and Regional Assimilation PrEdiction System), a new generation numerical prediction system developed by Chinese scientists, has become full operation recently after an extensive series of pre-operational trials, indicating that the strengthening of Chinese innovation capability as a whole. Besides the promotion of operational implements of GRAPES, new progresses in the development of GRAPES four dimensional variational data assimilation and other researches are made. Many successes not within the project of GRAPES have also been seen, including the new methodologies of data assimilation in new observations, precipitation prediction model, mesoscale ensemble prediction, and application in environmental problems, etc. Finally, some important scientific issues for further development of Chinese NWP and its prospects are discussed. The assimilation of remote sensing data, and the optimization and development of model physics fitting the climatic and geographic features in the East Asian monsoon area, are the key directions to increase the forecast accuracy of NWP in China.

**Key words:** progress, numerical weather prediction, data assimilation, high resolution model, global medium range prediction, ensemble prediction

## 1. Introduction

The key roles of numerical weather prediction (NWP) in the meteorological operations and services are recognized much more widely in recent years by Chinese atmospheric scientist community and decision makers than ever before, and the development of new NWP systems based on the state of art technologies is emphasized in the national research and development programs. This situation brings the new era in Chinese NWP development which is featured by the prominent achievements in the development of Chinese new generation NWP systems.

As the results of the national key research and development project “ Global and Regional Assimilation Prediction System (GRAPES in short)”, whose objectives and main components has been reviewed in an earlier paper ( Xue, 2004), the new regional NWP system GRAPES-Meso is now run operationally and pre-operational experiments of the new global NWP system GRAPES-Global are conducted in Chinese National Meteorological Center (CNMC) and some regional meteorological centers. In comparison with the operational NWP systems formerly used in most Chinese operational NWP centers and in numerical modeling researches by most Chinese scientists, all components of GRAPES are developed with the efforts of Chinese scientists. This fact indicates the enhancement of Chinese innovative capability in the areas of numerical model and relevant sciences, and prefigures more pronounced progresses in the numerical prediction directly related to the Chinese high impact weather events in the future. After the project mentioned above is ended by the end of 2005, a new national key research and development

project has been launched which focuses on the operational application of GRAPES systems and ensures the further development of GRAPES systems.

In addition to the works and results under the framework of GRAPES, researches in NWP dealing with much wider topics are also underway funded by some other national projects. All these researches stress the potential improvements of NWP for high impact weathers in China by introducing new concepts or methodologies, even though they may not have direct operational goals as GRAPES does. Among them is the national fundamental theoretical research project “Studies on the flooding rains in the South China” which takes the development of cloud resolving model as one of its main goals. It is no exaggeration to say that the past years are among the most fruitful periods in Chinese history of NWP development.

This paper reviews the recent progresses of NWP researches since the last overview (Xue, 2004) is published, with the stresses in the achievements of GRAPES project, for they constitute the main advances in NWP in China. Important results other than GRAPES project are also summarized in order to depict the panorama of development of NWP in China. The context is organized in a way to give prominence to results of great importance in promoting NWP development.

## **2. Data Assimilation**

### **2.1 Development of GRAPES-Var and GRAPES-EnKF**

GRAPES-Var is the variational data assimilation component of GRAPES, including GRAPES-3DVar( GRAPES Three Dimensional Variational analysis) and GRAPES-4DVar( GRAPES Four Dimensional Variational analysis). The global version of

GRAPES-3DVar inherits most subroutines from the regional version, which has been developed in 2001-2002 and briefly described by Xue (2005), except that a spectral filter takes the place of a recursive filter in the latter for preconditioning of control variables. Assimilation cycles combining GRAPES-3DVar, both for regional and global versions, and GRAPES prediction models are built up and an extensive series of pre-operational trials are conducted. After revises based on the batch experiments GRAPES-3DVar is capable of directly assimilating both conventional and unconventional observation data, such as radiances from polar orbital satellite NOAA15, NOAA16 and NOAA17, atmospheric vectors from geostationary satellites and Velocity Azimuth Display (VAD) data from Doppler radar, etc. The use of remote sensing data in GRAPES-3DVar is of great significance in alleviation of the sparseness of conventional observational data in NWP.

Following GRAPES-3DVar, GRAPES-4DVar is developed (Xue, 2006). It is the extension of GRAPES-3DVar in such a way that the time integration of prediction model is introduced into the assimilation system to assimilate all observations distributed within a time window, thereby get the flow-dependent background error distribution. Preliminary results of experiments of GRAPES-4DVar with real conventional and unconventional observational data are encouraging, showing substantial improvements of forecasts in comparison with those of GRAPES-3DVar. GRAPES-4DVar is the first four dimensional variational assimilation system capable of implementation in real operational environment developed in China, and among a few variational assimilation systems based on non-hydrostatic prediction model currently available all over the world. Its accomplishment means a breakthrough in the area of data assimilation in China, and sets up the foundation for further updating of Chinese data assimilation system. The tangent linear and adjoint of GRAPES prediction model in GRAPES-4DVar are completed by using an automatic

differential tool YHTAD developed by mathematicians participating in GRAPES project. The tangent linear and adjoint of GRAPES may be used in studies of sensitivity of forecast errors to the initial conditions and other model parameters, as well as application in ensemble forecast systems.

GRAPES-EnKF (GRAPES- Ensemble Kalman Filter) developed recently is an alternative in data assimilation of GRAPES. Its outstanding feature is that it is based on the GRAPES-3DVar so that it shares most codes, including optimization algorithm and observation operators of 3DVar, with the covariance matrix of background error derived from ensemble statistics so as to take the flow-dependent features of model errors into account. GRAPES-EnKF may superior to 4DVar for only the forward model rather than the linear tangential and adjoint is integrated, the latter two being controvertible in cases when strong nonlinear physical processes dominate. It will be a candidate in the future assimilation focusing on severe storms, and adopted in constructing an ensemble prediction system combining the assimilation and creation of initial perturbation as one complete step. A diagnostic system based on ensemble transform Kalman filter(ETKF) in frame of GRAPES-EnKF has also been built to study the approaches to identifying the areas to which the prediction errors are sensitive and the impacts of targeted observations on model forecasts. Case studies show positive effects of extra observations in the upstream over the northwestern Pacific on the prediction of tropical cyclones landing on China.

## **2.2 New Methodologies of Data Assimilation**

The researches on data assimilation not within the project of GRAPES in recent years focus mainly on the new approaches of variational data assimilation or methodologies different from

3DVar or 4DVar. A new approach called “3-dimensional variational data assimilation of mapped observation (3DVM)” is proposed, based on the new concepts of mapped observation and backward 4DVar (Wang and Zhao, 2005). 3DVM produces an optimal initial condition (IC) that is consistent with the prediction model by taking the model as dynamical and physical constraints and is best fitted to the observations within the assimilation window through the model solution trajectory. The main difference between the concepts of 3DVM and the 4DVar lies in that the IC derived from 3DVM is referred to the end rather than the beginning of the assimilation window. The new approach reduces the computing cost greatly and also improves the assimilation accuracy, for the tangent linear and adjoint approximations in calculating the gradient of cost function are avoided. It is shown in a case study of assimilation of AMSU-A (Advanced Microwave Sounding Unit- A) data that the new approach produces better IC for 72-hour simulation than 4DVar does with 1/7 computing costs of 4DVar. Mu et al. (2003) study the problem in variational data assimilation related to the “on-off” switches in physical parameterizations of the NWP models. They analyze the impacts of different treatments of switches in tangent linear models on the minimizing the cost function in 4DVar and indicate that keeping the switches in the tangent linear model same as in the forward model might yield a local minimum rather than the global minimum if the cost function has multiple minima. They propose a new way to obtain the global descent direction which is helpful to find the global minimum ( Mu et al., 2005).

Qiu and Chou (2005) propose an approach of four-dimensional data assimilation called 4DSVD based on Singular Value Decomposition (SVD) derived from a coupled data set which is created by integrating the NWP model and simulated observational operators. The analysis is simply completed by projecting the observational data onto the space spanned by the singular

vectors. Four-dimensional data assimilation is simplified to a linear inverse problem with their approach so that the adjoint of both prediction model and observational operators and the covariance matrix of background error are no longer needed.

### **2.3 Remote Sensing Data Assimilation**

The development of GRAPES-Var builds a base for assimilation of most remote sensing data, among which the ATOVS(Advanced TIROS Operational Vertical Sounder) onboard the polar orbiting satellites of NOAA series dominates by far the volume currently ingested into GRAPES system. Results from a number of trials have demonstrated the positive impacts of direct assimilation of ATOVS data with GRAPES-3DVar on predictions of track and intensity of tropical cyclones (Dong et al., 2005) . In order to improve the practical effects of the assimilation of satellite data, a few scientific issues have been studied. Dong et al. (2005) test an algorithm to improve the estimation of emissivity of land surface in microwave band. The land surface emissivity is firstly retrieved from specific channels sensitive to land surface characteristics, and then these retrieved values are fed into the radiation transfer model for other channels. Real data experiments show that the new scheme results in better performance of GRAPES-Var.

Direct assimilations of the data of radial velocity and reflectivity derived by Doppler weather radars have also been studied in the frames of GRAPES-3DVar. In order to assimilate these data, new control variables of vertical velocity and the parameters of cloud microphysics and new observation operators are introduced into GRAPES-Var. It is shown that Radar data assimilations not only improve the analysis of wind field, but also provide cloud information, resulting in positive impacts on the prediction of mesoscale storms ( Gu, 2006). The assimilation of radar data gives a way to initialize the clouds for time integration of NWP model with explicit cloud scheme

rather than using convective parameterization. This so called “hot start” of model integration results in better forecast in a trial of rainstorm event than so called “cold start” and has the potential to improve very short term forecast (Liu, 2006). Positive contributions of remote sensing data on the mesoscale NWP are also shown by researches with GRAPES or other systems (e.g. Xu et al., 2004; Wan et al., 2006; Li et al, 2006; Zhang and Ni, 2006).

With the increase of the number of available ground and space based GPS data, more and more scientists devote to assimilating this kind data into NWP models, most showing obvious positive impacts. An experiment with the data of atmospheric precipitable water ( PW ) obtained from a net of 11 ground GPS receivers in the Yangtze River Delta show that using GPS PW results in better forecasts of 6h accumulated precipitation prediction in earlier hours of model integration ( Yuan, et al., 2004). The observational operators for space based GPS in terms of bending angle or ray-tracing method are developed with improved parallel computing algorithm, setting up a base for assimilation of GPS/MET (Wang et al., 2003; Zhang et al., 2003).

### **3. High Resolution Model and Quantitative Precipitation Forecast**

GRAPES is designed to meet the need of numerical prediction for different scales with the stress on very-high-resolution modeling. A number of idealized tests, such as the density flow and mountain wave, and the spectral analyses of kinetic energy derived from GRAPES model output with different resolution are conducted in order to evaluate the ability of the model to simulate the atmospheric motions in different scales. The results accord well with the theoretical solutions and the non-hydrostatic models developed in recent years abroad. These results show that upgrading model resolution and introducing non-hydrostatic dynamics improve the modeling of small scale motion without harmful impact on large scale motions, and the use of semi-Lagrangian scheme of

time integration for non-hydrostatic model with very high resolution is acceptable, supporting the feasibility of an unified dynamic core applied to models for diverse usages in GRAPES (Xue, 2006).

The prediction model of GRAPES may be implemented with limited area or global configurations and a number of options of model physical schemes are provided. Table 1 lists physical parameterization schemes currently available in GRAPES model for regional setting. The regional GRAPES model and GRAPES-Var constitute an assimilation and prediction system GRAPES-Meso which is in fully operational implementation in the national and a few of regional meteorological centers after long time pre-operational experiments. The performance of the new operational NWP system is comparable to those of operational NWP models of other countries. In cases of typhoon or tropical cyclones over northwestern Pacific, the new typhoon model based on GRAPES-Meso gives the minimal forecast error of the tracks during 2003-2005.

AREM is an advanced version of a regional Eta-coordinate model (REM) developed since 1980s which intends to handle effects of the Tibetan Plateau and many other steep mountains in NWP model. The recent developments include increasing spatial resolutions and updating physical parameterizations. It is run operationally in Hunan, Hubei and Anhui Provincial Bureau of Meteorology along the Yangtze River, researches showing the great capabilities of AREM in forecasting the heavy rainfall events over most of China region. Case studies show that the AREM captures reasonable structures and evolutions of the rainfall systems along the Yangtze River (Yu et al., 2004).

A high resolution non-hydrostatic tropical atmospheric model is developed by using a ready-made regional atmospheric modeling system (Shen and Sumi, 2005). The motivation is to

investigate the convective activities associated with the tropical intra seasonal oscillation (ISO) through a cloud resolving calculation. Due to limitations in computing resources, a 2000 km×2000 km region covering the forefront of an ISO-related westerly is selected as the model domain, in which a cloud-resolving integration with a 5-km horizontal resolution is conducted. The results indicate the importance of stratus-cumulus interactions in the organization of the cloud clusters embedded in the ISO. In addition, comparative integrations with 2-km and 5-km grid sizes are conducted, which suggest no distinctive differences between the two cases although some finer structures of convections are discernible in the 2-km case. The significance of this study resides in supplying a powerful tool for investigating tropical cloud activities without the controversy of cloud parameterizations. The parallel computing method applied in this model allows sufficient usage of computer memory, which is different from the usual method used when parallelizing regional model.

#### **4. Development of Global Medium Range Prediction**

GRAPES-Global is the first global medium range assimilation and prediction system developed by Chinese scientists, and is one of a few non-hydrostatic global models in the world. It inherits many features of GRAPES-Meso with the refinements of model focused on reducing the errors due to the spherical geometry and optimization of physical parameterization schemes for diverse geographic and climatic condition. Besides, efficient scheme of parallel computing for global configuration needs to be handled. The prototype of GRAPES-Global is completed around 2004. To verify the dynamical frame of GRAPES-Global, three experiments: poleward flow, balanced flow and Haurwitz wave experiments are conducted. Results from these experiments

demonstrate the coherency with other mature global models or the theoretical solutions. A series of hindcase trials have been undertaken using GRAPES-Global assimilation and prediction system since 2005. Figure 1 presents 500hPa height anomaly correlation coefficient (ACC) averaged over five months in the summer and winter of 2005. For comparison, the results of current national operational global medium range assimilation and prediction system (T213) are also displayed. The significant improvement in forecast skill of GRAPES-Global is seen in this figure. Tests for selected cases of high impact weather events in recent years, e.g. typhoon Matsa (Fig.2), give similar results. The success of GRAPES-Global demonstrates the overall progress of Chinese NWP, and has profound significance for future innovation in atmospheric sciences and technologies.

GRAPES-Global is currently discretized in latitudinal-longitudinal grid mesh, with which the polar singularity is always a tough issue hard to deal with. To avoid the problems completely, a new mesh called Yin-Yang grid is studied as an alternative candidate of grid mesh for future GRAPES-Global model. The Yin-Yang grid is a newly developed grid system in spherical geometry with two perpendicularly-oriented latitude-longitude grid components (called Yin and Yang respectively) that overlap each other, and this effectively avoids the coordinate singularity and the grid convergence near the poles. In this overset grid, the way of transferring data between the Yin and Yang components is the key to maintaining the accuracy and robustness in numerical solutions. Li et al.(2006) design a numerical interpolation for boundary data exchange, which maintains the accuracy of the original advection scheme and is computationally efficient. The semi-Lagrangian advection scheme is implemented on a new quasi-uniform overset (Yin-Yang) grid on the sphere. Numerical results show that the quasi-uniform Yin-Yang grid can get around

the problems near the poles, and the numerical accuracy in the original semi-Lagrangian scheme is effectively maintained. A new version of GRAPES-Global adopting Yin-Yang grid is being developed. The development of global 3DVar with Yin-Yang grid has also succeeded, showing comparable results with original global 3DVar and ease in coding. Besides the progress of GRAPES-Global, national operational global medium range assimilation and prediction system has been upgraded from T106 to T213 in 2003.

## 5. Model Physics

Unlike the earlier works on model physics, recent researches in this field pay more attention to understanding the inherent mechanism of physical processes related to the formation and evolution of the weather system in China, and attempt to improve the parameterization scheme based on more physical considerations. The researches deal with almost all processes in the NWP models.

Chen et al. (2003) investigate the impacts of schemes of diabatic processes, including cumulus convection, planetary boundary layer (PBL), radiation on the predictions of model variables in cases of heavy rain events. Their results show that the PBL and convection parameterization dominate the contribution of diabatic physical processes to the short term forecasts of precipitation, giving a clue of the primary issue in refining the NWP models.

Study on the dynamic and thermodynamic conditions for middle cloud formation over eastern China indicates that the middle stratiform clouds downstream of the Tibetan Plateau are maintained by the frictional and blocking effects of the plateau. In addition, it is found that the temperature inversion at plateau height over eastern China generated by the warm air advected

from the plateau provides a favorable thermodynamic condition for middle clouds. Both diurnal variations of the mid-level divergence and the inversion over eastern China dominate the cloud diurnal cycle. The middle cloud amount decreases and the cloud top falls in the daytime, but reverses at night (Li et al., 2005). Zhou et al. (2005) introduced a radiation transfer scheme based on delta-4 stream, correlated- $k$  distribution into PSU/ NCAR MM5, resulting in detailed information about cloud radiative properties. Their results present the importance of radiation process in the mesoscale precipitations.

Sun et al. (2005) develop a new Planetary Boundary Layer (PBL) model (namely MY-4) with reference to Mellor-Yamada's Level 4 turbulent closure concept. Having been coupled with mesoscale model MM5, it is utilized to simulate a heavy-rain process, taking place over South China during June 8-9, 1998. Its model outputs indicated that the rainfall process is better captured in terms of its intensity and geographical distribution by more accurate simulation of the major weather systems and reduction of the false rainfall centers.

Up to now no convective parameterization scheme is developed based upon observations in China. It is widely accepted that the optimization of convective parameterization scheme in climatic conditions of East Asia monsoon is one of the key issues to improve the prediction of precipitation. A number of works evaluate the performances of various convective parameterization schemes in modeling heavy rain events in China (e.g. Xu et al., 2006). It is found that different convective schemes often results in obvious discrepancy in predicted precipitation field. This discrepancy further causes different feedback to large scale environment and precipitation in grid scale. However, most works of this kind are conducted with a few selected cases and their conclusions are diverse. More studies with batch cases are necessary in order to

reach the goal of refining the parameterization scheme in climatic condition of China.

## **6. Ensemble Prediction**

Ensemble prediction attracts more and more Chinese scientists in recent years, with stress on the mesoscale ensemble techniques. The strategy of multi-model ensemble is adopted by a number of researchers. Some of works simply use different suites of schemes of model physics in the same dynamic frame, taking into account the fact that in the model physics dominates the uncertainty of model forecasts in the mesoscale regime. This simple approach gets satisfactory results in case studies. Chen et al.(2006) design a new initial perturbation method called DPMM (Different Physical Mode Method) for ensemble prediction of heavy rain. DPMM attempts to generate initial perturbation reflecting the uncertainty of convection instability by introducing the difference in prediction due to the use of various cumulus convective parameterization schemes. Huang et al. (2006) propose an approach perturbing the initial location and intensity of tropical cyclone combining with the Bogus Data Assimilation scheme to generate a series of bogus vortex and initial conditions for model integrations. Although these experiments are preliminary, the results are encouraging.

The development of global ensemble prediction system (GEPS) has been an important task in the National Meteorological Center since later 1990s ( Li and Chen, 2002). Since the performance of the original GEPS based on singular vectors is not satisfactory, a new GEPS is being developed based on breeding growing modes (Gong, personal communication). Meanwhile the study on GRAPES-GEPS is underway combined with ETKF.

## 7. Application in Environmental Problems

GRAPES-Meso provides a base for numerical prediction of air quality in urban areas or large domains. The NWP model of sand and dust storm GRAPES-DAM is developed by coupling GRAPES-Meso with an aerosol module which includes emission, dispersion, dry deposition, rain out and scavenging of sand and dust particles in the air. The pre-operation tests are undertaken in the Chinese academy of Meteorological Sciences. Similarly, based on the GRAPES-Meso, a forecast system towards city environments, GRAPES-Mega City, is developed. GRAPES-MegaCity includes the parameterization scheme of urban canopy and introduces atmosphere chemistry and aerosol processes in order to improve the modeling effects of urban heat island and to predict the air quality. It further drives a simple dynamical model to simulate the air flow features in street scale and get the details of wind and temperature distribution in the city scale. These models have set up the foundation for the development of new generation air quality model, and are expected to be applied in the city meteorology service.

Similar researches are conducted based on other atmospheric models. Fang et al. (2004) established a user-oriented multi-scale numerical modeling system to simulate the urban meteorological environment. The system mainly involves three spatial scales: the urban scale, urban sub-domain scale, and single to few buildings scale. The effects of building distribution, azimuth and screening of shortwave radiation and the influence of anthropogenic heating are taken into account. The simulated results are reasonably in agreement with the observational data. Li et al. (2003) develop an urban canopy parameterization (UCP) based on some advanced canopy parameterization abroad, in which the effect of urban infrastructure and anthropogenic on urban boundary layer and rational representation of urbanization in mesoscale model is considered, and

couple it with MM5. Sun et al .(2003) develop an integrated dust storm numerical modeling system in which a physical based wind erosion scheme, a dust transportation model and mesoscale model (MM5) with a geographic information database were coupled. Results show that the model can simulate the dust emission and dust concentration in the air successfully.

## **8. Concluding Remarks**

The development of Chinese new generation numerical prediction model system GRAPES is one of Chinese prominent scientific achievements in the early years of new century. The advanced variational assimilation and non-hydrostatic prediction model of GRAPES will constitute new foundation of operational numerical predictions and modeling studies of high impact weather events in China. GRAPES also provides a new base for numerical prediction and modeling of environmental issues and climate events.

Significant progresses are also achieved other than GRAPES project. The efforts for the improvements of prediction of heavy rain events by introducing sophisticated scheme to deal with complex terrain in the model and the upgrading the model physics are successful and of great importance in the future development of NWP in China.

From a long-term view to push the sustained development of Chinese NWP current achievements either in or out GRAPES project are by far just primary. More efforts must be made to promote the operational application of GRAPES and to continuously improve its performance. Some scientific issues relevant to NWP should be emphasized in the near future. They are assimilation of radar and other high-resolution remote sensing data, numeric algorithms for high-resolution model to handle the complex topography in China, optimization of model physics

in the climatic conditions of East Asian monsoon area and coupling of atmospheric model with processes beyond atmosphere. With the base having been set up and improved observational networks and computer resources in China, the expectation of future development of NWP will be optimistic even though all works mentioned above are tough.

**Acknowledgements:** This work is jointly funded by the national key-research project “Innovative Researches on Chinese Numerical Weather Prediction System” (Grant No. 2004BA607B) and the project of National Natural Science Foundation of China “Study on Weather Prediction Associated with Heavy Precipitation in China” (Grant No. 40233036). The authors thank the scientist team of the project “Innovative Researches on Chinese Numerical Weather Prediction System” for generously providing a number of up to date achievements and allowing us to cite their part tables and figures.

#### References

- Chen Jing, Xue Jishan, and Yan Hong, 2003: The impact of physics parameterization schemes on mesoscale heavy rainfall simulation. *ACTA Meteorological Sinica*, 61, 203-218. (in Chinese)
- Chen Jing, Xue Jishan, and Yan Hong, 2006: A new initial perturbation method of ensemble mesoscale heavy rain prediction. *Chinese Journal of Atmospheric Sciences*, 29, 717-726. (in Chinese).
- Dong Peiming, and Xue Jishan. An adjusted parameter scheme of land surface emissivity for assimilation of microwave satellite data, *Proceedings of SPIE: Atmospheric and Environmental Remote Sensing Data Processing and Utilization: Numerical Atmospheric Prediction and Environmental Monitoring*, 274-280,

- Editors: Hung-Lung A. Huang, Hal J. Bloom, Xiaofeng Xu, Gerald J. Dittberner, 2005
- Dong Peiming, Liu Zhiqian, Xue Jishan, et al., 2005: The Use of ATOVS Microwave Data in the Grapes-3Dvar System. Proceedings of fourteenth International TOVS Study Conference, 2005, 274-280
- Fang Xiaoyi, Jiang Weimei, Miao Shiguang, et al., 2004: The multi-scale numerical modeling system for research on the relationship between urban planning and meteorological environment. *Advances In Atmospheric Sciences*, 21:103–112.
- Gu Jianfeng, Three dimensional variational method study on directly assimilation Doppler radar data, PhD dissertation (in Chinese), Chinese Academy of Meteorological Science, 2006
- Huang Yanyan, Wan Qilin, Yuan Jinnan, et al., 2006: Experiments of ensemble forecast of typhoon track using DBA perturbing method. *Journal of Tropical Meteorology*, 22, 49-54. (in Chinese)
- Li Xiaoli, He Jinhai, and Bi Baogui, 2003: The design of urban canopy parameterization of MM5 and its numerical simulation. *ACTA meteorological sinica*, 61: 526-539. (in Chinese)
- Li Xingliang, Chen Dehui, Peng Xingdong, et al., 2006: Implementation of the semi-Lagrangian advection scheme on a quasi-uniform overset grid on a sphere. *Advances in Atmospheric Sciences*, 23, 792-801.
- Li Yongping, Zhu Guofu, Xue Jishan, et al., 2006: Microphysical retrieval from Doppler radar reflectivity using variational data assimilation. *ACTA meteorological sinica*, 20, 20-27
- Li Yunying, Yu Rucong, Xu Youping, et al., 2005: AREM simulations of cloud features over Eastern China in February. *Advances in Atmospheric Sciences*, 22: 260–270.
- Li Zechun, and Chen Dehui, 2002: The development and application of the operational ensemble prediction system at national meteorological center. *Journal of Applied Meteorological Science*, 13: 1-15. (in Chinese)
- Mu Mu, and Wang Jiafeng, 2003: A method for adjoint variational data assimilation with physical “on-off” processes. *Journal of the atmospheric sciences*, 60, 2010-2018.

- Mu Mu, and Zheng Qin, 2005: Zigzag Oscillations in variational data assimilation with physical "on-off" processes. *Monthly weather review*, 133: 2711-2720.
- Qiu, C. and J. Chou, 2005: Four-dimensional data assimilation method based on SVD: Theoretical aspect, *Theor. Appl. Climatol.*, 83, 51-57.
- Shen Xueshun, and Akimasa Sumi, 2005: A high resolution non-hydrostatic tropical atmospheric model and its performance, *Advances in Atmospheric Sciences*, 22, 30-38.
- Sun Jian, Zhou Xiuji, and Zhao Ping, 2005: A planetary boundary layer model and its application to heavy rain modeling. *Chinese Science Bulletin*, 50, 275-285. (in Chinese)
- Sun Jianhua, Zhao Linna, and Zhao Sixiong, 2003: An integrated numerical modelling system of dust storm suitable to north China and its applications, *Climatic and Environmental Research*, 8, 125-142
- Wan Qilin, Xue Jishan, and Zhuang Shiyu, 2005: Study on the variational assimilation technique for the retrieval of wind fields from Doppler radar data. *ACTA Meteorologica Sinica*, 63, 129-145. (in Chinese)
- Wan Qilin, Xue Jishan, Chen Zhitong et al., 2006: The test of applying radar TREC wind in three-dimensional variational assimilation. *Journal of Tropical Meteorology*, 12, 59-66.
- Wang Bin, and Zhao Ying, 2005: A new data assimilation approach, *Acta Meteorologica Sinica*, 63, 694-701. (in Chinese)
- Wang Yunfeng, and Wang Bin, 2003: The variational assimilation experiment of GPS bending angle, *Advances in Atmospheric Sciences*. 20, 479-485.
- Xu Guoqiang, Wan Qilin, Huang Liping et al., 2006: Application and study of precipitation schemes in weather simulation in summer and winter over China, *ACTA meteorological sinica*, 20, 28-38
- Xu Xiaoyong, Zheng Guoguang, and Liu Liping, 2004: Dynamical and microphysical retrieval from simulated Doppler radar observations using the 4dvar assimilation technique, *ACTA meteorological sinica*, 62, 411-422.

(in Chinese)

Xue Jishan, 2004: Progresses of researches on numerical weather prediction in China: 1999–2002, *Advances in Atmospheric Sciences*, 21, 467–474.

Xue Jishan, 2005: Development of 3DVar for operational application in CMA. Proceedings of 4th WMO International Symposium on Assimilation of Observations in Meteorology and Oceanography, Czech, April 18-22, 2005, 142

Xue Jishan, 2006: Progress of Chinese numerical prediction in the early new century, *Applied Meteorological Science*, 17, 602-610. (in Chinese)

Xue Jishan, Zhang Hua, Zhu Guofu, Zhuang Shiyu. Development of a 3D Variational Assimilation System for ATOVS Data in China. Proceedings of Thirteenth International TOVS Study Conference, 2003, 30-36.

Yu Rucong, Xu Youping, 2004: Arem and its simulations on the daily rainfall in summer in 2003, *Acta Meteorological Sinica*, 62, 715-724. (in Chinese)

Yuan Zhaohong, Ding jincai, and Chen Min, 2004: Preliminary study on applying GPS observations to mesoscale numerical weather prediction model, *Acta Meteorological Sinica*, 62, 201-212.(in Chinese)

Zhang Lin, and Ni Yunqi, 2005: Four-Dimensional variational data assimilation of radar radial velocity observations. *Chinese Journal of Atmospheric Sciences*, 30, 433–440

Zhang Xin, Liu Yuewei, Wang Bin, et al., 2004: Parallel computing of a variational data assimilation model for GPS/MET observation using the ray-tracing method. *Advances in Atmospheric Sciences*, 21, 220-226

Zhou Guangqiang, Zhao Chunsheng, Ding Shouguo, et al. 2005: A study on impacts of different radiative transfer schemes on mesoscale precipitations. *Journal of Applied Meteorological Science*, 16, 148-158.

Table 1 physical parameterization schemes in GRAPES-Meso

Explicit precipitation	Convection precipitation	Longwave radiation	Shortwave radiation	Surface layer	Land surface	Boundary layer
(1) Kessler	(1)New	(1)RRTM	(1)Dudhia	(1)Similarity theory	(1)Thermal diffusion	(1)MRF
(2) Lin(Purdue)	Kain-Fritsch	(2)GFDL	simple short wave	(2)MYJ surface scheme	(2)OSU/MM5 LSM	(2)Mellor-Yamada-Janjic
(3) NCEP simple ice	(2)Betts-Milieu-Canion	(3)ECMWF	(2)DFDL	(3)GSFC	(3)improved NCAR LSM	(3) Second order turbulent closure scheme
(4) NCEP mixed phase	(3)Kain-Fritsch		(4)ECMWF			
(5) Eta old microphysics						
(6) Eta new microphysics						
(7) CAMS simply ice scheme						
(8) Large scale precipitation iterative coagulation scheme						
(9) ECMWF larger scale precipitation coagulation scheme						

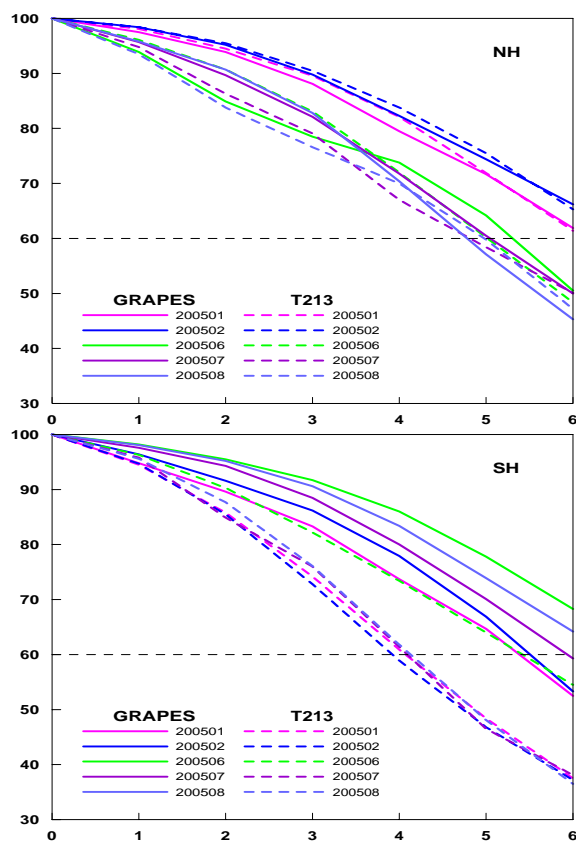


Fig. 1 500hPa height anomaly correlation coefficient averaged over five months in summer and winter of

2005 for both GRAPES-Global and T213 (provided by Yang Xuesheng)

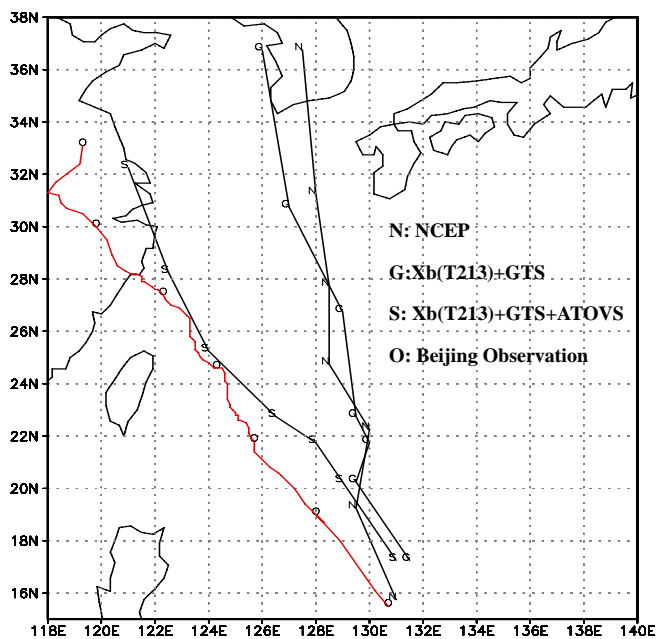


Fig. 2 Track prediction of typhoon Matsa in 2005 using GRAPES global assimilation and prediction system

(provided by Han Wei)

# PROGRESS IN THE DEVELOPMENT AND APPLICATION OF CLIMATE OCEAN MODELS AND OCEAN-ATMOSPHERE COUPLED MODELS IN CHINA

ZHOU Tianjun\* , YU Yongqiang, LIU Hailong, LI Wei, YOU Xiaobao, ZHOU Guangqing

(LASG, Institute of Atmospheric Physics, Chinese Academy of Sciences, Beijing 100029)

## ABSTRACT

A review is presented of the development and application of climate ocean models and ocean-atmosphere coupled models developed in China as well as a review of climate variability and climate change studies performed with these models. While the history of model development is briefly reviewed, emphasis has been put on the achievements made in recent five years. Advances in model development are described along with a summary on scientific issues addressed by using these models. Focus of the review is the climate ocean models and the associated coupled models, including both global and regional models, developed at the Institute of Atmospheric Physics, Chinese Academy of Sciences. Some typical progress of either coupled model development made by other institutions or climate modeling using internationally developed models are also reviewed. Although the authors attempt to outline the main contributions of Chinese scientists in this field, clearly it is beyond the authors' ability to summarize so large amount of literatures into a short paper.

**Key words:** Climate Ocean model, ocean-atmosphere coupled model, climate modeling

## 1. Introduction

The climate system is an interactive system consisting of five major components: the atmosphere, the hydrosphere, the cryosphere, the land surface and the biosphere. Internal variation of the climate involves a complex interplay of physical, chemical, and biological processes of the atmosphere, ocean, sea ice, and land surface. This system is also forced or influenced by various external forcing mechanisms. Any change, whether natural or anthropogenic, in the components of the climate system and their interactions, or in the external forcing, may result in climate variations (Houghton et al. 2001; Blackman et al. 2001). Addressing the interplay among different components or establishing the climate system's response to changes in anthropogenic emissions of greenhouse gases requires a coupled climate-system approach. The most complex climate models, termed coupled climate system models, involve coupling comprehensive three-dimensional atmospheric general circulation models (AGCMs), with ocean general circulation models (OGCMs), with sea-ice models, and with models of land-surface processes (see IPCC SAR for a extensive review, Houghton et al. 1995). Climate system models, as grand geophysical laboratories, are among the most powerful tools to both enhance our understanding of

the fundamental mechanisms of the climate system and make projections of future climate change.

Recognizing the central importance of climate models in climate studies, the Institute of Atmospheric Physics, Chinese Academy of Sciences (hereinafter IAP) has put much effort on GCM developments. The development and use of numerical models for the study of climate has been a central focus of the State Key Laboratory of Numerical Modeling for Atmospheric Sciences and Geophysical Fluid Dynamics's (hereinafter LASG) research activities since the establishment of the laboratory in 1985. Many pioneering Chinese models have been developed at LASG/IAP, including IAP Atmospheric General Circulation Model, Oceanic General Circulation Model, global coupled ocean-atmosphere models, and global atmosphere-tropical Pacific coupled models for research and seasonal forecasting (Wu et al. 1997; Zhou and Zeng, 1998; Zhang et al. 1999, 2000; Yu et al. 2004; Wang, 2005).

In recent years, more and more Chinese institutions have been involved in the development and applications of climate ocean models and coupled climate system models. For example, China Meteorological Administration has set up a plan to develop a new coupled climate system model for operational seasonal forecast and climate change studies (Wu 2006). In the mean time, many internationally developed climate ocean models such as the MOM (Pacanowski, 1995), coupled climate system models such as the Community Climate System Model (hereinafter CCSM) (Boville and Gent, 1998; Collins et al. 2006), the Bergen Climate Model (hereinafter BCM) (Furevik et al. 2003), and the Fast Ocean-Atmosphere Model (hereinafter FOAM) (Jacob, 1997) have been set up and used in many Chinese institutions. In addition to global ocean or coupled ocean-atmosphere models, regional climate ocean models (Li et al., 2002) and regional ocean-atmosphere coupled models (Ren and Qian, 2000) have also been developed in China. Here we summarize the achievements to date, and outline our current state of the development and simulation characteristics of the recent versions of the global climate ocean model and coupled climate system model in use at the IAP as well as a brief summary of the climate variability and change experiments conducted by Chinese scientists with some internationally developed models.

The outline is as follows: in Sect. 2 the development and applications of LASG/IAP global climate ocean model are described. The evolution and applications of LASG/IAP global ocean-atmosphere coupled models are described in Sect. 3. A review on the development and application of regional ocean models and the regional ocean-atmosphere coupled model is made in Sect. 4, while in Sect. 5 the use of other climate ocean models and ocean-atmosphere coupled models is described, along with some key results. A concluding discussion is presented in Sect. 6.

## **2. Development and applications of LASG/IAP climate ocean model**

\* E-mail: [zhoutj@lasg.iap.ac.cn](mailto:zhoutj@lasg.iap.ac.cn)

\* <http://www.gfdl.noaa.gov/~fms/>

### **2.1 Early achievements**

The family of LASG/IAP climate ocean model has been developing on the basis of succession during the past twenty years. The primary features of the model include a free surface, an energy conserving numerical differential scheme, and the  $\eta$ -coordinate in the vertical. LASG/IAP initiated its baroclinic OGCM from a 4-layer model in 1980's (Zhang and Liang 1989). The first version has a horizontal resolution of  $4^\circ \times 5^\circ$ , covering the scope of  $60^\circ\text{S}$ - $60^\circ\text{N}$ . The second version is the same as the first one except that the vertical layer was increased to 20-levels (ML20) and the model domain extends to the global scope except the North Pole (Chen, 1994; Zhang et al. 1996). The simulation of thermohaline circulation was improved in ML20 relative to the previous 4-layer model.

The third generation of LASG/IAP OGCM was developed by Jin et al. (1999). It has 30 layers in the vertical and the horizontal discretization is conducted based on a triangular spectral truncation with a zonal wave number of 63 (approximately  $1.875^\circ \times 1.875^\circ$ ) (hereinafter L30T63). The physical processes have been greatly improved in L30T63, including the parameterization of meso-scale eddies (Gent and McWilliams, 1990) and the inclusion of Richardson number dependent vertical diffusion scheme (Pacanowski and Philander, 1981). The permanent thermocline, the thermohaline circulation as well as the meridional heat transport were significantly improved in L30T63 (Zhang et al. 2003).

The developments of LASG/IAP climate ocean model are motivated for climate variability and climate change studies as well as large-scale ocean circulation simulations. Zhou et al. (2000) discussed the ocean circulation response to surface freshwater forcing and found the stability of the thermohaline circulation in ML20 was highly sensitive to the surface flux condition of salinity. Disturbance of the surface freshwater forcing might cause a collapse of the Atlantic thermohaline circulation. The stand-alone ocean model has also been used in the understanding of tropical ocean dynamics. Yu et al. (2001) drove the L30T63 model by observational monthly wind stress covering 1980-1989 and got a reasonable interannual variability in the tropical Pacific, proving a good performance of L30T63. The El Niño events are generally better simulated than La Niña events in L30T63. Liu et al. (2002) forced the L30T63 by daily wind stress and heat flux to address ocean's responses to the western wind burst (WWB) during TOGA-COARE Intensive Observation Period (September to December of 1992). They found that the L30T63 successfully reproduced the deepening of the mixed layer and the weakening of surface current over the warm pool during WWB event. The L30T63 model was also employed in paleo-climate simulations. Yu et al. (2003) performed a set of experiments with the oceanic bathymeter at present, 6Ma BP and 14MA BP respectively to investigate the effect of the north shift of Australian continent on the tropical ocean. They found a closure of Indonesian passage would result in a warming in tropical Pacific and a cooling in tropical Indian Ocean; the Indonesian through flow originates from the North Pacific at contemporary stage however from the south Pacific at 14 Ma BP.

## 2.2 Recent progress

The development of L30T63 has been an important milestone. However, later evaluations

revealed some limitations, which could be attributed to its coarse meridional resolution (Jin et al. 1999). These limitations include a weaker North Equatorial Countercurrent (NECC) and Equatorial Undercurrent (EUC), as well as a stronger South Equatorial Current (SEC) relative to observations. Recently, Liu et al. (2004a,b) established an eddy-permitting version with a uniform grid of  $0.5^\circ$  by  $0.5^\circ$ . This improved version was named as LICOM (LASG/IAP Climate Ocean Model). The  $0.5^\circ$  by  $0.5^\circ$  grids are marginal resolutions to resolve the equatorial Rossby radius of deformation. The complicate topographies surrounding the Indonesian seas, including the channels connecting the Pacific and Indian Oceans together, are well represented in LICOM. The horizontal viscosity and diffusivity schemes were also updated in LICOM. Evaluations on LICOM reveal many improvements, including better western boundary currents, stronger EUC and NECC, and an intensified meridional heat transport. The Ekman cells around the equator and the Deacon Cell of the Antarctic Circulation Current were also improved (Liu et al. 2004a,b).

To improve the simulation of tropical thermocline, Wu et al. (2005) has increased the vertical resolution of LICOM within the upper 150m and a more realistic cold tongue extending from the coast of Peru to the equator is found. Recently, the chlorophyll related solar radiation penetration scheme of Ohlmann (2003) was incorporated into LICOM by Lin and Liu (2006, personal communication). Efforts in improving the equatorial Pacific simulation have also been devoted to the advection treatment, and the two-step shape-preserving advection scheme of Yu (1994) was incorporated into LICOM by Xiao (2006). The excessively westward extension of the eastern Pacific cold tongue was reduced relative to the former version employing two-order central differential scheme.

The LICOM has been the ocean component of various versions of LASG/IAP coupled climate system model (Yu and Liu, 2004; Yu et al. 2004; Yu 2005; Zhou et al. 2005a,b; Wang 2005). In addition to global large scale ocean circulation simulations, the LICOM has also been used in regional sea studies. Li et al. (2004) and Liu et al. (2005) drove the LICOM by observational surface wind and finished 44-years integrations. The ITF transport from 1958 to 2001 was estimated. The LICOM represents a reasonable pathway of the ITF with the Makassar Strait serving as the major passage transferring the North Pacific water southward. The simulated annual mean ITF transport is 14.5 Sv, with 13.2 Sv in the upper 700 m. Both the annual mean and seasonal cycle of the ITF agree well with the observation. Analyses prove that the ENSO-related interannual variability of the Pacific is dominant in controlling the ITF transport. Cai et al. (2005) presents a quantitative estimate of the water exchange of the South China Sea with its adjacent ocean through 5 straits by using a 900-year integration of LICOM. They found that the annual transport is the largest in the Luzon Strait, then in the Taiwan Strait, and then in the Sunda Shelf, in the Balabac Strait and in the Mindoro Strait in turn. The largest monthly transport variation appears in the Luzon Strait and Sunda Shelf. The Indonesian Throughflow (ITF) contributes greatly to the mass and heat exchanges between the Pacific and Indian Ocean.

In addition, some ongoing work using LICOM includes the investigations of North Pacific

mode water (Liu et al., 2006, personal communication), meridional heat transport in the Indian Ocean (Wu et al., 2006, personal communication) and the interdecadal variation of western Pacific warm pool (Li et al., 2006, personal communication).

### **3. Development and applications of LASG/IAP global ocean-atmosphere coupled models**

#### **3.1 Early achievements**

The development of global ocean-atmosphere coupled models in China dates back to early 1990s. A four-layer OGCM was successfully coupled with the two-level AGCM by using a prediction-correction Monthly Flux Anomaly coupling scheme (referred to as MFA) (Zhang et al. 1992). With the MFA scheme, the twenty-layer OGCM of LASG/IAP was also coupled with the two-level AGCM (Guo et al. 1996), and a multi-level AGCM i.e. the nine-level and R15 spectral AGCM (L9R15) (Wu et al. 1996, Liu et al. 1996). Since both of these two coupled models have noticeable climate drifts, much effort has then been devoted to the improvements of the coupling scheme and a modified MFA scheme (referred to as MMFA) was presented (Yu and Zhang, 1998). By using the MMFA scheme, the twenty-layer OGCM of LASG/IAP has been successfully coupled with L9R15 AGCM to build up an ocean-atmosphere-land system model, i.e. GOALS/LASG model (Wu et al. 1997). Four versions of the GOALS model have been presented and all of them have been integrated for 100-200 years without serious climate drift. Relative to the preliminary version of GOALS (Wu et al. 1997), version 2 employs a daily coupling scheme instead of the original monthly coupling (Yu and Zhang, 1998), version 3 improves the atmospheric solar radiation by including its daily variation (Shao et al. 1998), and version 4 improved the coupling processes by including the ocean-atmospheric freshwater exchange (Zhou et al. 2000, 2001). For details of these early achievements, the author is referred to Zhang et al. (1999) and Yu et al. (2004).

The GOALS model has been widely used in the climate variability and climate change studies. It has played important roles in the studies of global ocean circulation. By using the long term integration of version 2 of GOALS, Zhou et al. (2000) studied the relationship between the North Atlantic thermohaline circulation (THC) and atmospheric circulation and they found a significant negative correlation between the THC and the North Atlantic Oscillation. Zhou (2001) identified the multi-spatial variability modes of the Atlantic THC in version 4 of GOALS, the THC either oscillates at decadal scales with strong cross-equatorial flow or fluctuates locally at interannual scales with weaker cross-equatorial flow. Recently, response of THC to global warming is examined by using version 4 of GOALS (Zhou et al. 2005). The evidence indicates that the gradually warming climate associated with the increased atmospheric carbon dioxide leads to a warmer and fresher surface water at the high latitudes of the North Atlantic, which prevents the down-welling of the surface water. The succedent reduction of the pole-to-equator meridional potential density gradient finally results in the decrease of the THC in intensity. When the atmospheric carbon dioxide is doubled, the maximum value of the Atlantic THC decreases

approximately by 8%. The associated poleward oceanic heat transport also becomes weaker. This kind of THC weakening centralizes mainly in the northern part of the North Atlantic basin, indicating briefly a local scale adjustment rather than a loop oscillation with the whole Atlantic “conveyor belt” decelerating. Similar basin or local scale adjustment of the THC were found in BCM (Bentsen et al. 2004; Zhou and Drange, 2005).

The discussion of ocean circulation in GOALS model is not limited to the Atlantic Ocean. Recently, sensitivity of the Pacific subtropical-tropical meridional cell (STC) to global warming is examined by using version 4 of GOALS. A weak response of the STC to the increasing of atmospheric carbon dioxide is found. At the time of atmospheric carbon dioxide doubling, the change of the meridional cell strength is smaller than the amplitude of natural variability (Zhou et al. 2006).

The GOALS model has played active roles in monsoon studies, e.g. the relationship between ENSO and East Asian monsoon is addressed by Wang (2001). Both data diagnosis and model analyses reveal that there exists a time-dependence in the relationship between East Asian monsoon and SST. The anomalous winter monsoon may have significant correlations with the succeeding summer monsoon, but this relationship may disappear in another time period. The GOALS model has also been a useful tool in climate change studies. Ma et al. (2004) drove the GOALS model by using historical greenhouse gases concentrations, the mass mixing ratio of sulfate aerosols, and reconstructed solar variations spanning 1900-1997. The model reproduced reasonable temporal and spatial distributions of the temperature change. The global warming during the 20th century is caused mainly by increasing greenhouse gas concentration especially since the late 1980s; sulfate aerosols offset a portion of the global warming.

### **3.2 Recent progress**

Enlightened by NCAR in developing Community Climate System Model (Boville and Gent, 1998) and GFDL in developing its Flexible Modeling System\* , in the late 1990s, LASG/IAP made a decision to consolidate and modernize the numerical modeling activities through the development of a new coupled system employing coupler structure. A preliminary experimental version was carried out in 2002 (Yu et al. 2002), which is temporarily called Flexible General Circulation Model (FGCM). The version 0 of FGCM (hereinafter FGCM0) is the same as NCAR CSM (Boville and Gent, 1998) except that the ocean component has been change to the fourth generation of LASG/IAP climate ocean model L30T63 (Jin et al. 1999).

The FGCM0 shows many improvements relative to the GOALS model. For example, Zhou et al. (2001) compared the atmospheric moisture transport and air-sea freshwater exchange in GOALS and FGCM0 and found the later has a better performance. Similar as many others “none flux adjustment” coupled models, however, the FGCM0 also suffers from the spurious “Double ITCZ” problem. Great efforts have been devoted to the improvement of this tropical bias. Based on the relation between the low-level cloud cover and the bulk stability of the low troposphere, Dai et al. (2003) modified the parameterization scheme of low-level cloud in CCM3, which is the

AGCM component of FGCM0, and found an improved simulation of the low-level cloud over the cold oceans, which then effectively reduces the SST warm biases in ITCZ north of the equator. Li et al. (2004) showed that the double ITCZ in FGCM0 is a result of non-local and nonlinear adjustment processes of the coupled system. The zonal gradient of the equatorial SST is too large in the ocean component and the amount of low-level stratus over the Peruvian coast is too low in the atmospheric component. Both of them contribute to the formation of “double ITCZ”. Improvements in wave-induced mixing also have significant impacts on the coupled model. Insufficient vertical mixing of OGCM would cause an overestimated SST and underestimated mixed layer depth in summer (Qiao et al 2004, 2006). The wave-induced vertical viscosity/diffusivity can be expressed as a function of wave number spectrum (Qiao et al, 2004; Yuan and Qiao, 2006) (hereinafter Qiao-Yuan scheme). By employing the Qiao-Yuan scheme into the ocean component of FGCM0, Song et al (2006) has reduced the tropical SST bias more than 0.8°C, with a maximum value of 1.2°C nearing 0° -3°N, 160° -180° E.

Benefit from the freely available NCAR CCSM2 (Kiehl and Gent, 2004), version 1 of FGCM was developed by changing the ocean component of CCSM2 to LICOM (Yu and Liu, 2004). This version was improved in 2005 by employing a new atmospheric component, i.e. the Grid Atmospheric Model of IAP/LASG (GAMIL) (Wang et al. 2004). The new version of the coupled model was normally named as FGOALS\_g1.0 (Flexible Global Ocean Atmosphere Land Sea-ice model) by LASG (Wang, 2005; Yu, 2005). A twin version of FGOALS\_g was developed by changing its atmospheric component to another AGCM developed at LASG/IAP, i.e. the Spectral Atmospheric Model of IAP/LASG (SAMIL) (Wu et al. 1996; Wang et al. 2004). This version of FGOALS model employing SAMIL as its atmospheric component was normally named as FGOALS\_s (Zhou et al. 2005a,b). Preliminary analyses on the land surface variables indicate an improvement in FGOALS\_s (Bao et al. 2006). Due to the bias in cloud-radiation process, however, there exists apparent cold bias in the tropical ocean (Zhou et al. 2005b), which in turn influences the strength of the mean meridional circulation and the westerly jets (Wang et al. 2006).

The FGOALS\_g1.0 model has been involved in many international model inter-comparison projects such as IPCC AR4 and PMIP (Yu, 2005; Masson-Delmotte et al. 2006). In a multi-model ensemble discussion on the El Nino mean state - seasonal cycle interactions, Guilyardi (2006) noted that the pre-industrial control El Nino amplitude of FGOALS\_g1.0 is large than observation, along with a too regular frequency. Saji et al. (2006) show that the tropical Indian Ocean response to ENSO is stronger than observation in FGOALS\_g1.0. In the mean time, however, the ENSO amplitude in FGOALS\_s, which shares the same ocean component of FGOALS\_g1.0, is weaker than observation (Zhou et al. 2005b), indicating the impact of the atmosphere on the ENSO intensity of the coupled system. The outputs of FGOALS\_g1.0 experiments for IPCC AR4 have been widely used in climate change and climate variability studies, e.g. the South Asian High (Zhou et al. 2006), the mechanism of 20<sup>th</sup> century surface air temperature evolution over China and the globe (Zhou et al. 2006), the polar sea ice simulation (Zhang and Walsh, 2006), and the

soil moisture studies (Zhang, 2006), among many others.

In addition to the improvements of FGOALS\_g and FGOALS\_s model, efforts in LASG/IAP have also been devoted to the development of a low resolution fast ocean-atmosphere coupled model, which will be used in the millennial scale climate simulations (Zhou et al. 2006, personal communication). By combing different versions together, LASG/IAP aims to create a common modeling infrastructure, which will be receptive to components of varying complexity and of varying resolutions, and which will balance scientific needs with resource availability. This model system would support diverse research activities, from seasonal monsoon evolution to anthropogenic climate change, and from millennial climate evolution to paleo-climate simulation.

Besides the global ocean-atmosphere coupled models, IAP also developed a global atmosphere-tropical Pacific Ocean coupled model for ENSO-prediction purpose (Zhou and Zeng, 1998, 2001). The tropical Pacific Ocean model has a horizontal resolution of  $2^\circ$  longitude by  $1^\circ$  latitude and 14 layers in the vertical, and the global atmosphere model is the IAP 2L AGCM (Zeng et al. 1989). This model has shown good performances in ENSO predictions (Zhou et al. 1999). Recently, Fu (2005) improved this model by increasing the horizontal resolution of the ocean model to be  $0.5^\circ$  by  $0.5^\circ$ . The atmospheric component was changed to IAP 9 layer AGCM, which is the new version of IAP 2L AGCM (Bi, 1993). This new coupled model shows great improvements in the simulations of equatorial Pacific Ocean circulation and East Asian monsoon (Fu, 2005).

#### **4. Development and application of regional ocean models and ocean atmosphere coupled models**

Besides the global OGCM, a regional Oceanic General Circulation Model (Hereinafter IAP-ROCM) with h coordinate and free surface has been developed in IAP (Li et al., 2002; Li and You, 2003). The IAP-ROCM has been applied to simulate the circulation in the South China Sea (SCS), and the influence of Kuroshio is considered through open boundaries (You et al. 2001; Li et al., 2003a,b). The IAP-ROCM successfully produced the anticyclonic meandering path of the Kuroshio, which appears west of the Luzon Strait, and a tongue with relatively high temperature and salinity, which spreads into SCS through the Luzon Strait and represents a intrusion of the Kuroshio in winter. In summer, the anticyclonic circulation in the southern SCS is mainly driven by the southwest monsoon. The cyclonic eddy in the northern SCS is formed due to the joint actions of Kuroshio, bottom topography effect and baroclinic effect. You et al. (2002) developed a 24-level tri-nested regional ocean model with a horizontal resolution of  $0.25^\circ \times 0.25^\circ$ . The current system in the China Seas, such as the Kuroshio, Mindanao Current, South China Sea Warm Current, Taiwan Warm Current, Yellow Sea Warm Current, Tsushima Warm Current and some mesoscale eddies, has been well reproduced.

Efforts have also been devoted to the development of regional air-sea coupled models in China. Ren and Qian (2001) developed a regional air-sea coupled model by using the Nanjing University regional climate model (P- $\sigma$  RCM) and a regional ocean model (POM). Case study on

the 1998 monsoon season (from May to August) proves that the model has a reasonable performance. This model, however, still has a cold bias, which was caused by the disagreement of the surface heat fluxes produced by the P- $\sigma$  RCM with those required by the POM (Ren and Qian, 2005). This model has been used in discussing the evolution of the South China Sea branch of the Kuroshio current in monsoon season (Ren and Qian, 2000; Ren et al., 2000).

To investigate the atmosphere–ocean dynamics of midlatitude North Atlantic storms, Ren et al. (2004) coupled the Canadian Mesoscale Compressible Community (MC2) atmospheric model to the Princeton Ocean Model. Case simulations show that late-summer storms encounter a thin mixed layer and produce a cold wake by inducing strong currents. Sea surface temperature can be depressed as much as 5°C or more. Although impacts on SSTs and the upper-ocean temperature profile tend to be weak, about 1°C or so, storm-induced ocean currents can be large.

## **5. The application of other ocean or ocean-atmosphere coupled models and model inter-comparisons**

In addition to the climate models developed by Chinese institutions, some internationally-developed general circulation models have also been used in China. Applications include studies of climate variability from interannual to interdecadal time scales, simulations of paleoclimate regimes, and projections of future anthropogenic climate change (Pu et al. 2004). The interannual variabilities of the tropical Pacific as well as the controlling mechanisms of ENSO evolution are investigated by using GFDL MOM2 model forced with monthly mean data of COADS covering 1945~1993, and the delayed oscillator mechanism is found to be active (Rong and Yang, 2000). In the tropical Indian Ocean, the ENSO related basin wide warming/cooling mode and the dipole mode are successfully simulated. The model also successfully simulates a ENSO-like mode of the SST variations in the tropical Atlantic. Rong and Yang (2005) discussed the MOM2 response to surface forcing and found that the model successfully captures the dominant mode of the SST anomalies on the decadal-to-interdecadal timescales, as well as the major feature of SST anomalies in the 1976-77 regime shift. Examination of the upper ocean heat budget in three key regions (central North Pacific, coast of California and Kuroshio-Oyashio Extension (KOE) region) reveals that the 1976-77 regime shift was caused by both the sustained heat flux input anomalies and the strong horizontal advection anomalies in the central North Pacific. In the Californian coastal region, only the heat flux input anomalies were found dominant, and the effect of the horizontal advection anomalies is negligible. In the KOE region, the vertical advection, heat flux and horizontal advection anomalies are important in producing the regime shift.

Rong and Yang (2003) discussed the sensitivity of ENSO characteristics in GFDL coupled model to change of climatological background state. They found that the ENSO characters including the frequency and the amplitude and its controlling mechanism strongly depend on the climatological background states. Two different ENSO modes were identified for the two different

background states. One is the “delayed oscillator” mode, corresponding to a background state close to the observation; and the other is a stationary mode, corresponding to a background state with a decreased zonal thermal gradient and a flat thermocline structure along the equatorial Pacific.

Climate variability involves complex processes of ocean-atmosphere feedbacks and teleconnection, our means of diagnosing these processes in a climate model are very limited. Recently, the modeling group at Physical Oceanography Laboratory of Ocean University of China is taking a novel modeling framework, referred to as “Modeling Surgery” (Wu et al. 2003), to address these issues. This new modeling strategy is specifically to diagnose ocean-atmosphere feedbacks and teleconnections through systematically modifying the coupling configuration and teleconnection pathways in a climate model. Using “Modeling surgery”, this group has been investigating the origins of the mid-70s’ North Pacific climate regime shift. By constraining the wind stress forcing of the North Pacific in a coupled model, they were able to find that the adjustment of the subtropical ocean circulation in response to the persistent wind stress prior to the climate shift can induce SST first in the western subtropical North Pacific, that can further induce a shift of the atmospheric circulation, leading a change of SST in the central Pacific and then in the KOE region (Wu et al. 2005a). This new hypothesis is further tested in a coupled model initial-value approach. They further proposed that the KOE region can be an important source of global decadal climate variability, which can induce SST in the tropical Indian Ocean, South Pacific, and north and tropical Atlantic through Asian winter monsoon and Arctic Oscillation/North Atlantic Oscillation (NAO) (Wu et al. 2005b).

Mid-latitude air-sea interaction was discussed by Zhou et al. (2006a) with focus on the North Atlantic. The North Atlantic inter-annual variability associated with the NAO is examined in 300 years integration of BCM. The dominant mode of the North Atlantic wintertime SST variability exhibits a meridional tri-polar pattern, with a colder sub-polar region, warmer mid-latitude, and a colder region between the equator and 30°N. The atmospheric circulation change associated with the tri-polar SST anomalies exhibits as NAO and has a barotropic structure. The tri-polar structure SST anomalies over the North Atlantic are mainly resulted from the barotropic driving of the NAO-like atmospheric forcing, and thermal process plays a dominant role in this process. Similar result was reported in Zhou et al. (2000). The feedback of the tri-polar SST anomalies on the atmosphere is weak. Zhou et al. (2006b) addressed the contribution of the tropical Pacific forcing to the North Atlantic interannual time scale variability in BCM and found that the dominant mode of the interannual time scale SST variability of the North Atlantic is partly forced by the atmospheric tele-connections originated from the middle and eastern equatorial Pacific. Positive phase of the tri-polar North Atlantic SST mode corresponds to a cold event in the equatorial Pacific. The response of the North Atlantic SST to the equatorial Pacific forcing has a lag time of 2-3 months.

Studies on the mid-latitude air-sea interaction have been extended to address the atmospheric

forcing on the ocean circulation. Zhou (2003) discussed the adjustment of the thermohaline circulation (THC) to the forcing of NAO and found that a positive phase NAO and thereby an intensified westerlies enhances the net heat flux loss of the Labrador Sea, in conjunction with the positive salinity anomaly over there, water at the surface then becomes denser, and deep convection occurs. Three months after the NAO reaches its maximum state, the Labrador Sea convection reaches its largest depth. Response of the North Atlantic thermohaline circulation to the Labrador Sea convection lags 3 years in the model. The oceanic poleward heat transport has a maximum simultaneous correlation with the THC.

Tropical inter-basin interaction has been studied by using coupled model. Wu et al. (2005c) discussed the influence of the tropical Atlantic on the tropical Pacific. Using so-called “partial-coupling” strategy, they were able to find that a north Atlantic SST anomaly can induce a meridional SST dipole in the eastern equatorial Pacific in spring, which can subsequently evolve into an ENSO-like pattern (Wu et al. 2005c). This finding may help interpret the global climatic impacts of THC collapse.

During El Nino events, the warm anomalies in the eastern tropical Pacific are seen to occur in conjunction with prominent warm anomalies in the North Pacific SSTs off the west coast of North America as well as with cold anomalies in the central North Pacific. By analyzing the long term integration of IPSL (Institute Pierre-Simon-Laplace des Sciences de l'Environnement Global, France) coupled model, Zhou et al. (2003) demonstrate that the North Pacific response to ENSO is achieved via an atmospheric bridge, i.e., the atmospheric response to ENSO in turn forces the extra-tropical SST anomalies associated with the El Nino event, thereby serving as a bridge between the tropical and extra-tropical Pacific. Zhou et al. (2004) demonstrate that this mechanism is also active in resulting in the warming of the Indian Ocean associated with ENSO events.

Chinese scientists have also benefited from the international modeling group in paleo-climate simulations. Liu et al. (2005) compared the reconstructed temperature anomalies in the eastern China with the output from a 1000-year ECHO-G simulation in an attempt to understand the causes of climate change in China over the last millennium. The Medieval Warm Period (MWP) during 1000-1300 A.D., the Little Ice Age (LIA) during 1300-1850 A.D. and the modern warming period after 1900 A.D. are all recognizable from both the simulated and reconstructed temperatures. Diagnosis of the model results indicates that, during the last millennium, variations in solar radiation and volcanic activity are the main controlling factors on regional temperature change, while in the recent 100 years, the change of the concentration of greenhouse gases plays most important role in explaining the rapid temperature rising.

## **6. Summary**

Climate system models play an instrumental role in understanding and simulating past, present, and future climate. Both global and regional climate ocean models and their associated coupled system model have been created to represent the principal components of the climate system and

their interactions. Development and applications of these models are carried out by the Chinese climate research community. This paper mainly reviewed the history, its current capabilities and applications of the climate ocean model and the associated ocean-atmosphere model developed at IAP, with the goals of providing a summary useful to present and future users. The development of regional ocean models and regional ocean-atmosphere coupled models in China, and applications of several internationally-developed climate ocean and ocean-atmosphere coupled models are also reviewed. Emphasis has been put on the achievements get in the recent five years.

Performances of both global climate ocean models and ocean-atmosphere coupled models developed at IAP have been significantly improved. The involvement of IAP model in many international climate model inter-comparison projects has greatly promoted the development and improvement of these models. Relative to global models, the history of regional ocean and ocean-atmosphere coupled model is shorter. However, great achievements have been made in recent years, which greatly facilitated our understandings of marginal sea ocean-atmosphere interactions. Applications of some internationally developed coupled climate models in China have made great contributions to our understanding of climate physics. The results of multi-model inter-comparison have been serving as guides for the improvement of Chinese models.

We are living in a world facing many scientific challenges of the climate problem. To address these challenges, we need to upgrade our model from climate system model, which consists of four components for the atmosphere, ocean, sea ice, and land surface, to earth system model through the incorporation of an integrated chemistry model and the inclusion of global prognostic biogeochemical components for land, ocean and atmosphere (Wang et al. 2004). In order to make such development possible, a wide intellectual participation is needed, as what NCAR has done in its development of the Community Climate System Model (Blackmon et al. 2001). In addition to the inclusion of new component models, development efforts should also focus on the incorporation and improvement of new representations of physical processes.

### **Acknowledgements**

We acknowledge Profs. Wu Lixin, Qiao Fangli, Ren Xuejuan and Yang Haijun for providing relevant literatures. This work was jointly supported by the Major State Basic Research Development Program of China (973 Program) under grant No. 2005CB321703, the International Partnership Creative Group entitled "The Climate System Model Development and Application Studies", and the National Natural Science Foundation of China (40375029, 40675050).

### **References**

- Bao Q., Y. Liu, T. Zhou, Z. Wang, G. Wu and P. Wang, 2006: The sensitivity of the new atmospheric general circulation model SAMIL-R42L26 of LASG/IAP to the land-atmosphere flux, *Chinese Journal of Atmospheric Sciences*, in press
- Bentsen M., H. Drange, T. Furevik, T. Zhou, 2004: Simulated variability of the Atlantic Meridional Overturning circulation, *Clim. Dyn.*, 22, 701-720.
- Bi X., 1993: IAP nine-level AGCM and its simulation of climate, Ph. D. Thesis, Institute of Atmospheric Physics,

- Chinese Academy of Sciences, 210pp. (in Chinese)
- Blackmon M. B., B. Boville, F. Bryan, R. Dickinson, P. Gent, J. Kiehl, R. Moritz, D. Randall, J. Shukla, S. Solomon, G. Bonan, S. Doney, I. Fung, J. Hack, E. Hunke, J. Hurrell, et al., 2001: The Community Climate System Model. *BAMS*, 82(11), 2357-2376.
- Boville, B. A. and P. R. Gent, 1998: The NCAR climate system model, Version One, *J. Climate*, 11, 115~1130.
- Cai S., H. Liu, W. Li, X. Long, 2005: Application of LICOM model to the numerical study of the water exchange between the South China Sea and its adjacent oceans, *Acta Oceanologica Sinica*, Vol. 24, No. 4, 10-19.
- Chen K., 1994: Improvements of IAP coupled global ocean-atmosphere general circulation model and its simulation of climate change induced by increasing greenhouse gases. Ph. D. Thesis, Institute of Atmospheric Physics, Chinese Academy of Sciences, 1-145pp (in Chinese).
- Collins W. D., C. M. Bitz, M. L. Blackmon, G. B. Bonan, C. S. Bretherton, J. A. Carton, P. Chang, S. C. Doney, J. Hack, T. B. Henderson, J. T. Kiehl, W. G. Large, D. S. McKenna, B. D. Santer, and R. D. Smith, 2006: The Community Climate System Model: CCSM3, *J. Climate*, 19(11), 2122-2143.
- Dai F., R. Yu, X. Zhang, Y. Yu, and J. Li, 2003: The impact of low-level cloud over the eastern subtropical Pacific in the "Double ITCZ" in LASG FGCM-0. *Adv. Atmos. Sci.*, 20(3), 461-474
- Fu W., 2005: A high resolution tropical Pacific OGCM and its coupling to a global AGCM, Ph. D. dissertation, Institute of Atmospheric Physics, Chinese Academy of Sciences, 169pp.
- Furevik T, M. Bentsen, H. Drange H et al. 2003: Description and evaluation of the Bergen climate model: ARPEGE coupled with MICOM. *Clim. Dyn.*, 21(1): 27-51.
- Gent P R, J.C. McWilliams, 1990: Isopycnal mixing in ocean circulation models. *Journal of Physical Oceanography*, 20: 150~155
- Guilyardi E., 2006: El Nino-mean state-seasonal cycle interactions in a multi-model ensemble, *Clim. Dyn.*, 26(4),329-348
- Guo Y., Y. Yu, K. Chen, X. Jin, and X. Zhang, 1996: Mean climate state simulated by a coupled ocean-atmosphere general circulation model. *Theor. and Appl. Climatol.*, 55, 99-112.
- Houghton J.T., L.G. Meira Filho, B.A. Callender, N. Harris, A. Kattenberg and K. Maskell (Eds), 1995: Climate Change 1995: The Science of Climate Change, Cambridge University Press, UK. pp 572
- Houghton, J. T., Y. Ding, D. J. Griggs, M. Noguer, P. J. van der Linden, X. Dai, K. Maskell, and C. A. Johnson, Eds., 2001: Climate Change 2001: The Scientific Basis. Cambridge University Press, 892 pp.
- Jacob,1997: Low frequency variability in a simulated atmosphere ocean system. PhD Thesis, University of Wisconsin, p 155
- Jin X., X. Zhang and T. Zhou, 1999: Fundamental framework and experiments of the third generation of IAP/LASG world ocean general circulation model, *Adv. Atmos. Sci.*, 16, 197-215.
- Kiehl J. T., and P. R. Gent. 2004: The Community Climate System Model, Version 2. *J. Climate*, 17, 3666~3682.
- Li D., X. You, M. Zhang, 2003: Numerical simulation of every monthly mean ocean currents in the South China Sea, *Scientia Meteorologica Sinica*, 23(1):22-38
- Li D., X. You, M. Zhang, 2003: A study on circulation mechanism of South China Sea in summer by numerical experiments, *Journal of Tropical Oceanography*, 22(6),54-63.
- Li J., X. Zhang, Y. Yu, F. Dai, 2004: Primary reasoning behind the double ITCZ phenomenon in a coupled ocean-atmosphere general circulation model. *Adv. Atmos. Sci.*, 21(6),857-867
- Li R., X. You, P. Wongwises, 2002: A three-dimensional coastal ocean circulation model, ISBN 974-90322-4-1, Bangkok, Thailand.
- Li R., X. You, 2003: The development and application of the oceanic general circulation models Part II. the regional oceanic general circulation models, *Chinese Journal of Atmospheric Sciences*, 27(4): 729-739 (in

Chinese)

- Li W., H. Liu, X. Zhang, 2004: Indonesian throughflow in an eddy-permitting oceanic GCM, *Chinese Science Bulletin*, 49(21), 2305-2310.
- Liu H., X. Jin, X. Zhang, G. Wu, 1996: A coupling experiment of an atmosphere and ocean model with a monthly anomaly exchange scheme. *Adv. Atmos. Sci.*, 13,133~146
- Liu H., W. Li, X. Zhang, 2005: Climatology and Variability of the Indonesian Throughflow in an Eddy-permitting Oceanic GCM, *Adv. Atmos. Sci.*, 22, 496-508
- Liu H., X. Zhang, Y. Yu, W. Li, 2004a: Manual for LASG/IAP Climate system ocean model. Science Press, Beijing, 1-108pp.(In Chinese)
- Liu H., X. Zhang, W. Li, Y. Yu, R. Yu, 2004b: An eddy-permitting oceanic general circulation model and its preliminary evaluations, *Adv. Atmos. Sci.*, 21, 675-690.
- Liu H., W. Li, X. Zhang and Y. Yu, 2002: Simulated response of SST to west wind bursts in the western equatorial Pacific warm pool, *Chinese Journal of Atmospheric Sciences*, 26, 172-184. (In Chinese)
- Liu H., X. Jin, X. Zhang and G. Wu, 1996: A coupling experiment of an atmosphere and an ocean model with a monthly anomaly exchange scheme, *Adv. Atmos. Sci.*, 13, 133-146.
- Liu J., H. Storch, X. Chen, E. Zorita, J. Zheng, S. Wang, 2005: Simulated and reconstructed winter temperature in the eastern China during the last millennium, *Chinese Science Bulletin*, 50 (24), 2872-2877.
- Liu X., 2001: The simulation and study of sea-ice-air interaction in the northern high latitude region, Ph.D. dissertation, Graduate School of the Chinese Academy of Sciences, 136pp.(in Chinese)
- Ma X., Y. Guo, G. Shi, Y. Yu, 2004: Numerical simulation of global temperature change during the 20th century with the IAP/LASG GOALS model, *Adv. Atmos. Sci.*, 21(2),227-235.
- Masson-Delmotte, V., M. Kageyama, P. Braconnot, S. Charbit, et al.,2006: Past and future polar amplification of climate change: climate model intercomparisons and ice-core constraints. *Clim. Dyn.*,26, 513–529.
- Ohlmann, J. C., 2003: Ocean radiant heating in climate models. *J.Climate*, 16, 1337–1351.
- Pacanowski R C, G. Philander, 1981: Parameterization of vertical mixing in numerical models of the tropical ocean. *Journal of Physical Oceanography*, 11,1442~1451
- Pacanowski R.C., 1995: MOM2 documentation users guide and reference manual. GFDL Ocean Technical Report No.3, Princeton, USA.
- Perrie W., X. Ren, W. Zhang, and Z. Long, 2004: Simulation of extratropical Hurricane Gustav using a coupled atmosphere-ocean-sea spray model, *Geophys. Res. Lett.*, 31, L03110, doi: 10.1029/2003GL018571
- Pu S., J. Zhao, W. Yu et al., 2004: Progress of large-scale air-sea interaction studies in China. *Adv. Atmos. Sci.*, 21(3), 383-398
- Qiao F., Y. Yuan, Y. Yang, Q. Zheng, C. Xia, J. Ma, 2004: Wave-induced mixing in the upper ocean: Distribution and application in a global ocean circulation model, *Geophysical Research Letter*,31:L11303,doi:10.1029/2004GL019824.
- Qiao F., Y. Yuan, T. Ezer, C. Xia, Y. Yang, Z. Song, 2006: A three-dimensional surface wave-ocean circulation coupled model: System description and initial testing. *Ocean Modelling* (In press)
- Ren X., and Y. Qian, 2005: A coupled regional air-sea model, its performance and climate drift in simulation of the East Asian summer monsoon in 1998, *Int. J. of Climatol.* 25, 679-692.
- Ren X., W. Pierrie, Z. Long, and J. Gyakum, 2004: Atmosphere-Ocean coupled dynamics of Cyclones in Midlatitudes, *Monthly Weather Review*, 132, 2432-2451
- Ren X., and Y. Qian, 2001: Development of a coupled regional air-sea model and its numerical simulation for summer monsoon in 1998, *Acta Meteorologica Sinica*, 15(4), 385-396.
- Ren X., Y. Qian, and Y. Zhang, 2000: Numerical simulations of oceanic elements in the South China Sea and its neighboring sea regions from January to August in 1998, *Journal of Tropical Meteorology*, 16(2), 139-147

- (in Chinese).
- Ren X. and Y. Qian, 2000: Numerical simulation of oceanic elements at East Asian coastal oceans from May to August in 1998 by using a coupled regional ocean-atmosphere model, *Climatic and Environmental Research*, 5(4), 482-485.
- Rong X., and X. Yang, 2003: Sensitivity of ENSO characteristics in a coupled ocean-atmosphere GCM to change of climatological background state, *Acta Meteorologica Sinica*, 61(1), 52-65
- Rong X. and X. Yang, 2005: The upper-ocean response and adjustment to surface forcing in an oceanic general circulation model: II Decadal-to-interdecadal variability, *Acta Oceanologica Sinica*, 27(3), 20-31.
- Saji N.H., S. -P. Xie , and T. Yamagata, 2006: Tropical Indian Ocean variability in the IPCC 20th-century climate simulations. *J. Climate*, in press.
- Shao H., Y. Qian, Q. Wang, 1998: Impact of solar radiation diurnal cycle on the simulation results of R51L9, *Plateau Meteorology*, 17, 158-168.
- Song Z., F. Qiao, Y. Yang, Y. Yuan, 2006: The improvement of the simulated tropical Pacific too cold tongue from a coupled ocean-atmosphere general circulation model by wave-induced vertical mixing, *Progress in Natural Sciences* (in press)
- Wang B., H. Wan et al., 2004: Design of a new dynamical core for global atmospheric models based on some efficient numerical methods, *Science in China*, Ser. A, 47 Supp, 4-21.
- Wang B., 2005: Introduction of the 4<sup>th</sup> generation of LASG/IAP climate system model FGOALS and its numerical experiments, Invited presentation at the 2004 Annual Academic Conference of the Institute of Atmospheric Physics, Chinese Academy of Sciences, Feb. 22, 2005, Beijing.
- Wang H.J., 2000: The interannual variability of East Asian monsoon and its relationship with SST in a coupled Ocean-Atmosphere-Land climate model. *Adv. Atmos. Sci.*, 17,31~47.
- Wang H., Y. F. Xu, T.J. Zhou et al. 2004: Atmospheric Science: A vigorous frontier science, *Adv. Atmos. Sci.*, 19(4), 31-38.
- Wang Z., G. Wu., T. Wu et al. 2004: User's Guide and Reference Manual of the ALGCM (R42), Technical Report of LASG/IAP, No.14, 73pp.
- Wang Z., R. Yu, Q. Bao, T. Zhou, G. Wu, Y. Liu, and P. Wang, 2006: A comparison of the atmospheric circulations simulated by the FGOALS-s and SAMIL, *Chinese Journal of Atmospheric Sciences*, in press
- Wu F., H. Liu, W. Li, X. Zhang, 2005: Effect of adjusting vertical resolution on the eastern equatorial Pacific cold tongue, *Acta Oceanologica Sinica*, 24(3), 1-12 .
- Wu G., X. Zhang, H. Liu, Y. Yu, X. Jin, Y. Guo, S. Sun, W. Li, B. Wang, G. Shi, 1997: Global ocean-atmosphere-land system model of LASG (GOALS/LASG) and its performance in simulation study, *Quart. J. Appl. Meteor.*, Supplement Issue, 15-28. (In Chinese)
- Wu G., H. Liu, Y. C. Zhao, and W. P. Li, 1996: A nine-layer atmospheric general circulation model and its performance, *Adv. Atmos. Sci.*, 13, 1-18.
- Wu L., D. Lee, and Z. Liu, 2005a: The 1976/77 North Pacific climate shift: The role of subtropical ocean adjustment and coupled ocean-atmosphere feedbacks. *J. Climate*, 18, 5125-5140.
- Wu L., Z. Liu, Y. Liu, Q. Liu, and X. Liu ,2005b: Potential global climatic impacts of the North Pacific Ocean, *Geophys. Res. Lett.*, 32, L24710, 10.1029/2005GL024812.
- Wu L., F. He, and Z. Liu, 2005c: Coupled ocean-atmosphere response to north tropical Atlantic SST: Tropical Atlantic dipole and ENSO. *Geophys. Res. Lett.*,32, L21712, 10.1029/2005GL024222.
- Wu L., Z. Liu, R. Gallimore, R. Jacob, D. Lee, and Y. Zhong, 2003: Pacific decadal variability: the Tropical Pacific mode and the North Pacific mode. *J. Climate*, 16,1101-1120
- Wu T.W., 2006:The coupled climate system model development plan of China Meteorological Administration and

- its recent progress, East Asian Climate (EAC) Workshop, 31 March -1 April, 2006, Sun Moon Lake, Nantou, Taiwan, China
- Xiao C., 2006: Adoption of a two-step shape-preserving advection scheme in an OGCM and its coupled experiment. Dissertation for Master Degree, Institute of Atmospheric Physics, Chinese Academy of Sciences, 89pp.
- You X., R. Li, M. Zhang, Q. Zeng, 2001: Numerical Calculation of the Wintertime Circulation in the South China Sea by using a Baroclinic Model, *Acta Oceanologica Sinica*, 23(6), 1-10.
- You X., G. Zhou, J. Zhu, R. Li, 2003: A Sea Temperature Data Assimilation System for the China Sea and Adjacent Areas, *Chinese Science Bulletin*, 48 (Supp II), 70-76.
- Yu R.C., 1994: A Two-Step Shape-Preserving Advection Scheme, *Adv. Atmos. Sci.*, 11(4), 479-490.
- Yu Y. and X. Zhang, 1998: A modified air-sea flux anomaly coupling scheme, *Chinese Science Bulletin*, 43, 866-870. (In Chinese)
- Yu Y., A. Izard, Y. Guo and X. Zhang, 2001: A Response of IAP/LASG Oceanic General Circulation Model to the Observed Wind Stress, *Chinese J. of Atmos. Sci.*, 25, 305-324.
- Yu Y., R. Yu, X. Zhang and H. Liu, 2002: A Flexible Global Coupled Climate Model, *Adv. Atmos. Sci.*, 19, 169-190.
- Yu Y., and X. Liu, 2004: ENSO and Indian Dipole Mode in Three Coupled GCMs, *Acta Oceanologica Sinica*, 23 (4) , 581-595.
- Yu Y., Z. Zhou, and X. Zhang, 2004: Impact of the closure of Indonesian seaway on climate: A numerical modeling study. *Chinese Sci. Bull.*, 48 Supp.II, 88-93.
- Yu Y., X. Zhang, Y. Guo, 2004: Global coupled ocean- atmosphere general circulation models in LASG/IAP. *Adv. Atmos. Sci.*, 21, 444-455.
- Yu Y., 2005: IAP Global Coupled Climate Model FGOALS and Its Application in Climate Change, MOST-DOE Science Team Meeting, 9-11 June, 2005, Beijing
- Yuan Y. and F. Qiao, 2006: Ocean dynamic system and marine numerical models, *Progress in Natural Sciences*, (In press)
- Zeng Q., X. Zhang, X. Liang, C. Yuan, and S. Chen, 1989: Documentation of IAP Two-Level Atmospheric General Circulation Model. TRO44, DOE/ER/60314-HI.
- Zhou G., and Q. Zeng, 1998: A coupled ocean-atmosphere general circulation model for ENSO prediction and 1997/1998 ENSO forecast. *Climatic and Environmental Research*, 3(4), 349-357. (in Chinese)
- Zhou G., Q. Zeng, and R. Zhang, 1999: An improved coupled ocean-atmosphere general circulation model and its numerical simulation. *Progress in Natural Science*, 9(5), 374-381.
- Zhou G., and Q. Zeng, 2001: Prediction of ENSO with a coupled atmosphere-ocean general circulation model. *Adv. Atmos. Sci.*, 18(4), 1587-1603.
- Zhou N., Y. Yu, and Y. Qian, 2006, Simulations of the 100 hPa South Asia High and Precipitation over the East Asia with IPCC Coupled GCMs. *Adv. Atmos. Sci.*, 23(3), 375-390.
- Zhou T., R. Yu, X. Zhang, Y. Yu, W. Li, H. Li, and X. Li, 2001: The features of atmospheric moisture transport, convergence and air-sea freshwater flux on coupled climate models, *Chinese Journal of Atmospheric Sciences*, 25(5), 598-608 (in Chinese).
- Zhou T., X. Zhang, S. Wang, 2000: The relationship between the thermohaline circulation and climate variability, *Chinese Science Bulletin*, 45(11), 1052-1056
- Zhou T., X. Zhang, Y. Yu, R. Yu, S. Wang, 2000: Response of IAP/LASG GOALS model to the coupling of air-sea freshwater exchange, *Adv. Atmos. Sci.*, 17(3), 473-486.
- Zhou T., X. Zhang, R. Yu, Y. Yu, S. Wang, 2000: The North Atlantic Oscillation Simulated by Version 2 and 4

- of IAP/LASG GOALS Model. *Adv. Atmos. Sci.*, 17(4), 601-616
- Zhou T., X. Zhang, Y. Yu, 2001: On the Coupling Procedure of Air-Sea Freshwater Exchange in Climate System Models, *Chinese Science Bulletin*, 46(1),83-85
- Zhou T., 2003: Multi-spatial variability modes of the Atlantic Meridional Overturning Circulation, *Chinese Science Bulletin*, 48, Supp. II, 30-35.
- Zhou T., Z. Li, Y. Yu, R. Yu, X. Zhang, 2004: Indian Ocean response to ENSO in IPSL air-sea coupled model, *Chinese Journal of Atmospheric Sciences*, 28(4), 313-330.
- Zhou T., and H. Drange, 2005: Climate impacts of the decadal and interannual variability of the Atlantic Thermohaline circulation in Bergen Climate Model, *Chinese Journal of Atmospheric Sciences*, 29(2), 167-177.
- Zhou T., R. Yu, X. Liu, et al., 2005: Weak response of the Atlantic thermohaline circulation to an increase of atmospheric carbon dioxide in IAP/LASG Climate System Model, *Chinese Science Bulletin*, 50(6), 592-598
- Zhou T., R. Yu, Z. Wang, and T. Wu, 2005a: The Atmospheric general circulation model SAMIL and the associated coupled model FGOALS\_s, Beijing, Meteorology Press, 288pp (in Chinese).
- Zhou T., Z. Wang, R. Yu, Y. Yu, Y. Liu, H.Liu, Q. Bao, P. Wang, W. Li, G. Wu, and T. Wu, 2005b: The climate system model FGOALS\_s using LASG/IAP spectral AGCM SAMIL at its atmospheric component, *Acta Meteorologica Sinica*, 63 (5), 702-715 (in Chinese).
- Zhou T., Y. Yu, H. Liu, W. Li, R. Yu, 2006: Numerical simulation of the sensitivity of the Pacific subtropical-tropical meridional cell to global warming, *Progress in Natural Science*, 16(5),507-511.
- Zhou T., and R. Yu, 2006: 20<sup>th</sup> Century surface air temperature over China and the globe simulated by coupled climate models, *Journal of Climate*, in press
- Zhang W., 2006: Spatial distribution and temporal variation of the observed and simulated soil moisture over China. Dissertation for Master Degree, Institute of Atmospheric Physics, Chinese Academy of Sciences, 119pp.
- Zhang X., and X. Liang, 1989:A numerical world ocean general circulation model. *Adv. Atmos. Sci.*, 6: 43~61
- Zhang X., N. Bao, R. Yu, W. Wang, 1992: Coupling scheme experiments based on an atmospheric and an oceanic GCM. *Chinese Journal of Atmospheric Sciences*, 16: 129~144
- Zhang X., K. Chen, X. Jin, W. Lin, Y. Yu, 1996: Simulation of thermohaline circulation with a twenty-layer oceanic general circulation model. *Theoretical and Applied Climatology*, 55: 65~87
- Zhang X., Y. Guo, C. Yuan, G. Shi, and G. Wu, 1999: Achievements in GCM studies at IAP, in *Greenhouse Effect and Climate Change*, Tao S., M. Riches, P. Chen, and W. Wang Eds, China Ocean Press, Beijing, 1999, 96-107pp.
- Zhang X., G. Shi, H. Liu, and Y. Yu (Eds) , 2000: IAP Global Ocean-Atmosphere-Land System Model, Science Press, Beijing, 251pp.
- Zhang X., Y. Yu and H. Liu, 2003: The Development and Application of the Oceanic Circulation Models, Part I. the Global Oceanic General Circulation Models, *Chinese Journal of Atmospheric Sciences*, 27, 607-617 (in Chinese).
- Zhang, X., and J. E. Walsh, 2006: Toward a seasonally ice-covered Arctic Ocean: Scenarios from the IPCC AR4 model simulations. *J. Climate*, 19, 1730–1747.

## RECENT PROGRESS IN THE STUDY IN CHINA OF THE IMPACT OF TIBETAN PLATEAU ON THE CLIMATE

*Liu Yimin (刘屹岷)<sup>1\*</sup> Bao Qing (包庆)<sup>1</sup> Duan Anmin (段安民)<sup>1</sup>*

*Qian Zhenan (钱正安)<sup>2</sup> and Wu Guoxiong (吴国雄)<sup>1</sup>*

<sup>1</sup>State Key Laboratory of Numerical Modeling for Atmospheric Sciences and Geophysical Fluid Dynamics

(LASG), Institute of Atmospheric Physics, Chinese Academy of Sciences, Beijing 100029

<sup>2</sup>Cold and Arid Regions Environmental and Engineering Research Institute,

Chinese Academy of Sciences, Lanzhou 730000

### Abstract

The studies of the impacts of the Tibetan Plateau (TP) on climate in China in recent 4 years are reviewed. New findings and insights are highlighted.

It is reported that the temperature and precipitation over the TP have increased during recent decades. From the satellite data analysis, it is demonstrated that most of the precipitation over the TP is from the deep convection clouds.

The huge TP mechanical forcing and extraordinary elevated thermal forcing impose remarkable impacts on the local circulation and global climate. Extensive studies in this aspect during the passed four years are summarized here. In winter and spring stream flow is deflected by the large obstacle and appears as an asymmetric dipole, making East Asia much colder than the Middle Asia in winter and forming the persistent rainfall in late winter and early spring over South China. In late spring, the TP heating contributes to the establishment and intensification of the South Asian High and the abrupt seasonal transition of the surrounding circulations. In summer, the TP heating in conjunction with the TP- Air-Pump cause the deviation stream field to resemble a cyclonic spiral, converging towards and rising over the TP. Together with Iran Plateau, the TP locates in the central and eastern parts of the Eurasian Continent. Therefore the prominent Asian monsoon climate over East Asia and the dry climate over Middle Asia in summer are forced by both the TP local forcing and the Eurasian continental forcing.

Due to the longer memory of the snow and soil moisture process the TP thermal status both in summer and in the late winter and spring can influence the variation of Eastern Asian summer rainfall. It is indicated that corresponding to the stronger TP heating in summer, more rainfall tends to occur along Yangtze River and Huaihe River and less rainfall in northern and southern China. A combined index using both the snow cover over the TP and ENSO index in winter show

---

\* E-mail: lym@lasg.iap.ac.cn

a better seasonal forecast.

The strong sensible heating over the Tibetan Plateau in spring contributes significantly to anchor the earliest Asian monsoon being over the eastern Bay of Bengal (BOB) and western Indochina Peninsula. Qualitative prediction of the BOB monsoon onset was attempted by using the sign of meridional temperature gradient in March in the upper-troposphere or at 400 hPa over the TP. It is also demonstrated by numerical experiment and theoretical study that the heating over the TP leads to a significant variability in the atmospheric circulation on a quasi-biweekly time-scale, bearing much similarity to those found from the observational studies. At last some important issues for further researches in understanding the impacts of TP are raised.

## 1. Introduction

The Tibetan Plateau (Qinghai-Xizang Plateau abbreviated as TP hereafter) is not only the terrain obstacle to the air flow, but also the strong heat source or sink, which intensifies the land-sea thermal contrast there. Therefore the TP functions as an important modulator of the regional climates over the Central- and Southern-Asia, particularly South Asian monsoon climate to its south; the East Asia monsoon to the east; the unique China-Mongolia mid-latitude drought climate to the north; the Central Asia desert and dry one to the west; and the unique Plateau monsoon climate over the TP.

Before 1950's, most of the studies concerned with the influence of large-scale topography upon atmospheric circulation and climate focused on its mechanical aspects. Queney (1948) summarized the studies on airflow over mountains and brought forward three critical scales to distinguish different mountain waves by using linearized equations. In 1957, Yeh et al. and Flohn respectively found that the Tibetan Plateau is a heat source of the atmosphere in summer. Since then the temporal and spatial distributions of the heating field over the Tibetan Plateau and their impacts on weather and climate have become an important research field in meteorology (Yeh and Tao et al, 1958; Yeh and Gao, 1979; Zhang et al, 1988; Wu et al, 1997; 2004). Recently, Yanai and Wu (2006) gave a thorough review of the past studies concerned with the effects of the TP. The review summarized from the research in the 1950's on the jet stream, the warm South Asian High, and the early progress of TP research in China. The review also discussed the mechanical effects of the TP on large-scale motion, the winter cold surge, and the summer negative vorticity source over the TP, as well as the heating source  $\langle Q_1 \rangle$  and  $\langle Q_2 \rangle$  used by Yanai et al. (1973).

Field experiment over the TP has been a national focusing topic in the TP study for a long time in China. The Qinghai-Xizang Meteorology Experiment (QXPME) in 1979 and the second Tibetan Plateau Atmosphere Science Experiment (TIPEX) in 1998 were conducted in China. There were intensive *in situ* meteorological observation and land surface physical process observation over the Plateau (Zhang et al., 1988; Tao et al., 2000 a, b, c; Zhou et al., 2000). During the last four years, such field experiments continued and became parts of international coordination. These include the Global Energy and Water Cycle Experiment (GEWEX) Asian Monsoon Experiment on the Tibetan Plateau (GAME/Tibet) and the Coordinated Enhanced

Observing Period (CEOP) Asia-Australia Monsoon Project (CAMP) on the Tibetan Plateau (CAMP/Tibet). Prominent progresses have been obtained (Ma et al., 2006a)

This paper reviews the recent advances of TP research in the last four years in China. Section 2 covers new observation facts over the Plateau; Section 3 and 4 describes the impacts of TP forcing on the synchronous and time-lag climate, respectively; research on heating over the Tibetan Plateau and the Asian Monsoon onset is presented in Section 5; Section 6 is devoted to the relationship between heating over the TP and low-frequency oscillation of circulation; In Section 7, some important issues for further researches in understanding the TP climate dynamics are raised.

## **2. New observation facts over the Tibetan Plateau**

### **2.1 Precipitation, surface air temperature and their variations**

Based on the three-year TRMM precipitation radar data, Fu (2005) and Fu et al. (2006) revealed that the tower mast shape of deep precipitation layer with the rain rate more than 2 mm/h can be seen over the TP summer (Fig. 1) with very strong diurnal cycle. Their work also indicated that the TRMM algorithm might have misclassified weak convections as stratiform rains. The fact that latent heat tower of well-lifted and well-penetrated into the middle troposphere confirms the earlier finding that convection heating is a dominant heating in summer over the TP (Yeh and Gao, 1979).

Utilizing the NCEP's monthly mean data, Cai and Qian (2004) calculated the air column precipitable water (PW) and showed that in winter the minimum PW is over the TP, with only 3 mm, even lower than that over North China and the eastern part of Northwest China. In summer, there is the maximum PW of 60 mm or more over the South and East Asian Monsoon regions, while the PW over the TP is about 10 mm. But the mean precipitation conversion rate of PW to real rainfall over the TP is double than that over the southern and eastern China and much more than the northern and northwestern China.

There are significant interannual and decadal variability in the TP rainfall. Wei et al. (2003), Cai et al. (2003), Ma and Hu (2005) and Wu S. et al. (2005) showed that the main trends of climate change are temperature rise and precipitation increase. Precipitation in most parts of the Plateau increases smoothly. The changes are detected in Qinghai and northwestern Sichuan in 1968, 1972 and 1986 separately (Ma and Hu, 2005, Duan et al., 2006). The increasing trends of the annual mean temperature, maximum and minimum temperature were confirmed by the recent

station data (Duan et al., 2006; Li S. C. et al., 2006) and satellite data (Xu et al., 2005).

## **2.2 Ground temperature and its variation**

Usually ground temperature (TG) is the 0 cm temperature measured by mercury thermometer at weather stations. Li D. et al (2006) showed that in the last 30 years the TG trends in the northern and southern TP are different. The TG over the northern and northeastern TP exhibits a significant increasing while the TG over the middle and southeast TP shows a decreasing trend. However Jiang et al. (2006) indicated that the difference between the TG on the bare surface measured by mercury thermometer and calculated by the radiation balance can be more than 4°C in day time in summer, and about -2°C during night. On the dense vegetation surface, the highest difference in day time can be over 16°C, and the negative difference at night can reach about -3°C. In this regard, the conclusion of Li et al. should be considered qualitative and further verification are needed.

## **2.3 Land-surface processes and boundary layer**

The climatological average of the surface sensible heat flux (SH) over the Plateau from recent data doesn't show much new results from the previous studies. The SH appears a weak negative value in a small range in winter, and it is positive in the rest seasons of a year (Li D et al., 2003 a). In detail, the western part of TP is a heating source in all seasons (Li G et al., 2003; Yu et al., 2004). The long variation of SH has a decrease trend in the northern and western parts of the Plateau, and has an increase trend in the middle and eastern parts of the Plateau in winter. In summer the SH in main TP and its eastern area increases year by year but has an opposite trend in the western part (Li D. et al., 2003 b)

Most of these studies are based on station data. A study of Wei and Li (2003) indicated that in the reanalysis data the long-term variations in air temperature and radiation flux over the TP calculated from NCEP reanalysis agree with the observations although the reanalyzed temperature are systematically lower than the observation due to the higher altitude of the Plateau in the reanalysis model. During the last 4 years, the studies from the diurnal to annual variation based on the data from TIPEX experiment and CEOP have been conducted and a parameterization method has been proposed to calculate the SH and determine the SH regional distribution over the TP (Gao Z. et al., 2003; Ma Y. et al., 2003; 2005 b; 2006 a and b; Ma and Ma, 2006)

Higher elevation of atmospheric boundary layer (ABL) over the Plateau has been indicated

from field observation. In 1998, it is as high as 3550 m above the ground at Ando in the central TP in dry season, but 2300m, in wet season (Zuo et al, 2004). In the Mt Qomolangma Region of Himalaya Ranges, the ABL altitude reaches even 4000 m in dry season of 2005 (Li S. M. et al, 2006 ). Moisture inversion phenomena were found over the TP during the TIPEX period (Liu H. et al, 2002; Peng Y. et al., 2005), presenting a unique character of the boundary layer over the TP (Bian et al., 2003).

### **3. TP forcing and the synchronous circulation and climate**

. The temporal and spatial distributions of the heating over the Tibetan Plateau and their impacts on weather and climate have been further studied during the past four years and new achievement have been obtained.

#### **3.1 The TP forcing in winter and persistent rainfall in early spring in South China**

In winter as a large obstacle, the TP together with the mountain to the north of TP retard the westerly jet flow and deflects it into northern and southern branches. The deviation stream flow then appears as an asymmetric dipole (TP-Dipole) with the convergent entrance on its eastern flank and the divergent outgoing on its western flank (Wu et al., 2005a). Figure 2 shows the 850 hPa stream fields difference between the experiments with and without an idealized elliptical mountain based on a spectral atmospheric general circulation model (GOALS-SAMIL) which has 9 vertical layers and is truncated at wave-number 42 (Wang et al., 2004). Even in such a highly simplified experiment, the asymmetric dipole in DJF is predominated. The huge anticyclonic deflected flow in the north has an important impact on atmospheric temperature distributions due to its horizontal advection, making East Asia much colder than the Middle Asia at the same latitudes north of 35°N (Jian, 2003). Its cyclonic deflected flow in the south has an important impact on the dry climate in South Asia and the moist climate in Southeast Asia and South China. In late winter and early spring over South China, the southward moving cold and dry air that flows along the northern anticyclonic circulation of the TP-Dipole meets with the northward moving warm and moist air that flows along the southern cyclonic circulation of the TP-Dipole. Persistent rainfall in early spring therefore occurs over South China until the Asian monsoon onset (Wan and Wu, 2007) (Fig. 3). In late spring, the TP heating also contributes to the establishment and intensification of the South Asian High and the abrupt seasonal transition of the surrounding circulations (Wu et al, 2007).

#### **3.2 TP forcing in summer and the Asian climate pattern**

In summer, the TP heating produces a large-scale cyclonic circulation in the lower

troposphere. Such a forcing in conjunction with the TP- Air-Pump (Wu et al., 1997) causes the deviation stream field to resemble a cyclonic spiral (Fig. 2b), converging towards and rising over the TP (Wu et al., 2007). Duan and Wu (2005) and Wu et al. (2005b) found that since the TP acts as a strong heat source in summer with the strongest heating lying in the lower layers (Fig. 4), the thermal adaptation results in a shallow and weak cyclonic circulation near the surface and a deep and strong anticyclonic circulation above it (Fig. 5). As a consequence, large amounts of moisture flux are transported from the tropics to the eastern flank of the TP and to its east, resulting in plentiful rainfall. On the contrary, dry climate is forced to the west of the TP (Fig. 2b).

Moreover, with long wave radiation cooling (CO), sensible heating (SH), condensation heating (CO) and double heating (D) as the local dominant heating appearing from west to east across each continent and its neighboring oceans, the continental-scale diabatic heating along the summer subtropics presents a quadruplet LOSECOD pattern (Wu and Liu, 2003; Liu et al., 2004). This LOSECOD quadruplet heating generates lower layer cyclonic circulation and upper layer anticyclone circulation over land areas (Cai and Qian, 2004). Therefore the circulation pattern forced by the continental-scale heating over Eurasian is in phase with the circulation patterns forced by the thermal forcing of the TP and Iran Plateau, and dry and hot climate in West and Middle Asia but strong monsoon and wet climate in East Asia are formed (Duan and Wu 2005; Liang, et al., 2005a; Liang et al., 2006).

Besides thermal forcing, it has been revealed that orographic forcing can also significantly contribute to the configuration of the summer circulation. Previous studies show that in winter, when westerlies dominate in the mid-latitudes and subtropical upper troposphere, orographic forcing plays a very important role. In summer the zonal flow across the TP is weak, and the zonal mean zero-westerly wind isoline at upper troposphere is over the TP. The importance of its thermal forcing has been stressed (Yeh, et al., 1957; Yania and Wu, 2006). Little attention has been paid to the role of the TP orographic forcing on the Asian summer monsoon flow. Recently, Liu et al., (2007) investigated the influence on the summer circulation over Asia of the orographic and thermal forcing of the TP using a sequence of idealised experiments based on a global primitive equation model. It is shown that there is some similarity between the responses to the separate orographic forcing and thermal forcing. The upper tropospheric Tibetan anticyclone is forced predominantly by the heating but also weakly by the orography. In the lower troposphere, both forcings produce air descending down the isentropic surfaces in an equatorward anticyclonic

circulation to the west and rising in a poleward circulation to the east (Fig. 6). These results explain why in the experiments based on a complex GCM, the Asian monsoon precipitation in summer is greatly enhanced with the existence of the TP comparing with that without the TP (Liang et al., 2005a; Wu et al., 2007).

The China-Mongolia (CM) arid area is also influenced by TP. Qian et al (2001) showed that this arid area is associated with the summer mean vertical circulations over the TP and its vicinity. The TP thermally inducing meridional cells exist not only along 90° E, but also along all of the meridians on the north sides of the TP. In the severe drought summers over the CM dry area, these meridional cells become intensified; whereas in the wetter summers, these meridional cells are not clear.

### **3.3 Variation of the summertime TP heating and its climate impact**

Hsu and Liu (2003) showed that the summer (JJA) column diabatic heating over the TP where the elevation is more than 3000 m shows an evident shift in the late 1970's. In the eight strong TP heating summers, the rainfall pattern exhibits a tripole structure over the eastern China, ie, with a zonal-elongated positive anomaly in the Yangtze River and Huaihe River Reaches, sandwiched by the negative anomaly in the northern- and southern-China, and vice versa in the eight weak TP heating summers. Such a tripole pattern of rainfall distribution resembles the leading EOF modes reported in the early studies (e.g., Tian and Yasunari, 1992; Huang et al, 2003). The study also agrees with the finding that there is a closed link between the TP heating and the East Asia Summer Rainfall (EASMR) (Bai, et al., 2003a; Zhao, et al., 2003; Jian et al, 2004; Zhang et al., 2006). To further understand the possible impacts of Tibetan plateau surface condition on the EASMR, a suite of sensitivity experiments was performed with the ECHAM atmospheric general circulation model (Bao et al., 2007). The land surface albedo was changed so that the TP land surface temperature was changed accordingly. The results show that a warmer surface temperature condition over the TP tends to enhance the upper tropospheric South Asian High and the westerly jet stream to its north and the Indian monsoon to its south, while the moisture transport in the lower troposphere towards East Asia increases. The precipitation pattern in the case of warmer TP surface is featured by increasing rainfall over the northwest India and enhanced *Mei-yu* and decreasing rainfall over the Bay of Bengal and in the regions under the control of the western Pacific Subtropical High (Fig. 7), in well agreement with the result from the

above data analysis.

Tibetan Plateau covers a broad coverage and complicated topography. Thus, a single heating index is not enough to represent geographic structure of heating over the TP. Based on the 1958~1999 monthly averaged NCEP/NCAR reanalysis data, the REOF analysis was applied to obtain the main spatial modes of normalized atmospheric heating source over the Tibetan Plateau (TP) in July (Duan and Wu, 2004). The results show that the TP heating cannot be properly presented by only few REOF components. However, since the reliability of the heating in reanalysis data sets is not certain, using new satellite data to validate all the above results and to reveal new facts are necessary.

#### **4. TP thermal status and the time-lag circulation and climate**

The TP thermal impact on the EASMR is not just in summers, but also in winter and spring due to the longer memory of the land process.

##### **4.1 Snow accumulation, freezing-thawing processes and the circulation and rainfall in summer**

The Impact of the TP winter snow cover on the EASMR has been studied by many Chinese scientists since the late 1970's (Chen and Yan, 1978). Recently in more detail, Zhang and Tao (2001) and Wu et al. (2003) and Wu and Qian et al (2000; 2003) showed that if the snow cover over the TP in winter is above normal, the TP heat source in the subsequent spring and summer is weakened, and so is the land-sea thermal contrast between the TP and Pacific. As a result, the east Asian summer monsoon is weakened and more precipitation occurs in the Yangtze River valley and less poor rain is observed in Northern-Southern China; and vice versa in the lighter TP snow years. Similar results were obtained also by Huang and Li (2003) and Lu et al. (2003).

However the relationship between EASMR pattern and the snow accumulation over the TP is not simple. First, Snow is not unique and the most important factor in determining the regional rainfall (Qian et al. 2003). Second, it has been found that the snow depth anomaly in winter over the Tibetan Plateau is relatively more important to the regional precipitation in China than the snow cover in winter and snow depth in spring. Liu et al. (2003) indicated that the relationship between the Plateau snow cover and the summer rainfall over China can be detected more

appropriately under the background of the interdecadal variation of Asian monsoon circulation. Chen (2005) and Peng J. et al. (2005) showed that in some areas of China the relationships between the winter snow cover (and SST) and summer rainfall is stronger in the interdecadal scales than in interannual scales. Furthermore, more or less winter-spring snow in the plateau is found well related to a stronger or weaker polar vortex over Europe and Asia and the subtropical anticyclone in winter (Wei et al., 2005).

Freezing and thawing process in the Tibetan Plateau is another process which may influence the East Asia circulation. Wang C. et al. (2003) showed that in July when the depth of frozen soil on the TP is lower, the South Asian high is stronger and shifts westward in location, and the 500 hPa subtropical high over the western Pacific is weaker and moves eastward. There are 3 belts where the correlation is significant between the mean frozen soil depth in TP and the precipitation in China in July. Therefore, the changes of moisture and heat associated with freezing-thawing process in the TP could act as an external thermal forcing and influence the East Asia climate. On the other hand Gao R. et al. (2003) and Nan et al. (2005) showed that the permafrost distribution over the TP is very sensitive to the climate change.

#### **4.2 TP thermal status in spring and climate anomaly in summer**

Simultaneous relationship between the atmospheric circulation or rainfall over East Asia and the heating over the TP in summertime cannot be used for prediction. Zhao and Chen (2001) showed that the heating status over the TP in April can give a clue to predict the forthcoming weather over regions between the Yangtze River and Huaihe River, and South China and North China. The number of days covered by snow and snowfall over the TP are also shown good relationship with the hemispheric extra-tropical atmospheric circulation and the East Asian summer monsoon rainfall (Zhao et al, 2007). An increase of spring (April-May) number of days covered by snow over the TP is associated with decreases of the tropospheric temperature and geopotential height in the spring and the early summer (June). These tropospheric anomalies over the TP are connected with changes in the hemispheric extra-tropical atmospheric circulation along the westerly jet stream that acts as a waveguide. Soil moisture in May-June might act as a bridge linking the spring snow anomaly and the subsequent summer monsoon.

The station data used in the above studies are mostly located in the eastern part of China. To further reveal the influence of the heating status over the TP before the East Asia summer monsoon onset upon the atmospheric circulation and rainfall in the forthcoming monsoon season, Duan et al. (2005) discussed sensible heat source over the TP region from April, May and June and

their influences upon the circulation and rainfall patterns in the subsequent July based on the NCEP/NCAR reanalysis after verifying their quality. The temporal variation of the April, May and June sensible heat source averaged over the TP is representative of the total diabatic heating, and their leading patterns during this period are almost the same. They found that when the sensible heat source over the TP is abnormally strong (weak), there will be more (less) rainfall in July over the Yunnan-Guizhou Plateau and the middle reaches of the Yangtze River and Huaihe River (Fig. 8). Correspondingly, there is lower-layer convergence (divergence) of water vapor flux in these regions. All these were well explained in terms of the thermal adaptation theory, the large-scale quasi-stationary barotropic vorticity equation and the good persistence of the thermal status over the TP. These results are in consistence with those presented in Section 3.3, and also agree with other results derived from either data diagnoses or modeling (Li, 2003; Li et al., 2003a; Bai et al., 2003b; Bi et al., 2004; Ning and Qian, 2006). Therefore, the heating status over the TP during April, May and June can be used as a useful predictor for the early summer rainfall and atmospheric circulation over East Asia, especially over the valley between the Yangtze and Huaihe Rivers.

#### **4.3 TP thermal status and sand storm days in northern China**

Li et al. (2004) found the abnormal surface sensible heating (SH) on the TP in spring is significantly related to the number of sand storm day in the Northern China. The results indicated that although individual sand storm may belong to different mesoscale weather process, sand storms in different years have a good coherence in space distribution. There are five natural sand sources: Gansu Hexi-Corridor, southern rim of south Xinjiang basin, Alashan Plateau, Eerduosi Plateau and the Hunshandake Sandlot. The trend of the sand storm occurrence has been decreasing since 1964. The number of sand storm day in 1990's is the least in recent 5 decades, but showed a hoist from end of 20 century to the beginning of 21 century. Moreover, the annual occurrence of sand storm in the northern China is well related to the TP surface heating. Zhong et al. (2004) decomposed the SH on the TP in winter and spring, and showed that when the first EOF mode is positive in spring, the number of sand storm day in northern China is significantly above normal.

### **5. Heating over the Tibetan Plateau and the Asian Monsoon onset**

In a review paper of the TP, Wu (2004) indicated that the strong sensible heating over the TP in spring contributes significantly to the abrupt seasonal transition of the East Asian circulation, resulting in the earliest Asian monsoon onset anchored over the eastern Bay of Bengal to the western Indochina Peninsula. Wu and his collaborators (2004) showed that due to the surface cooling in winter and heating in summer, the air column over the Tibetan Plateau descends strongly in winter and ascends strongly in summer. It acts as a huge air-pump and regulates the seasonal evolution of the lower layer circulation over the surrounding areas, contributing to the occurrence of the monsoons over South Asian, BOB, SCS and the western Pacific (Mao et al., 2002 a, b). However, without surface sensible heating, especially the surface heating on the sloping surfaces, such an air- pump will not expel or suck the surface air- flow (Wu et al., 2007).

Wu and Zhang (1998) showed that it is due to the mechanical as well as thermal forcing of the Tibetan Plateau that the Asian monsoon onset is composed of three consequential stages: the earliest over the eastern Bay of Bengal (BOB) to western Indochina Peninsula in early May. The BOB monsoon onset creates favorable conditions for the Southern China Sea monsoon onset in middle May (Liu et al., 2002). These lead to the great changes in both large-scale circulation and diabatic heating over Asia. Finally, the Indian monsoon onset appears in early June. The numerical simulation of Liang et al. (2005b) proves that the Tibetan Plateau heating in late spring greatly intensified the southern branch of the winter-time dipole of the 850 hPa stream field. This intensified southern branch of the dipole enhances the southerlies to the southeast of the Tibet and brings heavy rainfall and more latent heating over the eastern BOB and to its east, and the prevailing northerlies to the southwest of the Tibet, resulting in less rainfall and more sensible heating over Indian subcontinent. Therefore, the Tibetan Plateau anchors the onset site of Asian summer monsoon and the onset of Asian summer monsoon often takes place over the eastern sea shore of BOB to the south of the Tibetan Plateau (Fig. 9). It is also found that stronger surface sensible heating on the TP in spring lead to earlier seasonal transition in Eastern Asia (Wang L. et al., 2003; Duan et al., 2004; Mao and Duan, 2005).

## **6. Heating over the TP and low-frequency oscillation of circulation**

Tao and Zhu (1964) demonstrated that zonal shifting of the South Asian High over the TP

in summer leads the east-west movement of the 500 hPa subtropical anticyclone over the Western Pacific (SAWP) for few days. Krishnamurti and Bhalme (1976) showed that the sub-seasonal oscillations of the summer rainfall, which leads to the active and break monsoon, are related to a quasi-biweekly oscillation of the monsoon system including the Tibetan High. Liu et al. (2007) analyzed the transient behavior of the circulation from a sequence of idealized experiments based on a global primitive equation model. It is found that heating over the Plateau leads to a potential vorticity (PV) minimum over the TP in the upper troposphere. They further showed that if the heating is sufficiently strong, the background flow becomes unstable, and a quasi-biweekly oscillation is produced (Fig. 10). During this oscillation the Tibetan anticyclone in the upper troposphere changes between a single centre over the southwestern side of the TP and a split/double-center structure with one center over East China and the other over Middle East (Fig. 11). These characteristics are quite similar to the observed variability in the area. It is shown that the origin of such variability is due to the zonally extended PV minimum on a  $\theta$ -surface, as proposed by Hsu and Plumb (2000), and due to the tendency to reduce the PV above the heating over the Plateau and to the advection by the consequent anticyclone of high PV from the east and low PV to the west.

The above JJA numerical simulation results are consistent with those from data diagnosis. Gong et al. (2004, 2006) found that there are evident differences of the rainfall over the TP between weaker monsoon summer (1993) and stronger monsoon summer (1994). During the weaker monsoon summer of 1993, the TP rainfall concentrated in July and August which possessed the feature of the quasi-biweekly variations. The western Pacific subtropical high also presented a quasi-biweekly southward/northward oscillation during its northward shift from May to August. In contrast in 1994, the precipitation over the TP was stronger in May and June but weak in July and August, and the main variability was associated with 30- 60 day tropical oscillations.

## **7. Concluding remarks**

The studies of the Tibetan Plateau meteorology and Tibetan Plateau climate dynamics in recent 4 years in China are reviewed. The huge TP mechanical forcing and extraordinary elevated

thermal forcing have a large influence on regional as well as global climate. The TP is a weak heat sink in winter but a strong heat source in summer. It was found that converging impact of the TP on the atmospheric circulation in summer is stronger than its diverging impact in winter, because in the summer months there is a CISK-like positive feedback between the small-scale convection over the TP and the large-scale convergent spiral of the lower tropospheric circulation in the surrounding area (Wu et al., 2007). The analysis of the TRMM data proves that the precipitation over the TP is dominated by deep convection.

Relative to earlier work, one of the most important processes in understanding the TP climate impacts is the TP influences in different seasons. In winter as a large obstacle, the TP retards the westerly jet flow and deflects it into northern and southern branches. The deflected stream flow then appears as an asymmetric dipole (TP-Dipole), making East Asia much colder than the Middle Asia in high latitudes. In late winter and early spring over South China, the TP-Dipole circulation results in the persistent rainfall in early spring over South China till the Asian monsoon onset. In late spring, the TP heating also contributes to the establishment and intensification of the South Asian High and the abrupt seasonal transition of the surrounding circulations. In summer, the TP heating in conjunction with the TP-Air-Pump generate a zonal deviation stream field to resemble a cyclonic spiral, converging towards and rising over the TP.

The TP together with Iran Plateau are located in the central and eastern parts of the Eurasian Continent. The meridional and vertical motions generated by the Eurasian continental-scale heating are in phase with those generated by the TP local-scale forcing over Asia. The rising of the southerly flow over East Asia and the sinking of the northerly flow over Middle Asia therefore become enhanced. The East Asian monsoon climate and the Middle Asia dry climate in summer are intensified by the TP mechanical and thermal forcing.

It has been shown that the variation of the Eastern Asian summer rainfall is closely related to the TP thermal status both in summer and in late winter and spring. Generally corresponding to the stronger TP heating in summer, more rainfall trends to occur along the Yangtze River and Huaihe River and less rainfall in the northern and southern China. An index combining both the snow cover over the TP and ENSO index has been proposed and shown better ability on the seasonal climate forecast.

The influence of the TP on the Asian monsoon onset is another important issue receiving intensive study during the past four years. The strong sensible heating over the Tibetan Plateau in spring contributes significantly to the abrupt seasonal transition of the East Asian circulation, resulting in the earliest Asian monsoon onset being anchored over the eastern Bay of Bengal and western Indochina Peninsula. Moreover since the essence of summer monsoon onset is a result of the change in land-sea thermal contrast, a qualitative prediction of the BOB monsoon onset was attempted based on the thermal-wind balance and using the sign of meridional temperature gradient in the upper-troposphere or at 400 hPa over the TP. However, the climate system is a

nonlinear, dissipative and open system, and the timing and location of the Asian monsoon onset is influenced not only by the Tibetan Plateau heating, but also by other persistently external forcing and the low frequency oscillations in the atmosphere including the Madden-Julian Oscillation. Thus continuous efforts are needed to improve the monsoon prediction.

Numerical experiments have shown that the heating over the TP can lead to a significant variability of the atmospheric circulation on a quasi-biweekly time-scale that bears much similarity to those discussed in the observational studies.

In this paper we mainly review the studies of the TP impacts on the climate, not including its influence on the weather systems such as the local torrential rain (Chen and Li, 2005) and the Tibetan Plateau vortex (Liu and Li, 2006). These are very important and should be reviewed separately.

Despite the great efforts many aspects are still unclear. Most of the conclusions summarized here are still qualitative in nature. Unresolved questions include how radiation processes affect the thermal state of the TP, what is the role of the aerosol-cloud-radiation-monsoon circulation feedback, how the air-sea exchange processes interact with such a feedback, and how the TP-Air-Pump in conjunction with the thermal state over Indian Ocean and Australia affect the Asia-Australia monsoon? On the other hand, owing to the broad coverage and complicated topography, the precision, content and coverage of the satellite data and the *in situ* observation still can not satisfy the requirements of the study. Large errors still exist in the surface momentum flux, energy budget, cloud and precipitation in the reanalysis data. Up to now, there are no continuous observations on temporal and spatial variations of land processes. The reliability of numerical simulations is still limited by the uncertainties in models of cloud-radiation feedback, schemes of convection and land processes. Therefore, the priority areas that require improvement in the next few years are more field observation experiments and numerical modeling efforts. Further advance in the study of the Tibetan Plateau requires cooperation among scientists over the world.

**Acknowledgment** We thank Ms. Yu Jingjing for drawing Figure 2. This work was jointly supported by the National Key Basic Research and Development Project of China under grant No. 2004CB418302, 2006CB403607 and by the Natural Science Foundation of China under grants 40475027, 40221503, 40575028 and 40523001.

#### References

- Bai, J.Y., X.D. Xu and S.Q. Yu, 2003a: Summertime deep convection heating over southeast of Tibetan Plateau. *Meteorological Science and Technology*, **31**: 18-22.
- Bai, J.Y., X.D. Xu, Y.S. Zhou and X.J. Zhang, 2003b: Preliminary research on inhomogeneous distribution of Tibetan Plateau sensible heat fluxes in spring. *Journal Of Applied Meteorological Science*, **14**: 363-368.
- Bao, Q., B. Wang, Y.M. Liu, G.X. Wu, 2007: The impact of the Tibetan Plateau warming on the East Asia Summer Monsoon --An ECHAM model study. *Chinese J. A. S* (in press)
- Bi, Y., X. Li, Y.F. Qian, 2004: Relation between 300 hPa temperature anomalies over Iranian and Qinghai-Xizang Plateaus and precipitation of China, *Plateau Meteorology*, **23**: 465-471.
- Bian, L., X. Xu, L. Lu, Z. Gao, M. Zhou and H. Liu, 2003: Analyses of turbulence parameters in the nearsurface layer at Qamdo of the southeastern Tibetan Plateau. *Adv. Atmos. Sci.*, **20**(3): 369-378.
- Cai, Y., Z.A. Qian, 2004: Distribution, changes of atmospheric precipitable water vapor over Qinghai-Xizang Plateau and its surroundings, *Plateau Meteorology*, **23**(1):1-10.
- Cai, Y., D.L. Li, M.C. Tang and C.Y. Bai, 2003: Decadal temperature changes over Qinghai-Xizang Plateau in recent 50 years. *Plateau Meteorology*, **22**: 464-470.
- Chen, L.T., Z.X. Yan, 1978: Impact of QXP snow cover anomalies in winter and spring on the circulation and flood period precipitation in southern China, Selected papers on mid-and long-range hydrometeorology (I), Beijing: *Water and Electricity Press*, 185-195.
- Chen, Y. and Z.C. Li, 2005: diagnostic analysis and numerical simulation on a regional heavy-hard rain in northeast Qinghai-Xizang Plateau, *Acta Meteo. Sinica*, **63**: 289-300.
- Chen, L. T., 2005: The combined application of snow anomaly over the Tibetan Plateau and ENSO index to the forecast of rainfall in China. *Impacts of the land-sea thermal contrast on the climate in China*, Liu Yimin and Qian Zhenan, 2005, China Meteorological Press, Beijing, 177-185.
- Duan, A.M., G.X. Wu, 2005: Role of the Tibetan Plateau thermal forcing in the summer climate patterns over subtropical Asia. *Climate. Dynamics*. **24**, 793-807. DOI 10.1007/s00382-004-0488-8.
- Duan, A.M., G.X. Wu, 2004: Main heating modes over the Tibetan Plateau in July and the correlation patterns of circulation and precipitation over east Asia, *ACTA meteorological Sinica*, **18**,167-178.
- Duan, A.M., Y.M. Liu, G.X. Wu, 2005: Heating status of the Tibetan Plateau from April to June and rainfall and atmospheric circulation anomaly over east Asia in midsummer, *Science in China (D)*, **48**(2), 250-257.
- Duan, A.M., J.Y. Mao, G.X. Wu, 2004: Predictability Analysis and Preliminary Application of the Bay of Bengal Summer Monsoon Onset. *Plateau Meteorology*, **23**: 18-25.

- Duan, A.M., G.X. Wu, Q. Zhang, and Y.M. Liu, 2006: New proofs of the recent climate warming over the Tibetan Plateau as a result of the increasing greenhouse gases emissions, *Chinese Science Bulletin*, **51**(11), 1396-1400.
- Flohn, H., 1957: Large-scale aspects of the "summer monsoon" in South and East Asia. *J. Meteor. Soc. Japan*, **75th Ann. Vol.**, 180-186.
- Fu, Y.F., G.S. Liu, R.C. Wu et al, 2006: Tower mast of precipitation over the central Tibetan Plateau, *Geophy Res Lett*, 33: L05802, doi:10.1029/2005GL024713.
- Fu, Y.F., 2005: The difference of precipitation profiles among Tibetan Plateau, East Asia and tropics. *Impacts of the land-sea thermal contrast on the climate in China*, Liu Yimin and Qian Zhenan, 2005, China Meteorological Press, Beijing, 123-133.
- Gao, R., Z.G. Wei, W.J. Dong, C.H. Wang, H.L. Zhong, 2003: Variation of the snow and frozen soil over Qinghai-Xizang Plateau in the late twentieth century and their relations to climatic change. *Plateau Meteorology*, **22**:191-196.
- Gao, Z., L. Bian, J. Wang and L. Lu, 2003: Discussion on calculation methods of sensible heat flux during GAME/Tibet in 1998. *Adv. Atmos. Sci.*, **20**(3): 357-368.
- Gong, Y.F., L.R. Ji, T.Y. Duan, 2004: Precipitation character of rainy season of Qinghai-Xizang Plateau and onset over east Asia monsoon. *Plateau Meteorology*, **23**: 313-322.
- Gong, Y. F., M. L. Xu, J. H. He, L. X. Chen, 2006: On the relationship between the eastern Tibet Plateau rainfall and subtropical high shift in summer. *ACTA Meteorologica Sinica*, **64**: 90-99.
- Hsu, H. H., X. Liu, 2003: Relationship between the Tibetan Plateau heating and East Asian summer monsoon rainfall, *Geophy Res Lett*, **30**(20): 2066, doi: 10.1029/ 2003GL017909.
- Hsu, C. J. and R. A. Plumb, 2000: Nonaxisymmetric thermally driven circulations and upper-tropospheric monsoon dynamics, *J. Atmos. Sci.*, **57**, 1255-1276.
- Huang, R. H., J. L. Chen, L. T. Zhou et al, 2003: Studies on the relationship between the severe climatic disasters in China and the east Asian climate system, *Chinese J Atmos Sci*, **27**(4):770-787.
- Huang, Y. F. and Y. Q. Li, 2003: Analysis of the relationship between winter surface heating in Qinghai-Xizang Plateau and spring air temperature in Sichuan Chongqing Area, *Plateau Meteorology*, **22**: 33-39.
- Jian, A. L., 2003: The impacts of Tibetan Plateau on the climate of tropical China and on the cultivation of rubber tree. *Tropical Geography*, **23**: 199-203.
- Jian, M. Q., H. B. Luo and Y.T. Qiao, 2004: On the relationships between the summer rainfall in China and the

- atmospheric heat sources over the eastern Tibetan and the western Pacific warm pool. *J. Tropical Meteorol.*, **20**: 355-364.
- Jiang H, G. D. Cheng, K. L. Wang, 2006: Analyzing and measuring the surface temperature of Qinghai-Tibet Plateau *Chinese J. Geophys.*, **49** (2) : 391 ~ 397.
- Krishnamurti, T.N. and H.N. Bhalme, 1976: Oscillations of a monsoon system. Part I. Observational aspects. *J. Atmos. Sci.*, **33**, 1937-1954.
- Li, D. L., W. Li, W. J. Li, L. Z. Lü, H. L. Zhong, and G. L. Ji: 2003 a: The effect of surface sensible heat flux of the Qinghai-Xizang Plateau on general circulation over the Northern Hemisphere and climatic anomaly of China. *Climatic and Environmental Research*, **8**: 60-70.
- Li, D. L., H. L. Zhong, W. Li, L. Z. Lu, 2004: The abnormal sand-dust storm in Northern China during spring and its response to surface sensible heat on Qinghai-Xizang Plateau in winter. *Journal of Arid Land Resources and Environment*, **18**: 45-51.
- Li, D. L., W. J. Li, W. Li, H. L. Zhong, L. Z. Lü, and G. L. Ji, 2003 b: A diagnostic study of surface sensible heat flux anomaly over the Qinghai-Xizang Plateau. *Climatic and Environmental Research*, **8**: 71-83.
- Li, D. L., H. L. Zhong, Q. B. Wu, Y. J. Zhang, Y. L. Hou, M. C. Tang, 2006: Analyses on changes of surface temperature over Qinghai-Xizang Plateau. *Plateau Meteorology*, **24**: 291-298.
- Li, G. P., T. Y. Duan and G. F. Wu, 2003: the intensity of surface heat source and surface heat balance on the western Qinghai-Xizang plateau. *Scientia Geographica Sinica*, **23**: 13-18
- Li. S. C., L. Xu, Y. X. Guo, W. H. Qian, G. Q. Zhang, C. Li, 2006: Change of annual air temperature over Qinghai-Tibet Plateau during recent 34 years. *Journal Of Desert Research*, **26**: 27-34.
- Li, S. M., Y. Dei, Y. M. Ma, et al, 2006: Analyses of ABL structure and interaction of near surface in Mt Qomolangma region. *Plateau Meteorology*, **25**(5): 807-813.
- Li, Y. Q., 2003: Surface heating in the Tibetan Plateau and general circulation over it and their relations with the prediction of drought- flood at its eastern side. *Chinese Journal of Atmospheric Sciences*, **27**: 107-114.
- Liang, X. Y., Y. M. Liu and G. X. Wu, 2005b: Effect of Tibetan Plateau on the site of onset and intensity of the Asian summer monsoon. *ACTA Meteorologica Sinica*, **63**: 799-805.
- Liang, X. Y., Y. M. Liu, G. X. Wu, 2005a: The Impact of Qinghai-Xizang Plateau uplift on Asian general circulation in spring and summer. *Plateau Meteorology*, **24**: 837-845.
- Liang, X. Y., Y. M. Liu, G. X. Wu, 2006: Roles of tropical and subtropical land-sea distribution and the Qinghai-Xizang Plateau in the formation of the Asian summer monsoon. *Chinese J. Geophys.*, **49** (4) :

983 ~ 992.

- Liu, H. Q., Z. B. Sun, W. J. Zhu, 2003: Interdecadal relation between snow cover over the Tibetan Plateau and Asian monsoon circulation. *Journal of Nanjing Institute of Meteorology*, **26**: 733-739.
- Liu, H., H. Zhong, L. Bian, J. Chen, M. Zhou, X. Xu S. Li, and Y. Zhao, 2002: Characteristics of the Micrometeorology in the surface layer in the Tibetan Plateau. *Adv. Atmos. Sci.*, **19**(1): 73-88.
- Liu, X. R. and G. P. Li, 2006: Review and Prospect of Research on the Tibetan Plateau Vortex. *Ard Meteorol.*, **24**: 60-66
- Liu, Y. M., J. C. L. Chan, J. Y. Mao and G. X. Wu, 2002: The Role of Bay of Bengal Convection in the Onset of the 1998 South China Sea Summer Monsoon. *Mon. Wea. Rev.*, **130**: 2731-2744
- Liu, Y. M., G. X. Wu, and R. C. Ren, 2004: Relationship between the Subtropical Anticyclone and Diabatic Heating. *J. Climate*, 2004, **17**: 682-698.
- Liu, Y. M., B.J. Hoskins, M. Blackburn, 2007: Impacts of the Tibetan Topography and Thermal Forcing over Asia in Summer. *Met Soc Japan (Special 125th Anniversary Issue)* . in press
- Lu, J. H., G. P. Li, L. Shi, L. P. Hao, L. R. Zhou, 2003: Correlation research between low-pressure systems on the east side of Qinghai-Xizang Plateau and snow cover over Plateau. *Plateau Meteorology*, **22**: 121-126.
- Ma, X. B., Z. Y. Hu, 2005: Precipitation variation characteristics and abrupt change over Qinhai-Xizang Plateau in recent 40 years. *Journal of Desert Research*, **25**: 137-139.
- Ma, Y., H. Ishikawa, O. Tsukamoto, M. Menenti, Z. Su, T. Yao, T. Koike, and T. Yasunari 2003: Regionalization of surface fluxes over heterogeneous landscape of the Tibetan Plateau by using satellite remote sensing, *J. Meteorol. Soc. Jpn.*, **81**, 277– 293.
- Ma Weiqiang, Ma Yaoming, 2006, The annual variations on land surface energy in the northern Tibetan Plateau. *Environmental Geology*, 50(5). DOI 10.1007/s00254-006-0238-9
- Ma, Y., S. Fan, H. Ishikawa, O. Tsukamoto, T. Yao, T. Koike, H. Zuo, Z. Hu, and Z. Su 2005: Diurnal and inter-monthly variation of land surface heat fluxes over the central Tibetan Plateau area, *Theor. and Appl. Climatol.*, **80**, 259– 273.
- Ma, Y., L. Zhong, Z. Su, H. Ishikawa, M. Menenti, and T. Koike, 2006 b: Determination of regional distributions and seasonal variations of land surface heat fluxes from Landsat-7 Enhanced Thematic Mapper data over the central Tibetan Plateau area. *Journal of Geophysics Research*, 111, D10305, doi:10.1029/2005JD006742
- Ma, Y. M., T. D. Yao, J. M. Wan, 2006 a: Experimental study of energy and water cycle in Tibetan Plateau -The progress introduction on the study of GAME/ Tibet and CAMP/ Tibet. *Plateau Meteorology*, **25**: 344-351.

- Mao, J. Y. and A. M. Duan, 2005: The predictability of the reversal of the ridge of the subtropical anticyclone and the onset of the summer Asian Monsoon. *Impacts of the land-sea thermal contrast on the climate in China*, Liu Yimin and Qian Zhenan, 2005, China Meteorological Press, Beijing, 173-177.
- Mao, J. Y., G. X. Wu, Liu Yi-min, 2002a: Study on modal variation of subtropical high and its mechanism during seasonal transition part I: Climatological features of subtropical high structure. *Acta Meteor. Sinica*, **60**(4): 400~408.
- Mao, J. Y., G. X. Wu, Y. M. Liu, 2002b: Study on modal variation of subtropical high and its mechanism during seasonal transition part II: Seasonal transition index over Asian Monsoon Region. *Acta Meteor. Sinica*, **60**(4): 409~420.
- Nan, Z. T., S. X. LI, G. D. Cheng, 2005: Prediction of permafrost distribution on the Qinghai-Tibet Plateau in the next 50 and 100 years. *Science in China Ser. D Earth Sciences*, **48**(6), 797-804.
- Ning, L. and Y. F. Qian, 2006: Oscillation characteristics of sensible heat in north Africa and Qinghai-Xizang Plateau and their impacts on the rainfall in east China. *Plateau Meteorology*, **25**: 357-365.
- Peng, J. B., L. T. Chen, Q. Y. Zhang, 2005: Multi-scale variations of snow cover over QXP and Tropical Pacific SST and their influences on summer rainfall in China. *Plateau Meteorology*, **24**: 366-377.
- Peng, Y., H. S. Zhang, H. Z. Liu, L. G. Bian, S. M. Li, L. Kang, J. Y. Chen, M. Y. Zhou, X. D. Xu, 2005: Characteristics of micro-meteorology in the surface layer over Tibetan Plateau area. *Acta scientiarum naturalium, Universitatis Pekinensis*, **41**: 180-190.
- Qian, Y. F., Y. Zhang, Y. Q. Zheng, 2003: Impacts of the Tibetan Plateau snow anomaly in winter and spring on precipitation in China in spring and summer. *Arid Meteorology*, **21**: 1-7.
- Qian, Z.A., T. W. Wu, X. Y. Liang, 2001: Feature of mean vertical circulation over the QXP and its Neighborhood, *Chinese J. Atmos. Sci*, **25**(3): 237-249.
- Queney, P., 1948: The problem of air flow over mountains: A summary of theoretical studies. *Bull. Ame. Meteor. Soc.* **29**, 16-29
- Tao, S. Y., L. S. Chen, X. D. Xu, 2000a: Progresses of theoretical study in the second Tibetan Plateau atmosphere scientific experiment. Part I: Beijing, China Meteorological Press, 348 pp
- Tao, S. Y., L. S. Chen, X. D. Xu, 2000b: Progresses of theoretical study in the second Tibetan Plateau atmosphere scientific experiment Part. II: Beijing, China Meteorological Press, 396 pp
- Tao, S.Y., L. S. Chen, X. D. Xu, 2000c: Progresses of theoretical study in the second Tibetan Plateau atmosphere scientific experiment. Part III: Beijing, China Meteorological Press, 203 pp
- Tao, S. Y. and F.K. Zhu, 1964: The variation of 100 mb circulation over south Asia in summer and its association with arch and withdraw of west pacific Subtropical High. *Acta Meteorological Sinica*, **34**, 385~395.
- Tian, S.F., T. Yasunari, 1992: Time and space structure of interannual variations in summer rainfall over China, *J Meteor Soc Japan*, **70**: 585-596.

- Wan, R. J., G. X. Wu, 2007: Mechanism of the Spring Persistent Rains over southeastern China. *Sciences in China*. In press
- Wang, C. H., D. W. Jie, Z. G. Wei, 2003: Study on relationship between the frozen thaw process in Qinghai-Xizang Plateau and circulation in east-Asia. *Chinese Journal of Geophysics*, **46**: 309-316.
- Wang, L. N., Q. L. Zheng, Q. L. Song, 2003: Numerical simulation of the influences of west central Qinghai-Xizang Plateau on East Asia seasonal transition. *Plateau Meteorology*, **22**: 179-184.
- Wang, Z. Z., G. X. Wu, T. W. Wu, R. C. Yu, 2004: Simulation of the seasonal variations of Asian monsoon with the climate model R42L9/LASG, *Adv. Atmos. Sci.*
- Wei L., and D. L. Li, 2003: Evaluation of NCEP/PDOE surface flux data over Qinghai-Xizang Plateau. *Plateau Meteorology*, **5**: 478-487.
- Wei, Z. G., R. H. Huang, and W. J. Dong, 2003: Interannual and interdecadal variations of air temperature and precipitation over the Tibetan Plateau. *Chinese Journal of Atmospheric Sciences*, **27**: 157-170.
- Wei, Z., R. H. Huang, W. Chen, 2005: The Causes of the interannual variation of snow cover over the Tibetan Plateau. *Journal of Glaciology and Geocryology*, **27**: 491-497.
- Wu, G. X. and Y. M. Liu, 2003: Summertime quadruplet heating pattern in the subtropics and the associated atmospheric circulation. *Geophys. Res. Lett.*, **30**(5), 1201
- Wu, G. X., 2004: Recent advances in QXP climate dynamic research, *Quarterly Science*, **24**( 1): 1-9..
- Wu, G. X., W. P. Li, H. Guo, 1997: Tibetan Plateau sensible heat pump and Asia summer monsoon. Ye Duzheng (main editor), *Memorial corpus for Zhao Jiuzhang*. Beijing, Science publishing company, 116~126
- Wu, G. X. and Y. S. Zhang, 1998: Tibetan Plateau forcing and the timing of the monsoon onset over South Asia and the South China Sea. *Monthly Weather Review*, **126**: 913~927
- Wu, G. X., Y. M. Liu, J. Y. Mao, 2004: Adaptation of the atmospheric circulation to thermal forcing over the Tibetan Plateau: Observation, theory and modeling of the atmospheric variability, Selected papers of Nanjing Institute of meteorology alumni in Commemoration for Professor Zhang Ji-ja, Edited by Xun Zhu et al.
- Wu, G. X., J. Wang, X. Liu, Y. M. Liu, 2005a: Numerical modeling of the influence of Eurasian orography on the atmospheric circulation in different seasons. *Acta Meteorological Sinica*, **63**(5): 603-612.
- Wu, G. X., Y. M. Liu, X. Liu, A. M. Duan, and X. Y. Liang, 2005b: How the heating over the Tibetan Plateau affects the Asian climate in summer. *Chinese Journal of Atmospheric Sciences*, **29**: 47-56.
- Wu, G. X., Y. X. Liu, T. M. Wang, R. J. Wan, X. Liu, W. P. Li, Z. Z. Wang, Q. Zhang, A. M. Duan and X. X. Liang, 2007: The Influence of the Mechanical and Thermal Forcing of the Tibetan Plateau on the Asian Climate. *J. Hydrometeorology*. In press
- Wu, S. H., Y. H. Yin, D. Zheng and Q. Y. Yang, 2005: Climate changes in the Tibetan Plateau during the last 3

- decades. *Acta Geographica Sinica*, **60**: 3-11.
- Wu, T. W., Z.A. Qian, 2000: Further studies of relation between QXP winter and spring snow anomaly and east China summer precipitation, *Acta Meteorologica Sinica*, **58**(5): 570-581.
- Wu, T. W., Z. A. Qian, 2003: The relation between the Tibetan winter snow and the Asian summer monsoon and rainfall: an observation investigation, *J Climate*, **16**: 2038-2051.
- Xu, X. K., H. Chen, and G. Q. Zhou, 2005: The spatiotemporal distribution of land surface features in the Tibetan Plateau. *Climatic and Environmental Research*, **10**: 409-420.
- Yanai, M., S. Esbensen, and J.-H.Chu, 1973: Determination of bulk properties of tropical cloud clusters from large-scale heat and moisture budgets. *J. Atmos. Sci.*, **30**., 611-627.
- Yanai. M. and G. X. Wu, 2006: Effects of the Tibetan Plateau. Chap. 13, *The Asian Monsoon*, Ed. B. Wang. Springer, Chichester, 2006: 513-549.
- Yeh, T. C. , S. Y. Tao et al, 1958: Abrupt phenomenon of general circulation in June and October. *Acta Meteorologica Sinica*, **29**: 249-263.
- Yeh, T. C., Y. X. Gao, 1979: Qinghai-Xizang Plateau Meteorology, Beijing: *Science Press*,1-278.
- Yeh, T. C., S. W. Lo and P. C. Chu, 1957: The wind structure and heat balance in the lower troposphere over Tibetan Plateau and its surrounding. *Acta Meteor. Sinica*, **28**, 108-121
- Yu, J. H., Liu Jinmiao and Ding Yuguo, 2004: Annual and Diurnal Variations of Surface Fluxes in Western Qinghai-Xizang Plateau. *Plateau Meteorology*, **23**: 353- 359
- Zhang, J. J., B. Z. Zhu, F. K. Zhu, 1988: Tibetan Plateau meteorological progresses. Science publishing company, Beijing, 268
- Zhang, Q. Y., Z. H. Jin and J. B. Peng, 2006: The relationship between convection over the Tibetan Plateau and circulation over East Asian. *Chinese Journal of Atmospheric Sciences*, **30**: 802-812.
- Zhang, S. L. , S. Y. Tao, 2001: Diagnostic and numerical studies on the impacts of Qinghai-Xizang Plateau snow cover on Asian monsoon., *Chinese J Atmos Sci*, **25**(3): 372-390.
- Zhao, P., and L. X. Chen, 2001: Climatic features of atmospheric heat source/sink over the Qinghai-Xizang (Tibetan) Plateau in 35 years and its relation to rainfall in China. *Science in China (Series D)*, **44**, 858-864.
- Zhao, S. R., Z. S. Song and L. R. Ji, 2003: Heating effect of the Tibetan Plateau on rainfall anomalies over north china during rainy season. *Chinese Journal of Atmospheric Sciences*, **27**: 883-893.
- Zhao, P., Z. J. Zhou, and J. P. Liu, 2007: Variability of Tibetan spring snow and its associations with the hemispheric extra-tropical circulation and East Asian summer monsoon rainfall: An observational investigation. *Journal of Climate*, **20**, in press.
- Zhong, H. L., D. L. Li and W. Li, 2004: The abnormal sand-dust storm in northern China during spring and its

response to surface sensible heat on Qinghai-Xizang Plateau in winter. *Journal Of Desert Research*, **24**: 323-329.

Zhou, M. Y., X. D. Xu, L. G. Bian et al., 2000: The observation, diagnosis and dynamics of the atmospheric boundary over the Tibetan Plateau. Beijing: Meteorological Press. 125 pp.

Zuo, H. C., Y. Q. Hu, S. H. Lu et al, 2004: Transfer of dry and wet seasons at Ando region of QXP and their ABL features, *Advances in Nature Sciences*, **14**(5): 535-540.

Figure Captions

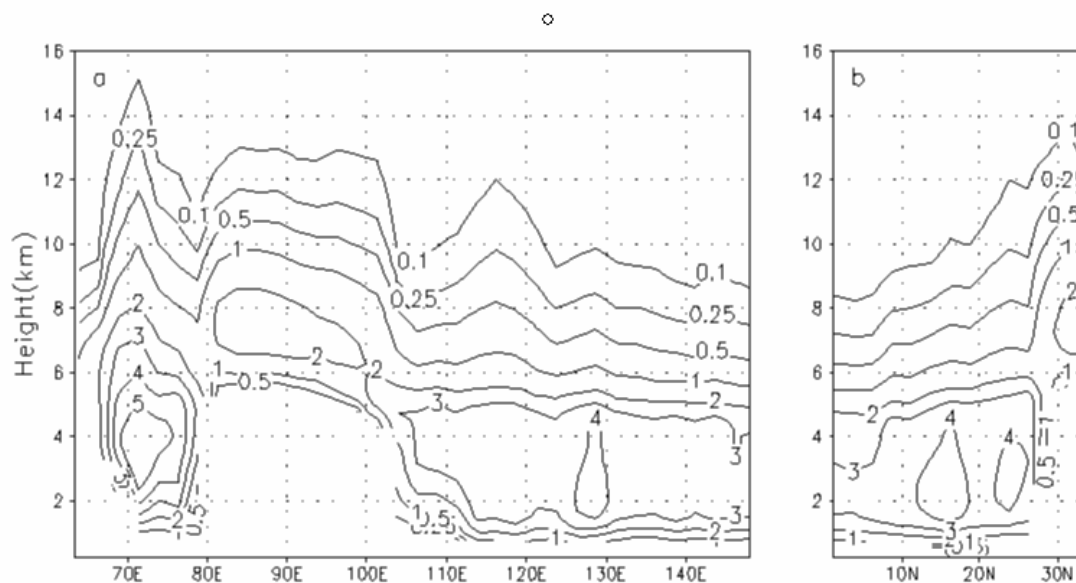


Fig. 1 The mean rain rate over the Tibetan Plateau, which is calculated from the TRMM received radar-reflectivity ( $Z$ ) profiles by averaging rain-only bins at each level of the profiles. The averaging period covers June, July and August of three years from 1998 to 2000 (unit: mm/h). (a) Height-longitude cross-section averaged between  $30^{\circ}\text{N}$  and  $35^{\circ}\text{N}$  and (b) height-latitude cross section averaged between  $85^{\circ}\text{E}$  and  $90^{\circ}\text{E}$ . From Fu et al. (2006).

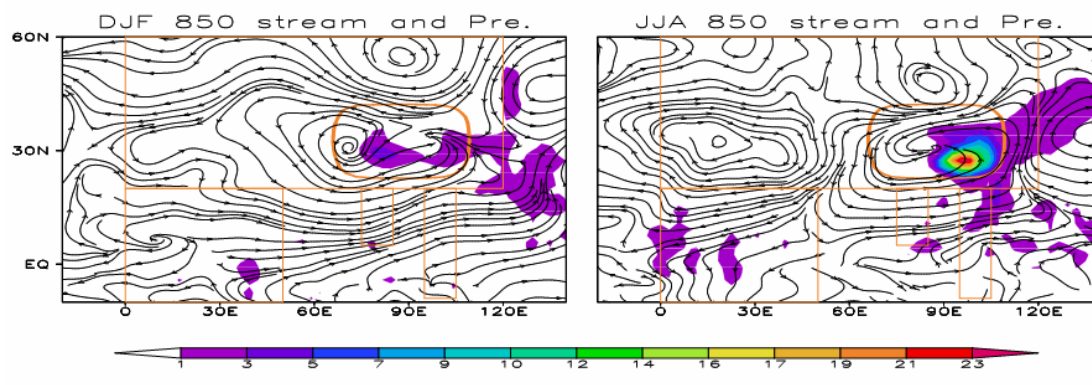


Fig. 2 The 850 hPa stream field difference between the experiments with and without the ellipsoidal orography which is centred at  $(90^{\circ}\text{E}, 33^{\circ}\text{N})$  with a maximum elevation of 5 km and a domain of  $50^{\circ}$  long \*  $30^{\circ}$  lat, mimicking Tibetan Plateau as marked by the heavy elliptic at the elevation of 100 m. The experiments use an idealised landmark to present the Africa-Eurasian Continent, which is embedded on the aqua surface of the GOALS-SAMIL model. Both experiments were integrated for 10 years and the results from the last 8 years are extracted for the calculation. (a) December-February; (b) June-August.

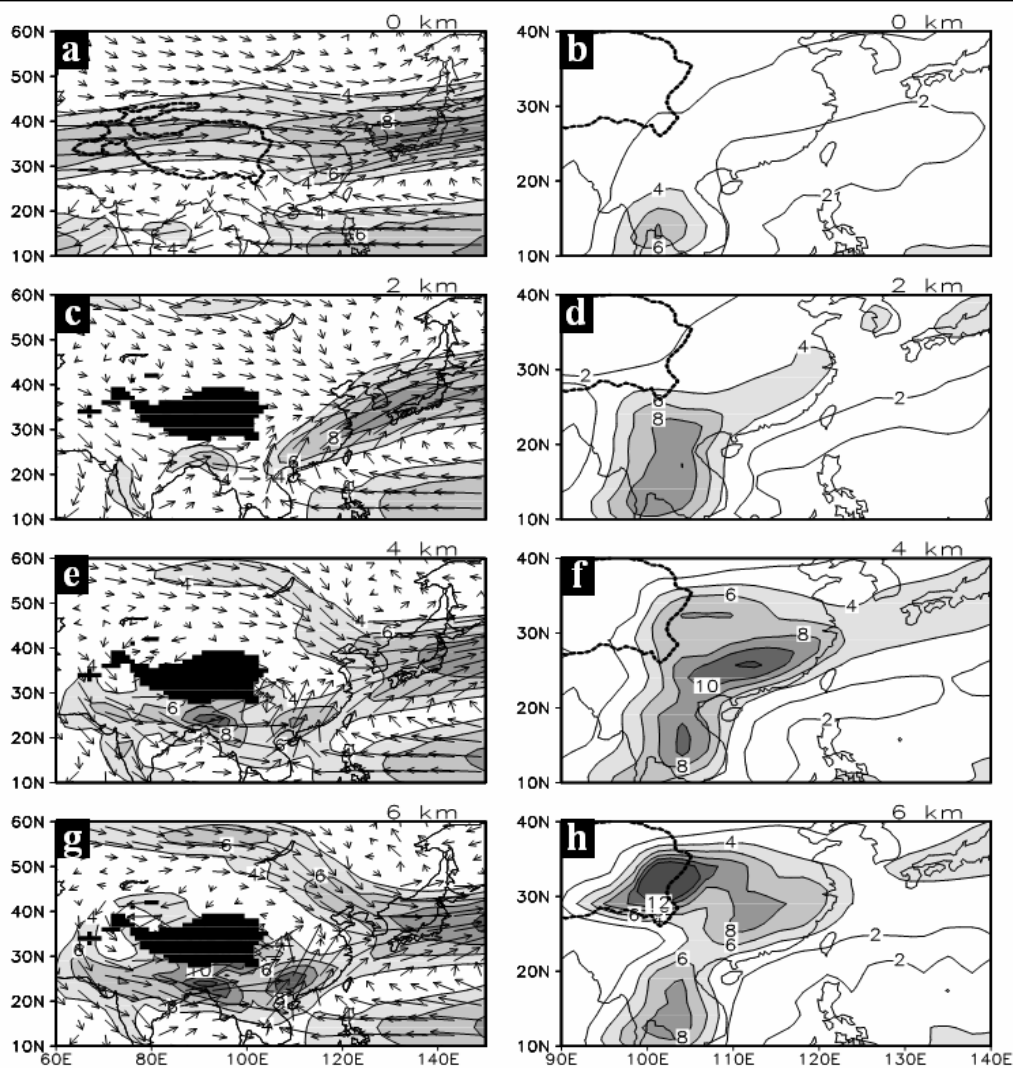


Fig. 3 Distributions of wind vector and isotach at 850 hPa (left panels, unit is  $\text{m s}^{-1}$ , shaded indicate exceeding  $4 \text{ m s}^{-1}$ ) and rain (right panels, unit is  $\text{mm d}^{-1}$ ) in the perpetual spring sensitivity experiments with different TP elevations and averaged over 30 months by using GOALS-SAMIL. The black shaded in left panels and bold solid curve in right panels are the main part of TP. The TP maximum elevation is 0 km in (a) and (b), 2 km in (c) and (d), 4 km in (e) and (f), and 6 km in (g) and (h). From Wan and Wu (2006).

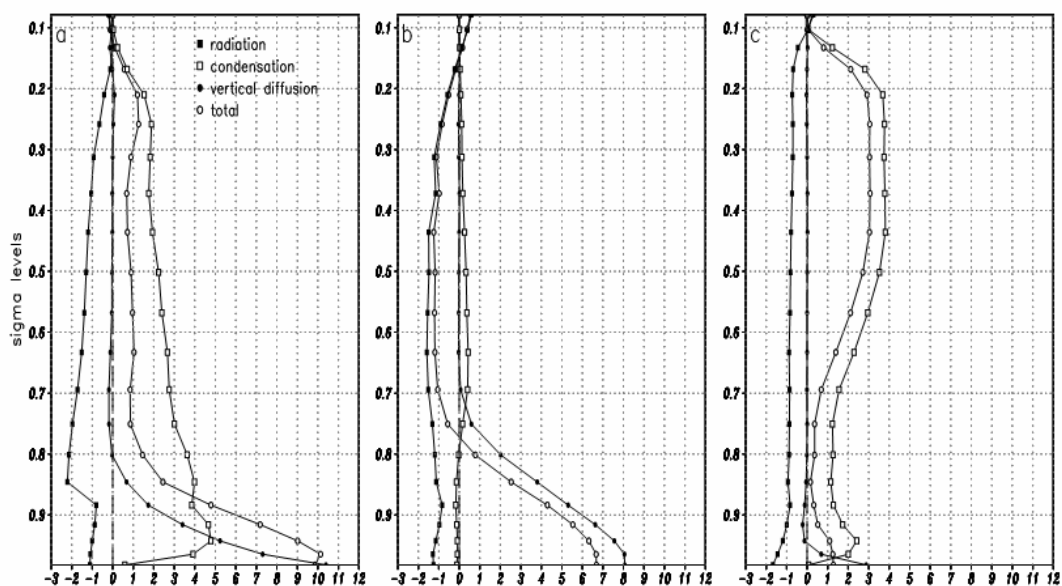


Fig. 4 July mean area-averaged profile of the total and individual diabatic heating rate over (a): TP region; (b): Middle Asia region; and (c): East China region from NCEP/NCAR for 1980-1999. Units:  $K day^{-1}$ . From Duan and Wu (2005).

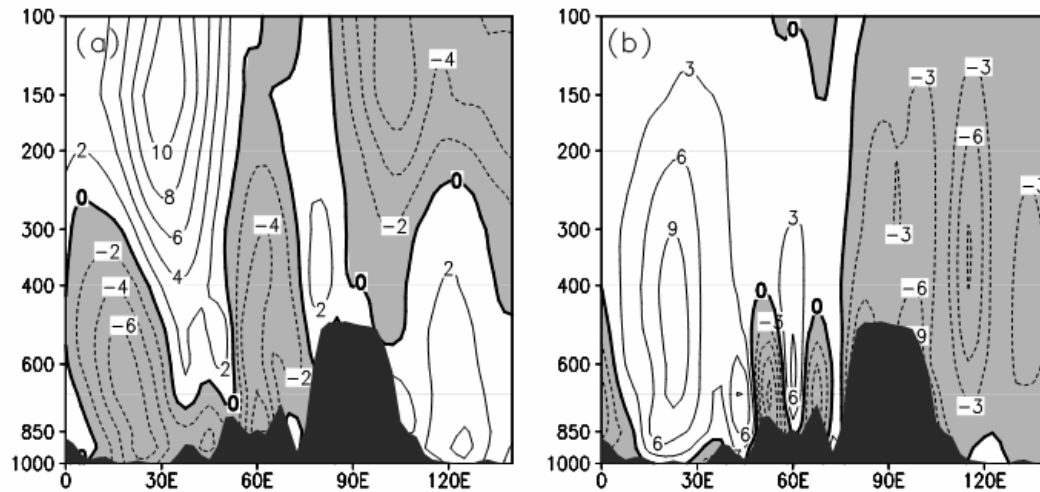


Fig. 5 Longitude-pressure cross-sections along  $32.5^{\circ}N$  of the July mean meridional wind (a, unit is  $m s^{-1}$ ) and vertical velocity in  $p$ -coordinates (b, unit is  $10^{-1} Pa s^{-1}$ ) from NCEP/NCAR for 1981-1999. From Duan and Wu (2005).

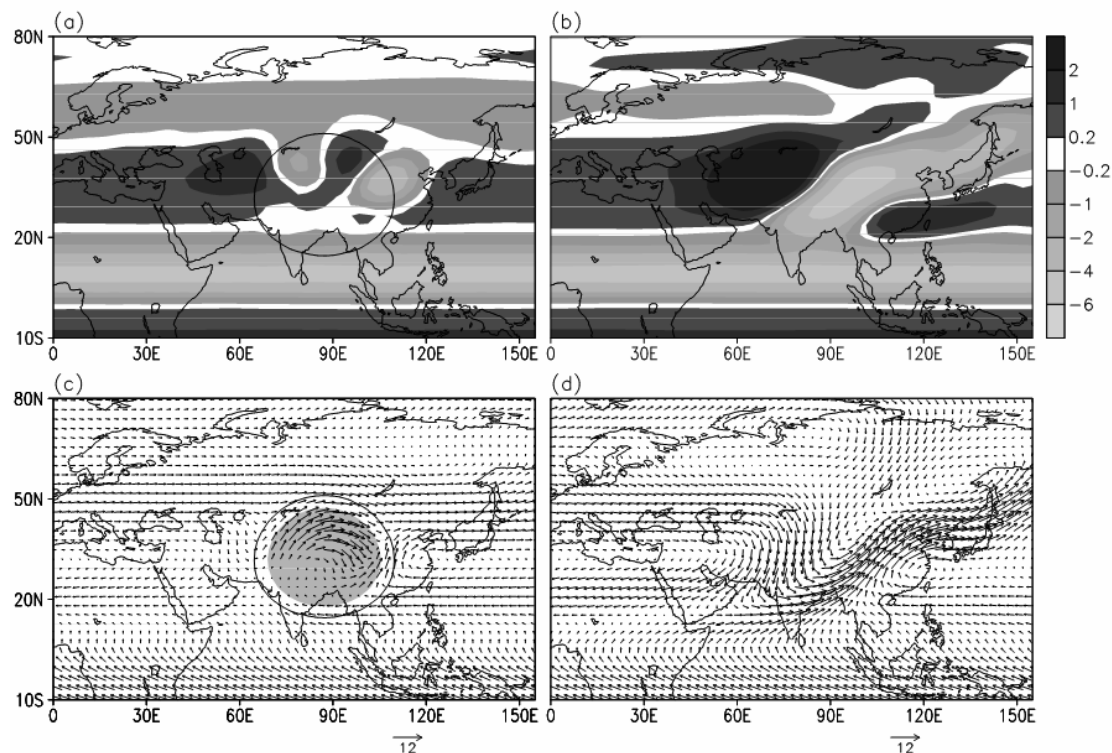


Fig. 6 Comparison of the mean of days 15-70 of the idealized orography experiment (right) and idealized heating experiment (right). (a) and (b) 400 hPa  $\omega$  (units  $10^{-2} \text{ Pa s}^{-1}$ ), and (c) and (d) wind vectors at 850 hPa wind vectors (units  $\text{m s}^{-1}$ ) based on a global primitive equation model. The maximum altitude of the idealised orography is 5580m at  $32^\circ\text{N}$ ,  $87^\circ\text{E}$  and the height of 500 m is depicted by the bold contour in (a) and (c), and in (c) the region where the 850-hPa surface below ground is shaded. The idealised heating has the same horizontal distribution as the idealised orography. In the vertical it has a profile which is constant from  $\sigma=1.0$  to  $0.8$  and then decreases linearly to zero at  $\sigma=0.2$  (near 100 hPa over the highest topography). The maximum heating rate, near the surface at the centre, is  $5 \text{ K day}^{-1}$ . From Liu et al. (2007).

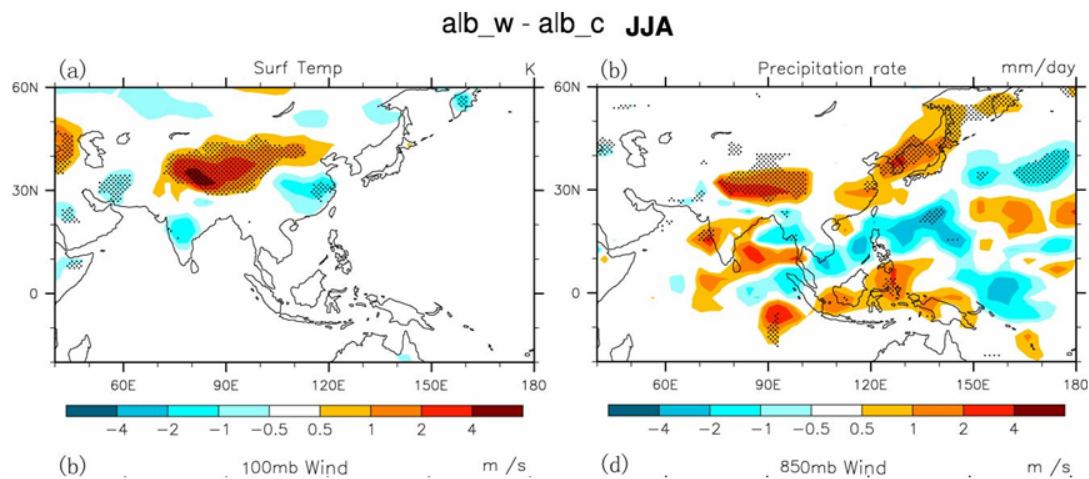


Fig. 7 The ensemble mean differences between sensitivity tests of the land surface albedo over the TP region being reduced 50% and increased with 150% using ECHAM4 T42L19 model in boreal summer. (a) Surface temperature (K); (b) Precipitation rate (mm/day); The stippling is the significant regions at 0.05 level based on student's t test.

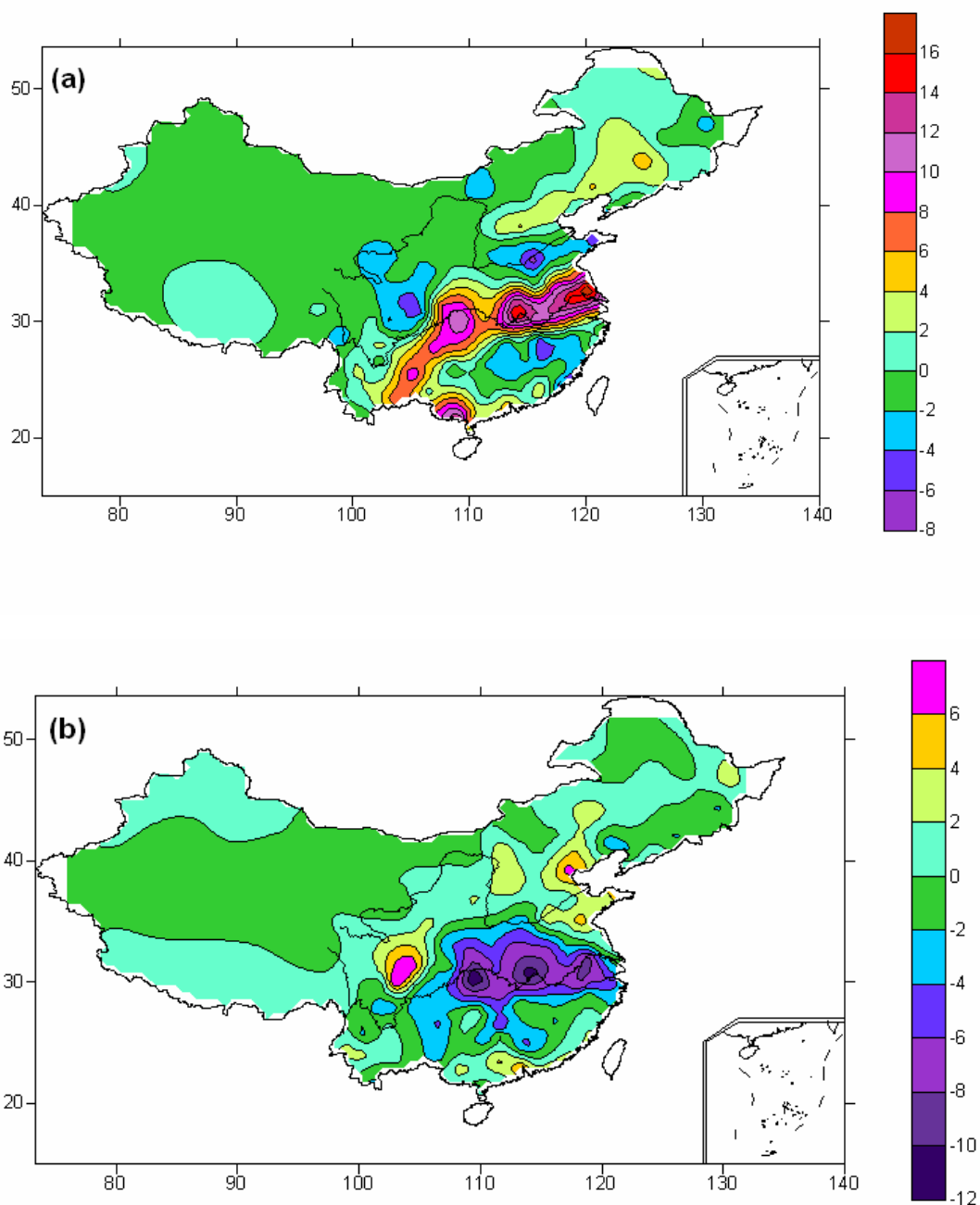


Fig. 8 The composite rainfall anomaly in July with strong (a) and weak (b) May sensible heating in the Tibetan Plateau from NCEP/NCAR for 1981-1999. Unit: mm/day. From Duan et al. (2005).

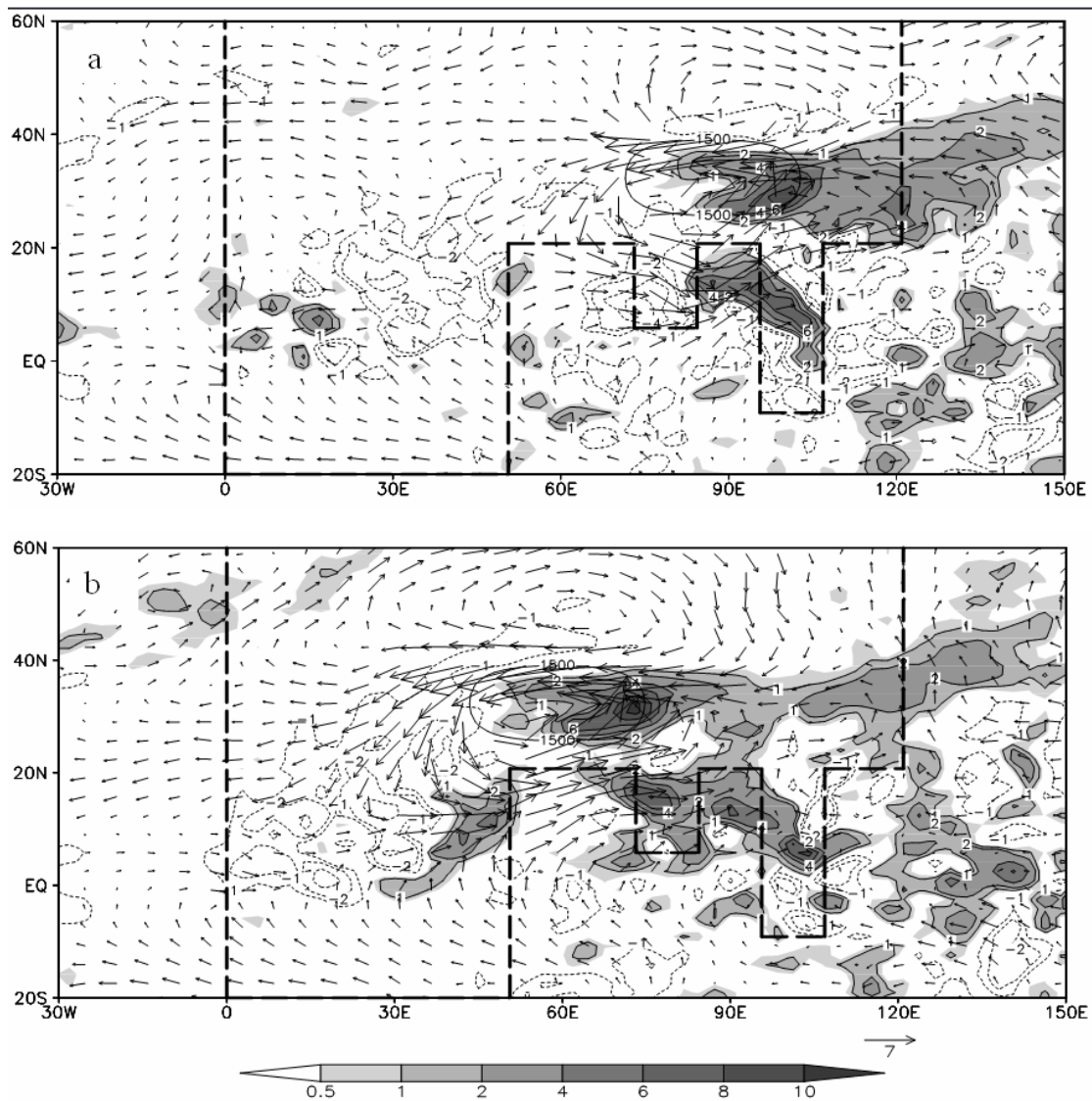


Fig. 9 Differences of precipitation (mm day<sup>-1</sup>) (shading) and wind vector (m s<sup>-1</sup>) at 850 hPa between with and without TP experiments during the Asian summer monsoon onset time (a) differences between TP-90 and EL experiments, (b) differences between TP-60 and EL experiments by using GOALS-SAMIL model. From Liang et al. (2005b).

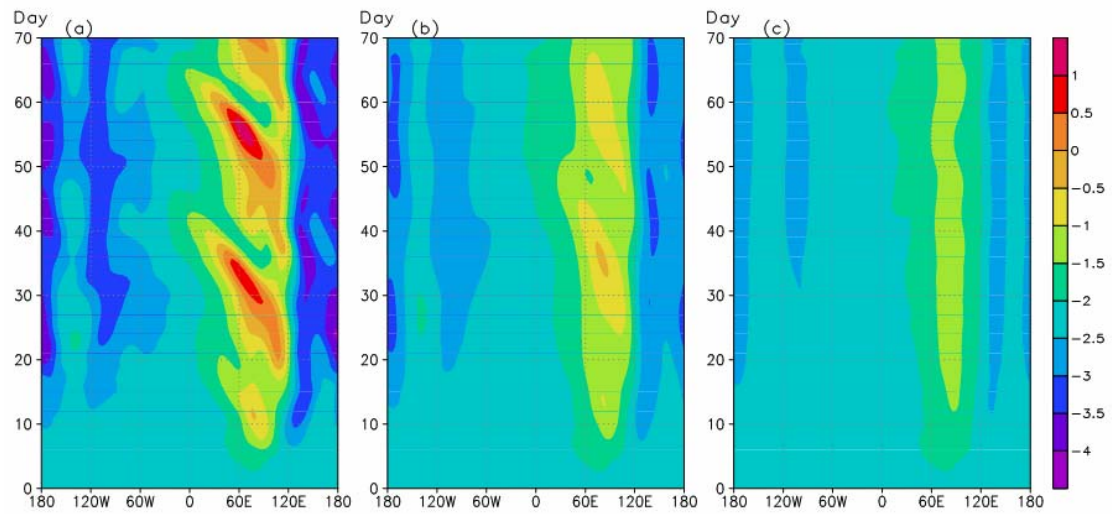


Fig. 10 Time-longitude cross-section of 25-35°N averaged 200 hPa streamfunction (units  $10^7\text{m}^2\text{s}^{-1}$ ) for (a) the experiment with idealized orography and heating, (b), as in (a) but with the magnitude of the idealized heating reduced by a factor of two, and (c) as in (a) but with the magnitude of the idealized heating reduced by a factor of four. From Liu et al. (2007).

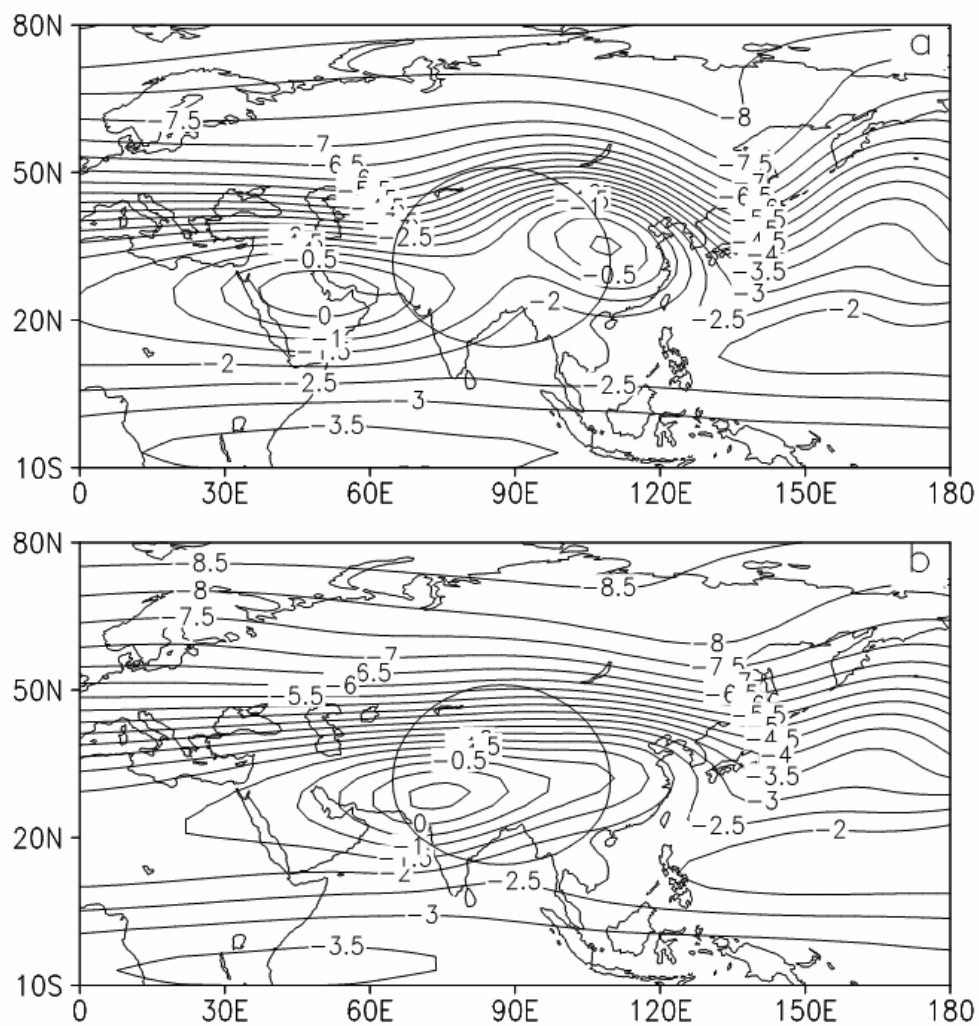


Fig. 11 For the idealised TP orography and idealised TP heating experiment, composites of the 200 hPa streamfunction for (a) the split/double mode (the average of days 21, 38, 58, and 76), and (b) the single mode (the average of days 12, 32, 53 and 70). The units are  $10^7 \text{m}^2 \text{s}^{-1} \text{day}$ . From Liu et al. (2007).

# REVIEW OF THE STUDY OF NONLINEAR ATMOSPHERIC DYNAMICS IN CHINA (2003-2006)

DING Ruiqiang<sup>\*1</sup> (丁瑞强), FENG Guolin<sup>2</sup> (封国林), LIU Shida<sup>3</sup> (刘式达), LIU Shikuo<sup>3</sup> (刘式适), HUANG Sixun<sup>4</sup> (黄思训), and FU Zuntao<sup>3</sup> (付遵涛)

<sup>1</sup>State Key Laboratory of Numerical Modeling for Atmospheric Sciences and Geophysical Fluid Dynamics (LASG), Institute of Atmospheric Physics, Chinese Academy of Sciences, Beijing 100029

<sup>2</sup>Laboratory for Climate Studies of China Meteorological Administration, National Climate Center,

Beijing 100081

<sup>3</sup>School of Physics, Peking University, Beijing 100871

<sup>4</sup>Institute of Meteorology, PLA University of Science and Engineering, Nanjing 211101

## ABSTRACT

Recent advances in the study of nonlinear atmospheric dynamics in China are briefly reviewed. This review includes the major achievements in the following eight aspects: nonlinear error dynamics and predictability; nonlinear analysis of observational data; eddy-forced envelope Rossby soliton theory; sensitivity and stability of ocean's thermohaline circulation; nonlinear waves dynamics; nonlinear analysis on fluctuations in the atmospheric boundary-layer; the basic structures of atmospheric motions; some applications of variational methods.

**Key words:** nonlinear dynamics; predictability; blocking; stability; nonlinear waves; variational method

## 1. Introduction

The atmosphere is a complex, nonlinear system, which involves complex, nonlinear interactions among all components of the atmosphere. So the study of nonlinear atmospheric dynamics is very important. Nonlinear atmospheric dynamics is an interdisciplinary branch of atmospheric sciences, geophysical fluid dynamics and nonlinear sciences, whose complexity and nonlinearity present many physical and mathematical challenges for scientists in many fields (Li and Wang, 2006). Continuous development of nonlinear atmospheric dynamics plays an important role in understanding the basic processes in the atmosphere as well as providing the theory and

---

\* Email: drq@mail.iap.ac.cn

method for the prediction of atmospheric motions. The research activities of Chinese Scientists in this field are vigorous and productive during the last three decades, and some important advances in nonlinear adjustment process, nonlinear stability and instability, predictability study, multiple equilibria dynamics, meso- and micro-scale nonlinear dynamics, and nonlinear blocking dynamics etc. have been made (Li and Chou, 2003; Diao et al., 2004). Since the last International Union of Geodesy and Geophysics (IUGG) General Assembly (2003), four years passed. In the recent four years, some new studies in China have been carried out in many aspects of nonlinear atmospheric dynamics. This paper summarizes the major results.

## **2. Nonlinear error dynamics and its applications to the predictability of weather and climate**

Because atmosphere itself is a complex nonlinear system and there exist a lot of limitations using the linearized error growth equation to study the atmospheric predictability (Lacarra and Talagrand, 1988; Mu, 2000), it is necessary to propose a new approach based on nonlinear error growth dynamics for quantifying the atmospheric predictability. Ding and Li (2006a) and Li et al. (2006) applied fully nonlinear error growth equations of nonlinear dynamical systems instead of linear approximation to error growth equations to discuss the evolution of initial perturbations, and first introduced the concept of nonlinear local Lyapunov exponent (NLLE). The NLLE depends generally on the initial state in the phase space, the initial error and evolution time, which is quite different from the global Lyapunov exponent or the local Lyapunov exponent based on linear error dynamics.

In order to study the average predictability of the whole system, the whole ensemble mean of the NLLE should be defined. According to the chaotic dynamical system theory and probability theory, Ding and Li (2006a) proved a saturation theorem of mean relative growth of initial error (RGIE) derived by the mean NLLE, that is, for a chaotic dynamic system, the mean RGIE will necessarily reach a saturation value in a finite time interval. Once the mean RGIE reaches the saturation, at the moment almost all predictability of chaotic dynamic systems is lost. Therefore, the predictability limit can be defined as the time at which the mean RGIE reaches its saturation level.

On the other hand, in order to measure predictability of specified state with certain initial uncertainties in the phase space and to investigate distribution of predictability limit in the phase space, Ding and Li (2006b) introduced the local ensemble mean of the NLLE. Then the local average predictability limit of a chaotic system could be quantitatively determined by examining the evolution of the local mean relative growth of initial error (LRGIE). The local ensemble mean of the NLLE different from the whole ensemble mean of the NLLE could show local error growth dynamics of subspace on an attractor in the phase space. Moreover, in practice the local average predictability limit itself might be regarded as a predictand to provide an estimation of accuracy of prediction results.

The NLLE defined in Ding and Li (2006a) and Li et al. (2006) actually only characterizes the growth rate of initial perturbation along the most rapidly growing direction. Li and Ding (2006) extended the concept of the NLLE from one dimension to multi-dimension. Based on the NLLE along the most rapidly growing direction, for an  $n$ -dimensional chaotic dynamic system, they obtained the first  $m$  NLLE spectra along other directions by the growth rate of the volume of  $m$ -dimensional subspace spanned by the first  $m$  error vectors ( $m=2,3,\dots,n$ ). In a chaotic system, each error vector tends to fall along the local direction of most rapid growth. Due to the finite precision of computer calculations, the collapse toward a common direction causes the orientation of all error vectors to become indistinguishable. Li and Ding (2006) further pointed out that this problem could be overcome by the repeated use of the Gram-Schmidt reorthonormalization (GSR) procedure on the vector frame.

The nonlinear error dynamics may be applied to the predictability study of the finite-size initial error, and demonstrates superiority in determining the limit of predictability of chaotic systems in comparison with linear one. Recently, Chen et al. (2006) applied the nonlinear error dynamics to the predictability analysis of atmospheric observation data, and obtained the temporal-spatial characteristics of the predictability limit of 500 hPa geopotential height field. Other questions including the temporal-spatial characteristics of the predictability limit of other different variables such as temperature, precipitation etc.; the decadal change of the predictability limit, the relationships among the predictability limits of motion on various time and space scales and the prediction of predictability et al. will be further subjects of future research by employing the nonlinear error dynamics.

### 3. Nonlinear analysis of observational data

Global change science is a new research domain nowadays, and one of the most important studies of which is the climate change, to which great attention is paid by all governments in world. For the further study on the past climate change, especially to reveal the rules of the global climate change in past 2000a and predict future climate change, Wan et al. (2005a) introduced a new method making use of the dynamical lag correlation exponent (named  $Q$  index), a dynamics exponent based on the phase-space reconstruction, which can effectively discern the similarities or differences between the dynamics of the two series. With  $Q$  index, they analyzed the dynamics structure of some typical climatic proxies. Their results showed that the dynamics of climatic proxies are almost similar, and the regional climate keeps the same change with the global. In other words, regional climate is controlled by the global climate change. Besides, they also found that there are two dynamics jump periods (namely 700-900a and 1300-1700a) in past 2000a of the climate system, which may correspond to the periods of the medieval warm period and the little ice age, respectively.

Climate system is nonlinear, non-stationary and hierarchical, which makes even harder to detect and analyze abrupt climate changes. Based on Student's  $t$ -test, Bernaola Galvan recently proposed a heuristic segmentation algorithm to segment the time series into several subsets with different scales, which is more effective in detecting the abrupt changes of nonlinear time series. Feng et al. (2005) tried to verify the effectiveness of heuristic segmentation algorithm in dealing with nonlinear time series by an ideal time series. Through detecting and analyzing the information of abrupt climate changes contained in recent 2000a's tree annual growth ring, they succeeded in distinguishing abrupt changes with different scales. The research based on the newly defined parameter of abrupt change density showed that human activities might have lead to the recent 1000a's unbalanced distribution of serial and spares segments of abrupt climate changes, which may be one of the manifestations of global temperature change.

Most of the present statistical climate prediction methods (mainly includes empirical, mathematical and physical statistics methods) are based on the hypothesis that the system is stationary. However, the observations, in particular for the climate data, are often

nonlinear/non-stationary and multi-hierarchical, which makes the prediction very difficult. Aiming at this problem, Wan et al. (2005b) introduced a new prediction model, in which, firstly, using the empirical mode decomposition the observation sequence are stationarized and a variety of intrinsic mode functions (IMF) are obtained; secondly the IMFs are predicted by the mean generating function model separately; finally with the optimal subset regression model the part of predictions are used as new samples to fit the original series directly or step by step and a system of prediction equations are set up. The climate sequences prediction research showed that the individual IMF, especially the eigen-IMF, has more stable predictability than that of its sources. The trend of development in climate prediction lies in researching the mechanism and hierarchy of the climate system, constructing the corresponding climate prediction model. An attempt has been accomplished in their work. It is believed that the model proposed can open up a new effective way for the climate prediction or evaluation.

#### **4. Eddy-forced envelope Rossby soliton theory**

Luo (2005a) proposed a new forced envelope Rossby soliton model in an equivalent barotropic beta-plane channel to describe the interaction between an incipient block (planetary scale) and short synoptic-scale eddies. It is shown that the planetary-scale projection of the nonlinear interaction between synoptic-scale eddies is the most important contributor to the amplification and decay of the planetary-scale blocking dipole or anticyclone, while the synoptic–planetary-scale interaction contributes significantly to the downstream development of preexisting synoptic-scale eddies. Large-scale topography plays a secondary role compared to the synoptic-scale eddies in exciting the block. However, it plays a role in inducing a standing planetary-scale ridge prior to block onset, which fixes the geographical location of the block and induces meridional asymmetry in the flow. In particular, the topographically induced planetary-scale ridge that is almost in phase with a dipole component of blocking flow is found to be a controlling factor for the northward deflection of storm tracks associated with blocking anticyclones.

Using the same block–eddy interaction model mentioned above but ignoring the effect of topography, Luo (2005b) first examined the role of westward traveling planetary waves in the

blocking circulations associated with synoptic-scale eddies. He found that a typical retrograde blocking anticyclone can arise through the interaction of an incipient block with synoptic-scale perturbations when a planetary-scale ridge with zonal wavenumber 1 shifts westward from the east of the dipole component in a preexisting planetary-scale flow prior to block onset. But a noticeable northward deflection of synoptic eddies cannot be observed in this case. Luo (2005c) also examined the relationship between blocked flow and deformed eddies using the numerical and analytical methods. It is found that the blocking flow and synoptic-scale eddies are symbiotically dependent upon one another during their interaction. The low-frequency variability in an isolated block flow and associated synoptic-eddy activity is caused by the low-frequency eddy forcing by the preexisting synoptic eddies prior to block onset. The interaction of preexisting eddies with an isolated blocked flow induces two types of eddies: Z-type eddies with a meridional monopole structure and M-type eddies having a meridional tripole structure, which play different roles in the deformation of eddies. These eddies tend to disperse their energy toward downstream with the same group velocity as that of the block. At the same time, the zonal wavenumbers of blocked flow and deformed (Z-type and M-type) eddies can be shown to satisfy two conserved quantities.

Besides, Luo (2005d) further extended the eddy-forced envelope Rossby soliton theory proposed in Luo (2005a) to include the zonal mean flow with a shear and discussed the impact of the horizontal shear of the basic flow on isolated vortex pair blocks in association with synoptic-scale eddies. To simplify the problem, an assumption of a weak shear is used to allow analytical solutions. The type of the shear of the mean flow is found to have a significant impact on the strength and persistence of isolated vortex pair blocks and the deformation of synoptic-scale eddies.

## **5. Sensitivity and stability of ocean's thermohaline circulation**

Mu et al. (2003) proposed a new approach of conditional nonlinear optimal perturbations (CNOPs) to investigate the nonlinear effects in the predictability study, sensitivity analysis and stability research (Also see Mu and Zhang, 2006). Mu et al. (2004) considered the sensitivity and stability of the thermohaline circulation (THC) to finite amplitude perturbations within a simple

model context by using approach of CNOP. It is shown that linearly stable thermohaline circulation states can become nonlinearly unstable and the properties of the perturbations with optimal nonlinear growth are determined. An asymmetric nonlinear response to perturbations exists with respect to the sign of finite amplitude freshwater perturbations, on both thermally dominated and salinity dominated thermohaline flows. This asymmetry is due to the nonlinear interaction of the perturbations through advective processes.

Sun et al. (2005) also utilized CNOP to investigate the decadal variation of THC in a simple coupled ocean-atmospheric two-box model. Specifically, the passive variabilities found in this model are due to non-normal and nonlinear growth of initial perturbations. These variabilities, measured as recovering time of perturbations, can cause decadal variability of THC. These results are of potential application to the interpretation of past climate change linked to THC variations in nonlinear regime.

## **6. Studies of nonlinear waves and their applications to studies of the atmosphere and ocean**

Liu et al. (2003a) and Fu et al. (2003a, b, c; 2004a, b) applied the special functions and related knowledge to the studies of nonlinear waves in a creative way. They proposed several methods to solve nonlinear evolution equations, including the Jacobi elliptic function expansion method, new transformation method, method related to elliptic equations, power series expansion method and so on. Especially for the Jacobi elliptic function expansion method, after it was proposed, the number of its citations gradually increased. Using these methods, they obtained the classical solitary wave solutions (Fu et al., 2004b, 2005a; Zhao et al., 2005); In addition, the generalized periodic wave solutions were also derived (Liu et al., 2003a; Fu et al., 2005a). These solutions are benefit to our understanding to the irregularities in period and multiple structures of the atmospheric motions (Chen et al., 2005; Fu et al., 2004c, d, 2005b). Actually, there are indeed ample patterns in motions of geophysical fluid from our studies to motions of atmosphere and ocean.

## **7. Nonlinear analysis on fluctuations in the atmospheric boundary-layer and in the fields related to weather and climate variables**

Starting from time series analysis, Liu et al. (2003b), Fu et al. (2003d), Wang et al. (2005), Shi et al. (2005), and Liu et al. (2005a) applied the new methods put forward in fluid mechanics, such as hierarchical similarity law and extended self-similarity, to analyze the statistical symmetry in fluctuations in the atmospheric boundary-layer and in meteorology variables. It showed that there exists hierarchical similarity in atmospheric motions over broad ranges, and there are different hierarchical similarity laws for different conditions, which is originated from the internal factors among atmospheric systems. For example, stratification is an important factor for velocity fluctuations in the atmospheric boundary layer, and it can influence the hierarchical similarity of velocity fluctuations. At last, the difference of the hierarchical similarity is determined by the gravity waves or solitary waves found in the atmospheric boundary layer. Due to the existence of these gravity waves or solitary waves, the statistical symmetry and energy cascade of turbulence will be changed in the atmospheric boundary layer.

## **8. The basic structures of atmospheric motions and the relation between solitary waves and wavelets**

Liu et al. (2003c, 2004a), Liu et al. (2003d, 2006), and Chi et al. (2004) found that the steady states of atmospheric motions were spiral patterns and these kinds of structures are originated from the balance among several forces such as dissipation force in the controlled equations of atmospheric motions. These kinds of spiral structures are related either to cone-shaped spirals or to column-shaped spirals, which are formed either from updraft due to surface convergence or downdraft due to divergence in high levels, or from downdraft due to convergence in high levels or updraft due to surface divergence.

Liu et al. (2003e, 2004b), Liu et al. (2003f, 2004c, 2005b), and Fu et al. (2005c) also found that the common Mexican hat wavelet satisfied linear ordinary differentiation equations with variable coefficients and its shape was also a kind of solitary waves. So this showed that wavelet was a kind of solitary waves.

## **9. Some applications of variational methods**

## 9.1 Inverse problems in atmospheric science and their applications

In recent years, a variety of methods have been proposed to boost accuracy of numerical weather prediction, such as variational data assimilation (VDA). The aim of VDA is to obtain initial and boundary conditions and parameters of models statistically or dynamically from observational data. Generally speaking, VDA problem is characterized by ill-posedness, and belongs to the category of inverse problem (Huang et al., 2005a; Huang et al., 2006a).

Initial condition and model parameter retrieval belong to the class of inverse problems. It is ill-posed to determine the initial condition and model parameters which are distributed in space and time with global and local observations by adjoint method. In the test of numerical experiments, the solution is very sensitive to the first guess and iteration steps, and the calculation is unstable to some extent without regularization. Huang and Wu (2001) and Zhang and Huang (2003) utilized the regularization method and overcame the ill-posedness of the problem to some extent. In the case of local observations, it improved the accuracy and stability of the solution, especially for the determination of model parameter in which the descent speed of the cost functional and the accuracy are both improved. However, the ill-posedness of the problem is very complicated, more efforts should be done in future (Pan and Huang, 2004; Du et al., 2004). In addition, Huang et al. (2004a), Huang and Han (2003), Gao et al. (2005), Fang et al. (2004), Fang and Huang (2004), and Wang et al. (2006) applied the VDA method combining with the regularization techniques and optimal control idea to retrieve the atmospheric and oceanic parameters, including the vertical eddy diffusion coefficient, the turbulivity of the atmospheric boundary layer, the wind with Doppler radar data, and GPS dropsonde's motion, obtaining good results.

Xiang et al. (2004, 2006) employed the adjoint method to a statistical-dynamical tropical-cyclone prediction model (SD-90). Their results indicated that by using the adjoint method, five tropical cyclone (TC) tracks are all fitted well and forces acting on TCs are well retrieved. They also applied the same method to a portion of the track data of TC 9804, which indicates that when the amount of data of a TC track is sufficient, the algorithm is stable. If TC track data are obtained every three hours, their results further prove the applicability of the algorithm to TCs with complicated mesoscale structures.

## 9.2 Variational adjustment of wind field and decomposition of wind field

The variational optimization analysis method (VOAM) for 2-D flow field suggested by Sasaki can be used efficiently in most case. However, in the cases where there are high frequency noises in 2-D or 3-D flow field, it appears to be inefficient. Based on Sasaki's VOAM, Huang et al. (2005b, c) and Lan et al. (2004) proposed a generalized variational optimization analysis method (GVOAM) with regularization ideas, which could deal well with flow fields containing high frequency noises. A numerical test shows that observational data can be both variationally optimized and filtered, and therefore the GVOAM is an efficient method.

By using the variational analysis, Huang et al. (2006b) used a linear and nonviscous 2-D Boussinesq equation on an  $f$ -plane to extract basic flows from observational wind field. Their results indicated that extracted basic flow can satisfy the controlling equations and can also make the functional--difference between it and observations--minimum after being taken integration average along the vertical direction. Subtracting basic flow from observational wind field gives disturbance wind fields which can be used to study instability problem and temporal evolvement of disturbance field (Huang et al., 2004b12).

## 9.3 Studies of variational data assimilation for a coupled air-sea model

For the prediction of ENSO, the accuracy of the model including the parameters and initial value of the model is important, which can be retrieved by the variational data assimilation methods developed in recent years. But when the nonlinearity of the model is strong enough, the effect of the improvement made by the 4-D variational data assimilation may be poor due to the bad approximation of the tangent linear model to the original model. So Du et al. (2006) introduced the ideas in the optimal control to improve the effect of 4-DVAR in the inversion of the parameters of a nonlinear dynamic ENSO model. Their results indicated that when the terminal controlling term is added to the cost functional of 4DVAR, which originated from the optimal control, the effect of the inversion may be largely improved comparing to the traditional 4DVAR, as can be especially obvious from the phase orbit of the model variables. In addition, their results

also suggested that the method of 4DVAR in combination with optimal control can not only reduce the error resulting from the inaccuracy of the model parameters but also can correct the parameters itself. This gives a good method in modifying the model and improving the quality of prediction of ENSO.

#### **9.4 New approach of variational data assimilation with “on-off” processes**

Moist physical processes characterized by the “on-off” switches are strongly nonlinear, the impact of “on-off” switches on the variational data assimilation (VDA) has been intensively investigated from idealized simple models to sophisticated forecast models in the recent years.

Mu and Wang (2003) present a new method based on the nonlinear perturbation equation (NPE) for an idealized model to calculate the gradient of the CF in the presence of “on-off” switches. This method provides the accurate gradient of CF in the time-continuous case. In the discrete case, it is useful to obtain the global descent direction of the CF in optimization and helpful to find the global minimum (Wang et al., 2002). In addition, the robustness of NPE method in using the VDA method to estimate both the initial condition (IC) and parameter is also verified (Wang et al., 2005).

Using an idealized PDE model, Mu and Zheng (2005) demonstrated that the traditional time discretization dealing with the nonlinearity caused by switches of the governing equation could induce awful zigzag in both of the CF and the numerical solution of the model. They proposed a method, which is a generalization of Xu’s intermediate interpolation method, to eliminate the zigzag phenomenon. The potential merits of this treatment are that the convergence in the minimization processes of the VDA is improved and the satisfactory optimization retrievals are obtained. Besides, they also demonstrate theoretically and numerically that if the “on-off” switches in the forward model are not properly numerical treated, the discrete CF gradients (even the one-sided gradient of CF) with respect to some ICs do not exist, and the solution of the corresponding tangent linear model (TLM) obtained by the conventional approach would not be a good first-order linear approximation to the nonlinear perturbation solution of the governing equation. Consequently, the validity of the adjoint approach in VDA with parameterized physical processes could not be guaranteed (Zheng and Mu, 2006).

## 10. Summary

The progresses in the study of nonlinear atmospheric dynamics achieved by Chinese Scientists in the period of 2003-2006 are reviewed in the following eight aspects: nonlinear error dynamics and predictability; nonlinear analysis of observational data; eddy-forced envelope Rossby soliton theory; sensitivity and stability of ocean's thermohaline circulation; nonlinear waves dynamics; nonlinear analysis on fluctuations in the atmospheric boundary-layer; the basic structures of atmospheric motions; some applications of variational methods. These achievements shed some light on the some atmospheric nonlinear phenomena and deepen our understanding of them. However, these progresses are far enough away from exposing the nature or cause of complex nonlinear phenomena. Many more achievements in this research area are expected to be realized in the future.

**Acknowledgments.** This work was supported by the National Natural Science Foundation of China (Grant Nos. 40325015, 40675046).

## References

- Cao Xiaoqun, Huang Sixun, and Du Huadong, 2005: Theoretical analysis and numerical experiments single-Doppler wind retrieval, *J. Hydrodynamics*, **20B**, 277-285. (in Chinese)
- Chen Baohua, Li Jianping, and Ding Ruiqiang, 2006: Nonlinear local Lyapunov Exponent and atmospheric predictability research, *Science in China (D)*, **49**, 1111-1120.
- Chen Zhe, Fu Zuntao, Liu Shikuo, 2005: Periodic structures of oceanic Rossby wave under the influence of wind stress, *Chaos, Solitons & Fractals*, **26**, 1467-1473.
- Chi Dongyan, Liu Shikuo, and Fu Zuntao, 2004: The steady motion and spiral pattern in Typhoon with condensed water, *Acta Scientiarum Naturalium Universitatis Pekinensis*, **40**, 788-796
- Diao Yina, Feng Guolin, Liu Shida, Liu Shikuo, Luo Dehai, Huang Sixun, Lu Weisong, and Chou Jifan, 2004: Review of the study of nonlinear atmospheric dynamics in China (1999-2002), *Adv. Atmos. Sci.*, **21**, 399-406.

- Ding Ruiqiang, and Li Jianping, 2006a: Nonlinear finite-time Lyapunov exponent and predictability, *Phys. Lett. A*, in press.
- Ding Ruiqiang, and Li Jianping, 2006b: A new method of local predictability study: Nonlinear local Lyapunov exponents, submitted to *Chinese J. Atmos. Sci.*.
- Du Huadong, Huang Sixun, and Shi Hanqing, 2004: Theoretical analyses and numerical tests for one-dimensional semigeostrophic shallow water model, *J. Hydrodynamics*, **19A**, 38-45. (in Chinese)
- Du Huadong, Huang Sixun, Cai Qifa, and Cheng Liang, 2006: Studies of variational assimilation for a coupled air-sea model, *J. Nanjing Inst. Meteor.*, accepted.
- Fang HanXian, Huang Sixun, and Wang Tingfang, 2004: Retrieval study of 1-d dropsonde's motion, *J. Hydrodynamics*, **19A**, 50-60. (in Chinese)
- Fang HanXian, and Huang Sixun, 2004: Theoretical analysis and numerical experiments of retrieval of 2-d dropsonde's motion, *Prog. Nat. Sci.*, **14**, 1257-1264.
- Feng Guolin, Gong Zhiqiang, Dong Wenjie, and Li Jianping, 2005: Abrupt climate change detection based on heuristic segmentation algorithm, *Acta Physica Sinica*, **54**, 5494-5499. (in Chinese)
- Fu Zuntao, Liu Shikuo, Liu Shida, and Zhao Qiang, 2003a: The JEFE method and periodic solutions of two kinds of nonlinear wave equations, *Commun. Nonlin. Sci. Numer. Simul.*, **8**, 67-75.
- Fu Zuntao, Liu Shikuo, and Liu Shida, 2003b: A new approach to solve nonlinear wave equations, *Commun. Theor. Phys.*, **39**, 27-30.
- Fu Zuntao, Liu Shida, and Liu Shikuo, 2003c: Solving nonlinear wave equations by elliptic equation, *Commun. Theor. Phys.*, **39**, 531-536.
- Fu Zuntao, Liu Shida, Chen Jiong, Liu Shikuo, and Liang Shuang, 2003d: Period 2, 3, 5 and their prediction for climatic jump points, *Earth Science Frontiers*, **10**, 415-418.
- Fu Zuntao, Liu Shikuo, and Liu Shida, 2004a: A new method to construct solutions to nonlinear wave equations, *Acta Physica Sinica*, **53**, 343-348.
- Fu Zuntao, Liu Shida, Liu Shikuo, 2004b: New solutions to mKdV equation, *Phys. Lett. A*, **326**, 364-374.
- Fu Zuntao, Zhang Lin, Liu Shida, and Liu Shikuo, 2004c: Basic pattern in atmospheric turbulence model, *Commun. Theor. Phys.*, **41**, 845-848.
- Fu Zuntao, Liu Shida, Liu Shikuo, and Chen Zhe, 2004d: Structures of equatorial envelope Rossby wave under the influence of new type of diabatic heating, *Chaos, Solitons & Fractals*, **22**, 335-340.
- Fu Zuntao, Liu Shikuo, and Liu Shida, 2005a: New rational form solutions to mKdV equation, *Commun. Theor.*

- Phys.*, **43**, 423-426.
- Fu Zuntao, Liu Shikuo, and Liu Shida, 2005b: Equatorial Rossby solitary wave under the external forcing, *Commun. Theor. Phys.*, **43**, 45-48.
- Fu Zuntao, Liu Shida, Liu Shikuo, Liang Fuming, and Xin Guojun, 2005c: Homoclinic (heteroclinic) orbit of complex dynamical system and spiral structure, *Commun. Theor. Phys.*, **43**, 601-603.
- Huang Sixun, and Wu Rongsheng, 2001: Methods of Mathematical Physics in Atmospheric Science. China Meteorological Press, Beijing, pp540. (in Chinese)
- Huang Sixun, and Han Wei, 2003: Application of techniques in inverse problems to VAR in meteorology and oceanography, Recent Development in Theories and Numerics, Inf. Conf. on Inverse Problem, World Scientific, 349-355.
- Huang Sixun, Han Wei, and Wu Rongsheng, 2004a: Theoretical analyses and numerical experiments of Variational assimilation for one-dimensional ocean temperature model with technique in inverse problems, *Science in China (D)*, **47**, 630-638.
- Huang Sixun, Zhang Ming, and An Jie, 2004b: Extract basic flow from observational wind, *J. Appl. Meteor. Sci.*, **15**, 572-578. (in Chinese)
- Huang Sixun, Xiang Jie, Du Huadong, and Cao Xiaoqun, 2005a: Inverse problems in atmospheric science and their application, *J. Phys.*, **12**, 45-57. (in Chinese)
- Huang sixun, Xu Dinghua, Lan Weiren, and Teng Jiajun, 2005b: Generalized variational optimization analysis for 2-D flow field, *J. hydrodynamics*, **17B**, 459-465.
- Huang sixun, Teng Jiajun, Lan Weiren, and Xiangjie, 2005c: Variational adjustment of 3-D wind field combining with the regularization method, *Chinese J. Theor. Appl. Mech.*, **37**, 399-407. (in Chinese)
- Huang Sixun, Cao Xiaoqun, Du Huadong, Wang Tingfang, and Xiang Jie, 2006a: Retrieval of atmospheric and oceanic parameters and the relevant numerical calculation, *Adv. Atmos. Sci.*, **23**, 106-117
- Huang Sixun, Cai Qifa, Xiang Jie, and Zhang Ming, 2006b: On decomposition of typhoon flow field, *Chinese Phys.*, accepted.
- Lacarra, J. F., and O. Talagrand, 1988: Short-range evolution of small perturbations in a barotropic model, *Tellus*, **40**, 81-95.
- Lan weiren, Huang Sixun, and Xiang Jie, 2004: Generalized method of variational analysis for 3-D Flow, *Adv. Atmos. Sci.*, **21**, 730-740.
- Li Jianping, and Chou Jifan, 2003: Advances in nonlinear atmospheric dynamics, *Chinese J. Atmos. Sci.*, **27**,

653-673. (in Chinese)

Li Jianping, Ding Ruiqiang, and Chen Baohua, 2006: Review and prospect on the predictability study of the atmosphere, China Meteorology Press, Beijing, pp96. (in Chinese)

Li Jianping, and Ding Ruiqiang, 2006: Multi-dimensional nonlinear local Lyapunov exponent in chaotic systems, submitted to *Phys. Lett. A*.

Li Jianping, and Wang Shouhong, 2006: Some mathematical and numerical issues in geophysical fluid dynamics and climate dynamics, submitted to.

Liu Shida, Liu Shikuo, Fu Zuntao, Ren Kui, and Guo Yan, 2003b: The most intensive fluctuation in chaotic time series and relativity principle, *Chaos, Solitons & Fractals*, **15**, 627-630.

Liu Shida, Liu Shikuo, Fu Zuntao, Xin Guojun, and Liang Fuming, 2003d: From 2-D geostrophic wind to 3-D vortex motions, *Chinese J. Geophys.*, **46**, 450-454. (in Chinese)

Liu Shida, Fu Zuntao, Liu Shikuo, Xin Guojun, Liang Fuming, and Feng Beiye, 2003f: Solitary wave in linear ODE with variable coefficients, *Commun Theor. Phys.*, **39**, 643-646.

Liu Shida, Fu Zuntao, Liu Shikuo, Xin Guojun, and Liang Fuming, 2004c: Solitary wave and wavelet, *Commun. Theor. Phys.*, **41**, 335-338.

Liu Shida, Shi Shaoying, Liu Shikuo, Fu Zuntao, Liang Fuming, and Xin Guojun, 2005b: Vortex of fluid field as viewed from curvature, *Commun. Theor. Phys.*, **43**, 604-606.

Liu Shida, Liu Shikuo, Liang Fuming, and Fu Zuntao, 2006: The spiral structure for atmospheric vortex, *Chinese J. Atmos. Sci.*, **30**, 849-853. (in Chinese)

Liu Shikuo, Fu Zuntao, Liu Shida, and Zhao Qiang, 2003a: Power series expansion method and its applications to nonlinear wave equation, *Phys. Lett. A*, **309**, 234-239.

Liu Shikuo, Wang Shaolin, Fu Zuntao, and Liu Shida, 2003c: Spiral patterns of the Rossby wave, *Chinese J. Geophys.*, **46**, 584-589. (in Chinese)

Liu Shikuo, Fu Zuntao, Liu Shida, Ren Kui, 2003e: Scaling equation for invariant measure, *Commun. Theor. Phys.*, **39**, 295-296.

Liu Shikuo, Liu Shida, Fu Zuntao, Xin Guojun, and Liang Fuming, 2004a: The structure and bifurcation of atmospheric motions, *Adv. Atmos. Sci.*, **21**, 557-561.

Liu Shikuo, Fu Zuntao, Liu Shida, Liang Fuming, and Xin Guojun, 2004b: Solitary wave and wave front as viewed from curvature, *Commun. Theor. Phys.*, **42**, 814-816.

Liu Shikuo, Liu Shida, Fu Zuntao, and Sun Lan, 2005a: A nonlinear coupled soil moisture -vegetation model, *Adv.*

- Atmos. Sci.*, **22**, 337-342.
- Luo Dehai, 2005a: A barotropic envelope Rossby soliton model for block–eddy interaction. Part I : Effect of topography, *J. Atmos. Sci.*, **62**, 5-21.
- Luo Dehai, 2005b: A barotropic envelope Rossby soliton model for block–eddy interaction. Part II : Role of westward-traveling planetary waves, *J. Atmos. Sci.*, **62**, 22-40.
- Luo Dehai, 2005c: A barotropic envelope Rossby soliton model for block–eddy interaction. Part III: Wavenumber conservation theorems for isolated blocks and deformed eddies, *J. Atmos. Sci.*, **62**, 3839-3859.
- Luo Dehai, 2005d: A barotropic envelope Rossby soliton model for block–eddy interaction. Part IV: Block activity and its linkage with a sheared environment, *J. Atmos. Sci.*, **62**, 3860-3884.
- Mu Mu, 2000: Nonlinear singular vectors and nonlinear singular values, *Science in China (D)*, **43**, 375-385.
- Mu Mu, Duan Wansuo, and Wang Bin, 2003: Conditional nonlinear optimal perturbation and its applications, *Nonlin. Proc. Geophys.*, **10**, 493-501.
- Mu M., and Wang JiaFeng, 2003: An adjoint method for variational data assimilation with physical “on-off” processes, *J. Atmos. Sci.*, **60**, 2010–2018.
- Mu Mu, and Zheng Qin, 2005: Zigzag oscillations in variational data assimilation with physical “on-off” processes, *Mon. Wea. Rev.*, **133**, 2711–2720.
- Mu, M., L. Sun, and H. A. Dijkstra, 2004: Sensitivity and stability of thermohaline circulation of ocean to finite amplitude perturbations, *J. Physical oceanography*, **34**, 2305-2315.
- Mu Mu, and Zhang Zhiyue, 2006: Conditional nonlinear optimal perturbations of a two-dimensional quasi-geostrophic model, *J. Atmos. Sci.*, **63**, 1587-1604.
- Pan Xiaoqiang, and Huang Sixun, 2004: Variational adjoint method for one-dimensional shallow water model: Theoretical analysis and numerical experiments, *Chinese J. Atmos. Sci.*, **28**, 175-186. (in Chinese)
- Shi Shaoying, Liu Shida, Fu Zuntao, Liu Shikuo, Liang Fuming, Xin Guojun, and Li Bailian, 2005: The characteristic analysis of weather and climate time series, *Chinese J. Geophys.*, **48**, 259-264. (in Chinese)
- Sun Liang, Mu Mu, Sun Dejun, and Yin Xieyuan, 2005: Passive mechanism of decadal variation of thermohaline circulation, *J. Geophys. Res.*, **110**, C07025, doi:10.1029/2005JC002897.
- Wan Shiquan, Feng Guolin, Zhou Guohua, Wan Bingmei, Qin Mingrong, and Xu Xiazhen, 2005a: Extracting useful information from the observations for the prediction based on EMD method, *Acta. Meteor. Sinica*, **63**, 516-525. (in Chinese)
- Wan Shiquan, Feng Guolin, Dong Wenjie, and Li Jianping, 2005b: From regional to global dynamics structure of

- the climatic proxy, *Acta Physica Sinica*, **54**, 5487-5493. (in Chinese)
- Wang Jiafeng, Mu Mu, and Zheng Qin, 2002: Adjoint approach to VDA of “on-off” processes based on nonlinear perturbation equation, *Prog. Nat. Sci.*, **12**, 869-973.
- Wang Jiafeng, Mu Mu, and Zheng Qin, 2005: Initial condition and parameter estimation in physical ‘on-off’ processes by variational data assimilation, *Tellus*, **57A**, 736-741.
- Wang Jingye, Fu Zuntao, Zhang Lin, and Liu Shida, 2005: Information entropy analysis on turbulent temperature series in the atmospheric boundary layer, *Plateau Meteor.*, **24**, 38-42. (in Chinese)
- Wang Tingfang, Huang Sixun, and Xiang Jie, 2006, Studies on retrieval of the turbulivity of atmospheric boundary layer, *J. Hydrodynamics*, **18B**, 177-183. (in Chinese)
- Xiang Jie, Wu Rongsheng, and Huang Sixun, 2004: Studies on application of the adjoint method to the statistic-dynamical prediction model for tropical cyclones (SD-90). I: Theoretical aspects and numerical tests, *Prog. Nat. Sci.*, **14**, 677-682. (in Chinese)
- Xiang Jie, Liao Qianfeng, Huang Sixun, Lan Weiren, Feng Qiang, and Zhou Fengcai, 2006: An application of the adjoint method to a statistical-dynamical tropical-cyclone prediction model (SD-90). II: real tropical cyclone cases, *Adv. Atmos. Sci.*, **23**, 118-126.
- Zhao Qiang, Liu Shikuo, and FU Zuntao, 2005: New soliton-like solutions for combined KdV and mKdV equation, *Commun. Theor. Phys.*, **43**, 615-616.
- Zheng Qin, and Mu Mu, 2006: The effects of the model errors generated by discretization of “on-off” processes on VDA, *Nonlin. Proc. Geophys.*, **13**, 309-320.

# THE MAJOR ADVANCES IN MESOSCALE ATMOSPHERIC DYNAMIC RESEARCH OF CHINA SINCE 2003

LU Hancheng<sup>1,2</sup>(陆汉城), GAO Shouting<sup>3</sup> (高守亭) , TAN Zhemin<sup>1</sup> (谈哲敏)

<sup>1</sup>Department of Atmospheric Sciences, Nanjing University, Nanjing 210093

<sup>2</sup>Meteorological College, PLA University of Science and Technology, Nanjing 211101;

<sup>3</sup>Institute of Atmospheric Physics, Chinese Academy of Sciences, Beijing 100029;

## Abstract

The advances in mesoscale meteorology during the past four years are reviewed. The major progresses in theoretical studies include a) Dynamic mechanism of mesoscale circulation; b) The heavy rain dynamics; c) Moist atmosphere dynamics. On the dynamic mechanism of mesoscale circulation, the followings are summarized: equilibrium dynamical problems; non-equilibrium dynamical problems(studied the instability of mesoscale such as symmetric instability and transverse wave instability in vortex atmosphere, non-linear convective symmetric instability, the interaction between forced flow and instable flow); the feature and energetic analysis of characteristic wave on mesoscale motion; mesoscale dynamics of Ekman layer; frontal circulation dynamics; wind helicity dynamics and tropical cyclone dynamics. Through the research of heavy rain dynamics and moist atmosphere dynamics, the possible mechanism for the formation and development of a meso- $\beta$  rainstorm system is proposed. The above studies give important explanation to revealing the developing mechanism of mesoscale circulation in the East Asia atmospheric circulation background.

Key words: mesoscale dynamics, mesoscale circulation, observational data diagnoses

## 1、 Introduction

Since 2003, with the quick development of Chinese economics, mesoscale meteorology research has acquired more national funds' support. In addition, modern atmospheric sounding technology and computer technology have made great progress, which lead to dramatic development in mesoscale-disastrous weather research make. Particularly, high frequency of recent year's intense storm and rainstorm heavily influenced national economy construction and people's lives and property. High attention is paid on the research of mesoscale disastrous weather mechanism, forecasting and pre-warning. Chinese meteorologists have carried out deep

probe into the observation research, dynamical diagnostic analysis and numerical forecasting of organic mesoscale convection system which form the mesoscale disastrous weather. The occurring and developing of mesoscale convective system in the East Asia atmosphere and circulation is observed, on the basis of which, dynamical theory of deep moist convection has reached innovative researching results. This paper synthetically discussed major advances of mesoscale weather dynamical research.

## 2 、 Dynamic mechanism of mesoscale circulation

Observational research shows that mesoscale convection system (MCS) is a convection storm formed by organic cumulus convection (Browning 1974, 1984, 1989; Emanuel et al 1986 ). Common mesoscale convection systems in middle latitude region include the followings: local convection system (local severe storm etc.), quasi-two dimensional line convection (squall line, frontal mesoscale rain belt etc.), mesoscale convection complex (MCC) with cluster structure like circular, and convection zone in typhoon with characteristics of vortex circulation (Lu et al 2001; Gao 2004; Tan 2004; Wu 2004). One of their shared characters is that there is a mesoscale circulation with very strong vertical motion on the quasi-two-dimension cross-section. Therefore, the dynamical mechanism of deep and moist convectional organic is the main scientific problem of mesoscale dynamics (Zhou et al 2004).

### 2.1 Equilibrium dynamical problems

Frontogenetical circulation theory which is based on approximation of frontal transverse circulation and semi-geostrophic momenta (Sawyer 1956; Eliassen 1962; Shapiro 1980), as well as symmetric instability theory (Bennetts and Hoskins 1979) put forward the genesis-mechanism of mesoscale circulation under the condition of base flow equilibrium (geostrophic equilibrium and thermal wind equilibrium), but they have great mathematical and physical difference, the former is induced by the forcing in the condition of elliptical equations, while the latter is time-varying unstable flow. Lu et al (2004) put forward the idea of applying equilibrium dynamical theory in the vortex atmosphere to discuss the occurrence and development of mesoscale disturbance, and applying the concept of “gradient wind momentary approximation”, which was similar to geostrophic momentary approximation (Wu 1990, 2002), to change the mesoscale primitive equations in cylinder coordinate system to the followings:

$$v = \tilde{v} + Du = \tilde{v} + D\tilde{u} - D^2(\tilde{v} + D\tilde{u}) + \dots, \quad u = \tilde{u} - Dv = \tilde{u} - D\tilde{v} - D^2(\tilde{u} - D\tilde{v}) + \dots,$$

$$\text{where } \mathbf{D} = \frac{d}{dt} = \frac{\partial}{\partial t} + u \frac{\partial}{\partial r} + v \frac{\partial}{r \partial \lambda} + w \frac{\partial}{\partial z}, \quad f_1 = \frac{v}{r} + f$$

Taking the first approximation, we will get  $\frac{d\tilde{u}}{dt} = f_1 v'$ ,  $\frac{d\tilde{v}}{dt} = -f_1 u'$ . Here we distinguish the tangential flow fulfilling gradient wind equilibrium and statistic equilibrium as generalized

thermal wind equilibrium:  $(\frac{2\tilde{v}}{r} + f) \frac{\partial \tilde{v}}{\partial z} = \frac{g}{\theta_0} \frac{\partial \theta}{\partial r}$ . In the condition of axial

symmetry,  $\frac{d\tilde{u}}{dt} = 0$ ,  $\frac{d\tilde{v}}{dt} = -f_1 u'$ . Let  $m = r(\tilde{v} + \frac{fr}{2})$ , we can get the diagnostic equations of the radial

secondary circulation:

$$\frac{1}{r} \frac{g}{\theta_0} \frac{\partial \theta}{\partial z} \frac{\partial^2 \psi}{\partial r^2} - \frac{2}{r} (\frac{2\tilde{v}}{r} + f) \frac{\partial \tilde{v}}{\partial z} \frac{\partial^2 \psi}{\partial r \partial z} + \frac{1}{r^2} (\frac{2\tilde{v}}{r} + f) \frac{\partial m}{\partial r} \frac{\partial^2 \psi}{\partial z^2} - \frac{1}{r^2} \frac{g}{\theta_0} \frac{\partial \theta}{\partial z} \frac{\partial \psi}{\partial r} + \frac{4}{r^2} \frac{g}{\theta_0} \frac{\partial \theta}{\partial r} \frac{\partial \psi}{\partial z} = 0$$

$$\text{Let } \frac{g}{\theta_0} \frac{\partial \theta}{\partial r} = S^2, \quad \frac{g}{\theta_0} \frac{\partial \theta}{\partial z} = N^2, \quad (\frac{2\tilde{v}}{r} + f) \frac{1}{r} \frac{\partial m}{\partial r} = F^2,$$

The ellipse condition for of the diagnostic equations is:  $F^2 N^2 - S^4 > 0$ , i.e.,  $(\frac{\partial m}{\partial r})_\theta \frac{\partial \theta}{\partial z} > 0$ ; while the

hyperbolic condition for the diagnostic equations is  $F^2 N^2 - S^4 < 0$ , i.e.,  $(\frac{\partial m}{\partial r})_\theta \frac{\partial \theta}{\partial z} < 0$ . Obviously, for

the ellipse condition  $(\frac{\partial m}{\partial r})_\theta > 0$ ,  $\frac{\partial \theta}{\partial z} > 0$  is only one of the cases, which is the existing condition for

radial circular flow in the condition of stable inertia and stratification. For hyperbolic

conditions:  $(\frac{\partial m}{\partial r})_\theta < 0$ ,  $\frac{\partial \theta}{\partial z} > 0$ , it is a sort of inertia instability on constant entropy surface in the

condition of stratification stability condition, and it is a symmetric instability. But equilibrium model can not be used to study unstable flow.

## 2.2 Non-equilibrium dynamical problem

The main theories for instability-generated convection are Conditional Symmetric Instability(CSI) or Moist Symmetric Instability(MSI) (Bennetts and Sharp 1982; Seltzer et al 1985; Reuter and Aktary 1993, 1995) and transverse wave instability. It is proved that symmetric instability with medium-size Rossby number is of quasi-two dimensional  $\beta$  mesoscale developing mechanism. Linear theories indicate that such instability is induced by disturbance non-thermal wind equilibrium in the condition of base flow thermal wind equilibrium. Deep research into non-equilibrium dynamical problems is paid much attention. Gao et al (2005) put forward the method of using convective vortex vector instead of potential vortex to diagnose meso-scale convective systems, while Lu et al (2004) put forward the non-equilibrium dynamical problem in

the vortex atmosphere.

### 2.2.1 Symmetric instability and transverse wave instability in vortex atmosphere

1、 Discuss symmetric unstable flow in the stationary gradient current(Fei and Lu 1996; Lu et al 2004). Linearizing the primitive equations in cylinder coordinate (using rotational flow thermal wind equilibrium), we can get a disturbance radial circular flow

$$\text{equation: } \frac{\partial^2}{\partial t^2} \left( \frac{1}{r^2} \frac{\partial^2 \psi}{\partial z^2} + \frac{1}{r^2} \frac{\partial^2 \psi}{\partial r^2} - \frac{1}{r^2} \frac{\partial^2 \psi}{\partial r} \right) = f_1 \frac{\partial}{\partial t} \left( \frac{\partial v'}{\partial z} \right) - \frac{g}{\theta_0} \frac{\partial}{\partial t} \left( \frac{\partial \theta'}{\partial r} \right)$$

Obviously, the development of radial circular flow is related with disturbance non-thermal wind equilibrium.

$$\begin{aligned} \frac{\partial^2}{\partial t^2} \left( \frac{1}{r} \frac{\partial^2 \psi}{\partial z^2} + \frac{1}{r^2} \frac{\partial^2 \psi}{\partial r^2} - \frac{1}{r^2} \frac{\partial^2 \psi}{\partial r} \right) = & -F^2 \left( \frac{1}{r} \frac{\partial^2 \psi}{\partial z^2} \right) + 2S^2 \left( \frac{1}{r} \frac{\partial^2 \psi}{\partial r \partial z} \right) - \frac{S^2}{r^2} \frac{\partial \psi}{\partial z} - \frac{N^2}{r} \left( \frac{\partial^2 \psi}{\partial z^2} - \frac{1}{r} \frac{\partial \psi}{\partial r} \right) \\ & + \frac{1}{r} \frac{\partial \psi}{\partial z} \left( \frac{\partial S^2}{\partial r} - \frac{\partial F^2}{\partial z} \right) - \frac{1}{r} \frac{\partial \psi}{\partial r} \left( \frac{\partial N^2}{\partial r} - \frac{\partial S^2}{\partial z} \right) \end{aligned}$$

When environmental parameters do not change with the spatial variation, we can get the

disturbance instability conditions  $R_i^* = \frac{F^2 N^2}{S^4} < 1 - \left( \frac{3}{2} + m \right)^{-2}$ , Where  $m = - \left[ \frac{3}{2} + \frac{c_1}{c_1 + c_2} \right]$  is the

eigenvalue of interflow hypergeometric equation ( kummer equation), and  $c_1, c_2$  are the eigenvalues of Hulukara equation.

It is indicated that the disturbance along vertical direction of tangential flow in the vortex atmosphere has the characteristic of inertia gravity wave. Symmetric instability is one of the developing mechanisms.

When the environmental parameters change with the spatial variation, we can get the energy-developing equations of symmetrical instability:

$$\begin{aligned} \frac{\partial}{\partial T} \int_{\tau} E d\tau = & \int_{\tau} \frac{E}{K^2 \omega^2} \left( kn \frac{\partial M_w^2}{\partial T} - \frac{n^2}{2} \frac{\partial F^2}{\partial T} - \frac{k^2}{2} \frac{\partial N_w^2}{\partial T} \right) d\tau + \int_{\tau} \frac{n^2 E}{K^4 \omega^2} \left( 2knC_r \frac{\partial M_w^2}{\partial R} - n^2 C_r \frac{\partial F^2}{\partial R} - k^2 C_r \frac{\partial N_w^2}{\partial T} \right) d\tau \\ & + \int_{\tau} \frac{n^2 E^2}{K^4 \omega^2} \left( -2knC_z \frac{\partial M_w^2}{\partial Z} + n^2 C_z \frac{\partial F^2}{\partial Z} + k^2 C_z \frac{\partial N^2}{\partial Z} \right) d\tau \end{aligned}$$

Therefore, variation of environmental field( including stratification、 temperature gradient、 wind shear)is the reason for the change of symmetric instability energy. But the circulation feature overlapped on change of environmental field can not be well demonstrated.

The transverse wave disturbance along tangential base flow of circular vortex is discussed. By using numerical method, Li and Lu et al (2003) study this instability of baroclinic flow which is

mesoscale inertia-gravity wave instability on the cylindrical coordinate. The growth rate of instability is influenced by stratification stability  $N^2$ , Coriolis parameter  $f_0$ , the vertical shear of tangential wind  $\overline{V}_z$  of the ambient atmosphere and the latent heat. In vortex atmosphere, there is also transverse wave instability in Eady mode and mesoscale mode. Furthermore, distribution character of mesoscale disturbance of transverse wave instability is studied. Anomalous “cat eye” structure and the character of the slowly spreading disturbance converges at low level and the quickly spreading disturbance converges at high level.

### 2.2.2 Non-linear convective symmetric instability

Xu (1986) pointed out the formation of rain belt calling ‘upscale’ formation. That is, first, a small scale convective cell appears arising from the development of moist convective instability, then the cell forms a meso-scale rain belt through the release of symmetric instability. But in the actual atmosphere, the fact that the convective instability and symmetric instability occur at the same time is always observed (Emanuel 1983; Seman 1994) calls such a meso-scale instability as nonlinear convective symmetric instability. The development of nonlinear convective-symmetric instability in the mesoscale convective system is analyzed by numerical experiment (Kou and Lu 2006) using ARPS (Advanced Regional Prediction System). The results show that, for the developing process of nonlinear convective-symmetric instability, at the beginning, convection develops, and it prepares the condition for the development of symmetric instability, then, the evolution of symmetric instability makes the convection systematization, strengthens the circulation and keeps the convection for a long time. There is a positive feedback between convection development and release of symmetric instability, and accordingly the concept of the interaction between the physical processes is presented.

In a numerical model especially set up in the work (Kou and Lu 2004) that includes disturbance and basic flows, the interactions between disturbances and symmetric instability are discussed comprehensively. The study shows that the interactions display the following features that(1) the basic flow, changed by the disturbance, has feedback on the latter, and(2)the mean transfer of disturbance changes the very structure of disturbance to affect its evolution. Slantwise circulation of disturbance as excited by symmetrically unstable basic flows has changed the ambient field so that the symmetrical instability keeps evolving. On the other hand, the influence as produced by mean transfer of disturbance is favorable for deeper evolution of the symmetrical

instability, with the latter being more important than the former.

An anelastic and non-hydrostatic two-dimensional numerical model is used to study the influence of initial disturbance's scale on the development of symmetric instability (Kou and Lu 2004). The results show that: The symmetrical instability does not have to be stirred by horizontal disturbance of correspondent scale of the symmetrical instability; the slant circulations, which are stirred by disturbances of different scales, have different specialties; there may be a minimum critical scale in symmetrical instability slant circulation; there is also an optimal horizontal scale to the development of symmetrical instability, while the vertical scale of disturbance throws less influence on symmetrical instability.

In addition, the conditional symmetry instability is the intermediate process between the stable and instable states of the atmosphere (Cheng and Lu 2006). The evolution of the atmosphere from the stable to unstable state or from unstable to stable comes through two stages. The convective-symmetric instability circulation is related with the state and type of the instability. When the conditional instability lies in the lower level and conditional symmetric instability in the upper level, the circulation will have vertical updrafts in the lower level and slantwise updrafts in the upper level. The release of conditional symmetric instability gives rise to a mesoscale rain belt. When the conditional symmetric instability lies in the middle level and conditional instability in the lower and upper levels, the circulation will have updrafts through the total column of the atmosphere. The release of conditional instability gives rise to a mesoscale rain belt.

### 2.2.3 The interaction between forced flow and instable flow

Slantwise convection caused by frontogenesis and Moist Symmetric Instability (MSI) also can lead to band rainfall. In virtual atmosphere, it's difficult to separate Front Genesis from Moist Symmetric Instability (MSI), because they are conjunctions with each other (David et al 1999). In the process of deep moist convection with the characteristic of long duration and larger scale, the interaction between forced and instable convection become more complex.

Based on the numerical method, the interaction between forced and instable convection in the process of the break and rebuilding of equilibrium state was discussed (Cheng and Lu 2006). The instable convection includes the conditional instability and conditional symmetric instability. A conclusion is drawn about the interaction of the forced convection and instable convection. The quantity of instable convection is ten times of that of forced convection. If the deep instability in

vertical or slantwise direction and the finite-amplitude ascending motion in forced convection are given, the instable convection will appear in three hours after the production of forced convection, or if the instable convection exists before the production of forced convection, the existing convection center will move to the forced convection center. On the contrary, if the finite-amplitude forced convection caused by ambient field shows the descending motion or the weak ascending motion, it makes against the creation of the instable convection, and the relevant ascending motion center couldn't create in actual vertical speed field. So whether ambient field can force out ascending motion to improve the instable energy release. The forced convection is trigger mechanism of instable convection.

### 2.3 The feature and energetic analysis of characteristic wave on mesoscale motion

#### 2.3.1 Characteristic wave and its structure of mesoscale motion

The characteristic wave and instability of meso- $\beta$  scale disturbance is discussed (Zhang and Shi 2004; Zhang and Deng 2005) using the means of numerical calculation by Boussinesq equations. The results show that the characteristic of wave spectrum of meso- $\beta$  scale waves is related to basic field. When having vertical shear in basic flow, a pair of gravitational inertial waves and a branch vortex wave all exist continuous spectrum. The continuous spectrums occur to overlap with the increase of wind shear. The spectral functions also change in the overlap spectrum area, namely the disturbance structure change. It is different from the characteristic wave of meso- $\alpha$  scale disturbance.

The structure of three kinds of instability disturbance are calculated and analyzed in different basic field(Zhang and Shi 2004). The results are as follows: The structure of symmetry instability of meso- $\beta$  scale is different from that of meso- $\alpha$  scale. The vertical wave number of instability inertia-gravitational wave increases with decrease of horizontal scale. The structure of heterotropic disturbance is similar to that of transverse wave disturbance. When Richardson number is small, the stream function shows that the shape of "cat eye". When Richardson number is great, the stream function shows the shape of anomaly wave in vertical structure. This result shows that two kinds of instability of meso- $\beta$  scale disturbance are same source.

In the context of the Boussinesq approximation equations for transversal wave-type(TWT) disturbances in zonal basic flow (Shen and Ni 2005), it is analyzed that vertical windspeed shear of basic flow causes instabilities of the TWT perturbation; considering the second derivative of

basic-flow wind with respect to  $z$  (denoted by  $\overline{U_{zz}} \neq 0$  which is simply given as  $\beta_*$  hereafter) the expression for the phase velocity of vortex Rossby wave (VR<sub>0</sub>W) is obtained, which is unidirectional in propagation with respect to basic flow; VR<sub>0</sub>W has its physical origin from  $\beta_*$ , i.e., from  $z$ -varying heterogeneities of  $y$ -direction averaged vorticity of the basic flow field; VR<sub>0</sub>W phase velocity is associated with zonal number  $k$ , its energy is dispersive and the group velocity exists in the  $x$  direction; when windspeed meets the condition of  $\beta_*$ , the TWT disturbance instability may be that of mixed VR<sub>0</sub>W and inertia-gravity wave.

The so-called “Meiyu front” over the Changjiang River basin is actually an equivalent-barotropic zone in which the horizontal thermal gradient is negligibly weak but the humidity gradient is very strong particularly in the lower troposphere (Hu 2005). In the Meiyu season most of the severe MCSs (mesoscale convective systems) with torrential rain may form, develop, move and newly emerge up and down-stream along such “low-level moisture frontal zone”. What kind of wave disturbance most relevant to these activities of MCSs are likely the deep mesoscale inertia-gravitational waves in company with the microscopic cumulus cloud ensemble heating, which will be named “inertia-gravitational wave CISK” hereafter.

### 2.3.2 Energetic analysis of Characteristic wave

The transversal wave type (TWT) disturbances are utilized to investigate the features in distribution of the related physical quantities and the energy sources (Shen and Ni 2005). Evidence suggests that in such a TWT synoptic system disturbance pressure  $p'$  and vorticity  $\xi'$  are in the same or opposite phase in the  $x$  direction, so are the disturbance divergence  $D'$  and vertical velocity  $w'$ , but  $\xi'$  differs by  $\pi/2$  in phase from  $D'$  in their propagation except that their distributions differ to some extent in the  $z$  direction; the total energy of the local disturbance development originates largely from the available potential energy and kinetic energy averaged over the environmental field.

A refined gravity-wave-drag scheme is presented based on McFarlane's parameterization scheme of gravity wave drag. Both the drag effect of the momentum flux and the dissipation effect of gravity wave breaking on the mean zonal flow are included in the refined parameterization scheme. Motivated by ageostrophic interactions of wave and basic flow, the generalized relationships between 3-D Eliassen-Palm flux and basic flows are derived (Ran and Gao 2004),

suitable for small-amplitude and finite-amplitude disturbances. The expressions of the new 3-D Eliassen-Palm flux and wave activity are presented in terms of Eulerian quantities so that they can be readily calculated by using observation data or model output data.

An ageostrophic Generalized E-P flux in baroclinic stratified atmosphere are developed (Gao et al 2004), aimed at limitation and deficiency of the traditional Eliassen-Palm flux associated with wave-meanflow interaction and its subsequent generalization based on the Boussinesq approximation or quasi-geostrophic approximation. This generalized E-P flux can be conveniently used to diagnose and analyze such important phenomena as the upper-level jet acceleration, gravity wave breaking-up and stratospheric erupt warming.

Using a multi-scale method, the interaction of eddy and barotropic basic flow in virtue of new E-P flux are investigated (Ran et al 2004) without introducing residual meridional circulation. The results show that the evolution of the zonally symmetric barotropic basic flow is completely dominated by the new zonal-averaged E-P flux divergence.

The relation between the barotropic basic zonal flow and a new Eliassen-Palm flux, which is applicable to diagnose the acceleration and deceleration of upper-level basic zonal flow, is examined by using the multi-time scale method (Ran et al 2005). It shows that the acceleration and deceleration of basic zonal flow mainly result from the meridional transportation of perturbation momentum.

#### 2.4 Mesoscale Dynamics of Ekman Layer

Based on the classical Ekman theory, a series of intermediate boundary layer models, which retain the nonlinear advective process while discard embellishments, have been proposed with the intention to understand the complex nonlinear features of the atmospheric boundary layer and its interaction with the free atmosphere (Tan and Fang et al 2006). It is found that the qualitative descriptions of the nonlinear nature in Ekman layer made by the intermediate models are fairly consistent though the details may be different. It is shown that the intermediate boundary-layer models have great potential in illustrating the low-level structures of the weather and climate systems as they are coupled with the free atmospheric models. In addition, the important remaining scientific challenges and a prospectus for future research on the intermediate model are also discussed.

Tang et al (2006) pointed out that a slab boundary layer model with a constant depth is used to

analyze the boundary-layer wind structure in a landfalling tropical cyclone. Asymmetry is found in both the tangential and radial components of horizontal wind in the tropical cyclone boundary layer at landfall. For a steady tropical cyclone on a straight coastline at landfall, the magnitude of the radial component is greater in the offshore-flow side and the tangential component is greater over the sea, slightly offshore, therefore the greater total wind speed occurs in the offshore-flow side over the sea.

A two-dimensional nonlinear baroclinic Eady wave model is used to study the dynamical mechanisms for the rapid growth of initial balanced perturbations in the baroclinic system (Yuan and Tan 2006). The advection effect of baroclinic shear flow on perturbation potential vorticity leads to the “potential vorticity unshielding” of initial perturbation potential vorticity (PV), which induces the rapid growth of initial perturbations in the linear system.

A time-dependent semi-geostrophic Ekman boundary layer model (SG), including slowly varying eddy diffusivity with height and inertial term effects, is developed to investigate the diurnal wind variation in the planetary boundary layer (PBL) (Zhang and Tan 2002). An approximate analytical solution of this model is derived by using the WKB method. The features of the diurnal wind variation in the PBL mainly depend on three factors: the latitude, horizontal momentum advection and eddy viscosity.

Using a three-dimensional nonhydrostatic mesoscale numerical model (MM5) (Zhang and Tan 2006), the evolution and structures of baroclinic waves with and without surface drag in case of dry and moist atmosphere are simulated, with special emphases on the effects of surface drag on the low-level frontal structure and frontogenesis.

Zhang and Tan (2006) studied the evolution of baroclinic waves with and without surface drag in the dry atmosphere, with special emphases on the structure of upper level front and the mechanism that tropopause folding remotes the surface cyclogenesis.

## 2.5 Frontal circulation dynamics

The interaction of mesoscale convection and frontogenesis is dealt with using the thermodynamical equation and frontogenetical function (Peng and Fang 2004). The results show that the outbreak of the severe storm is closely related to the local frontogenesis. In fact, the interaction between the shearing instability of the low-level jet (LLJ) and the topographic forcing generates an gravity-inertia wave as well as local frontogenesis ( the first front), which

consequently induce the onset of the severe storm.

Energetics of geostrophic adjustment in rotating flow is examined in detail with a linear shallow water model. The initial unbalanced flow considered first falls under two classes (Fang and Wu 2002). The impact of topography on the geostrophic adjustment process is discussed (Fang and Wu 2005) with a simple two-layer shallow water model, in which the lower-layer fluid is rest initially while the upper-layer is perturbed by the impulsive injection of momentum. During the geostrophic adjustment process of this ideal model, the initial kinetic energy is released and a fraction of it is converted into potential energy of the final geostrophically adjusted state. Thus, after the geostrophic adjustment, the kinetic energy of the system is reduced while the potential energy is enhanced.

By using towing-tank equipments, the lee vortex which is triggered when rotating and stratified flow passes over the large obstacle is investigated (Gao and Ping 2003, 2005). The results show that Froude number is of most importance and that different factors play a vital role in the formation of lee vortex in the non-rotational and rotational cases.

A series of laboratory experiments are carried out (Ping and Gao 2005) by towing-tank equipments to simulate the airflow passing over a large terrain, with focus on the generation and development of lee vortices for the low Froude number density stratified flow passing over an isolated obstacle. It shows that lee vortices can appear in the non-rotational and rotational cases but with different formation mechanisms.

Jing and Lu (2004) studied a heavy rain case caused by interaction between a move-in front and topographical heterogeneities on Taiwan Island.

## 2.6 Wind Helicity Dynamics

The concept of helicity is generalized as shearing wind helicity (SWH). Dynamically, it is found that the average SWH is directly related to the increase of the average cyclonic rotation of the weather system. Physically, it is also pointed out that the SWH, as a matter of fact, is the sum of the torsion terms and the divergence term in the vorticity equation. Thermal wind helicity (TWH), as a derivative of SWH, is also discussed (Han and Wu et al 2006). Xu and Wu (2003) discussed the conservation of helicity in hurricane Andrew (1992) and the formation of the spiral rainband. A simplified helicity equation is derived (Lu and Gao 2006) from the basic momentum equations by dimensional analysis, and the effect factors of helicity variation are discussed.

Furthermore, the characteristics of the horizontal helicity and the vertical helicity are investigated.

### 2.7 Tropical Cyclone Dynamics

Peng et al (2006) discussed the formation of concentric eyewalls with heat sink in a simple tropical cyclone model, the result suggests that thermodynamic adjustments to changes in the heating of a tropical-cyclone-core region may contribute to the formation of the double-eyewall phenomenon.

Duan et al (2005) summarizes the achievement of research in the change in intensity of tropical cyclone made in recent years. It mainly includes (1)the achievements of tropical cyclone genesis and its maximum potential intensity; (2) the effects of gradient of planetary vorticity, environmental uniform flow, vertical shear of environmental flow and the interaction between the outflow of tropical cyclone and environmental flow on the change in intensity of tropical cyclone; (3) the relationship between the change in the structure of tropical cyclone and its intensity variation, particularly in the field of asymmetric structure induced by the environment flow, the application of verifying of the theory of the slant vorticity development and theory of vorticity Rossby wave in the change in tropical cyclone intensity; (4)summarizing the role of the thermal regime of ocean and sea spray on the change in intensity of tropical cyclone.

Lu and Kang et al (2004) discussed the dynamic feature of mixed vortex Rossby-gravity inertia waves in a simulated hurricane. On one hand, positive (negative) geopotential height perturbations mainly correspond to negative (positive) vorticity perturbation and anticyclonic (cyclonic) circulation in the inner region within the eye wall, which are the characteristics of the vortex Rossby waves. However, such a relationship is not applicable outside the region. On the other hand, this kind of waves has obviously non-gradient winds and strong convergence/divergence, resulting in intensified geopotential motion, which is one of the features of the gravity inertia waves. The azimuthal propagation velocity of the waves is about 30 m/s, which is between theoretical vortex Rossby wave velocity and gravity inertia wave velocity. According to those features, we call such mesoscale wave in the hurricane as mixed vortex Rossby-gravity inertia waves.

A model is proposed (Xiang and Wu 2005) relating a variety of factors of tropical cyclones (TCs) to their tracks, and attentions are paid to the influence of the asymmetric wind structures of TCs. Ideal numerical calculation shows that the asymmetric wind structures of TCs have

conspicuous influence on their motion tracks.

The evolution of tropical cyclone Bilis(2000) from a very weak depression into tropical storm and it is found in the typhoon simulation(Xu and Wu 2005) that the evolution of asymmetric momentum in the low level and its transformation to symmetric momentum play an important role in the genesis of Bilis.

A limited-area primitive equation model (Duan and Wu et al 2004) is used to study the role of the  $\beta$ -effect and a uniform current on tropical cyclone (TC) intensity. It is found that TC intensity is reduced in a non-quiet environment compared with the case of no uniform current. On an f-plane, the rate of intensification of a tropical cyclone is larger than that of the uniform flow. A TC on a  $\beta$ -plane intensifies slower than one on an f-plane.

Xu et al (2003) discussed the effects of cold surges from southern hemisphere on tropical cyclone formation.

### 3 The heavy rain dynamics

A heavy rainfall event, mainly caused by the successive mesoscale convective systems (MCSs) along the Meiyu front(Liao and Tan 2005). There were four different vertical circulations within the Meiyu front, which were important for the interactions among the different scales weather systems in both the upper- and lower-levels. These vertical circulations possessed the different structures and dynamic roles at different rainfall stages.

Zhang et al (2004) analyzed the three types of heavy rain associated with the Meiyu front. Li et al (2005) did the comparative studies of three types of heavy rainstorms associated with the Meiyu front by numerical simulations.

Long et al (2004) did the numerical simulation and analysis for Meiyu front rainstorm and the low vortex with shear line.

Dong et al (2004) diagnostically studied the mesoscale lows on Meiyu front and associated heavy rainfall.

Improved research on Meiyu front system includes the followings:

The concept of a dew-point front is introduced (Zhou et al 2004), and forms the Meiyu front system (MYFS) with the Meiyu front. Through a diagnostic study of their formation and structures, it is found that strong ascending motion in the passageway between the two fronts is surrounded by subsidence, and that the convergence and deformation of the horizontal wind are

important factors responsible for both the formation and development of the Meiyu front system.

Further study (Cui et al 2005) discusses the physical mechanism of the formation of the bimodal distribution. It is found that atmospheric moisture gradients, as well as temperature gradients, mainly contributed to the variation of atmospheric potential temperature gradients, and thus variations of the Meiyu front system.

#### 4. Moist atmosphere dynamics

Considering that the condensed liquid water will partially drop out of the air parcel after an infinitesimal perturbation (Liu and Gao 2003), a new form of Brunt-Vaisala frequency  $N_m^2$  with the mixing ratio of saturated vapor  $\theta_e$  is derived and discussed. So is a refined equivalent potential temperature.

The moist potential vorticity equation is derived (Cui et al 2003) from complete atmospheric equations including the effect of mass forcing, with which the theory of Up-sliding Slantwise Vorticity Development (USVD) is proposed based on the theory of Slantwise Vorticity Development (SVD). Several numerical simulations, such a torrential rain event in the Changjiang-Huaihe Meiyu front and a frontal cyclogenesis over the Western Atlantic Ocean, are performed and they all show the applicability and importance of USVD in the development and movement of these synoptic systems.

The impacts of cloud-induced mass forcing on the development of the moist potential vorticity (MPV) anomaly associated with torrential rains are investigated (Gao et al 2004), and show a positive tendency for MPV anomaly. It may be used to track the propagation of rain systems for operational applications.

The condensation probability function is originally introduced (Gao et al 2005) into the thermodynamic framework with  $(q/q_s)^k$ . The generalized moist potential vorticity (GMPV) is thus defined and its tendency equation is derived. (Gao et al 2004) A series of the dynamical properties of GMPV are applied to the operational nowcasting. Using its indicative sense to hot and humid weather, hot and humid weather in Beijing city in summer can be identified and predicted in a short time.

Moist ( $\vec{\zeta} \times \nabla q_v / \rho$ , MVV) and dynamic ( $\vec{\zeta} \times \vec{V} / \rho$ , DVV) vorticity vectors are introduced (Gao et al 2004; Gao et al 2005) to study 2-D tropical convection. It is found that the vertical

component of the MVV and both zonal and vertical component of DVV are closely associated with tropical convection. With the derived tendency equations for the MVV and DVV, the mechanisms of these two new vectors are discussed and their potential applications to operational dynamic nowcasting have been studied. These are all studied for the first time around the world.

The contribution of both the moisture sinks and the cloud sinks to the surface rain rate are examined (Gao et al 2005), using a cloud-resolving model and it is found that such partition of the surface rain rate into the moisture and cloud processes could have many potential applications.

The features of Gregory cumulus parameterization scheme are researched (Ping et al 2003), and then this scheme is developed and improved according to the characteristics of area precipitation over China. The improvements include (i) the full estimation of the effects of the large-scale convergence in the lower layer upon cumulus convection, (ii) the revision of the initial convective mass flux, and (iii) the regulation of convective-scale down draft.

## 5、 Summary

The advances in mesoscale meteorology during the past four years are reviewed. The major progresses in theoretical studies include a) Dynamic mechanism of mesoscale circulation; b) The heavy rain dynamics; c) Moist atmosphere dynamics. On the dynamic mechanism of mesoscale circulation, the followings are summarized: equilibrium dynamical problems, non-equilibrium dynamical problems, the feature and energetic analysis of characteristic wave on mesoscale motion, mesoscale dynamics of Ekman layer, frontal circulation dynamics, wind helicity dynamics and tropical cyclone dynamics. Through the research of heavy rain dynamics and moist atmosphere dynamics, the possible mechanism for the formation and development of a meso- $\beta$  rainstorm system is proposed. The above studies give important explanation to revealing the developing mechanism of mesoscale circulation in the east Asia atmospheric circulation background. We believe that mesoscale meteorological research has a positive future in China, with great progress of modern atmospheric sounding technology and computer technology and the rapid increase of available observational data.

Acknowledgments. The authors wish to thank Prof. Wu for his constructive suggestion. This work was supported by the National Nature Science Foundation of China (Grant No.40575022.....)

**Reference:**

- [1] Bennetts, D, A., and B. J. Hoskins, 1979: Conditional symmetric instability-A possible explanation for frontal rain bands. *Quart. J. Roy. Meteor. Soc.*, 105, 945-962.
- [2] Bennetts, D, A., and J. C. Sharp, 1982: The relevance of conditional symmetric instability to the prediction of mesoscale frontal rainbands. *Quart. J. Roy. Meteor. Soc.*, 108, 595-602.
- [3] Bennetts, D, A., and P. Ryder, 1984: A study of mesoscale convective bands behind cold fronts. Part I: Mesoscale organization. *Quart. J. Roy. Meteor. Soc.*, 110, 121-145.
- [4] Bennetts, D, A., and J. R. Grant et al, 1988: An introductory review of fronts. Part I: Theory and observations. *Meteor. Mag.*, 117, 357-370.
- [5] Bosart L. 1984: An overview of physical processes associated with coastal frontogenesis. *Dynamics of Mesoscale Weather Systems*, 293-231.
- [6] Browning K A et al, 1974: Structure and mechanism of precipitation and effect of orography in a wintertime warm-sector. *Quart. J. Roy. Meteor. Soc.*, 100, 309-330.
- [7] Browning K A ,1989: The mesoscale data base and its use in mesoscale forecasting. *Quart. J. Roy. Meteor. Soc.*, 115(488), 717-762.
- [8] Byrd, G. P., 1989: A composite analysis of winter season overrunning precipitation bands over the Southern Plains of the United States. *J. Atmos. Sci.*, 46, 1119-1132.
- [9] Cheng Yanhong, and Lu Hancheng, 2004: The difference of influence of dry and moist convection on circumstance[J]. *Journal of Tropical Meteorology*, 6, 146-152. (in Chinese)
- [10] Cheng Yanhong, and Lu Hancheng, 2006: The evolution and circulation feature of convective-symmetric instability[J]. *Journal of Tropical Meteorology*, 3, 47-52. (in Chinese)
- [11] Cheng Yanhong, and Lu Hancheng, 2006: The interaction between forced and unstable convection[J]. *Chinese Journal of Atmospheric Sciences*, 4, 609-618. (in Chinese)
- [12] Cui Xiaopeng, and Wu Guoxiong et al, 2003: An experiment study of frontal cyclones over the western atlantic ocean. *Acta Meteorologica Sinica*, 17(3), 321-336. (in Chinese)
- [13] Cui Xiaopeng, and Gao Shouting et al, 2003: Moist Potential Vorticity and Up-Sliding Slantwise Vorticity Development. *Chin. Phys. Lett.*, 20(1), 167-169 (SCI). (in Chinese)
- [14] Cui Xiaopeng, and Gao Shouting et al, 2003: Up-sliding slabwise vorticity development and the complete vorticity equation with mass forcing. *Advances in Atmospheric Sciences*, 20(5), 825-836 (SCIE).
- [15] Cui Xiaopeng, and Gao Shouting et al, 2005: Physical mechanism of formation of the bimodal structure in the

- Meiyu front system. *Chin.Phys.Lett* , 22 (12), 3218-3220 (SCI) (in Chinese)
- [16]Dong Peiming, and Zhao Shixiong, 2004: A diagnostic study of mesoscale lows (disturbances) on Meiyu front and associated heavy rainfall[J]. *Chinese Journal of Atmospheric Sciences*, 6,876-891. (in Chinese)
- [17]Duan Yihong, and Wu Rongsheng et al, 2004: The role of  $\beta$ -effect and a uniform current on tropical cyclone intensity [J]. *Advances in Atmospheric Sciences*, 1, 77-88. (in Chinese)
- [18]Duan Yihong, and Yu Hui et al, 2005: Review of the research in the intensity change of tropical cyclone. *Acta Meteorologica Sinica*, 5, 636-645. (in Chinese)
- [19]Eliassen, A., 1962: On the vertical circulation in frontal zones. *Geofys. Publ.*, 24, 147-160.
- [20]Emanuel, K, A., 1979: Inertial instability and mesoscale convective systems. Part I: Linear theory of inertial instability in rotating viscous fluids. *J. Atmos. Sci.*, 36, 2425-2449.
- [21]Emanuel, K, A., 1982: Inertial instability and mesoscale convective systems. Part II: Symmetric CISK in a baroclinic flow. *J. Atmos. Sci.*, 39, 1080-1098.
- [22]Emanuel, K, A., 1983a: The lagrangian parcel dynamics of moist symmetric instability. *J. Atmos. Sci.*, 40, 2368-2376.
- [23]Emanuel, K, A., 1983b: On assessing local conditional symmetric instability from atmospheric soundings. *Mon. Wea. Rev.*, 111, 2016-2033.
- [24]Emanuel, K, A., 1985: Comments on “inertial instability and mesoscale convective systems. Part I”. *J. Atmos. Sci.*, 42, 747-752.
- [25]Fang Juan, and Wu Rongsheng et al, 2005: Topographic effect on the energetics of geostrophic adjustment[J]. *Acta Meteorologica Sinica*, 1, 19-30. (in Chinese)
- [26]Fei Jianfang and Lu Hancheng et al, 1996: Study on instability in baroclinic vortex symmetric disturbance under effect of nonuniform environment parameters. *Advances in Atmospheric Sciences*,13(4),471-488. (in Chinese)
- [27]Gao Shouting and Ping Fan, 2003: Laboratory studies of the stratified rotating flow passing over an isolated obstacle. *Chin.Phys.Lett.*, 20(7), 1094-1097 (SCI). (in Chinese)
- [28]Gao Shouting, and Ran Lingkun,2003: 重力波上传破碎对中层纬向平均流拖曳的参数化方案. *Chinese Science Bulletin*, 48(7),726-729. (in Chinese)
- [29]Gao Shouting and Ran Lingkun, 2003: On the parameterization scheme of gravity wave drag effect on the mean zonal flow of mesosphere. *Chinese Science Bulletin*, 48(10), 1020-1023 (SCI). (in Chinese)
- [30]Gao Shouting, and Zhao Sixiong, 2003: Progress of research on sub-synoptic scale and mesoscale torrential

- rain systems. *Chinese Journal of Atmospheric Sciences*, 27(4), 618-627. (in Chinese)
- [31]Gao Shouting, and Zhang Hengde et al, 2004: Ageostrophic generalized E-P flux in baroclinic atmosphere. *Chin.Phys.Lett.*, 21(3), 576-579 (SCI). (in Chinese)
- [32]Gao Shouting, and Zhou Yushu et al, 2004: Impacts of cloud-induced mass forcing on the development of moist potential vorticity anomaly during torrential rains. *Advances in Atmospheric Sciences*, 21(6), 923-927 (SCIE).
- [33]Gao Shouting, and Zhou Yushu et al, 2005: Analyses of hot and humid weather in Beijing city in summer and its dynamical identification. *Science in China Ser. D Earth Sciences*, 48(Supp. II), 128-137. (in Chinese)
- [34]Gao Shouting, and Ping Fan, 2005: An experiment study of lee vortex with large topography forcing. *Chinese Science Bulletin*, 50(3), 248-255(SCI). (in Chinese)
- [35]Gao Shouting, and Ping Fan et al, 2006: Tropical heat\water vapor quasi-equilibrium and cycle as simulated in a 2D cloud-resolving model. *Atmospheric Research*, 79, 15-29 (SCI). (in Chinese)
- [36]Gao Shouting, and Ping Fan et al, 2006: Cloud microphysical processes associated with the diurnal variations of tropical convection: A 2D cloud resolving modeling study. *Meteorol. Atmos. Phys.*, 91(1), 9-16 (SCI). (in Chinese)
- [37]Gao Shouting et al, 2004: Generation of generalized moist potential vorticity in a frictionless and moist adiabatic flow. *Geophys. Res. Lett.*, 31, L12113,doi:10.1029/2003GL019152 (SCI). (in Chinese)
- [38]Gao Shouting et al, 2004: A convective vorticity vector associated with tropical convection: A twodimensional cloud-resolving modeling study. *J. Geophys. Res.*, 109, D14106, doi: 10.1029/2004JD004807 (SCI). (in Chinese)
- [39]Gao Shouting et al, 2005: Surface rainfall processes as simulated in a cloud-resolving model, *J. Geophys. Res.*, 110, D10202, doi:10.1029/2004JD005467 (SCI). (in Chinese)
- [40]Gao Shouting et al, 2005: A modeling study of moist and dynamic vorticity vectors associated with two-dimensional tropical convection. *J. Geophys. Res.*, 110, D17104, doi:10.1029/2004JD005675 (SCI). (in Chinese)
- [41]Han Ying, and Wu Rongsheng et al, 2006: Shearing wind helicity and thermal wind helicity[J]. *Advances in Atmospheric Sciences*, 4, 20-28. (in Chinese)
- [42]Hoskins, B. J., 1971: Atmospheric frontogenesis models, some solutions. *Quart. J. Roy. Meteor. Soc.*, 97, 139-153.
- [43]Hoskins, B. J., 1974: The role of potential vorticity in symmetric stability and instability. *Quart. J. Roy. Meteor.*

- Soc.*, 100, 480-482.
- [44]Hoskins, B. J., M. E. McIntyre, and A. W. Robertson, 1985: On the use and significance of isentropic potential vorticity maps. *Quart. J. Roy. Meteor. Soc.*, 111, 877-946.
- [45]Hu Bowei, 2005: Evolution and propagation of MCSs over meiyu fronts and inertia-gravitational wave-CISK related to “low-level moisture frontal zone”. *Chinese Journal of Atmospheric Science*, 6, 845-853. (in Chinese)
- [46]Huang Yong, and Zhang Xiaofang et al, 2006: Diagnosis of a heavy rain by use of average storm –relative helicity. *Scientia Meteorologica Sinica*, 2, 57-62. (in Chinese)
- [47]Jing Li, and Lu Hancheng et al, 2004: The effects of front and topography on the heavy rain Taiwan[J].*Scientia Meteorologica Sinica*, 1, 35-44. (in Chinese)
- [48]Jing Li, and Lu Hancheng et al, 2004: A Mesoscale Analysis of Heavy Rain Caused by Frontal and Topographical Heterogeneities on Taiwan Island [J]. *Advances in Atmospheric Sciences*, 6, 75-88. (in Chinese)
- [49]Kou Zheng, and Lu Hancheng et al, 2004: The numerical study on the relation between symmetrical instability and the scale of initial disturbance[J]. *Journal of Tropical Meteorology*, 1,82-90. (in Chinese)
- [50]Kou Zheng, and Lu Hancheng et al, 2004: Evolution of symmetrically unstable mesoscale circulation under the interactions between waves and basic flows[J].*Journal of Tropical Meteorology*, 3,66-78. (in Chinese)
- [51]Kou Zheng, and Lu Hancheng, 2005: The nonlinear convective-symmetric instability during the development of mesoscale convective system[J]. *Chinese Journal of Atmospheric Sciences*, 4,636-644. (in Chinese)
- [52]Li Bo and Pei Lei et al, 2003: Diagnosing the hurricane Andrew in the whole developing course by MPV[J], *Journal of PLA University of Science and Technology(Natural Science)*, 6,86-91. (in Chinese)
- [53]Li Hongjin, and Lu Hancheng et al, 2003: Transverse wave instability of circular vortex atmosphere[J]. *Chinese Journal of Atmospheric Sciences*, 5,909-919. (in Chinese)
- [54]Liu Dong, and Gao Shouting, 2003: The Brunt-Vaisala frequency in a saturated atmosphere and the revised equivalent potential temperature. *Acta Meteorologica Sinica*, 61(3),379-383. (in Chinese)
- [55]Liao Jie, and Tan Zhemin, 2005: Numerical simulation of a heavy rainfall event along the Meiyu front: influences of different scale weather systems. *Acta Meteorologica Sinica*, 5, 771-788. (in Chinese)
- [56]Lu Hancheng, and Zhong Ke et al, 2001: Mesoscale characters of the 1992 hurricane Andrew [J]. *Chinese Journal of Atmospheric Sciences*,6, 827-836. (in Chinese)
- [57]Lu Hancheng, and Zhong Ke et al, 2002: A possible developing mechanism of the slantwise updraft in the eyewall of the 1992 hurricane Andrew-nonlinear convective and symmetrical instability[J].*Chinese Journal of Atmospheric Sciences*,1, 83-90. (in Chinese)

- [58]Lu Hancheng, and Kou Zheng et al, 2004: Some problems of unbalanced dynamics in the development of the mesoscale convective system [J]. *Scientia Meteorologica Sinica*, 1,120-126. (in Chinese)
- [59]Lu Hancheng, and Kang Jianwei et al, 2004: Dynamical characteristics of mesoscale mixed-waves in cyclones[J]. *Progress in Nature Science*, 5, 63-68+124. (in Chinese)
- [60]Lu Hancheng, and Yang Guoxiang, 2004: The theory and forecasting of the meso-scale weather. *China Meteorological Press*. (in Chinese)
- [61]Li Kun, and Xu Youping et al, 2005: Comparative Studies of Three Types of Heavy Rainstorms Associated with the Meiyu Front by Numerical Simulations[J]. *Chinese Journal of Atmospheric Sciences*, 2,236-248. (in Chinese)
- [62]Lu Huijuan, and Gao Shouting, 2006: On the helicity and the helicity equation. *Acta Meteorologica Sinica*, 6, 684-691. (in Chinese)
- [63]Ping Fan, and Gao Shouting et al, 2003: A Comparative Study of the Numerical Simulation of the 1998 Summer Flood in China by Two Kinds of Cumulus Convective Parameterized Methods. *Advances in Atmospheric Sciences*, 20(1), 149-157 (SCIE).
- [64]Ping Fan, and Gao Shouting et al, 2003: An Improvement of the Mass Flux Convection Parameterization Scheme and its Sensitivity Tests for Seasonal Prediction over China. *Advances in Atmospheric Sciences*, 20(6), 978-990.(in Chinese)
- [65]Ping Fan, and Gao Shouting et al, 2003: The development and improvement of cumulus parametrization scheme and its application in season climate prediction model. *Chinese Science Bulletin*, 48(7),708-717. (in Chinese)
- [66]Peng Jiayi, and Wu Rongsheng et al, 2002: Initiation mechanism of meso- $\beta$  scale convective systems[J]. *Advances in Atmospheric Sciences*, 5,108-122. (in Chinese)
- [67]Ping Fan, and Gao Shouting et al, 2003: Development and improvement of mass flux convection parameterization scheme and its applications in the seasonal climate prediction model. *Chinese Science Bulletin*, 48(10), 1006-1015 (SCI). (in Chinese)
- [68]Peng Jiayi, and Fang Juan et al, 2004: Interaction of mesoscale convection and frontogenesis[J]. *Advances in Atmospheric Sciences*, 5,141-150. (in Chinese)
- [69]Ping Fan and Gao Shouting, 2004: Study on the chosen parameterized schemes of cumulus convection and the test of their simulated effects in the short-term climate. *Journal of the Graduate School of the Chinese Academy of Science*, 21(3), 366-373. (in Chinese)

- [70]Ping Fan and Gao Shouting, 2005: Laboratory studies of low vortices in a low Froude number flow pasting over an isolated obstacle. *Chin. Phys. Lett.*, 22 (1), 150-153 (SCI). (in Chinese)
- [71]Ran Lingkun, and Gao Shouting, 2004: Ageostrophic theory of zonal flow acceleration and wave-activity conservation law. *Acta Meteorologica sinica.*, 18(1), 87-94. (in Chinese)
- [72]Ran Lingkun, and Gao Shouting et al, 2004: Effect of a new Eliassen-Palm Flux on barotropic Basic flow. *Chin. Phys. Lett.*, 21(5), 980-982 (SCI). (in Chinese)
- [73]Ran Lingkun, and Gao Shouting et al, 2005: Relation between acceleration of basic zonal flow and EP flux in the upper-level jet stream region. *Chinese Journal of Atmospheric Sciences*, 29(3), 409-416. (in Chinese)
- [74]Ran Lingkun, and Gao Shouting et al, 2005: Relation between acceleration of zonal basic flow and EP flux in the upper-level jet stream region. *Chinese Journal of Atmospheric Sciences*, 29(4), 417-425. (in Chinese)
- [75]Ran Lingkun, and Gao Shouting et al, 2005: Propagation of low frequency Rossby wave with divergent wind. *Acta Meteorologica Sinica*, 63(1), 13-20. (in Chinese)
- [76]Reuter, G. W., and N. Aktary, 1993: A slantwise Showalter index based on moist symmetric instability: Results for central Alberta. *Atmos.-Ocean.*, 31, 379-394.
- [77]Seltzer, M., R. E. Passarelli, and K. A. Emanuel, 1985: The possible role symmetric instability in the formation of precipitation bands. *J. Atmos. Sci.*, 42, 2207-2219.
- [78]Seman, C. J., 1991: Numerical study of nonlinear convective-symmetric instability in a rotating baroclinic atmosphere. *Ph. D. dissertation, 185 pp.* [Available from University of Wisconsin-Madison, Dept. of Atmospheric and Oceanic Sciences, Madison, WI 53706.]
- [79]Seman, C. J., 1994: A numerical study of nonlinear nonhydrostatic conditional symmetric instability in a convectively unstable atmosphere. *J. Atmos. Sci.*, 51, 1352-1371.
- [80]Shen Xinyong, and Ni Yunqi et al, 2005: A possible mechanism of the genesis and development of meso- $\beta$  rainstorm system Part I. Phase velocity of vortex Rossby waves. *Chinese Journal of Atmospheric Sciences*, 5,727-733. (in Chinese)
- [81]Shen Xinyong, and Ni Yunqi et al, 2005: A possible mechanism of the genesis and development of meso- $\beta$  rainstorm system Part II. Formation of vortex Rossby waves[J].*Chinese Journal of Atmospheric Sciences*, 6,854-863. (in Chinese)
- [82]Shen Xinyong, and Ding Yihui et al, 2006: Properties and stability of a meso-scale line-form disturbance[J]. *Advances in Atmospheric Sciences*, 2,120-128. (in Chinese)
- [83]Shi Lianjun, and Zhang Lifeng, 2002: The distribution of instability growing rate of  $\beta$  meso-scalep[J]. *Scientia*

- Meteorologica Sinica*, 3,23-28. (in Chinese)
- [84]Tan Zhemin, and Fang Juan et al, 2005: Ekman Boundary layer dynamic theories. *Acta Meteorologica Sinica*, 5, 543-555. (in Chinese)
- [85]Tan Zhemin, and Fang Juan et al, 2006: Nonlinear Ekman layer theories and their applications[J]. *Acta Meteorologica Sinica*, 2, 83-96. (in Chinese)
- [86]Tang Xiaodong, and Tan Zhemin, 2006: Boundary-layer wind structure in a landfalling tropical cyclone[J]. *Advances in Atmospheric Sciences*, 5,81-93. (in Chinese)
- [87]Thorpe, A. J. Emanuel, 1985: Frontogenesis in the presence of small stability to slantwise convection. *J. Atmos. Sci.*, 42, 1809-1824.
- [88]Wang Chunming, and Wang Yuan et al, 2004: The effect of model horizontal resolution on quantitative precipitation forecast for Meiyu front torrential rainfall. *Journal of Hydrodynamics*, 1, 74-83. (in Chinese)
- [89]Wu Rongsheng, 2002: Atmospheric Dynamics. *China Higher Educational Press*. (in Chinese)
- [90]Xiang Jie, and Wu Rongsheng, 2005: The effect of asymmetric wind structures of tropical cyclones on their tracks[J]. *Acta Meteorologica Sinica*, 1, 52-59. (in Chinese)
- [91]Xu, Q., 1989b: Frontal circulation in the presence of small viscous moist symmetric stability and weak forcing. *Quart. J. Roy. Meteor. Soc.*, 115, 1325-1353.
- [92]Xu Yamei, and Wu Rongsheng, 2003: The effects of cold surges from southern hemisphere on tropical cyclone formation. *Acta Meteorologica Sinica*, 5, 540-547.
- [93]Xu Yamei, and Wu Rongsheng, 2003: The conservation of helicity in hurricane Andrew (1992) and the formation of the spiral rainband[J]. *Advances in Atmospheric Sciences*, 6, 94-104. (in Chinese)
- [94]Xu Yamei, and Wu Rongsheng, 2005: The numerical simulation of the genesis of tropical cyclone Bilis (2000): The evolution and transformation of asymmetric momentum. *Chinese Journal of Atmospheric Sciences*, 1, 79-90. (in Chinese)
- [95]Yuan Xian, and Tan Zhemin, 2004: Influence of friction and nonlinear on the initial baroclinic perturbation development[J]. *Chinese Journal of Atmospheric Sciences*, 6,48-64. (in Chinese)
- [96]Zhang Min, and Deng Bing, 2005: A numerical study of instability of the mesoscale perturbation[J]. *Chinese Journal of Atmospheric Sciences*, 2, 249-258. (in Chinese)
- [97]Zhang Lifeng, and Shi Lianjun, 2004: Characteristic wave of meso- $\beta$  scale disturbance in shear basic flow[J]. *Chinese Journal of Atmospheric Sciences*, 4,589-600. (in Chinese)
- [98]Zhang Lifeng, and Shi Lianjun, 2004: Instability structure of meso- $\beta$  scale disturbance[J], *Chinese Journal of*

*Atmospheric Sciences*, 6,931-940. (in Chinese)

[99]Zhong Wei ,and Lu Hancheng, 2004: Storms severity index of severe convective weather in the middle and lower tropospheric jet[J]. *Journal of PLA University of Science and Technology(Natural Science)*, 6, 68-71. (in Chinese)

[100]Zhou Xiaoping, and Lu Hancheng et al, 2004: A review of major progress in mesoscale dynamic research in China since 1999.*Advances in Atmospheric Sciences*, vol(21),3, 497-504. (in Chinese)

[101]Zhou Yushu, and Gao Shouting et al, 2004: A diagnostic study of formation and structures of the Meiyu front system over East Asia. *Journal of the Meteorological Society of Japan*, 82(6), 1565-1576 (SCI). (in Chinese)

# PROGRESSES IN PREDICTABILITY STUDIES IN CHINA (2003-2006)

*Duan Wansuo, Xu Hui*

LASG, Institute of Atmospheric Physics

Chinese Academy of Sciences, Beijing 100029, China

E-mail: duanws@lasg.iap.ac.cn, Tel: 86-010-82995302, Fax: 86010-82995172.

**Abstract** Since the last International Union of Geodesy and Geophysics (IUGG) General Assembly (2003), the predictability studies in China have made progresses. In this paper, we review these progresses. In dynamical forecast, two novel approaches of conditional nonlinear optimal perturbation and nonlinear local Lyapunov exponent were proposed to attack the predictability problems of weather and climate and shown to be superior to the corresponding linear theory. A possible mechanism of "spring predictability barrier" phenomenon for ENSO was provided based on a theoretical model. To improve the forecast skill of an intermediate coupled ENSO model, a new initialization scheme was developed, and the hindcast experiments showed its applicability. By using the reconstruction phase space theory and the spatio-temporal series predictive method, Chinese scientists also proposed a new approach to improving the dynamical extended range (monthly) prediction and successfully applied it to the monthly scale predictability of short-term climate variation. In the statistical forecast, it was obtained that the effects of SST on precipitation in China have obvious spatial and temporal distribution features, and that summer precipitation patterns over East China are closely related to the northern atmospheric circulation. And in ensemble forecast, a new initial perturbation method for ensemble forecast was given and then used to the mesoscale heavy rain forecast. In the heavy rain cases of Guangdong and Fujian Provinces on June 8, 1998, this new method showed itself the applicability. Besides, the ensemble forecast approach was also used to the prediction of tropical Typhoon. For downscaling forecast, to improving the prediction of the monthly mean precipitation, a new downscale model consisting of dynamical and statistical methods was provided. By comparing its hindcast results with those of the issued operational forecast, this new downscaling model showed itself a relatively high score.

**Keywords** predictability, prediction, perturbation, weather, climate

## 1. Introduction

Predictability is a fundamental issue in both atmospheric and oceanic research and numerical weather and climate predictions. The studies on predictability have received considerable attention in recent decades due to the pioneering work of the atmospheric scientist Lorenz in the early 1960s (Lorenz, 1962; 1963; 1965; 1969).

One of the great efforts is the exploration of the fundamental limits to predictability (Smith et al., 1999). The predictability of a system is strongly dependent on its stability properties (Smith et al., 1999; Moore and Kleeman, 1996). If the system is particularly unstable, any initial uncertainty that projects significantly onto one of these instability will severely limit the skill of an

initial-value forecast. Lorenz (1975) showed that the extreme sensitivity of weather predictions to initial conditions means that detailed forecasts are, in general, impossible beyond around 2 weeks. This kind of initial-value problem is referred to as the first kind of predictability problem (Lorenz, 1975). In the studies of first kind of predictability problem, the models are usually assumed to be perfect. Generally, the medium-range weather forecasts with an atmosphere model and seasonal forecast with a coupled ocean-atmosphere model are considered to fall in this scenario (Palmer, 1996). The second kind of predictability problem aims to estimate how a given dynamical system responds to a change in some prescribed parameter or external forcing (Lorenz, 1975). The response of El Nino-Southern Oscillation (ENSO) to the stochastic forcing related to MJO, westerly burst events, etc., or of an atmospheric GCM to a prescribed change in SST, are all predictions of the second kind of predictability. Uncertainties in such predictions may arise from the accuracy in the prescribed change itself, or from uncertainties in model formulation. In practice, of course, many forecasts do not fall exclusively into either of these two categories. Even though prediction of the second kind of predictability are, by construction, not sensitive to initial conditions, the underlying instabilities of the flow play an important role in determining the associated predictability.

Both model error and initial uncertainties can cause the prediction error. But it is difficult to identify their respective contribution to the prediction uncertainties when both of them are in activity. Besides, the complexities and the nonlinearities of atmospheric and oceanic motions also limit the exploration of predictability. Nevertheless, within the frame of the two kinds of predictability problems proposed by Lorenz (1975), some studies on predictability have been conducted, which can be grouped into two types: the analysis of the factors and mechanism that cause the forecast uncertainties, and the search for methods and approaches to reducing these uncertainties.

In the predictability studies, three types of approaches have been used. The first is statistical method, which calculates the variance of a time series or the correlation coefficients of the forecast results and observations, or determines the evolution of the difference between two "analogues" states from historical data (Lorenz, 1969), and the second approach is dynamical method and consists of investigating the evolution of the initial errors by numerical model, in which the Lyapunov exponents (Oseledec, 1968) and linear singular vector (LSV) (Lorenz, 1965) are two important methods. The third is the mixture of the statistical and dynamical methods (Lorenz, 1969).

To reduce the prediction errors caused by initial uncertainties, a statistical prediction involving an ensemble of possible projections has become commonplace in weather and climate prediction since Leith in the early 1970s (Leith, 1974). Another effective approach is the variational data assimilation approach, which may be the most effective one in formalizing initial analysis field of model prediction. For the prediction uncertainties caused by model error, multi-models ensemble forecast could be a useful approach (Palmer et al., 2004).

By using the above approaches, scientists obtained many instructive results during the last decades. Lorenz (1962; 1963) discovered the upper limit of about two weeks for weather predictability. Webster and Yang (1992) demonstrated the "spring predictability barrier" (SPB) of ENSO forecast by analyzing the correlation between El Niño and Southern Oscillation. And Samelson and Tziperman (2001) showed the growth-phase predictability barrier of El Niño. Recently, Chen et al. (2004) performed the hindcast experiments and successfully hindcasted two-year SSTA.

Chinese scientists have also made some significant contributions in predictability studies. Chou (1989) used the cell-to-cell mapping theory to obtain the global predictability limit of a system. Li et al. (2000), Li (2000), and Li et al. (2001) demonstrated the dependence of the model predictability time on the machine precision and the model itself. Li (2000) and Li et al. (2001) also provided an optimal numerical integration method of step by step adjustment and made the numerical model achieve the best predictability. Based on the two kind of predictability problems (Lorenz, 1975), Mu et al. (2002) classified three predictability problems in numerical weather and climate prediction including maximum predictability time, maximum prediction error, and maximum allowable initial error. To explore the nonlinearity on predictability, Mu (2000) and Mu and Wang (2001) proposed the concept of nonlinear singular vector and nonlinear singular value. Recently, Chou (2002) and Li and Chou (2003) established the monotonicity principle of predictability.

Since the last International Union of Geodesy and Geophysics (IUGG) General Assembly (2003), four years have passed. During this period, Chinese scientists have further made progresses in the study of predictability. In the rest of this paper, we briefly review these progresses.

## 2. Predictability in dynamical forecast

### 2.1. Theoretical studies

#### 2.2.1 Conditional nonlinear optimal perturbation

LSV is the fastest growing perturbation of a linear model, which has been widely used in predictability studies (Lorenz, 1975). But it is always associated with the sufficiently small initial perturbations (Oortwijn and Barkmeijer, 1995; Mu et al., 2003). Considering this limitation of LSV in revealing the effect of nonlinearity on predictability, Mu (2000) provided an approach of nonlinear singular vector (NSV). Given the information of initial observation, the nonlinear optimal perturbations should be less than an upper bound of initial observational error. However, Mu and Wang (2001) found that there exists local NSVs, which could exceed the upper bound. To overcome this weakness, Mu et al. (2003) further proposed a new approach of conditional nonlinear optimal perturbation (CNOP) to attack the predictability problems (see Fig.1).

CNOP is an initial perturbation whose nonlinear evolution attains the maximal value of a given cost function at prediction time (Mu et al. 2003; Mu and Duan, 2003), where the cost function measures the evolution of initial perturbations in terms of the chosen measurement (for

example, a norm  $\|\cdot\|$ ). Mathematically, it is the global maximum of the cost function. In some cases, there exists local maximum. And the corresponding initial perturbations are called local CNOPs.

The computation of CNOP is related to a nonlinear optimization problem, so it is difficult to solve it analytically. Mu et al.(2003), Duan et al. (2004), Mu et al.(2004), and Sun et al. (2005), etc. used some simple models consisting of a set of ordinary differential equations (ODEs) and solved numerically the CNOPs. Some common characteristics of CNOP were found. First, when linear approximation of nonlinear model is not valid, CNOP is significantly different from LSV, and cannot be approximated by LSV. Second, the (global) CNOPs and local CNOPs are all located on the boundary of the domain defined by the given constraint. These characteristics may be intrinsic for CNOPs.

To test the intrinsic properties of CNOPs, Mu and Zhang (2006) employed a two-dimensional quasigeostrophic model, which is a partial differential equations (PDEs), to compute the CNOPs. The results demonstrated that when the initial perturbations were large, or the time periods were long, or both, CNOPs and LSVs showed the remarkable difference. First, LSV stands for the optimal growing direction, while CNOPs represent a kind of initial perturbations that have largest effects on the predictability. That is to say, CNOP is only a "pattern" rather than a "direction" due to the nonlinearity in model. Consequently, when the linearized model is not a good approximation to the corresponding nonlinear model, the CNOPs and the corresponding LSVs are remarkably different for a long time or/and a finite magnitude of initial perturbation. In addition, the differences between CNOPs and LSVs were also shown by investigating the dynamical evolutions. When the initial perturbations are sufficiently small, the evolutions of LSVs and CNOPs are trivially different. With the increasing magnitude of initial perturbations, the differences between the linear and nonlinear evolutions of CNOPs (LSVs) and between the nonlinear evolution of CNOPs and linear evolution of LSVs become more and more considerable. Second, Mu and Zhang (2006) illustrated that the CNOPs of the QG model located the boundary of the constraint. Thus, Mu and Zhang (2006) verified the results of simple models with respect to CNOP by the relatively realistic model. Mu and Zhang (2006) therefore implied the feasibility of CNOP approach in realistic numerical models.

The above researches has demonstrated that the distinct feature of CNOP approach lies in its applicability in revealing the effect of nonlinearity on predictability, which is therefore superior to LSV approach. It is expected that CNOP can be widely used in the studies of atmosphere and ocean sciences. Also, considering the application of LSV to ensemble forecast and target observation, we should also explore the applicability of CNOP approach in these fields.

### 2.1.2 Error growth

As mentioned in introduction, the atmosphere itself is a complex nonlinear system. There exist a lot of limitations in using the linear theory of error growth to study the atmospheric predictability (Lacarra and Talagrand, 1988; Mu, 2000). It is therefore necessary to develop a

nonlinear theory for quantifying error growth. Upon this request, Li et al. (2006) and Ding and Li (2007) introduced a novel concept of nonlinear local Lyapunov exponent (NLLE) (see Fig.2). The NLLE generalized the linear theory of Lyapunov exponents to the nonlinear field. Due to the effect of nonlinearity, the NLLE depends on initial states, initial errors and the time intervals, which is therefore quite different from the global (and local) Lyapunov exponent. These characteristics of the NLLE approach may feature its advantages.

By using the NLLE, Ding and Li (2007) presented a saturation theorem of mean relative growth of initial error (RGIE). That is, for a chaotic system, the mean RGIE will certainly reach a saturation value in a finite time interval. Also, they demonstrated that the average predictability limit of a chaotic system could be quantitatively determined as the time when the mean RGIE reaches its saturation level. To measure the predictability of a given state with certain initial uncertainties, the concept of the local ensemble mean of the NLLE was also given to quantify the local average predictability limit of a chaotic system.

The NLLE was also used by Chen et al. (2006) to investigate the predictability of daily 500 hPa geopotential height field. The results showed that the predictability of daily 500 hPa geopotential height field appears a zonal belt distribution with maximum predictable time around 12 days over the tropics, the second about 8-9 days over the Antarctic, the third about one week over the Arctic and the minimum around 3-4 days in the subtropics and middle latitudes.

Additionally, they demonstrated that the atmospheric predictability varies with the seasons. For most regions in the Northern Hemisphere, the predictability in winter is higher than that in summer.

The NLLE is a new idea for predictability study. There is a mass of work including the theory itself to be awaited for further investigations.

## 2.2 Applications of CNOP to atmosphere predictability

Jiang (2006) used CNOP approach to study the stability and sensitivity of small-scale vortices motions in Jupiter's atmosphere. By a two-layer quasi-geostrophic model and its adjoint model, Jiang (2006) solved the CNOPs related to Jupiter atmospheric motions and compared it to the corresponding LSVs. The results showed that CNOPs can capture the nonlinear characteristics of small-scale vortices motions in Jupiter's atmosphere and showed significant difference from LSVs for large initial perturbations. Besides, in some basic states, local CNOPs were also found. Then it emphasized the effect of nonlinearity on Jupiter atmospheric motion. Jiang (2006) thought that the application of the CNOPs to the theoretical models of small-scale vortex motions in Jupiter's atmosphere may provide the chance for comparing the stability of Jupiter's atmospheric motions and the Earth's atmosphere motions, which then helps us to further understand the law of Earth's atmospheric motions. Even if these works, it is still urgently needed to apply CNOP approach to the studies of Earth's atmospheric predictability.

## 2.3. Applications of CNOP to ENSO forecast

### 2.3.1 The optimal precursors for ENSO

Moore and Kleeman (1996) and Thompson (1998) demonstrated that it is of great significance for improving ENSO predictability to find out the precursors for ENSO events. They have attempted using the LSV approach to identify optimal growing initial pattern for ENSO, that is, the optimal precursors. However, as mentioned above, LSV is of limitations in revealing nonlinearity. Considering this point, Duan et al. (2004) employed CNOP to study the optimal precursors for ENSO events by the couple model of Wang and Fang (1996) (WF96). It was shown that the CNOP of annual cycle evolves into the positive SSTA nonlinearly, which takes a striking resemblance to the development of El Nino and therefore acts as a precursor for El Nino event in WF96 model. Although the corresponding LSV also develops into an El Nino, the intensity is considerably weaker than that of CNOP (see Fig.3). In this sense, CNOP was regarded as the optimal precursor for El Nino by Duan et al. (2004). For the local CNOP of annual cycle, Duan et al. (2004) showed that it acts as the optimal precursor of La Nina event (Fig.4). In addition, Duan et al.(2004) found that when using LSV to study the intensity of ENSO events, the corresponding El Nino and La Nina events in linearized model are of the equal amplitude, or say, the El Nino and La Nina events are symmetric in amplitude (Fig.5) . While in CNOP approach, the El Nino event is obviously stronger than the La Nina event under the condition that the (global) CNOP and local CNOP are of the same large amplitude (Fig.5), which is consistent with the observed ENSO asymmetry after 1976. So they demonstrated that the linear theory of singular vector cannot reveal the nonlinear asymmetry of El Nino and La Nina. It was therefore indicated that ENSO asymmetry may be caused by the nonlinear feedback mechanism of coupled ocean-atmosphere.

The above results involved the ENSO amplitude asymmetry after 1970s. Duan and Mu (2006) further investigated the change of the ENSO amplitudes asymmetry before and after 1970s. They showed that the ENSO asymmetry had become considerable since the famous 1976 climate shift. Along the thinking of how the tropical background field modulates ENSO cycle, Duan and Mu (2006) explored the effect of the climatological basic-state change on the ENSO asymmetry by applying the approach of CNOP in a theoretical coupled model. They reproduced the observed decadal change of ENSO asymmetry qualitatively. Based on the physics described by the model, the mechanism of ENSO asymmetry change on inter-decadal scale was explored by Duan and Mu (2006). They demonstrated that the decadal change of ENSO asymmetry may be induced by the changing nonlinear temperature advection, which is closely related to the decadal change of the tropical background state. Then Duan and Mu (2006) indicated that the decadal change of ENSO asymmetry may result from the combined effect of the changes of the tropical background state and the nonlinearity.

In view of the simplicity of the WF96 model, an intermediate coupled ENSO model of Zebiak and Cane (1987) (CZ model) was also used to investigate the precursors for ENSO (Xu, 2006). The numerical experiments demonstrated that the CNOPs, rather than LSVs, of the climatological basic-state annual cycle acts as the optimal precursors of ENSO, whose configuration of SSTA

and thermocline depth anomaly reveals the fact that the transition phase of thermocline depth displacement leads to the sea surface temperature (SST) variation and supports the results of Duan et al.(2004). Then the results obtained by CZ model further showed the spatial structure of the CNOP and emphasized the locality of optimal precursors for ENSO in space distribution.

### 2.3.2 "Spring predictability barrier" for ENSO events

Considering that many state-of-the-art coupled ocean-atmosphere models have particular difficulty in prediction of ENSO prior to boreal spring and the causes of this spring predictability barrier (SPB) remain controversial and elusive, Mu et al.(2007a) used the above WF96 model to investigate this problem from the point of view of initial error growth associated with ENSO anomalies using CNOP approach. The results showed that the largest growth rate of the CNOP for El Nino occurs during boreal spring during the onset of ENSO warm event, which coincides with the time of the predictability barrier of ENSO models. With increasing magnitudes of CNOPs, the amplitude of spring error growth for El Nino becomes progressively large. Although the largest error growth of El Nino during spring during the onset of ENSO warm is also shown through LSV, the CNOP growth is significantly larger than the corresponding LSV growth for large-amplitude initial perturbations. This has the implication that the nonlinearity plays an important role in error growth of ENSO warm event. Furthermore, Mu et al.(2007a) compared the seasonal variations of the CNOP growth for ENSO events with those of a large ensemble of initial errors chosen randomly from a constrained initial domain. It was demonstrated that not all initial errors tend to induce prominent seasonal variation of error growth, it is the CNOP of El Nino that exhibits the most prominent seasonal variation. But for the La Nina events, even if the initial errors are taken to be of the types of CNOPs, their evolutions do not tend to exhibit the prominent seasonal dependence. Therefore, Mu et al. (2007a) concluded that the seasonal variation of error growth for El Nino may result from the combined effect of the climatological mean state, the El Nino event itself and the initial error, which is different from the viewpoints of the previous studies. The previous studies either emphasized the role of climatological annual cycle (Moore and Kleeman, 1996; Chen et al.,1997), or demonstrated that of El Nino itself (Van Oldenborgh et al., 1999), and did not consider the effect of initial uncertainties. Then Mu et al. (2007a) did not only point out the importance of initial error pattern in SPB, but also emphasized the combined effect of these three factors on SPB.

In addition, Mu et al.(2007b) used CZ model to test the results of WF96 model with respect to SPB. The results supported those of WF96 model. Then they found that the CNOP-type error of SSTA component of El Nino events tends to centralize locally in the equatorial central and eastern Pacific (Fig.6). This indicates that the observation accuracy of this region may be important for reducing uncertainty of ENSO prediction.

It was emphasized that it is CNOP that induces the most prominent predictability barrier of ENSO (Mu et al., 2007a,b). That is to say, if an initial error is not of the type of CNOP, the ENSO prediction may be less uncertain. Therefore, Mu et al.(2007a,b) suggested that if a data

assimilation method or/and target observation could filter this kind of CNOP-type initial errors, ENSO predictability could be improved. Of course, these results were derived from the simple models by investigating the dynamical behavior of initial uncertainties. It is expected that the effect of model uncertainties on SPB will be studied in the future.

#### 2.4. Predictability of seasonal and monthly forecast

In section 2.3.2, the results emphasized the importance of initial uncertainty in ENSO predictability. The following work may also show this point.

Duan and Mu (2005) used a nonlinear optimization method (Mu et al., 2002) to investigate the predictability of a numerical model for El Niño-Southern Oscillation (ENSO). Then a lower bound of maximum predictability time for the model ENSO events, an upper bound of maximum prediction error, and a lower bound of maximum allowable initial error were established based on the model, all of which potentially quantified the predictability of ENSO in adopted model. The numerical results revealed the phenomenon of SPB for the model ENSO event and supported the previous views on SPB.

It had been demonstrated that the ICM developed by Keenlyside and Kleeman (2002) (KK2002) was able to predict ENSO at 6-month lead time with an initialization scheme (Zhang et al., 2003). To further improve the forecast of this ICM, Zheng et al. (2006) developed a new initialization procedure, which was designed by considering both the magnitude of the nudging parameter and the duration of the assimilation and then running the coupled model with SST anomalies nudged to the observations to generate the initial conditions for atmosphere and ocean. Two sets of hindcasts experiments were performed to test the advantage of the initialization. The numerical results demonstrated that the initialization scheme can generate realistic thermal fields and surface dynamic fields in the equatorial Pacific. Then the prediction ability of the KK2002 model was increased beyond that demonstrated by Zhang et al. (2003) (Fig.7). Besides, by an ideal experiment, Zheng et al.(2006) got the optimal nudging parameters that include the nudging intensity and nudging time length. The twelve-month-long hindcast experiments for the periods of 1984-2003 and 1997-2003 further demonstrated the superiority of the new initialization (Fig.7).

In seasonal predictability, the contribution of initial atmospheric conditions to model skill were generally neglected, or the integrations started from several initial atmospheric fields and forced by observational SST lasted for many years (Sugi et al., 1997; Rowell, 1998; Kumar, 2003). Consequently, the corresponding seasonal predictability as well as inter-seasonal predictability differences may be underestimated or indefinite. To explore the effect of initial atmospheric conditions on model forecast skill, Lang and Wang (2005) used the real-time initial atmospheric data to IAP9L-AGCM (9-level global atmospheric general circulation model developed at Institute of Atmospheric Physics, Chinese Academy of Sciences) and investigated the model potential predictability of the seasonal mean climate and its response to the strong SST anomalies (SSTA) signal in both the Niño-3 region and the North Pacific (NP). It followed that there are slightly

inter-seasonal differences in the model potential predictability in the Tropics: in the region with northern middle and high latitudes, the prediction skill of IAP9L-AGCM is low in spring and relatively high either in summer for surface air temperature and middle and upper tropospheric geopotential height or in winter for wind and precipitation. Lang and Wang (2005) also demonstrated that in different regions, the prediction skill of the model is also in different. Generally, the model prediction skill rises notably in western China, especially in northwestern China, when SSTA signals in the Nino-3 region are considerable. Of course, if one predicts summer climate in the other regions of China, the attention should also be paid to the SSTA in the NP.

Besides, in Lang and Wang (2005), a comparison between the results of IAP9L-AGCM and those of Sugi et al. (1997) based on an AMIP-type simulation was performed. It was demonstrated that for the seasonal mean surface air temperature (SAT) over East Asia, the predictability of IAP9L-AGCM is greater than that demonstrated in Sugi et al.(1997). And for the seasonal mean 500hPa geopotential height (H500), the predictability of IAP9L-AGCM in the region with 30°-60°N during Dec-Jan-Feb and in north of 30° during Jun-Jul-Aug is higher than those suggested by Sugi et al. (1997).

Now we review the work on monthly scale predictability. Considering that the zonal mean circulation errors can cause the significant forecast errors in the numerical prediction model (Saha, 1992; Baumhefner, 1996), Chen et al. (2003) developed a new approach to improve the dynamical extended-range (monthly) prediction. Firstly, the monthly pentad-mean nonlinear dynamical regional prediction model of the zonal-mean height field was constituted by employing the reconstruction phase space theory and the spatio-temporal series predictive method. Then the resultant zonal height was transformed to its counterpart in the numerical model and was further used to correct the numerical model prediction during the integration process. Thus, the two different kinds of prediction approaches were combined. The numerical experiments showed that this hybrid approach not only reduced the systematical error of the numerical model, but also improved the forecast of the non-axis symmetric components due to the wave-flow interaction. Then this hybrid approach was used to conduct the forecast experiments of zonal mean flow (Chen et al., 2004). It was shown that for the 12-month forecast experiments of 1996, the results of the nonlinear model are better than those of persistent, climate prediction and T42L9 model either over the high-and mid-latitude areas of the northern and southern hemisphere, or over the tropical area (Fig.8). The monthly-mean height root-mean-square of T42L9 model decreased considerably with a change of 30.4%, 26.6%, 82.6% and 39.4% respectively over the high-and mid-latitude of the Northern Hemisphere, over the high-and mid-latitude of the Southern Hemisphere, over the tropics, and over the Globe. Nevertheless, by nonlinear correction after integration, the corresponding anomaly correlation coefficients over the four areas were respectively increased from 0.306 to 0.312, from 0.304 to 0.429, from 0.739 to 0.746, and from 0.360 to 0.400 (averagely a relative change of 11.0% over the Globe). Therefore, Chen et al.(2004) thought that

the forecasts produced by nonlinear model provides more useful information than those of T42L9 model.

### 3. Predictability in statistical forecast

In climate prediction, many studies demonstrated that the SST change can predetermine the tendency of the climate change and then plays an important role in the prediction of drought and waterlogging (Huang et al., 1999; Chen et al., 2002). However, there are still two issues to be addressed. One is to what extent the SST predetermines the China precipitation, the other is whether there exists some spatio-temporal distribution law of precipitation. To explore these two questions, Yan et al. (2003) investigated the impact of Pacific SST variations on precipitation predictability in China, where the data of monthly precipitation of 160 stations in China and the Pacific SST were used. The results showed that the effects of SST on precipitation have obvious spatial and temporal distribution features. From the point of views of time, the precipitation in April and November could be predicted effectively by using SST. And from the point of views of space, there exists a teleconnection relationship between SST and the precipitation.

The contribution of SST to the precipitation in Northwest China was greater than that in East China.

Based on the data of monthly mean 500 hPa height field and the observation of 160 stations in summer of China from the National Climate Center from 1951-2002, Yan et al. (2006) investigated the relationship between summer rain patterns over East China and the northern atmospheric circulation from January to May by using the composite analysis and multi-variable factors variance. It was found that there is a significant correlation between the spatial and temporal evolution of atmospheric circulation at 500 hPa during the period from January to February and the distribution of rain patterns in rainy season over China. But since spring is the transition season, this kind of correlation is generally not obvious in this season. Even though the distribution of rain patterns in rainy season responds to different previous atmospheric circulation fields, there are still only three key areas which pass the significance test in the previous periods, especially in January and February. Yan et al. (2006) further indicated that the longitude range of westerly index in the key areas is consistent with that of height anomaly field. The 1st and 2nd key areas are respectively located in 150°E-170°E and 100°W-80°W in January and February, which lie respectively in the front of East Asian trough and the backside of North American trough. The 3rd key area lies in 80°W-45°W of the Atlantic Ocean in February. In the significant key areas, the higher (lower) westerly index is usually corresponding to negative (positive) anomaly of height field from January to February. That is to say, if there is higher westerly index around the area of the Atlantic Ocean (80°W-45°W) and the anomaly of height field in the 3rd key area is consistent with the mean of 500 hPa geopotential height, especially in February, the 1st rain pattern will appear in the coming summer. If the westerly index is lower and the anomaly of height field is positive in the 1st key area, and the distributions of westerly index and the anomaly of height field are opposite synchronously in the 2nd key area, the 2nd rain pattern will appear in the coming

summer, and contrariwise, the 3rd rain pattern will appear. These show that there is a close relationship between the westerly index and the rain patterns in rainy season over China too. Therefore, it is valuable to analyze the influence of middle high latitude atmosphere circulation in winter for finding some new prediction clues of the summer precipitation over China.

#### 4. Predictability in ensemble and downscaling forecast

##### 4.1 Ensemble forecast

##### 4.1.1 Convective instability in the atmosphere

With the focus on the convective instability in the atmosphere, Chen et al.(2005) designed a new method to generate initial perturbations for ensemble forecast of mesoscale heavy rain, namely Different Physical Mode Method (DPMM). In Chen et al. (2005), the initial perturbations that reflect the uncertainty of convection instability were generated by DPMM, where the differences between the predictions with the different Cumulus Convective Parameterization (CCP) schemes were used. The methodology and mathematic scheme of DPMM demonstrated by Chen et al.(2005) are as follows. First, the prediction differences of moisture flux divergence at 500 hPa at 12-h prediction are employed to generate the normalized initial perturbation mode; secondly, the observation errors of the atmosphere are used to determine the perturbation amplitude of zonal wind  $u$ , meridional wind  $v$ , and temperature  $T$ ; thirdly, the perturbation of specific humidity  $q$  is calculated by temperature  $T$  and relative humidity  $r$ ; finally, by adding the perturbation value and deducting it from the control initial condition, the initial perturbations can then be generated. By using the above DPMM method, Chen et al. (2005) performed an ensemble forecast experiment with respect to a heavy rain case occurring in Guangdong and Fujian Provinces on 8 June 1998 within the frame of non-hydrostatic MM5. The results showed that the DPMM normalized initial perturbation mode is not evenly distributed with reasonable mesoscale circulation structure. The horizontal structure and scale are similar to those of the atmosphere gravity wave mode. The area of maximum perturbation amplitude appears in the warm and humid air belt associated with the southwest low-level jet on the west side of the western Pacific subtropical high, where the heavy rain mainly occurs according to the previous studies. Different initial perturbations can trigger different convective activities with apparent differences of location and strength of precipitation among ensemble members. The ensemble outputs of 24-h accumulated precipitation, including the ensemble mean, the probability exceeding 50 mm and the spread, showed that the ensemble predictions can obviously improve the controlling prediction by DPMM initial perturbation methods. Both the structures of normalized initial perturbations and ensemble outputs demonstrated that the DPMM can find the convection sensitive area and reflect the prediction uncertainty in the sensitive regions of convection instability.

##### 4.1.2 Typhoon

The application of ensemble forecast (EF) to the problem of tropical cyclone (TC) motion and intensity predictions is still in its infancy and more researches are necessary to establish the viability of the EF technique as an alternative to the traditional deterministic solution in such

predictions (Chan, 2002). Even if such a necessity, there were only few studies in this scenario. A fundamental issue in EF is what method can be used to generate the initial perturbations. Although the breeding of growing modes (BGM) has been tested in TC forecast by Cheung (2001), its effectiveness remains to be ascertained, especially when compared with other dynamic techniques such as the lagged-averaged forecast (LAF). Considering this point, Zhou et al. (2006) investigated the effectiveness of these two different EF techniques in predictability of tropical cyclone by using a baroclinic model. In the BGM experiments, the vortex and the environment were perturbed separately (named BGMV and BGME). TC motions in two difficult situations were studied: a large vortex interacting with its environment, and an apparent binary interaction. The former is Typhoon Yancy and the latter involves Typhoon Ed and super Typhoon Flo, all occurring during the Tropical Cyclone Motion Experiment TCM-90. The adopted model was the baroclinic model of the University of New South Wales. The lateral boundary tendencies were computed from atmospheric analysis data. Only the relative skill of the ensemble forecast mean over the control run was used to evaluate the effectiveness of the EF methods, although the EF technique was also used to quantify forecast uncertainty in some studies. In the case of Yancy, the ensemble mean forecasts of each of the three methodologies were better than that of the control (see Fig.9), with LAF being the best. The mean track of the LAF was close to the best track, and it predicted landfall over Taiwan. The improvements in LAF and the full BGM suggested the importance of combining the perturbation of the vortex and environment when the interaction between the two was appreciable. In the binary interaction case of Ed and Flo (see Fig.10), the forecasts of Ed appeared to be insensitive to perturbations of the environment and/or the vortex, which apparently resulted from erroneous forecasts by the model of the interaction between the subtropical ridge and Ed, as well as from the interaction between the two typhoons, thus reducing the effectiveness of the EF technique. Nevertheless, the forecast tracks in some cases were improved over that of the control. On the other hand, the EF technique had little impact on the forecasts of Flo because the control forecast was already very close to the best track. Based on these results, Zhou et al.(2006) thought that this study may provide a basis for the future development of the EF technique.

#### 4.2 Downscaling forecast

By downscaling method, the small-scale processes in weather forecast such as precipitation and air temperature can be predicted through the large-scale weather system of strong predictability. Two approaches are generally used to perform the downscaling forecast: dynamical and statistical downscaling. The dynamical downscaling has definite physical meaning; although the statistical one is of ambiguous physics, it can be conveniently used (Li and Chen, 1999). Considering these facts of downscaling forecast, Li and Chen (1999) presented a blending method of dynamical and statistical approaches, which established a relationship between monthly precipitation anomaly and monthly circulation. Based on this relationship, Chen et al. (2003) further developed a new downscale model, which combines the dynamical and statistical

downscaling of precipitation forecast. Statistical weights of each item of the relationship (the downscaling model) were derived from the monthly NCEP/NCAR reanalysis data (500hPa) and China's observed precipitation data during the control period from January in 1951 to December in 1991. Then a hindcast test was performed by using the data from January in 1992 to December in 2001. It was demonstrated that the new downscale model has a high score skill for monthly mean precipitation forecast. By using the 500 hPa height forecast obtained from T63/NCC GCM from January to June 2002, Chen et al.(2003) compared the monthly forecast of precipitation amounts between the issued operational forecast and the downscale model. The results demonstrated that the downscale model has a higher forecast score than the issued operational forecast.

## 5. Summary and discussion

In this paper, we review the progresses in predictability studies achieved by Chinese scientists during 2003-2006. The works consist of two parts: theoretical and practical investigations. In the former, Chinese researchers proposed two novel concepts of CNOP and NLLE, then used them to address the effect of nonlinearity on weather and climate predictability. Concerning the practical investigations, they studied the phenomenon of SPB for ENSO and presented a possible mechanism of SPB. Besides, to improve the predictability of some forecast models, new approaches were developed, which include the design of a new initialization scheme of an ICM, the use of the real-time initial atmospheric data in IAP9L-AGCM and of the reconstruction phase space theory and the spatio-temporal series predictive method in a nonlinear dynamical regional prediction model. The relations between SST and the precipitation in China and between summer precipitation pattern and the atmospheric circulation were also explored by the historical observational data. In ensemble forecast studies, a new initial perturbation method was used to the mesoscale heavy rain forecast and its applicability was shown in the hindcast of the heavy rain case of Guangdong and Fujian Provinces on June 8, 1998. Furthermore, the ensemble forecast approach was adopted to investigate the predictability of tropical Typhoon. In downscaling forecast, considering the respective weakness of dynamical and statistical down-scaling, Chinese scientists developed a new downscale model, which is a mixture of dynamical and statistical methods and does not only have definite physical meaning, but also consist of a great deal of historical data. Furthermore, this new downscale model can be conveniently used. In hindcast experiments, it showed a higher score than the issued operational forecast.

It is well known that atmospheric and oceanic motions are very complex. The corresponding numerical models are only a very rough approximation to them, and do not consider sufficiently the "history" and there is a lack of pertinency of the forecast objective. The predictability of weather and climate is therefore limited. Wang (1993) pointed out that although there exist these essential limitations, we should not think that we do not need to develop the numerical models. In contrast, we do not only develop the models, but also consider the applications of the theoretical results in models. In the studies of predictability theories, it is important to understand the

dynamics of uncertainties. Tennekes (1991) proclaimed that no forecast was complete without an estimate of the forecast error. The forecast errors can be caused by initial errors and model errors. In "perfect model scenario", a perfect model is usually assumed. Then the predictability is limited only by the growth of initial uncertainties. However, the practical predictability experiments are often carried out with an imperfect model forecasting observational data. Model error exists in the particular model employed. The predictability quantified by numerical models may under- or over-estimate the inherent predictability. That is to say, the different models may show different predictability due to the model errors.

During the period of 2003-2006, Chinese scientists conducted theoretically many studies on initial uncertainties with the assumption of perfect model. It is therefore expected that the effect of model error on predictability can be involved in future studies. It is hopeful that the combination of theoretical studies and practical applications can help the improvement of forecast skill.

**Acknowledgements.** The authors thank three anonymous reviewers for their valuable comments. This work was jointly sponsored by KZCX3-SW-230 of the Chinese Academy of Sciences, the National Nature Scientific Foundation of China (Nos. 40505013, 40675030), and 973 project (2006CB403606).

#### References

- [1] Baumhefner D. B., 1996: Numerical extended-range prediction: Forecast skill using a low-resolution climate model. *Mon. Rev. Wea.*, 124, 1965-1980.
- [2] Chan, J. C. L., 2002: Ensemble forecasting of tropical cyclones. *WMO Bulletin*, 51, 247C252.
- [3] Chen, Y., D. S. Battisti, T.N. Palmer, J. Barsugli, and E.S. Sarachik, 1997: A study of the predictability of tropical Pacific SST in a coupled atmosphere-Ocean model using singular vector analysis: the role of the annual cycle and the ENSO cycle. *Mon. Wea. Rev.*, 125, 831-845.
- [4] Cheung, K.K.W., 2001: Ensemble forecasting of tropical cyclone motion: comparison between regional bred modes and random perturbations. *Meteorology and Atmospheric Physics*, 78, 23-34.
- [5] Chen Yuejue, Jian Jun, and Zhou Renjun, 2002: Relations between East Asia summer monsoon and ENSO, *Plateu Meteorology (in Chinese)*, 21, 536-545.
- [6] Chen, D., M.A. Cane, A. Kaplan, S.E. Zebiak, and D.J. Huang, 2004: Predictability of El Nino over the past 148 years. *Nature*, 428, 733-736.
- [7] Chen Baohua, Li Jianping, and Ding Ruiqiang, 2006. Nonlinear local Lyapunov Exponent and atmospheric predictability research, *Science in China*, 49(10): 1111-1120.
- [8] Chen Bomin, Ji Liren, Yang Peicai, Zhang Daomin, Wang Geli, 2003: A new approach to improving monthly dynamical extended prediction, *Chinese Science Bulletin (in Chinese)*, 48, 513-520.
- [9] Chen Lijue, Li Weijing, Zhang Peiqun, and Wang Jinggui, 2003: Application of a new downscaling model to monthly precipitation forecast. *Journal of Applied Meteorological Science (in Chinese)*, 14, 648-655.
- [10] Chen Bomin, Ji Liren, Yang Peicai, Zhang Daomin, 2004: Monthly extended prediction experiments with nonlinear regional prediction I: Prediction of zonal mean flow. *Acta Meteorologica Sinica (in Chinese)*, 62, 1-10.
- [11] Chen Jing, Xue Jishan, Yan Hong, 2005: A new initial perturbation method of ensemble mesoscale heavy rain prediction, *Chinese Journal of Atmospheric Sciences (in Chinese)*, 29, 717-726.

- [12] Chou Jifan, 1989: Predictability of the atmosphere. *Adv. Atmos. Sci.*, 6, 335C346.
- [13] Chou Jifan, 2002: Nonlinearity and complexity in atmospheric Sciences (in Chinese). China Meteorology Press, Beijing, 166p.
- [14] Ding Ruiqiang, and Li Jianping, 2007: Nonlinear finite-time Lyapunov exponent and predictability. *Physics Letters A*, 364, 396C400.
- [15] Duan Wansuo, Mu Mu, Bin Wang, 2004: Conditional nonlinear optimal perturbation as the optimal precursors for El Nino-Southern Oscillation events, *J. Geophys. Res.*, 109, D23105, .
- [16] Duan Wansuo, and Mu Mu, 2006: Investigating decadal variability of El Nino-Southern Oscillation asymmetry by conditional nonlinear optimal perturbation, *J. Geophys. Res.*, 111, C07015, doi:10.1029/2005JC003458.
- [17] Duan Wansuo, Mu Mu, 2005: Applications of nonlinear optimization methods to quantifying the predictability the predictability of a numerical model for El Nino-Southern Oscillation, *Progress in Natural Science*, 15, 915-921.
- [18] Huang Ronghui, Xu Yuhong, and Zhou Liantong, 1999: The interdecadal variation of summer precipitations in China and the drought trend in north China. *Plateu Meteorology (in Chinese)*, 18: 465-476.
- [19] Jiang Zhina, 2006: Applications of conditional nonlinear optimal perturbation to the study of the stability and sensitivity of the Jovian atmosphere, 23, 775-783.
- [20] Keenlyside, N., and R. Kleeman, 2002: On the annual cycle of the zonal currents in the equatorial Pacific. *J. Geophys. Res.*, 107, doi: 10.1029/2000JC0007111.
- [21] Kumar, A., 2003: Variability, and predictability of 200-mb seasonal mean heights during summer and winter. *J. Geophys. Res.*, 108, 4169, doi: 10.1029/2002JD002728.
- [22] Lang Xianmei and Wang Huijun, 2005: Seasonal difference of model predictability and the impact of SST in the Pacific. *Adv. Atmos. Sci.*, 22, 103-113.
- [23] Leith C. S., 1974: Theoretical skill of Monte Carlo forecasts. *Mon. Wea. Rev.*, 102, 409-418
- [24] Li Jianping, 2000: Computational uncertainty principle: Meaning and implication. *Bulletin of Chinese Academy of Sciences*, 15, 428C430. (in Chinese)
- [25] Li Jianping, Zeng Qingcun, and Chou Jifan, 2000: Computational uncertainty principle in nonlinear ordinary differential equations. I: Numerical results. *Science in China (Series E)*, 43, 449-460.
- [26] Li Jianping, Zeng Qingcun, and Chou Jifan, 2001b: Computational uncertainty principle in nonlinear ordinary differential equations. II: Theoretical analysis. *Science in China (Series E)*, 44, 55-74.
- [27] Li Jianping, and Chou Jifan, 2003: The global analysis theory of climate system and its applications. *Chinese Science Bulletin*, 48, 1034-1039.
- [28] Li Jianpin, Ding Ruiqiang, and Chen Bohua, 2006: Review and prospect on the predictability study of the atmosphere (in Chinese), Beijing: China Meteorology Press, 96-100.
- [29] Li Weijing, Chen Lijuan, 1999: Research on reexpansion and reanalysis method of dynamical extended range forecast products, *Acta Meteorologic Sinica (in Chinese)*, 57, 338-345.
- [30] Lacarra, J. F. and O. Talagrand, 1988: Short-range evolution of small perturbations in a barotropic model, *Tellus*, 40A, 81-95.
- [31] Lorenz E.N., 1962: The statistical prediction if solution of dynamic equations. *proc. Intern. Symp. Numer. Weather Pred.* Tokyo: Meteorology Society of Japan, 629-635.
- [32] Lorenz E.N., 1963: The predictability of hydrodynamic flow. *Transactions of the New York Academy of Sciences, Series II, Vol.25*, 409-432.
- [33] Lorenz E.N., 1965: A study of the predictability of a 28-variable atmospheric model, *Tellus*, 17, 321-333.
- [34] Lorenz E. N., 1969: Three approaches to atmospheric predictability. *Bulletin of the American Meteorological*

- Society, 50, 345-349.
- [35] Lorenz E.N., 1975: Climate predictability, Appendix 2.1 in GARP Publ. Ser., No.16, WMO Geneva, 265pp.
- [36] Moore, A. M., and R. Kleeman, 1996: The dynamics of error growth and predictability in a coupled model of ENSO, *Q. J. R. meteorol. Soc.*, 122, 1405-1446.
- [37] Mu Mu, 2000: Nonlinear singular vectors and nonlinear singular values, *Science in China (D)*, 43, 375-385.
- [38] Mu Mu, and Wang Jiacheng, 2001: Nonlinear fastest growing perturbation and the first kind of predictability, *Sciences in China (D)*, 44, 1128-1139.
- [39] Mu Mu, Duan Wansuo, Wang Jiacheng, 2002: The predictability problems in numerical weather and climate prediction, *Adv. Atmos. Sci.*, 19, 191-204.
- [40] Mu, Mu, Duan Wansuo, and Wang Bin, 2003: Conditional nonlinear optimal perturbation and its applications, *Nonlinear Processes in Geophysics*, 10, 493-501.
- [41] Mu Mu, and Duan Wansuo, 2003: A new approach to studying ENSO predictability: conditional nonlinear optimal perturbation, *Chinese Sci. Bull.*, 48, 1045-1047.
- [42] Mu Mu, Sun Liang, Henk D.A., 2004: The sensitivity and stability of the ocean's thermohaline circulation to finite amplitude freshwater perturbations, *J. Phys. Oceanogr.*, 34, 2305-2315.
- [43] Mu, Mu, and Zhang Zhiyue, 2006: Conditional nonlinear optimal perturbation of a barotropic model, *J. Atmos. Sci.*, 63: 1587-1604.
- [44] Mu Mu, Duan Wansuo, Wang Bin, 2007a: Season-dependent dynamics of nonlinear optimal error growth and ENSO predictability in a theoretical model, *J. Geophys. Res.*, 112, D10113, doi:10.1029/2005JD006981.
- [45] Mu Mu, Xu Hui, Duan Wansuo, 2007b: A kind of initial errors related to "spring predictability barrier" for El Nino events in Zebiak-Cane model. *Geophys. Res. Lett.*, 34, L03709, doi:10.1029/2006GL027412.
- [46] Oseledec, V. I., 1968: A multiplicative ergodic theorem: Lyapunov characteristic numbers for dynamical systems. *Transl. Moscow. Math. Soc.* 19, 197C231.
- [47] Oortwijn, J., and J. Barkmeijer, 1995: Perturbations that optimally trigger weather regimes, *J. Atmos. Sci.*, 52, 3932-3944.
- [48] Palmer, T.N., F. J. Doblas-Reyes, R. Hagedorn, A. Alessandri, S. Gualdi, U. Andersen, H. Feddersen, P. Cantelaube, J.-M. Terres, M. Davey R. Graham, P. D'el'ecluse, A. Lazar, M. D'equ'e, J.-F. Gu'er'emy, E. Diez, B. Orfila, M. Hoshen, A. P. Morse, N. Keenlyside, M. Latif, E. Maisonave, P. Rogel, V. Marletto, M. C. Thomson, 2004: Development of a European multimodel ensemble system for seasonal-to-interannual prediction (DEMETER), *Bulletin of the American Meteorological Society*, 85, 853-872.
- [49] Palmer T.N., 1996: Predictability of the atmosphere and oceans: From days to decades. *Decadal Climate Variability: Dynamics and Predictability*, D. L. T. Anderson and J. Willebrand, Eds., Springer-Verlag.
- [50] Rowell, D. P., 1998: Assessing potential seasonal predictability with an ensemble of multidecadal GCM simulations. *J. Climate*, 11, 109C120.
- [51] Saha S., 1992: Response of the NMC MRF model to systematic error correction with integration. *Mon Wea Rev.*, 120, 345-360.
- [52] Smith L.A., C. Ziehmann, and K. Fraedrich, 1999: Uncertainty dynamics and predictability in chaotic systems, *Q.J.R. Meteorol. Soc.*, 125, 2855-2886.
- [53] Samelson, R.G., and E. Tziperman, 2001: Instability of the chaotic ENSO: The growth-phase predictability barrier, *J. Atmos. Sci.*, 58, 3613-3625.
- [54] Sugi, M., R. Kawamura, and N. Sato, 1997: A study of SST-forced variability and potential predictability of seasonal mean fields using the JMA global model. *J. Meteor. Soc. Japan*, 75, 717-736.
- [55] Sun Liang, Mu Mu, Sun Dejun, and Yin Xieyuan, 2005: Passive mechanism of decadal variation of

- thermohaline circulation, *J. Geophys. Res.*, 110, C07025, doi:10.1029/2005JC002897.
- [56] Tennekes H., 1991: Karl popper and the accountability of numerical forecasting. In new developments in predictability, ECMWF Workshop Proceedings, Shinfield Park, Reading, UK.
- [57] Thompson, C.J., 1998: Initial conditions for optimal growth in a coupled ocean-atmosphere model of ENSO, *J. Atmos. Sci.*, 55, 537-557.
- [58] van Oldenborgh, G. J., G. Burgers, S. Venzke, and C. Eckert, 1999: Tracking down the ENSO oscillator with an adjoint OGCM, *Mon. Wea. Rev.*, 127, 1477-1495.
- [59] Wang Shaowu, 1993: The studies of climate prediction and modeling (in Chinese). China Meteorological Publication Press, Beijing, 346pp.
- [60] Wang, B., and Z. Fang, 1996: Chaotic oscillation of tropical climate: A dynamic system theory for ENSO, *J. Atmos. Sci.*, 53, 2786-2802.
- [61] Webster P.J. and S. Yang, 1992: Monsoon and ENSO: Selectively interactive systems, *Quart. J. Roy. Meteor. Soc.*, 118, 877-926.
- [62] Xu Hui, 2006: Applications of conditional nonlinear optimal perturbation in predictability studies of Zebiak-Cane ENSO model. PhD dissertation (in Chinese), Institute of Atmospheric Physics, Chinese Academy of Sciences, 145pp.
- [63] Yan Huasheng, Wang Huijun, Yan Xiaodong, Cao Jie, and Han Jinping, 2003: Analysis of the impact of Pacific SST variations on prediction predictability in China, *Plateau Meteorology* (in Chinese), 22, 155-161.
- [64] Yan Huasheng, Yang Suyu, Hu Juan, and Chen Jiangang, 2006: A study of the relationship between the winter middle high latitude atmospheric circulation change and the principal rain patterns in rainy season over China, *Chinese Journal of Atmospheric Sciences* (in Chinese), 30, 285-292.
- [65] Zheng Fei, Zhu Jiang, Zhang Ronghua, and Zhou Guangqing, 2006: Improved ENSO forecasts by assimilating sea surface temperature observations into an intermediate coupled model. 23, 615-624.
- [66] Zebiak, S.E., and A. Cane, 1987: A model El Nino-Southern oscillation, *Mon. Wea. Rev.*, 115, 2262-2278.
- [67] Zhang, R.H., S.E. Zebiak, R. Kleeman, and N. Keelyside, 2003: A new intermediate coupled model for El Nino simulation and prediction. *Geophys. Res. Lett.*, 30(19), 2012, doi:10.1029/2003GL018010.
- [68] Zhou Xiaqiong, and Johnny C.L. Chen, 2006: Ensemble forecasting of tropical cyclone motion using a baroclinic model. *Adv. Atmos. Sci.*, 23, 342-354.

#### Figure Captions

Fig.1 Diagram showing conditional nonlinear optimal perturbation and its applications in predictability studies

Fig.2 Same as Fig.1 except for nonlinear local Lyapunov exponent.

Fig.3 Nonlinear and linear evolutions of the nondimensional model variable T (SSTA) corresponding to CNOP and LSV of annual cycle, respectively.  $u^g(u^g)$  and  $u^g(u^g)$ : the

$$\delta N LN \delta L LL$$

nonlinear and linear evolutions of SSTA of the CNOP (the LSV), which are two El Nino events. CNOP acts as the optimal precursor for El Nino (from Duan et al.(2004))

Fig.4. Same as Fig.1 except for La Nina events related to the local CNOP (the corresponding LSV) (from Duan et al. (2004)).

Fig.5. Comparisons between El Nino and La Nina amplitudes.  $u_{\delta N}^g(u_{LL}^g)$ : SSTA nonlinear (linear) evolution of CNOP (the corresponding LSV);  $v^1(v^1)$ : nonlinear (linear) evolution of

$$\delta N LL$$

T (negative anomaly of SST) of local CNOP (the corresponding LSV), indicating the amplitude of La Nina events (from Duan et al. (2004)).

Fig.6. The patterns of CNOP-type error for a given basic-state El Nino. In the left (right) column are SSTA (thermocline depth anomaly) components for the start month being (a) January, (b) April, (c) July, and (d) October (from Mu et al. (2007)).

Fig.7. Anomaly correlations and RMS error for the Nino-3.4 SST anomalies that were respectively forecasted by the intermediate coupled model (ICM) with original initialization (solid line with circles; Zhang et al., 2003), by the model with the new initialization (solid line with squares), and by persistence prediction (dot line with squares). All the results are for the period 1984-2003 (from Zheng et al.(2006)).

Fig.8. The RMSE of the pentad zonal-mean height of the persistence, climatic and nonlinear forecasts over (a) the Northern Hemisphere, (b) the Southern Hemisphere and (c) the tropical (the average of 12 cases in 1996) (from Chen et al.(2004)).

Fig.9. Ensemble tracks (thin lines) of Yancy (Y1700) using the LAF (solid line with triangles), BGM (dot line) and BGMV (dashed line with triangles) techniques. The best track is shown with black dots, the control run with open circles. Positions are plotted every 6 h (from Zhou and Chen (2006)).

Fig.10. Ensemble tracks (thin lines) of Ed and FLo from (a) 0000 UTC 14 September (E1400, F1400) in LAF and (b) 0000 UTC 15 September (E1500, F1500) in LAF, (c) E1400 and F1400 in BGME, (d) E1500 and F1500 in BGME, (e) E1400 and F1400 in BGMV, (f) E1500 and F1500 in BGMV. The best track is plotted with closed circles, the ensemble mean with triangles, the control with open circles. Positions are plotted every 6 h (from Zhou and Chen (2006)).

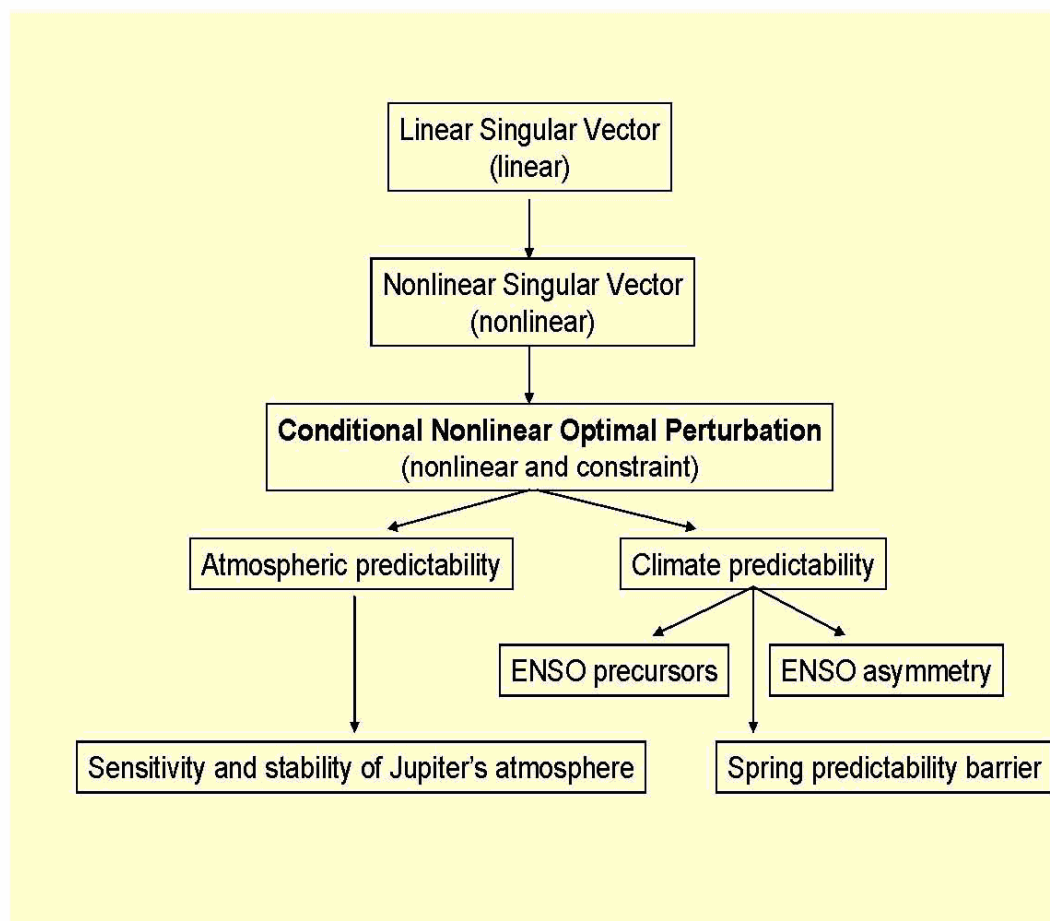


Fig.1 Fig.1 Diagram showing conditional nonlinear optimal perturbation and its applications in predictability studies

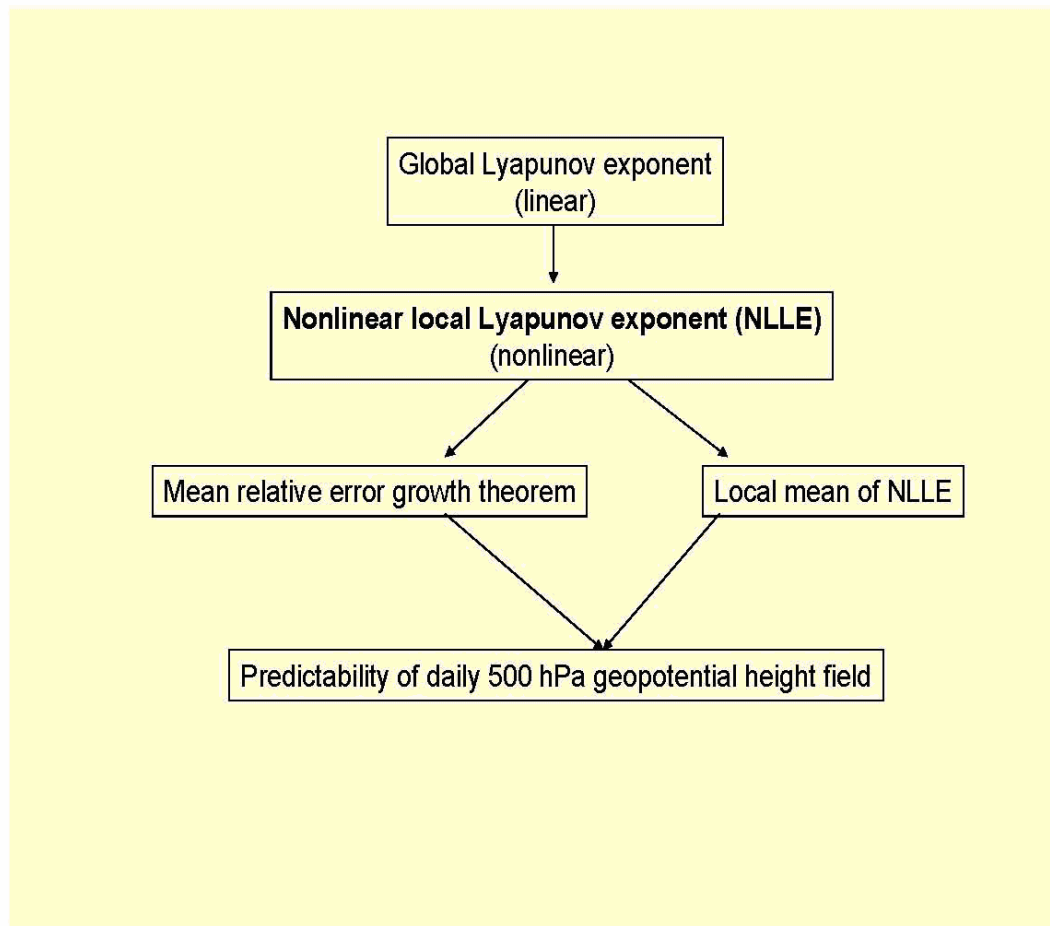


Fig.2

Fig.2 Same as Fig.1 except for nonlinear local Lyapunov exponent.

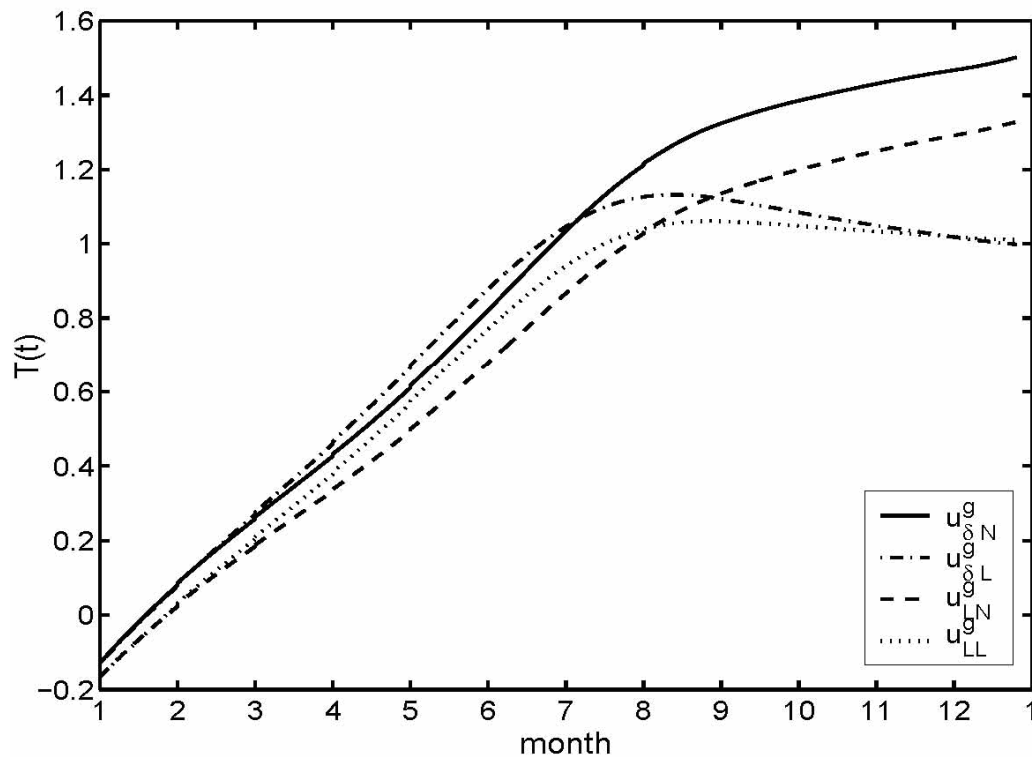


Fig.3

Fig.3 Nonlinear and linear evolutions of the nondimensional model variable T (SSTA) corresponding to CNOP and LSV of annual cycle, respectively.  $u_{\delta N}^g(u_{LN}^g)$  and  $u_{\delta L}^g(u_{LL}^g)$ : the nonlinear and linear evolutions of SSTA of the CNOP (the LSV), which are two El Nino events. CNOP acts as the optimal precursor for El Nino (from Duan et al.(2004))

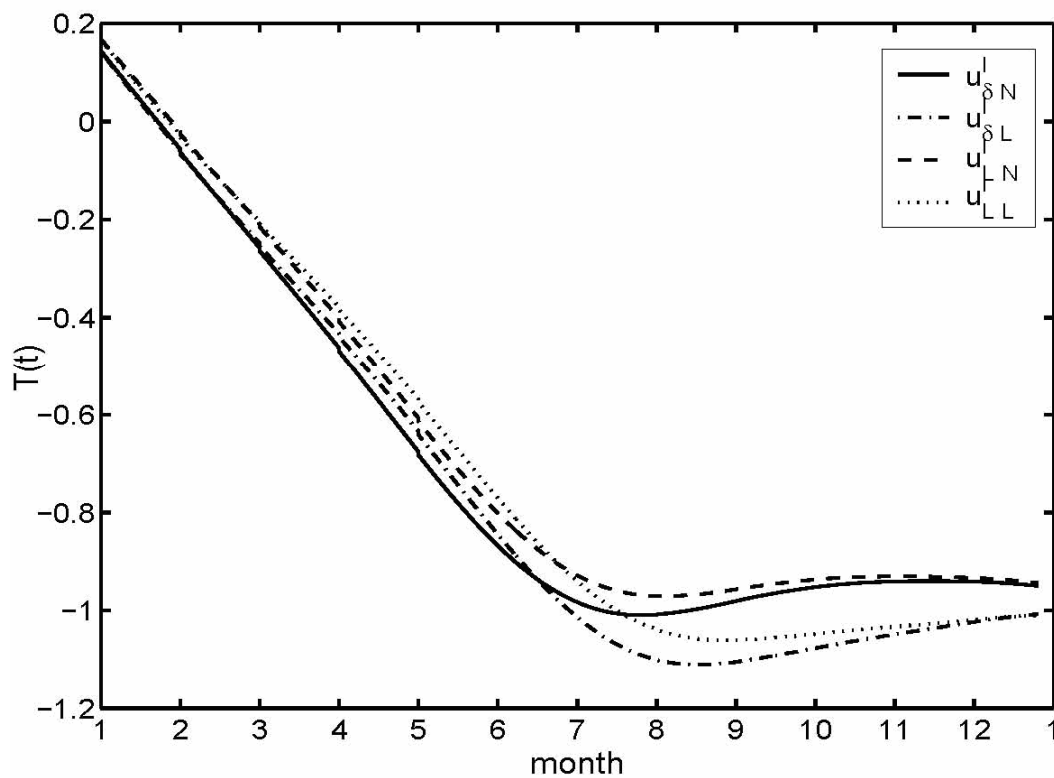


Fig.4 Fig.4. Same as Fig.1 except for La Nina events related to the local CNOP (the corresponding LSV) (from Duan et al. (2004)).

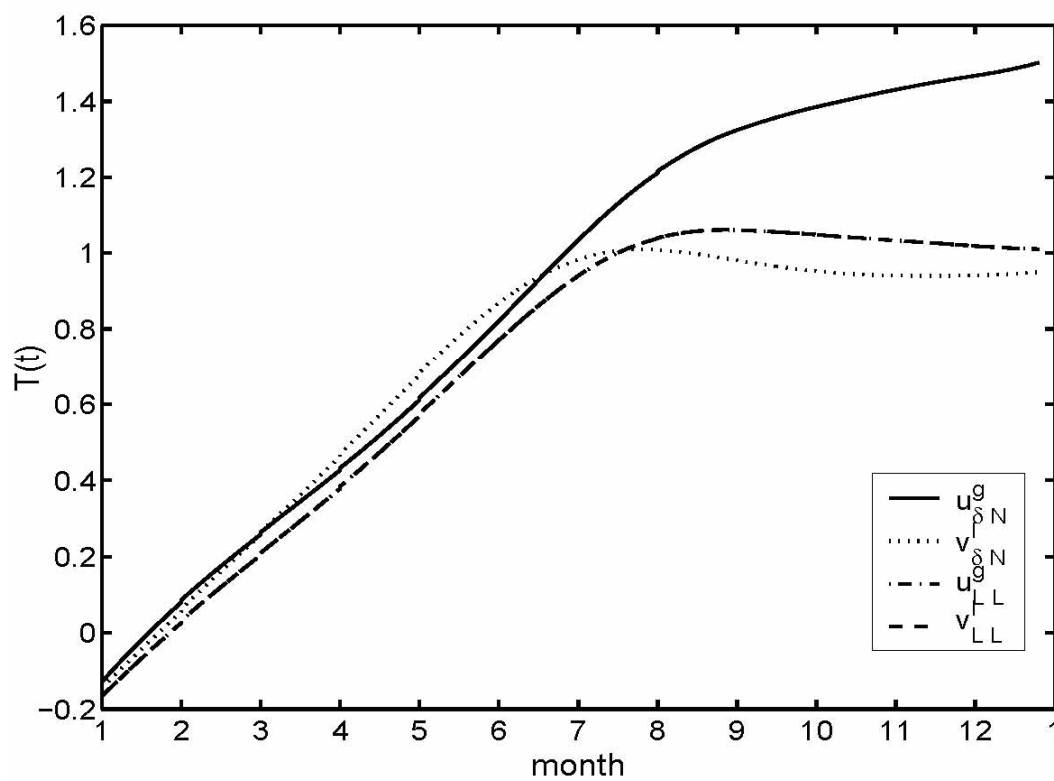


Fig.5 Fig.5. Comparisons between El Nino and La Nina amplitudes.  $u_{\delta N}$  ( $u_{\delta L}$ ): SSTA nonlinear